



Corso di dottorato di ricerca in:
"Scienze e Biotecnologie Agrarie"

Ciclo 36°

"Innovative technologies enabling plants to increase resilience as a pivotal feature in the conservation of agro-ecosystems"

Dottoranda
Dott.ssa Dora Scarpin

Supervisore
Prof. Enrico Braidot

Co-supervisore
Dott.ssa Elisa Petrusa

Anno 2024

TABLE OF CONTENTS

Summary.....	3
CHAPTER 1 - General Introduction.....	5
Climate change and new challenges for agriculture	6
New technologies for agricultural sustainability.....	7
Nanotechnology in agriculture.....	9
Multi-scale phenotyping.....	17
Aim of the thesis	20
References.....	21
CHAPTER 2 - Characterization and functionalization of chitosan nanoparticles as carriers for double stranded RNA (dsRNA) molecules towards sustainable crop protection	35
Abstract.....	37
Introduction.....	38
Results.....	40
Discussion.....	48
Experimental procedures.....	53
Conclusions.....	58
Author Contributions	59
Acknowledgements	59
References.....	60
Supporting information.....	66
CHAPTER 3 - Calcium Phosphate Particles Coated With Humic Substances: A Potential Plant Biostimulant From Circular Economy	71
Abstract.....	73
Introduction.....	74
Results.....	75
Discussion.....	83
Materials and methods.....	85
Conclusions.....	88
Author Contributions	89
Acknowledgments.....	89
References.....	90
Supporting information.....	94

CHAPTER 4 - Innovative multi-scale approach to study leaf phenotypic plasticity in weedy <i>Amaranthus</i> spp. young seedlings	100
Abstract	102
Introduction	103
Materials and methods.....	104
Results.....	107
Discussion.....	114
Author contributions	117
References	118
Supporting information.....	127
CHAPTER 5 - From plant traits to ecosystem: new perspective for the upscaling of salt marsh response to flooding stress with remote sensing tools.....	135
Abstract	137
Introduction	139
Results.....	140
Discussion.....	148
Materials and methods.....	151
Author Contributions	155
Acknowledgements	155
References	156
Supporting information.....	164
CHAPTER 6 - Final Dissertation.....	169
Impact of this work and future prospects	170
References	173
APPENDIX - Conferences, Other Contributions, Training Activities.....	176
Conferences and Workshops – Abstracts	177
Oral communications	177
Poster communications	182
Educational activities	193
Training activities.....	194
Acknowledgements	196

SUMMARY

Relentless global population growth, anthropogenic activity and the resulting climate change are causing significant damage to the environment and agricultural systems. Worsening environmental stresses on plants, inefficient use of resources and the general alteration of interactions between organisms in an ecosystem are just some of the problems we will be forced to face in the next future.

In the perspective of the ecological transition, different strategies are being explored to develop sustainable solutions that could ensure adequate production efficiency and limited impact, guaranteeing the maintenance of ecological balances.

In this context, the primary goal of the present research was to develop efficient methods to synthesise sustainable agrochemicals from natural nanomaterials obtained through circular economy and then functionalized with active biomolecules.

Studies were carried out primarily on the synthesis and characterisation of chitosan nanoparticles (NPs) for the defence of crops against fungal pathogens. These NPs have been utilized as carriers for specific double-stranded RNA (dsRNAs) sequences, with the aim of improving the efficiency of *Spray-Induced Gene Silencing* technology. This strategy may enable disease control through topical application of dsRNAs targeting pathogen essential genes on plant material. After preliminary analyses on NP-functionalized properties and on their fate when sprayed on *Nicotiana benthamiana* leaves, inhibition tests on *Botrytis cinerea* were carried out conveying dsRNAs with interfering function on fungal metabolism.

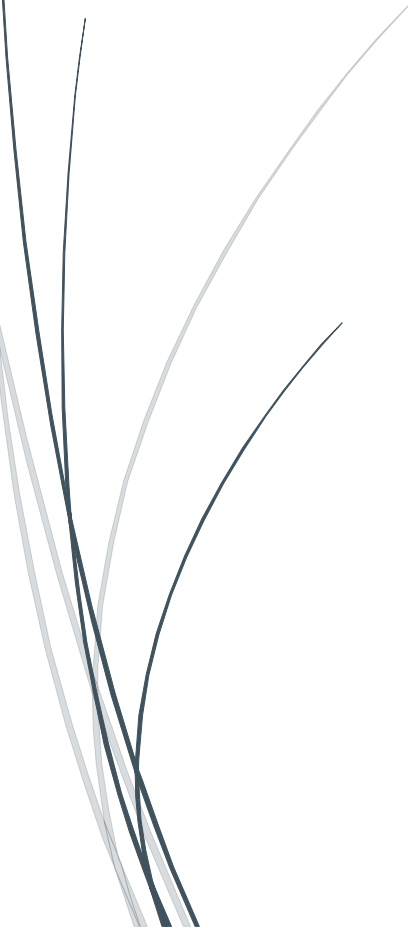
In addition, the production of a biostimulant from Calcium-Phosphate (CaP) NPs obtained by thermal treatment of *Salmo salar* bones was also investigated. In this case, CaP-NPs were combined with natural humic substances (HSs) and tested on *Valerianella locusta* and *Diplotaxis tenuifolia* to evaluate their nutrient uptake ability.

The second step was to investigate the field of plant phenotyping as an innovative approach for managing agricultural or natural systems. New methods useful for agri-environmental monitoring were developed through two different studies, using imaging techniques at different analytical scales.

Firstly, the leaf morpho-anatomical traits of four *Amaranthus* species were measured through image acquisition devices at full-scale and microscopic scale and subsequent image processing with specific software. The aim was to identify differences between species at a juvenile stage, that is notoriously difficult to analyse, but also the most critical phenological phase for weed competition with crops. In a second study, remote sensing compared with laboratory analysis was used to correlate the stress response of lagoon plant communities with multispectral indices. The aim was to investigate the power of imaging techniques to detect the environmental effect of flooding in salt marshes, with a view to understanding whether the method could be employed for environmental monitoring.

Both lines of research, although they still require a lot of experimental work to be fully validated, deserve to be developed. Their effectiveness would be improved by combining them, integrating complementary practices together for a multidisciplinary problem-solving approach. The innovativeness of these tools and the holistic perspective with which to employ them would permit to revolutionize the sustainable management of different ecosystems.

CHAPTER 1 - General Introduction



CLIMATE CHANGE AND NEW CHALLENGES FOR AGRICULTURE

Climate change is one of the most critical issues today. Enhanced anthropogenic activities have altered the composition of the global atmosphere (Malhi et al., 2021a; Solomon et al., 2007) causing an increase in the concentration of greenhouse gases (GHGs) such as carbon dioxide (CO₂), methane (CH₄) and nitrous oxide (N₂O), which lead to ozone depletion and subsequent global warming (Malhi et al., 2021a; Montzka et al., 2011). Human-caused climate change has affected widespread and rapid transformations in oceans, cryosphere and biosphere, leading to many extreme weather and climate phenomena that are increasing in intensity and frequency. This has led to negative impacts to nature and people, both in environmental and economic terms. Damage has occurred unevenly in different parts of the world, even worsening the already critical situation of the most disadvantaged countries (Calvin et al., 2023; Malhi et al., 2021a) or the most undisturbed environments such as the polar zones.

Looking at the primary production sector, recent IPCC reports (Calvin et al., 2023) state that climate change has compromised food and water security: in fact, although overall agricultural productivity has increased, environmental alterations have globally slowed this process over the past 50 years (Calvin et al., 2023), while the world population continues to grow. Moreover, climate-exposed sectors are suffering increasing economic damages, and among them, in addition to tourism and the energy sector, agriculture, forestry and fishery are importantly involved (Calvin et al., 2023).

In particular, agriculture is the most vulnerable to climate change due to its sensitivity to weather parameters (Mendelsohn, 2008). The effect of rising temperatures, changing precipitations and CO₂ concentration greatly influence crop yields (Adams et al., 1998), as well as their response to stresses. Some altered environmental factors may partially offset the effect of others (Adams et al., 1998; Long et al., 2006), but the final balance is almost negative: plants will increasingly face various abiotic stresses, including salinity, drought, heat or cold stresses (Malhi et al., 2021b), low water availability, and loss of soil fertility (Baul and McDonald, 2015). In addition, expected climatic changes may influence the development and survival of pathogens (Elad and Pertot, 2014). An increase in the susceptibility of crops to various pests and diseases is expected (Rosenzweig et al., 2001) with, for example, a possible 10-25% increase in losses due to insect infestations if the temperature rises by one degree (Shrestha, 2019). Invasion by migrating pests, a prolongation of the pest development season and a change in the synchronisation between pests and crops is possible (Reddy, 2013). At the same time, the competition of weeds with crops can also be strongly influenced, both by the use of resources and by the varying degree of adaptation to changes in temperature and CO₂ in the atmosphere (Korres et al., 2016; Malhi et al., 2020). Climate change can even affect the mode of action of herbicides (Varanasi et al., 2016) and pesticides (Matzrafi, 2019), altering their efficacy.

Looking at the issue from another angle, the agricultural sector is not only a victim of climate change, but also a cause of it. In fact, it contributes 15% to total emissions, mainly methane and nitrous oxide (Malhi et al., 2021a). The livestock sector is the largest producer of GHG emissions (8-10.8% according to the IPCC) (Malhi et al., 2021a; O'Mara, 2011), but also the contribution by manufacturing and use of chemical nitrogen fertilisers is significant (Kahrl et al., 2010). Global non-agricultural GHG emissions will increase until 2055, but are expected to grow at a higher rate if food preferences and food energy consumption shifts towards high-value products such as milk and meat (Popp et al., 2010). At the same time, inefficient agronomic practices provoke excessive nitrogen use that could be reduced by up to 38%, without taking energy waste into account. In fact, better crop management would reduce the energy consumption by 11%, increasing production and further lowering GHG emissions (Soltani et al., 2013) and environment eutrophication.

Hence, it seems clear that technological and managerial implementation is fundamental in both livestock and agronomic fields, to make production processes more efficient. Choices for the future of agriculture must consider on the one hand reducing impacts and on the other developing production methods that are adaptable to environmental changes. The formulation of climate-resilient technologies needs an interdisciplinary approach (Malhi et al., 2021a) and environmental policies should be dynamic, enacted with flexibility, since the negative impacts will be dependent on the climate scenario of different countries (Zilberman et al., 2004).

NEW TECHNOLOGIES FOR AGRICULTURAL SUSTAINABILITY

The use of traditional and agro-ecological management systems can help farmers adopt climate resilient technologies (Altieri and Nicholls, 2017; Venkateswarlu and Shanker, 2009). However, there is a clear need to focus on interventions that have both adaptation and mitigation characteristics (Arbuckle et al., 2015). Some approaches, such as the so-called Climate-Smart Agriculture (CSA) (Lipper et al., 2014), aim to transform and reorient agricultural systems from multiple points of view: the purpose is to operate not only on resource efficiency management (*water-smart* and *nutrient-smart practices*) and on resilience to climate change (*weather-smart* and *carbon-smart activities*), but also on the social, political and economic aspects, including the widespread dissemination of knowledge.

New technologies can help to accomplish the first two objectives complementing already widespread practices (biodiversification, more efficient soil and water handling, resource conservation, etc.) grouped under the concept of integrated agriculture (Altieri and Nicholls, 2017; Barzman et al., 2015; Hendrickson et al., 2008).

In recent years, agricultural and environmental management have profited from numerous innovations that are radically transforming the related sectors. These include, for example:

- **Resources-saving techniques.** Some of them aim to preserve soil fertility and reduce erosion through the use of cover crops, crop rotation and conservation agriculture (Giller et al., 2015); others, instead, like soilless farming, enable more efficient food production with reuse of substrates, water and nutrients, reducing pressure on agricultural land and shortening the supply chain (Pradhan and Deo, 2019).
- **Synthetic biology and New Genomic Techniques (NGTs).** These technologies enable the genetic modification of plants to make them not only more productive, but also more resistant to diseases, pests and environmental stresses (drought, excess salinity, extreme temperatures) (Clapp and Ruder, 2020; Giudice et al., 2021).
- **Precision agriculture and sensors.** Useful for collecting a wide range of data to better monitor environment and crops, also allow more targeted management of irrigation, fertilisation and crop protection, thus reducing waste and improving overall efficiency (Clapp and Ruder, 2020).
- **Alternatives to agrochemicals.** They consist of a range of less impactful and biodiversity-friendly crop nutrition and defence tools. These include the use of biopesticides (products derived from living organisms such as bacteria, fungi and viruses that can control diseases), biological control agents (predatory insects and parasitoids that reduce populations of harmful pests) (Anwer, 2017), biostimulants and products of natural origin for nutrition or integrated pest management (Yakhin et al., 2017), and, finally, latest-generation biotechnology-based products (Parisi et al., 2015).

Obviously, a part of these approaches or tools are determined simply by the reorganisation or rediscovery of cultivation management practices, while others are entirely new and have developed thanks to technological progress. Some of the latter, such as certain devices exploiting artificial intelligence and products based on biotechnology or genetic engineering, are still in a testing phase and are often not yet available on the market (Clapp and Ruder, 2020; Parisi et al., 2015).

Given the urgency of revolutionising agri-environmental systems to address climate change issues, it is necessary to focus research precisely on the development of these tools. The key idea is to exploit all the methods described above in a balanced and integrated manner, so as to adapt management practices to the peculiarities of the territory and to the actual situation. Among the various possibilities, that of tackling the same phenomenon by complementary means emerges (Uiterkamp and Vlek, 2007). This really occurs, for example, searching for alternative methods to save resources or to reduce the environmental damage of agricultural activities. In such cases it is necessary to integrate multiple fields of knowledge and to act at different scale levels (*e.g.*, it is important to know the effect of a specific intervention on the individual down to the entire ecosystem in which it is embedded).

With this approach in mind, the present work offers insights into two currently leading subjects: nanotechnology for the production of next-generation agrochemicals and imaging techniques. These two topics, although different, fit into the concept of the multidisciplinary approach: they can be used to achieve similar goals from multiple modes of action. Among all the targets, first and foremost the limitation of environmental impact of agronomic treatments should be considered.

NANOTECHNOLOGY IN AGRICULTURE

Nanotechnology has already enabled progress in medicine and pharmacology, but only recently its application in the agri-environmental sector attracted large interest (Cătălin Balaure et al., 2017). As studies have progressed in the last years, the advanced agronomic application of nanotechnology in plants, known as phyto-nanotechnology, turned out to be crucial for securing sustainable agriculture and food production (Wang et al., 2016). Applications of nanotechnology in agricultural systems can in fact promote smart progress in crop management, lowering resource use and improving the efficiency of conventional agricultural practices, thus offering numerous environmental benefits without reducing productivity. Due to the diverse areas where nanomaterials are applicable, and to the many materials that can be used, nanotechnology in agribusiness is becoming promising to be further understood and developed (Jiang et al., 2021).

Special properties of NMs and their interaction with plants

Starting from an initial definition, nanomaterials (NMs) are particles that have three- or two-dimensional external dimensions or internal surface structures ranging from 1 to 100 nm (Fincheira et al., 2021). The physicochemical properties of NMs, which include enhanced reactivity, specific surface structure and high surface-to-volume ratio, differ from those of their molecular counterparts (Rodrigues et al., 2017): this makes NPs suitable for performing different and optimized functions than ordinary materials (Wang et al., 2021). Engineering NPs with desired characteristics, such as shape, pore size, and surface properties is easily achievable, allowing them to be used in various ways (Khandelwal et al., 2016). Moreover, NPs can be utilized either directly as protectants or biostimulants (Worrall et al., 2018), or as carriers for precise and targeted delivery through adsorption, encapsulation, or conjugation of an active substance (Khandelwal et al., 2016).

The uptake, translocation and transport of NPs in crops play a role in strengthening both direct action and efficient delivery of active molecules. In general, NMs can be introduced into the plant system through two paths, namely via roots or leaves. In leaf uptake, NMs can be translocated via stomata or cuticle (Maluin and Hussein, 2020). The former pathway is the easiest, as the typical size of the stomatal opening is approximately 3-10 μm wide and 25 μm long (Eichert et al., 2008), while the cuticle pores have smaller sizes (0.6-4.8 nm) (Eichert and Goldbach, 2008; Popp et al., 2005)

that limit the passage of certain types of NPs. Uptake through root tissues, on the other hand, can occur by cuticular route or by root diffusion, based on the concentration gradient between the soil and roots. The penetrated NMs are then translocated and transported to other parts of the plant via the phloem and/or xylem (Maluin and Hussein, 2020). The movement of the systemic phloem during foliar application follows the symplastic pathway and is multidirectional, from the source to the sinks. The movement of the systemic xylem, on the other hand, follows the symplastic and apoplastic pathway and is unidirectional, *i.e.* only in the upward direction (Maluin and Hussein, 2020).

Hence, the uptake and accumulation of particles are greatly influenced by the route of NPs translocation (Ma et al., 2018), but this is substantially determined also by their properties. Many studies have shown that the nanometric form of various materials has enabled better absorption within plant tissues (Jiang et al., 2021) compared to bulk materials, leading to the conclusion that the characteristics of NPs, such as size, surface activity, aggregation level, crystallinity, porosity and redox potential, clearly influence their ability to interact with crops and to transport and release functionalising agents. Moreover, surface charge, hydrophilicity, lipophilicity and physical adsorption of NPs affect aggregation and translocation levels (Jiang et al., 2021).

In addition, coating NPs with various materials (*e.g.* iron, humic acids or other organic macromolecules, organic acids, different polymers) can influence their penetration and translocation into crops by modifying their surface structure (Jiang et al., 2021) and charge (Hu et al., 2020). Based on their own characteristics, these coatings can prevent NPs aggregation (*e.g.* hydroxyapatite, chitosan) (Jiang et al., 2021) and make them more stable on the leaf surface (*e.g.* protein encapsulation) (Rathore and Tarafdar, 2015) or, on the contrary, more easily absorbed. This happens especially when they create a hydrophilic protective sheet (Shahrekizad et al., 2015) or when the coating material is able to prevent the stomata closure (Su et al., 2019). Furthermore, the bioavailability of NPs is enhanced by functional groups and surfactants since they increase their adhesion to the leaf surface (Elmer and White, 2016; Yu et al., 2017).

Considering the composition of nanomaterials, some NPs inherently exhibit beneficial properties, and thus can also be employed on their own. For example, metal NPs, such as silver, copper, zinc oxide, and titanium dioxide have been shown to have antibacterial, antifungal and antiviral functions (Gogos et al., 2012; Kah and Hofmann, 2014; Kim et al., 2018), but also chitosan has similar properties (Worrall et al., 2018), to which are added biodegradability, biocompatibility, non-allergenicity, and low toxicity (Cota-Arriola et al., 2013). Chitosan NPs are very popular because, in addition to inducing numerous effects on organisms (Malerba and Cerana, 2016), they are also suitable as nanocarriers, together with silica NPs, solid lipid NPs and clays (layered double hydroxides), all of which have been tested for crop defence through their functionalization with synthetic or natural bioactive molecules (Worrall et al., 2018). These are just examples, but there are several other materials being studied for their use in sustainable agriculture.

Despite the numerous advantages described, NMs can be an attracting tool for the development of new sustainable technologies for agriculture after in-depth studies to understand their characteristics and effects on the ecosystem. It is important to carefully test a material and its dopant molecules to highlight any phytotoxicity (Ma et al., 2018), how they enter or interact with plants or pathogens, and their effects on the metabolism of target and non-target organisms. At the same time, it must be ensured that the NMs themselves are not adversely affected by external factors (*e.g.* root exudates, extracellular polymeric substances in the rhizosphere, climatic agents) (Anderson et al., 2018) and that the substrate or distribution medium is the most suitable to ensure greater efficacy (Ma et al., 2018). Upon verification of their safety, these materials have a great potential to revolutionise modern crop agriculture.

NPs applications in agriculture

Due to their versatile physico-chemical properties, NMs can be used in a large number of agricultural practices. Currently, studies are deepening knowledge on the application of nanotechnology into several macro-areas (Jiang et al., 2021), which could be divided as follows:

- Crop nutrition and growth
- Crop yield and quality
- Stress mitigation (*e.g.*, environmental factors due to climate change)
- Sustainable crop protection
- Postharvest preservation
- Genetic engineering
- Other applications (nanosensors, nanobarcoding) (Hayles et al., 2017)

Given the extent of materials that can be used to synthesise NPs and the molecules with which they can be functionalised, studies on this subject are numerous and varied. For this reason, only the topics most pertinent to this thesis work will be explored in greater detail.

Agronanochemicals: crop nutrition and disease management

The use of NPs for nutrition and disease management can take place through two different mechanisms: using NPs that directly provide benefits to crops or employing them as carriers of existing agrochemicals or other active ingredients, including those of natural origin (Worrall et al., 2018). This second mode is nowadays the most appreciable, as it offers numerous advantages over conventional products. As vectors, NPs can provide protection for active molecules, increasing their durability and stability even under environmental pressures (UV, rain); they can also guarantee better solubility, reduced toxicity and greater site-specific absorption in the target organism (Hayles et al., 2017). This allows for a specific action, thus also reducing the occurrence of antimicrobial resistances. In addition, NMs can be either simple stabilising agents

that permit slow release of the dopants, or their conveyers within plants or pests. All these functions are advantageous compared to the use of free active molecules, as they allow the dose and number of applications to be significantly reduced, thus decreasing costs and environmental impact (Worrall et al., 2018).

Nanofertilisers – Nanofertilisers are attracting considerable interest as they can solve some of the major issues associated with conventional nutrient products. As they are able to regulate the release of nutrients and employ smaller quantities, they would overcome problems of eutrophication and resource-use inefficiency and comply with legislative environmental restrictions (Chhipa, 2017; Jiang et al., 2021).

According to their functions, nanofertilisers can be categorised as nanocomposite fertilisers, controlled-release fertilisers, or controlled-loss fertilisers (Jiang et al., 2021). The sustained release of nutrients is one of the key points to be developed, as, in addition to making distribution more efficient by accommodating crop needs (Abdel-Aziz et al., 2016), it can also improve soil health by regulating microorganisms in the rhizosphere (Wang et al., 2020). Indeed, these NMs can induce them to produce secondary metabolites (Khan et al., 2018; Panichikkal et al., 2019), enhancing plant growth and promoting colonisation of the root surface (Jiang et al., 2021). NMs are particularly advantageous for their small size, which allows the surface mass ratio of the particles to increase. Due to this property, various nutrient ions can be desorbed and adsorbed slowly and constantly (Monreal et al., 2016), minimising loss through leaching or adsorption and prolonging the effect during time (Shalaby et al., 2016). This feature is crucial, for example, in the case of nitrogen, where its runoff is a major issue in conventional fertilisers (Cai et al., 2014; Kahrl et al., 2010), and phosphorus, whose highly insoluble compounds formed in the soil make it hardly available to plants (Paz-Ares et al., 2022). In addition, several studies demonstrated that the use on crops of various NMs (ZnO-NPs, Fe/Fe₂O₃-NPs, Cu/CuO-NPs, Au-NPs, nanocalcite, etc.) could enable also a regulatory effect on the uptake of elements other than those constituting the NPs (Jiang et al., 2021).

Ultimately, it is evident that nanofertilisers are able to balance nutrition during the plant life cycle and increase crop production. Despite this, there is a need for an evaluation of the fate of nanofertilisers in soils with different physiochemical characteristics, in order to define the best efficacy conditions for a particular crop or substrate (Jiang et al., 2021).

Nanopesticides and Nanoherbicides – Interest in the application of nanotechnology in crop protection replacing conventional methods has increased rapidly in recent years. This is because the defence techniques used to date are highly polluting and inefficient: it is true that at least 90% of pesticides fail to achieve their objectives of effective pest or pathogen control, and frequently leak into ecosystems (Nuruzzaman et al., 2016), damaging also non-target organisms. This situation leads to the deterioration of the environment, but also increases crop production costs. To solve

these serious issues, nano-formulation of agrochemicals proves to be an effective solution. In particular, nano-encapsulation processes can be performed, where the active ingredients of pesticides or herbicides are bound to NMs (Jiang et al., 2021), or other engineered nano-structures with beneficial characteristics for crop protection can be obtained (Ul-Haq and Ijaz, 2019). Again, these formulations are useful for the controlled release and persistence of active ingredients; moreover, since they act in an extremely specific way on the target organism, they offer a chance to overcome the multi-resistance development, which today noticeably affects crop management (Jiang et al., 2021). NPs employment also helps to enhance the water solubility of active ingredients, a limitation of conventional products, which in turn causes increased resistance to target organisms (Ul-Haq and Ijaz, 2019). In addition, nano-formulation and nano-encapsulation of bioactive molecules also allow the increase of their thermal stability, crystallinity, permeability and biodegradability, which are essential for sustainable agricultural systems (Dwivedi et al., 2016).

Looking specifically at pest and pathogen management, studies have been carried out in recent years on nanomaterials to be used mainly as carriers of active ingredients. Essential oils, conventional products and biocidal molecules with various modes of action have been tested as functionalizing agents of lipid, chitosan, silica, polymer mixes and other NPs, achieving good results in crop protection. The target organisms were mainly cutworms, mites, aphids, whiteflies and common fungi (*Fusarium*, *Aspergillus*, *Botrytis* spp., etc.) (Worrall et al., 2018), some of which have also been the subject of studies with simple metal oxide NPs (Elmer et al., 2018; Malandrakis et al., 2019; Shenashen et al., 2017).

The various trials have allowed to improve active molecules' solubility and stability, to reduce volatility and ultimately to be more effective if compared with conventional insecticides and fungicides. Conversely, the results of toxicity studies have not always been positive, indicating the need for further investigation (Worrall et al., 2018).

Finally, also in the weed management field nanotechnology-driven innovations are promising for solving not only the weaknesses shared by all agrochemicals, but also those specific to herbicides. As an example, nanotechnology could overcome the limitation of most currently available commercial formulations, which only target the above-ground sections of the weeds, leaving roots, rhizomes and tubers vital (Hess, 1993): by means of special nano-encapsulated molecules it is possible to target receptors in the roots and prevent the glycolysis process, eliminating weeds completely (Jiang et al., 2021). Moreover, NPs are also able to detoxify herbicide residues, thus reducing pollution and avoiding limitations in crop development (Satapanajaru et al., 2008).

Plant growth and biostimulation

Some NMs show useful properties for improving the growth and development of plants at different stages of their life cycle. Several studies on horticultural and field crops have demonstrated such an effect by NPs of various origins, including metal

oxide NPs, Zn-NPs, carbon nanotubes, Mesoporous silica NPs, Au-NPs, SiO₂-NPs and chitosan NPs (Jiang et al., 2021).

NMs have positive effects on crops in different ways depending on their intrinsic properties and concentration (Jiang et al., 2021). They can induce, directly or through the transport of other molecules, various responses which may be related to yield quality or to the acceleration of certain physiological functions (Nair, 2016). Studies have shown that some NMs can increase seed water uptake and, by penetrating the seed coat, can stimulate its enzyme system (Abou-Zeid et al., 2021; Li et al., 2021), although the mechanisms underlying the advantage of NMs over traditional materials remains unknown to date (Jiang et al., 2021). It has been reported that NPs can also enhance photosynthesis enzyme activity and chlorophyll content, thus improving overall plant growth (Jiang et al., 2021; Rossi et al., 2019). At the physiological level, some NPs can in fact stimulate the activity of Rubisco or of carbonic anhydrase (Jiang et al., 2021). At the molecular level, on the other hand, it has been shown that TiO₂-NPs can induce the light-harvesting complex II (LHCII) gene and increase the chloroplast's light absorption efficiency (Ze et al., 2011), while Si-NPs can stimulate the expression of genes related to chlorophyll biosynthesis (Li et al., 2023). NPs can influence also crop yield and quality by modifying plant physiology and biochemistry, improving mineral uptake, chlorophyll content, enzyme activity and plant growth (Jiang et al., 2021), influencing also the vernalization and flowering pathways (Ke et al., 2020).

Finally, also in the case of biostimulation, NPs can be a useful tool for delivering other active molecules precisely to the target site, saving resources and avoiding dispersion in the environment. One of the objectives to reach is the easing of nutrient absorption, which is stimulated for example by humic substances (Jindo et al., 2020).

Given the promising results to date, further investigations into dose-dependency, long-term exposure effects and metabolomics or proteomics studies (Jiang et al., 2021) may be a gateway tool to determine the exact function of NPs or transported molecules.

In summary, thanks to phyto-nanotechnology a revolution in agro-ecosystems could be achieved by increasing crop yield and productivity, minimizing losses and increasing input efficiency. Despite the need for further studies on these products to verify the toxicity of NPs and the safety of different applications, the potential is unquestionably high. The contemporary maintenance of environmental sustainability, ecological and economic stability would result in a relevant solution to make the development of agrosystems and of related sectors feasible. (Acharya and Pal, 2020).

An insight on the combination of new molecular approaches with nanotechnology

Other technologies that work on a small scale are those that act on the manipulation of gene expression. For a long time, traditional breeding or genetically modified organisms (GMOs) have been used to cope with biotic and abiotic stresses and to implement quality characteristics of crops. However, emerging diseases and unpredictable climatic changes require alternative solutions to adapt crops to new conditions. Innovative biotechnological techniques, such as cisgenesis and genome editing, are emerging solutions for the selection of more stress-tolerant crops (Giudice et al., 2021), but still have to face the obstacles of technological development, public perception, consumer preferences and legal regulation (Dayé et al., 2023; Giudice et al., 2021).

A new approach to overcome plant transformation and its limitations is to employ strategies based on the *RNA – interference* (RNAi) mechanism (Dubrovina and Kiselev, 2019). In plants, RNAi is a natural regulatory and defence strategy that plays key roles in the regulation of plant response to environmental stresses, growth, and development (Dubrovina and Kiselev, 2019; Rosa et al., 2018; Singh et al., 2018), but it is also a trigger for plant immunity against pests and pathogens, modulating plant-microbe interactions and their virulence (Giudice et al., 2021). In particular, the mechanism called *cross-kingdom RNAi* allows for bidirectional exchange of small RNA molecules between different interacting organisms, inducing gene silencing in each other (Cai et al., 2018; Ma et al., 2020). This further proves that RNAi can be used to control plant diseases caused by fungi, viruses, nematodes and insects (Giudice et al., 2021). It is still a matter of debate the assumption that RNAi is only capable to interfere with pathogen translation-machinery lowering virulence or even to stimulate plant response downregulating endogenous plant genes.

Specifically, the RNAi machinery is based on the diffusion of exogenous long dsRNAs or hpRNAs (hairpin RNAs) into tissues (of plants and of other organisms where the mechanism is conserved) that are transformed into siRNAs, microRNAs or other small RNAs, leading to the induction of silencing of target genes. This occurs when they are recognised and transformed by DICER-like ribonucleases (Borges and Martienssen, 2015; Dubrovina and Kiselev, 2019). The resulting small RNAs are then incorporated into the RNA-induced silencing complex (RISC) that drives translational repression or sequence-specific degradation of homologous target mRNAs (Dubrovina and Kiselev, 2019). In plants, the RNA silencing signal seems to move over short distances from one cell to another, probably through plasmodesmata, or long distances through the phloem. Although information on the nature of the mobile silencing signal is limited and sometimes inconsistent, several reports argue that 21-24 nt siRNAs or miRNAs could be responsible (Dubrovina and Kiselev, 2019; Mermigka et al., 2016).

Various studies show that the RNAi mechanism can affect the mRNA levels of target genes in plant genome or in plant pathogens or pests also when exogenous sequences come into artificial contact with plants, and not only when crops are under attack. For

this reason, RNAi could be a viable alternative for sustainable and eco-compatible wood (Bragg and Rieske, 2022) or crop protection without the use of chemicals. The *in vitro* or *in vivo* application of siRNA or dsRNAs obtained by bacterial-mediated biosynthesis has shown promising results on insects (Gogoi et al., 2017), viruses (Kaldis et al., 2018; Mitter et al., 2017b; Nilon et al., 2021; Taliansky et al., 2021) and fungi (Koch et al., 2016; McLoughlin et al., 2018; Nerva et al., 2020; Song et al., 2018), using different methods of treatment such as trunk injection, soil/root drenching, mechanical inoculation, petiole absorption and high or low pressure spraying (Dalakouras et al., 2020, 2018; Dubrovina and Kiselev, 2019; Nerva et al., 2020).

The latter, in particular, also called SIGS (*Spray Induced Gene Silencing*), could be a methodology closer to common agronomic treatments, and thus easily deployable on a large scale, relying on direct applications of exogenous RNAs on plants or pests. Although several developments (both technological and environmental impact assessment) are still needed to achieve their widespread use as protective molecules in crops (Giudice et al., 2021), some strategies are already demonstrated to be able to improve their efficacy. Specifically, to mitigate the great susceptibility of dsRNAs to rapid degradation, encapsulating techniques for protecting them and facilitating their delivery are currently being investigated. To this aim, the use of nanomaterials as carriers for these molecules becomes feasible: different materials have been employed for their delivery to facilitate the dsRNAs or siRNAs uptake and survival in plant or pest tissues, such as clay nanosheets (Mitter et al., 2017a; Yong et al., 2021), carbon nanotubes (Demirer et al., 2020), Carbon Quantum Dots (Das et al., 2015), gold nanoclusters (Zhang et al., 2021a), silica (Das et al., 2015) and chitosan NPs (Das et al., 2015; Dhandapani et al., 2020; Xu et al., 2023; Zhang et al., 2010). In the case of chitosan NPs and other materials, moreover, it would be possible to exploit not only their usefulness as vectors, but also their intrinsic biostimulant properties towards pathogens or plants (Stasińska-Jakubas and Hawrylak-Nowak, 2022). This would make it possible to enhance the efficacy of dsRNAs and/or to achieve several different effects with a single treatment.

In addition, in some cases specifically-designed nanocarriers may also be useful simply for long-term protection outside the plant, since cellular internalisation of nanocargoes is not always necessary for RNA delivery (Zhang et al., 2021b): this would further extend the number of employable nanomaterials, taking into account even those NPs that are not particularly suitable for penetration into tissues.

Finally, by developing appropriate formulations of nanoparticle-dsRNAs and optimising their distribution modalities, the amount of nucleotide material could be drastically reduced (instead of applying it naked), thus making this practice significantly cheaper and more accessible for widespread use (Dalakouras et al., 2020; Giudice et al., 2021) and this is another point in favour of this approach.

Given all these benefits, the combination of molecular techniques and nanotechnology also deserves further study in the next years, as an integrated strategy for crop

protection where the use of other molecules (even those carried by nanomaterials) does not exert the same protection.

MULTI-SCALE PHENOTYPING

Another approach to address the challenges of ecological transition is to study how plants interact with their environment. This information is crucial for understanding how plants respond to stresses, what competitive relationships they establish with other organisms and ultimately how an entire ecosystem may vary in response to climate change. Such knowledge is crucial for both natural and anthropized systems, aiming to facilitate decision makers and politician in setting up future strategies for agricultural and environmental management.

Plant phenotyping through modern imaging techniques is one of the tools enabling to obtain such answers.

Research has made significant advances in genetic sequencing techniques and genome analysis, revolutionising our understanding of biology and making it possible to predict the metabolic activities and growth patterns of plants. Nevertheless, the interaction between genes and environmental factors is quite difficult to study, and its in-depth investigation is crucial to fully understand an organism's relationship with its environment. The phenotype of an individual is not only expressed in morphology, but also concerns traits observable in developmental processes, physiological, biochemical and behavioural properties. In plants, moreover, these characteristics are more pronounced given their great plasticity to different environmental conditions, which makes understanding them even more complex (Dhondt et al., 2013; Pieruschka and Schurr, 2019).

Phenotyping is a medium to characterise individuals endowed with traits that give them an adaptive advantage in terms of stress resistance and productive capacity (Carvalho et al., 2021). From molecular to population analyses, this approach can be applied at different scale levels of organization to evaluate plant phenotypes based on anatomical, ontogenetic, physiological, and biochemical properties in specific environmental and genotypic conditions (Demidchik et al., 2020; Pieruschka and Schurr, 2019; Walter et al., 2015).

Modern phenotyping methods allow the detailed study of plant growth, development and reproduction processes such as photosynthesis, respiration, water turnover, mineral nutrition, productivity regulation mechanisms and stress resistance (Demidchik et al., 2020; Dhondt et al., 2013). In the agri-food sector, many progresses in phenotyping techniques are directed by the objectives of crop selection and management (Pieruschka and Schurr, 2019), nonetheless these tools also lend themselves for the improvement of environmental handling practices, especially in view of the global changes facing planetary ecosystems.

Phenotyping approaches can be invasive or non-invasive. The former method requires the extensive sample manipulation through a destructive process, which prevents any subsequent measurements and provides information only up to the time of analysis. Non-invasive methods, on the other hand, collect information from any tissue through non-destructive analysis, which allows forthcoming measurements of the individual, enabling changes in phenotype to be tracked over the entire life cycle of the plant or under varying growth conditions (Langstroff et al., 2022).

As expected, nowadays great interest is directed towards non-destructive techniques, in particular those based on automated image capture. By analysing the spectral properties of plants, these methods allow high-throughput quantitative evaluation of individual plant traits under controlled conditions, or of entire plant populations in an open air environment (field phenotyping) (Walter et al., 2015). The most widely applied techniques are those based on 2D and 3D imaging sensors using visible light, hyperspectral, thermal, stereo and time-of-flight cameras. These can be employed directly for individual analyses or mounted on different platforms, ranging from satellites to manned or unmanned aerial aircrafts or ground robots (Dhondt et al., 2013; Pieruschka and Poorter, 2012). Acquisitions can also be validated in a controlled environment or by means of laboratory analyses, to allow comparisons at different precision levels. Furthermore, in order to make the data available within the scientific community, the MIAPPE (Minimal Information About Plant Phenotyping Experiments) recommendations have been developed, which are continuously updated to allow the description of all metadata, including environmental ones, via national and international institutional networks. Although to date most complete phenotyping data remain unavailable, it may prove to be a useful resource for the future (Gehan and Kellogg, 2017; Pieruschka and Schurr, 2019).

Plant spectral behaviour and its interpretation

Vegetation has specific spectral behaviours at different wavelengths, which depend on the interactions of reflection, transmission and absorption of light due to the biochemical, structural and morphological specificities of leaves and of entire plant. The course of the obtainable reflectance curve therefore varies according to the content and type of leaf pigments, the internal structure of the leaf, the water and protein proportion, cellulose and other structural components, as well as to the canopy architecture. It follows that it is possible to draw useful information on the plants' different leaf structure and density, on phenological stage, on biomass production and on any stress they are suffering from (Liu et al., 2020).

Such indications are obtained by applying specific algorithms, as is the case of vegetation indices. With the spread of remote sensing technologies, various vegetation indices have been exploited, including, for example, *Normalized Difference Vegetation Index* (NDVI), *Green Normalized Difference Vegetation Index* (GNDVI) and *Enhanced Vegetation Index* (EVI), which explain, respectively, the level of vigour, the

photosynthetic activity and the vegetative development (Kothari and Schweiger, 2022; Liu et al., 2020; Ustin and Jacquemoud, 2020).

In order to quantitatively measure the phenotype through the interaction between light and plants, various imaging sensors are available, which can be divided into the following categories:

- Passive sensors, designed to detect electromagnetic energy in the environment: RGB (digital), thermographic, multi- and hyperspectral cameras, stereo-vision cameras etc. (Gibbs et al., 2016; Xie and Yang, 2020).
- Active sensors, that emit electromagnetic energy to scan the subject to be imaged: time-of-flight (*e.g.*, LiDAR – *Light Detection and Ranging*) or structured-light systems (Chandrashekar et al., 2018; Gibbs et al., 2016).
- Other sensors: Fluorescence and Magnetic Resonance Imaging, X-ray Computed Tomography (Kolhar and Jagtap, 2021; Li et al., 2014).

Through these devices it is possible to study plants at different scale levels. Numerous platforms permit to perform high-throughput phenotyping, ranging from satellites, Unmanned Aircraft Systems (UAS), ground vehicles (robots) and finer sensing systems used in controlled environments, laboratories and growth chambers (Araus et al., 2022; Liu et al., 2020; Volpato et al., 2021; Xu and Li, 2022).

With the abovementioned imaging techniques, the plant organism can be analysed in its entirety or in its individual parts by examining three components: (i) structural, *i.e.* morphological attributes, such as the number, shape and size of leaves; (ii) physiological, which influence the processes that regulate growth and metabolism, such as chlorophyll content, leaf surface temperature and photosynthesis efficiency; (iii) temporal, such as the pattern of growth or adaptation to certain conditions (Das Choudhury et al., 2019).

Nowadays, these advanced methods are not only fundamental for ecophysiological studies, but also for planning in agronomic or environmental management. For example, techniques that exploit radiation outside the visible spectrum allow to identify and quantify disease symptoms in advance (Dhondt et al., 2013); fluorescence methods can estimate photosynthetic activity; several devices can map root development; hyperspectral imaging is employable to determine biomass, water use efficiency and thus drought tolerance, responses to nutrient deficiency, plant overheating and to early detect biotic or abiotic stresses (Das Choudhury et al., 2019; Dhondt et al., 2013). This information can, in addition, be further deepened by processing the data with specific algorithms: some segmentation and skeletonisation systems make it possible to describe plant components (*e.g.*, leaves) in great detail, demonstrating the genetic influence on temporal or environmental variations (Das Choudhury et al., 2019; Dhondt et al., 2013; Kolhar and Jagtap, 2021; Schunck et al., 2021). Furthermore, through implementation with *deep learning* techniques, it is possible to develop 3D vegetation models and forecast models (Das Choudhury et al., 2019; Kolhar and Jagtap, 2021) useful for various purposes, from crop management planning to predicting future scenarios in natural environments.

Ultimately, phenotyping techniques have great potential as an integrative tool in ecological transition, both for the management of anthropised and non-anthropised areas. Validation of the reliability of information obtained by conventional destructive methods in comparison with data from non-destructive remote surveys becomes essential at this point. The possibility of repeating these measurements over time would also guarantee a monitoring distributed in the long term, to better understand the effect of environmental drivers that act for prolonged periods and the consequent adaptation/acclimatisation strategies developed by plants.

AIM OF THE THESIS

The aim of this work was to study and develop new technologies to support the ecological transition in agro-ecosystems, investigating methodologies that apply at different scale levels.

The main focus was on the development, characterisation and application of eco-compatible nanomaterials with a view to making progress in the field of nano-enabled agriculture. In particular, the objective of the experimental plan principally concerned the use of biodegradable polymers, such as chitosan NPs, as nanocarriers of bioactive molecules for the defence of crops against pathogens. In this context, *RNA-interference* technology was also exploited, using specific dsRNA sequences as functionalising agents for NPs to target the inhibition of post-harvest pathogenic *Botrytis cinerea*. In addition, the potential use of Calcium-Phosphate (CaP) NPs carrying humic acids as nutritional uptake stimulants in leafy crops was also explored.

Furthermore, the field of plant phenotyping was also investigated, as another innovative approach for the management of agro-ecosystems. Two different studies, using imaging techniques at different analytical scales of observation, were performed to develop new methods useful for agro-environmental monitoring.

In the first case, leaf morpho-anatomical traits of four weedy *Amaranthus* species were measured at full- and microscopic scale level to identify their phenotyping variation at juvenile stage, critical for weed competition with crops. Secondly, a remote sensing upscaling approach was also tested in the field of ecosystem monitoring, by measuring plant functional traits linked to submergence and the interplay with soil features on the salt marsh-key species *Salicornia fruticosa* and comparing the results with conventional destructive analyses.

REFERENCES

- Abdel-Aziz, H., Hasaneen, Mohammed Nagib, Omer, A., 2016. Nano chitosan-NPK fertilizer enhances the growth and productivity of wheat plants grown in sandy soil. *Spanish Journal of Agricultural Research* 14, e0902. <https://doi.org/10.5424/sjar/2016141-8205>
- Abou-Zeid, H.M., Ismail, G.S.M., Abdel-Latif, S.A., 2021. Influence of seed priming with ZnO nanoparticles on the salt-induced damages in wheat (*Triticum aestivum* L.) plants. *Journal of Plant Nutrition* 44, 629–643. <https://doi.org/10.1080/01904167.2020.1849288>
- Acharya, A., Pal, P., 2020. Agriculture nanotechnology: Translating research outcome to field applications by influencing environmental sustainability. *NanoImpact* 19, 100232. <https://doi.org/10.1016/j.impact.2020.100232>
- Adams, R.M., Hurd, B.H., Lenhart, S., Leary, N., 1998. Effects of global climate change on agriculture: an interpretative review. *Climate Research* 11, 19–30.
- Altieri, M.A., Nicholls, C.I., 2017. The adaptation and mitigation potential of traditional agriculture in a changing climate. *Climatic Change* 140, 33–45. <https://doi.org/10.1007/s10584-013-0909-y>
- Anderson, A.J., McLean, J.E., Jacobson, A.R., Britt, D.W., 2018. CuO and ZnO Nanoparticles Modify Interkingdom Cell Signaling Processes Relevant to Crop Production. *J. Agric. Food Chem.* 66, 6513–6524. <https://doi.org/10.1021/acs.jafc.7b01302>
- Anwer, M.D.A., 2017. Status of biopesticides and biocontrol agents in agriculture: An overview, in: *Biopesticides and Bioagents*. Apple Academic Press.
- Araus, J.L., Buchailot, M.L., Kefauver, S.C., 2022. High Throughput Field Phenotyping, in: Reynolds, M.P., Braun, H.-J. (Eds.), *Wheat Improvement: Food Security in a Changing Climate*. Springer International Publishing, Cham, pp. 495–512. https://doi.org/10.1007/978-3-030-90673-3_27
- Arbuckle, J.G., Morton, L.W., Hobbs, J., 2015. Understanding Farmer Perspectives on Climate Change Adaptation and Mitigation: The Roles of Trust in Sources of Climate Information, Climate Change Beliefs, and Perceived Risk. *Environment and Behavior* 47, 205–234. <https://doi.org/10.1177/0013916513503832>
- Barzman, M., Bàrberi, P., Birch, A.N.E., Boonekamp, P., Dachbrodt-Saaydeh, S., Graf, B., Hommel, B., Jensen, J.E., Kiss, J., Kudsk, P., Lamichhane, J.R., Messéan, A., Moonen, A.-C., Ratnadass, A., Ricci, P., Sarah, J.-L., Sattin, M., 2015. Eight principles of integrated pest management. *Agron. Sustain. Dev.* 35, 1199–1215. <https://doi.org/10.1007/s13593-015-0327-9>
- Baul, T., Mcdonald, M.A., 2015. Integration of Indigenous knowledge in addressing climate change. *Indian journal of traditional knowledge* 1, 20–27.
- Borges, F., Martienssen, R.A., 2015. The expanding world of small RNAs in plants. *Nat Rev Mol Cell Biol* 16, 727–741. <https://doi.org/10.1038/nrm4085>

- Bragg, Z., Rieske, L.K., 2022. Feasibility of Systemically Applied dsRNAs for Pest-Specific RNAi-Induced Gene Silencing in White Oak. *Front Plant Sci* 13, 830226. <https://doi.org/10.3389/fpls.2022.830226>
- Cai, D., Wu, Z., Jiang, J., Wu, Y., Feng, H., Brown, I.G., Chu, P.K., Yu, Z., 2014. Controlling nitrogen migration through micro-nano networks. *Sci Rep* 4, 3665. <https://doi.org/10.1038/srep03665>
- Cai, Q., Qiao, L., Wang, M., He, B., Lin, F.-M., Palmquist, J., Huang, S.-D., Jin, H., 2018. Plants send small RNAs in extracellular vesicles to fungal pathogen to silence virulence genes. *Science* 360, 1126–1129. <https://doi.org/10.1126/science.aar4142>
- Calvin, K., Dasgupta, D., Krinner, G., Mukherji, A., Thorne, P.W., Trisos, C., Romero, J., Aldunce, P., Barrett, K., Blanco, G., Cheung, W.W.L., Connors, S., Denton, F., Diongue-Niang, A., Dodman, D., Garschagen, M., Geden, O., Hayward, B., Jones, C., Jotzo, F., Krug, T., Lasco, R., Lee, Y.-Y., Masson-Delmotte, V., Meinshausen, M., Mintenbeck, K., Mokssit, A., Otto, F.E.L., Pathak, M., Pirani, A., Poloczanska, E., Pörtner, H.-O., Revi, A., Roberts, D.C., Roy, J., Ruane, A.C., Skea, J., Shukla, P.R., Slade, R., Slangen, A., Sokona, Y., Sörensson, A.A., Tignor, M., Van Vuuren, D., Wei, Y.-M., Winkler, H., Zhai, P., Zommers, Z., Hourcade, J.-C., Johnson, F.X., Pachauri, S., Simpson, N.P., Singh, C., Thomas, A., Totin, E., Arias, P., Bustamante, M., Elgizouli, I., Flato, G., Howden, M., Méndez-Vallejo, C., Pereira, J.J., Pichs-Madruga, R., Rose, S.K., Saheb, Y., Sánchez Rodríguez, R., Ürge-Vorsatz, D., Xiao, C., Yassaa, N., Alegría, A., Armour, K., Bednar-Friedl, B., Blok, K., Cissé, G., Dentener, F., Eriksen, S., Fischer, E., Garner, G., Guivarch, C., Haasnoot, M., Hansen, G., Hauser, M., Hawkins, E., Hermans, T., Kopp, R., Leprince-Ringuet, N., Lewis, J., Ley, D., Ludden, C., Niamir, L., Nicholls, Z., Some, S., Szopa, S., Trewin, B., Van Der Wijst, K.-I., Winter, G., Witting, M., Birt, A., Ha, M., Romero, J., Kim, J., Haites, E.F., Jung, Y., Stavins, R., Birt, A., Ha, M., Orendain, D.J.A., Ignon, L., Park, S., Park, Y., Reisinger, A., Cammaramo, D., Fischlin, A., Fuglestvedt, J.S., Hansen, G., Ludden, C., Masson-Delmotte, V., Matthews, J.B.R., Mintenbeck, K., Pirani, A., Poloczanska, E., Leprince-Ringuet, N., Péan, C., 2023. IPCC, 2023: Climate Change 2023: Synthesis Report. Contribution of Working Groups I, II and III to the Sixth Assessment Report of the Intergovernmental Panel on Climate Change [Core Writing Team, H. Lee and J. Romero (eds.)]. IPCC, Geneva, Switzerland. Intergovernmental Panel on Climate Change (IPCC). <https://doi.org/10.59327/IPCC/AR6-9789291691647>
- Carvalho, L.C., Gonçalves, E.F., Marques da Silva, J., Costa, J.M., 2021. Potential Phenotyping Methodologies to Assess Inter- and Intravarietal Variability and to Select Grapevine Genotypes Tolerant to Abiotic Stress. *Frontiers in Plant Science* 12. <https://doi.org/10.3389/fpls.2021.718202>
- Cătălin Balaure, P., Gudovan, D., Gudovan, I., 2017. 4 - Nanopesticides: a new paradigm in crop protection, in: Grumezescu, A.M. (Ed.), *New Pesticides and Soil Sensors*.

- Academic Press, pp. 129–192. <https://doi.org/10.1016/B978-0-12-804299-1.00005-9>
- Chandrashekar, A., Papadakis, J., Willis, A., Gantert, J., 2018. Structure-From-Motion and RGBD Depth Fusion. pp. 1–8. <https://doi.org/10.1109/SECON.2018.8478927>
- Chhipa, H., 2017. Nanofertilizers and nanopesticides for agriculture. *Environ Chem Lett* 15, 15–22. <https://doi.org/10.1007/s10311-016-0600-4>
- Clapp, J., Ruder, S.-L., 2020. Precision Technologies for Agriculture: Digital Farming, Gene-Edited Crops, and the Politics of Sustainability. *Global Environmental Politics* 20, 49–69. https://doi.org/10.1162/glep_a_00566
- Cota-Arriola, O., Onofre Cortez-Rocha, M., Burgos-Hernández, A., Marina Ezquerra-Brauer, J., Plascencia-Jatomea, M., 2013. Controlled release matrices and micro/nanoparticles of chitosan with antimicrobial potential: development of new strategies for microbial control in agriculture. *Journal of the Science of Food and Agriculture* 93, 1525–1536. <https://doi.org/10.1002/jsfa.6060>
- Dalakouras, A., Jarausach, W., Buchholz, G., Bassler, A., Braun, M., Manthey, T., Krczal, G., Wassenegger, M., 2018. Delivery of Hairpin RNAs and Small RNAs Into Woody and Herbaceous Plants by Trunk Injection and Petiole Absorption. *Front. Plant Sci.* 9, 1253. <https://doi.org/10.3389/fpls.2018.01253>
- Dalakouras, A., Wassenegger, M., Dadami, E., Ganopoulos, I., Pappas, M.L., Papadopoulou, K., 2020. Genetically Modified Organism-Free RNA Interference: Exogenous Application of RNA Molecules in Plants. *Plant Physiol.* 182, 38–50. <https://doi.org/10.1104/pp.19.00570>
- Das Choudhury, S., Samal, A., Awada, T., 2019. Leveraging Image Analysis for High-Throughput Plant Phenotyping. *Frontiers in Plant Science* 10. <https://doi.org/10.3389/fpls.2019.00508>
- Das, S., Debnath, N., Cui, Y., Unrine, J., Palli, S., 2015. Chitosan, Carbon Quantum Dot, and Silica Nanoparticle Mediated dsRNA Delivery for Gene Silencing in *Aedes aegypti*: A Comparative Analysis. *ACS applied materials & interfaces* 7. <https://doi.org/10.1021/acsami.5b05232>
- Dayé, C., Spök, A., Allan, A.C., Yamaguchi, T., Sprink, T., 2023. Social Acceptability of Cisgenic Plants: Public Perception, Consumer Preferences, and Legal Regulation, in: Chaurasia, A., Kole, C. (Eds.), *Cisgenic Crops: Safety, Legal and Social Issues, Concepts and Strategies in Plant Sciences*. Springer International Publishing, Cham, pp. 43–75. https://doi.org/10.1007/978-3-031-10721-4_3
- Demidchik, V.V., Shashko, A.Y., Bandarenka, U.Y., Smolikova, G.N., Przhevalskaya, D.A., Charnysh, M.A., Pozhvanov, G.A., Barkosvkyi, A.V., Smolich, I.I., Sokolik, A.I., Yu, M., Medvedev, S.S., 2020. Plant Phenomics: Fundamental Bases, Software and Hardware Platforms, and Machine Learning. *Russ J Plant Physiol* 67, 397–412. <https://doi.org/10.1134/S1021443720030061>

- Demirer, G.S., Zhang, H., Goh, N.S., Pinals, R.L., Chang, R., Landry, M.P., 2020. Carbon nanocarriers deliver siRNA to intact plant cells for efficient gene knockdown. *Sci. Adv.* 6, eaaz0495. <https://doi.org/10.1126/sciadv.aaz0495>
- Dhandapani, G., Mogilicherla, K., Palli, S., 2020. Chitosan nanoparticles help double-stranded RNA escape from endosomes and improve RNA interference in the fall armyworm, *Spodoptera frugiperda*. *Archives of Insect Biochemistry and Physiology* 104, e21677. <https://doi.org/10.1002/arch.21677>
- Dhondt, S., Wuyts, N., Inzé, D., 2013. Cell to whole-plant phenotyping: the best is yet to come. *Trends Plant Sci* 18, 428–439. <https://doi.org/10.1016/j.tplants.2013.04.008>
- Dubrovina, A.S., Kiselev, K.V., 2019. Exogenous RNAs for Gene Regulation and Plant Resistance. *IJMS* 20, 2282. <https://doi.org/10.3390/ijms20092282>
- Dwivedi, S., Saquib, Q., Al-Khedhairy, A., Musarrat, J., 2016. Understanding the Role of Nanomaterials in Agriculture. pp. 271–288. https://doi.org/10.1007/978-81-322-2644-4_17
- Eichert, T., Goldbach, H.E., 2008. Equivalent pore radii of hydrophilic foliar uptake routes in stomatous and astomatous leaf surfaces – further evidence for a stomatal pathway. *Physiologia Plantarum* 132, 491–502. <https://doi.org/10.1111/j.1399-3054.2007.01023.x>
- Eichert, T., Kurtz, A., Steiner, U., Goldbach, H.E., 2008. Size exclusion limits and lateral heterogeneity of the stomatal foliar uptake pathway for aqueous solutes and water-suspended nanoparticles. *Physiologia Plantarum* 134, 151–160. <https://doi.org/10.1111/j.1399-3054.2008.01135.x>
- Elad, Y., Pertot, I., 2014. Climate Change Impacts on Plant Pathogens and Plant Diseases. *Journal of Crop Improvement* 28, 99–139. <https://doi.org/10.1080/15427528.2014.865412>
- Elmer, W., De La Torre-Roche, R., Pagano, L., Majumdar, S., Zuverza-Mena, N., Dimkpa, C., Gardea-Torresdey, J., White, J.C., 2018. Effect of Metalloid and Metal Oxide Nanoparticles on Fusarium Wilt of Watermelon. *Plant Dis* 102, 1394–1401. <https://doi.org/10.1094/PDIS-10-17-1621-RE>
- Elmer, W.H., White, J.C., 2016. The use of metallic oxide nanoparticles to enhance growth of tomatoes and eggplants in disease infested soil or soilless medium. *Environ. Sci.: Nano* 3, 1072–1079. <https://doi.org/10.1039/C6EN00146G>
- Fincheira, P., Tortella, G., Seabra, A.B., Quiroz, A., Diez, M.C., Rubilar, O., 2021. Nanotechnology advances for sustainable agriculture: current knowledge and prospects in plant growth modulation and nutrition. *Planta* 254, 66. <https://doi.org/10.1007/s00425-021-03714-0>
- Gehan, M.A., Kellogg, E.A., 2017. High-throughput phenotyping. *American Journal of Botany* 104, 505–508. <https://doi.org/10.3732/ajb.1700044>

- Gibbs, J.A., Pound, M., French, A.P., Wells, D.M., Murchie, E., Pridmore, T., 2016. Approaches to three-dimensional reconstruction of plant shoot topology and geometry. *Funct Plant Biol* 44, 62–75. <https://doi.org/10.1071/FP16167>
- Giller, K.E., Andersson, J.A., Corbeels, M., Kirkegaard, J., Mortensen, D., Erenstein, O., Vanlauwe, B., 2015. Beyond conservation agriculture. *Frontiers in Plant Science* 6.
- Giudice, G., Moffa, L., Varotto, S., Cardone, M.F., Bergamini, C., Lorenzis, G.D., Velasco, R., Nerva, L., Chitarra, W., 2021. Novel and emerging biotechnological crop protection approaches. *Plant Biotechnology Journal* n/a. <https://doi.org/10.1111/pbi.13605>
- Gogoi, A., Sarmah, N., Kaldis, A., Perdakis, D., Voloudakis, A., 2017. Plant insects and mites uptake double-stranded RNA upon its exogenous application on tomato leaves. *Planta* 246, 1233–1241. <https://doi.org/10.1007/s00425-017-2776-7>
- Gogos, A., Knauer, K., Bucheli, T.D., 2012. Nanomaterials in Plant Protection and Fertilization: Current State, Foreseen Applications, and Research Priorities. *J. Agric. Food Chem.* 60, 9781–9792. <https://doi.org/10.1021/jf302154y>
- Hayles, J., Johnson, L., Worthley, C., Losic, D., 2017. 5 - Nanopesticides: a review of current research and perspectives, in: Grumezescu, A.M. (Ed.), *New Pesticides and Soil Sensors*. Academic Press, pp. 193–225. <https://doi.org/10.1016/B978-0-12-804299-1.00006-0>
- Hendrickson, J.R., Hanson, J.D., Tanaka, D.L., Sassenrath, G., 2008. Principles of integrated agricultural systems: Introduction to processes and definition. *Renewable Agriculture and Food Systems* 23, 265–271. <https://doi.org/10.1017/S1742170507001718>
- Hess, F.D., 1993. *Herbicide Effects on Plant Structure, Physiology, and Biochemistry, in: Pesticide Interactions in Crop Production*. CRC Press.
- Hu, P., An, J., Faulkner, M.M., Wu, H., Li, Z., Tian, X., Giraldo, J.P., 2020. Nanoparticle Charge and Size Control Foliar Delivery Efficiency to Plant Cells and Organelles. *ACS Nano* 14, 7970–7986. <https://doi.org/10.1021/acsnano.9b09178>
- Jiang, M., Song, Y., Kanwar, M.K., Ahammed, G.J., Shao, S., Zhou, J., 2021. Phytonanotechnology applications in modern agriculture. *Journal of Nanobiotechnology* 19, 430. <https://doi.org/10.1186/s12951-021-01176-w>
- Jindo, K., Canellas, L.P., Albacete, A., Figueiredo dos Santos, L., Frinhani Rocha, R.L., Carvalho Baia, D., Oliveira Aguiar Canellas, N., Goron, T.L., Olivares, F.L., 2020. Interaction between Humic Substances and Plant Hormones for Phosphorous Acquisition. *Agronomy* 10, 640. <https://doi.org/10.3390/agronomy10050640>
- Kah, M., Hofmann, T., 2014. Nanopesticide research: Current trends and future priorities. *Environment International* 63, 224–235. <https://doi.org/10.1016/j.envint.2013.11.015>

- Kahrl, F., Li, Y., Su, Y., Tennigkeit, T., Wilkes, A., Xu, J., 2010. Greenhouse gas emissions from nitrogen fertilizer use in China. *Environmental Science & Policy* 13, 688–694. <https://doi.org/10.1016/j.envsci.2010.07.006>
- Kaldis, A., Berbati, M., Melita, O., Reppa, C., Holeva, M., Otten, P., Voloudakis, A., 2018. Exogenously applied dsRNA molecules deriving from the Zucchini yellow mosaic virus (ZYMV) genome move systemically and protect cucurbits against ZYMV. *Molecular Plant Pathology* 19, 883–895. <https://doi.org/10.1111/mpp.12572>
- Ke, M., Li, Y., Qu, Q., Ye, Y., Peijnenburg, W.J.G.M., Zhang, Z., Xu, N., Lu, T., Sun, L., Qian, H., 2020. Offspring toxicity of silver nanoparticles to *Arabidopsis thaliana* flowering and floral development. *J Hazard Mater* 386, 121975. <https://doi.org/10.1016/j.jhazmat.2019.121975>
- Khan, S.T., Ahmad, J., Ahamed, M., Jousset, A., 2018. Sub-lethal doses of widespread nanoparticles promote antifungal activity in *Pseudomonas protegens* CHA0. *Sci Total Environ* 627, 658–662. <https://doi.org/10.1016/j.scitotenv.2018.01.257>
- Khandelwal, N., Barbole, R.S., Banerjee, S.S., Chate, G.P., Biradar, A.V., Khandare, J.J., Giri, A.P., 2016. Budding trends in integrated pest management using advanced micro- and nano-materials: Challenges and perspectives. *Journal of Environmental Management* 184, 157–169. <https://doi.org/10.1016/j.jenvman.2016.09.071>
- Kim, D.-Y., Kadam, A., Shinde, S., Saratale, R.G., Patra, J., Ghodake, G., 2018. Recent developments in nanotechnology transforming the agricultural sector: a transition replete with opportunities. *Journal of the Science of Food and Agriculture* 98, 849–864. <https://doi.org/10.1002/jsfa.8749>
- Koch, A., Biedenkopf, D., Furch, A., Weber, L., Roszbach, O., Abdellatef, E., Linicus, L., Johannsmeier, J., Jelonek, L., Goesmann, A., Cardoza, V., McMillan, J., Mentzel, T., Kogel, K.-H., 2016. An RNAi-Based Control of *Fusarium graminearum* Infections Through Spraying of Long dsRNAs Involves a Plant Passage and Is Controlled by the Fungal Silencing Machinery. *PLoS Pathog* 12, e1005901. <https://doi.org/10.1371/journal.ppat.1005901>
- Kolhar, S., Jagtap, J., 2021. Plant trait estimation and classification studies in plant phenotyping using machine vision – A review. *Information Processing in Agriculture* S2214317321000238. <https://doi.org/10.1016/j.inpa.2021.02.006>
- Korres, N.E., Norsworthy, J.K., Tehranchian, P., Gitsopoulos, T.K., Loka, D.A., Oosterhuis, D.M., Gealy, D.R., Moss, S.R., Burgos, N.R., Miller, M.R., Palhano, M., 2016. Cultivars to face climate change effects on crops and weeds: a review. *Agron. Sustain. Dev.* 36, 12. <https://doi.org/10.1007/s13593-016-0350-5>
- Kothari, S., Schweiger, A.K., 2022. Plant spectra as integrative measures of plant phenotypes. *Journal of Ecology* 110, 2536–2554. <https://doi.org/10.1111/1365-2745.13972>

- Langstroff, A., Heuermann, M.C., Stahl, A., Junker, A., 2022. Opportunities and limits of controlled-environment plant phenotyping for climate response traits. *Theor Appl Genet* 135, 1–16. <https://doi.org/10.1007/s00122-021-03892-1>
- Li, L., Zhang, Q., Huang, D., 2014. A Review of Imaging Techniques for Plant Phenotyping. *Sensors* 14, 20078–20111. <https://doi.org/10.3390/s141120078>
- Li, Y., Liang, L., Li, W., Ashraf, U., Ma, L., Tang, X., Pan, S., Tian, H., Mo, Z., 2021. ZnO nanoparticle-based seed priming modulates early growth and enhances physio-biochemical and metabolic profiles of fragrant rice against cadmium toxicity. *Journal of Nanobiotechnology* 19, 75. <https://doi.org/10.1186/s12951-021-00820-9>
- Li, Y., Xi, K., Liu, X., Han, S., Han, X., Li, G., Yang, L., Ma, D., Fang, Z., Gong, S., Yin, J., Zhu, Y., 2023. Silica nanoparticles promote wheat growth by mediating hormones and sugar metabolism. *J Nanobiotechnology* 21, 2. <https://doi.org/10.1186/s12951-022-01753-7>
- Lipper, L., Thornton, P., Campbell, B.M., Baedeker, T., Braimoh, A., Bwalya, M., Caron, P., Cattaneo, A., Garrity, D., Henry, K., Hottle, R., Jackson, L., Jarvis, A., Kossam, F., Mann, W., 2014. Climate-smart agriculture for food security. *Nature Climate Change* 4, 1068–1072. <https://doi.org/10.1038/nclimate2437>
- Liu, H., Bruning, B., Garnett, T., Berger, B., 2020. Hyperspectral imaging and 3D technologies for plant phenotyping: From satellite to close-range sensing. *Computers and Electronics in Agriculture* 175, 105621. <https://doi.org/10.1016/j.compag.2020.105621>
- Long, S.P., Ainsworth, E.A., Leakey, A.D.B., Nösberger, J., Ort, D.R., 2006. Food for Thought: Lower-than-Expected Crop Yield Stimulation with Rising CO₂ Concentrations. *Science* 312, 1918–1921.
- Ma, C., White, J.C., Zhao, J., Zhao, Q., Xing, B., 2018. Uptake of Engineered Nanoparticles by Food Crops: Characterization, Mechanisms, and Implications. *Annu Rev Food Sci Technol* 9, 129–153. <https://doi.org/10.1146/annurev-food-030117-012657>
- Ma, X., Wiedmer, J., Palma-Guerrero, J., 2020. Small RNA Bidirectional Crosstalk During the Interaction Between Wheat and *Zymoseptoria tritici*. *Frontiers in Plant Science* 10.
- Malandrakis, A.A., Kavroulakis, N., Chrysikopoulos, C.V., 2019. Use of copper, silver and zinc nanoparticles against foliar and soil-borne plant pathogens. *Science of The Total Environment* 670, 292–299. <https://doi.org/10.1016/j.scitotenv.2019.03.210>
- Malerba, M., Cerana, R., 2016. Chitosan Effects on Plant Systems. *Int J Mol Sci* 17. <https://doi.org/10.3390/ijms17070996>
- Malhi, G., Rana, M.C., Rana, S., Kaushik, P., 2020. EFFECT OF INDIVIDUAL OR COMBINED APPLICATION OF HERBICIDE IMAZETHAPYR ON NUTRIENT UPTAKE BY BLACKGRAM (*Vigna mungo* L.). *Journal of Experimental Biology and Agricultural Sciences* 8, 441–446. [https://doi.org/10.18006/2020.8\(4\).441.446](https://doi.org/10.18006/2020.8(4).441.446)

- Malhi, G.S., Kaur, M., Kaushik, P., 2021a. Impact of Climate Change on Agriculture and Its Mitigation Strategies: A Review. *Sustainability* 13, 1318. <https://doi.org/10.3390/su13031318>
- Malhi, G.S., Kaur, M., Kaushik, P., Alyemeni, M.N., Alsahli, A.A., Ahmad, P., 2021b. Arbuscular mycorrhiza in combating abiotic stresses in vegetables: An eco-friendly approach. *Saudi J Biol Sci* 28, 1465–1476. <https://doi.org/10.1016/j.sjbs.2020.12.001>
- Maluin, F.N., Hussein, M.Z., 2020. Chitosan-Based Agronanochemicals as a Sustainable Alternative in Crop Protection. *Molecules* 25, 1611. <https://doi.org/10.3390/molecules25071611>
- Matzrafi, M., 2019. Climate change exacerbates pest damage through reduced pesticide efficacy. *Pest Management Science* 75, 9–13. <https://doi.org/10.1002/ps.5121>
- McLoughlin, A.G., Wytinck, N., Walker, P.L., Girard, I.J., Rashid, K.Y., de Kievit, T., Fernando, W.G.D., Whyard, S., Belmonte, M.F., 2018. Identification and application of exogenous dsRNA confers plant protection against *Sclerotinia sclerotiorum* and *Botrytis cinerea*. *Sci Rep* 8, 7320. <https://doi.org/10.1038/s41598-018-25434-4>
- Mendelsohn, R., 2008. The Impact of Climate Change on Agriculture in Developing Countries. *Journal of Natural Resources Policy Research* 1, 5–19. <https://doi.org/10.1080/19390450802495882>
- Mermigka, G., Verret, F., Kalantidis, K., 2016. RNA silencing movement in plants. *J Integr Plant Biol* 58, 328–342. <https://doi.org/10.1111/jipb.12423>
- Mitter, N., Worrall, E., Robinson, K., Li, P., Jain, R., Taochy, C., Fletcher, S., Carroll, B., Lu, G., Xu, Z., 2017a. Clay nanosheets for topical delivery of RNAi for sustained protection against plant viruses. *Nature Plants* 3, 16207. <https://doi.org/10.1038/nplants.2016.207>
- Mitter, N., Worrall, E., Robinson, K., Xu, Z., Carroll, B., 2017b. Induction of virus resistance by exogenous application of double-stranded RNA. *Current Opinion in Virology* 26, 49–55. <https://doi.org/10.1016/j.coviro.2017.07.009>
- Monreal, C., Derosa, M., Mallubhotla, S., Bindraban, P.S., Dimkpa, C., 2016. Nanotechnologies for Increasing the Crop Use Efficiency of Fertilizer-Micronutrients. *Biology and Fertility of Soils* 52. <https://doi.org/10.1007/s00374-015-1073-5>
- Montzka, S.A., Dlugokencky, E.J., Butler, J.H., 2011. Non-CO₂ greenhouse gases and climate change. *Nature* 476, 43–50. <https://doi.org/10.1038/nature10322>
- Nair, R., 2016. Effects of Nanoparticles on Plant Growth and Development, in: Kole, C., Kumar, D.S., Khodakovskaya, M.V. (Eds.), *Plant Nanotechnology: Principles and Practices*. Springer International Publishing, Cham, pp. 95–118. https://doi.org/10.1007/978-3-319-42154-4_5


- Nerva, L., Sandrini, M., Gambino, G., Chitarra, W., 2020. Double-Stranded RNAs (dsRNAs) as a Sustainable Tool against Gray Mold (*Botrytis cinerea*) in Grapevine: Effectiveness of Different Application Methods in an Open-Air Environment. *Biomolecules* 10, 200. <https://doi.org/10.3390/biom10020200>
- Nilon, A., Robinson, K., Pappu, H.R., Mitter, N., 2021. Current Status and Potential of RNA Interference for the Management of Tomato Spotted Wilt Virus and Thrips Vectors. *Pathogens* 10, 320. <https://doi.org/10.3390/pathogens10030320>
- Nuruzzaman, M., Rahman, M.M., Liu, Y., Naidu, R., 2016. Nanoencapsulation, Nano-guard for Pesticides: A New Window for Safe Application. *J Agric Food Chem* 64, 1447–1483. <https://doi.org/10.1021/acs.jafc.5b05214>
- O'Mara, F.P., 2011. The significance of livestock as a contributor to global greenhouse gas emissions today and in the near future. *Animal Feed Science and Technology, Special Issue: Greenhouse Gases in Animal Agriculture - Finding a Balance between Food and Emissions* 166–167, 7–15. <https://doi.org/10.1016/j.anifeedsci.2011.04.074>
- Panichikkal, J., Thomas, R., John, J.C., Radhakrishnan, E.K., 2019. Biogenic Gold Nanoparticle Supplementation to Plant Beneficial *Pseudomonas monteilii* was Found to Enhance its Plant Probiotic Effect. *Curr Microbiol* 76, 503–509. <https://doi.org/10.1007/s00284-019-01649-0>
- Parisi, C., Vigani, M., Rodríguez-Cerezo, E., 2015. Agricultural Nanotechnologies: What are the current possibilities? *Nano Today* 10, 124–127. <https://doi.org/10.1016/j.nantod.2014.09.009>
- Paz-Ares, J., Puga, M.I., Rojas-Triana, M., Martínez-Hevia, I., Díaz, S., Poza-Carrión, C., Miñambres, M., Leyva, A., 2022. Plant adaptation to low phosphorus availability: Core signaling, crosstalks, and applied implications. *Molecular Plant* 15, 104–124. <https://doi.org/10.1016/j.molp.2021.12.005>
- Pieruschka, R., Poorter, H., 2012. Phenotyping plants: genes, phenes and machines. *Funct Plant Biol* 39, 813–820. https://doi.org/10.1071/FPv39n11_IN
- Pieruschka, R., Schurr, U., 2019. Plant Phenotyping: Past, Present, and Future. *Plant Phenomics* 2019, 1–6. <https://doi.org/10.34133/2019/7507131>
- Popp, A., Lotze-Campen, H., Bodirsky, B., 2010. Food consumption, diet shifts and associated non-CO2 greenhouse gases from agricultural production. *Global Environmental Change, Governance, Complexity and Resilience* 20, 451–462. <https://doi.org/10.1016/j.gloenvcha.2010.02.001>
- Popp, C., Burghardt, M., Friedmann, A., Riederer, M., 2005. Characterization of hydrophilic and lipophilic pathways of *Hedera helix* L. cuticular membranes: permeation of water and uncharged organic compounds. *J Exp Bot* 56, 2797–2806. <https://doi.org/10.1093/jxb/eri272>
- Pradhan, B., Deo, B., 2019. Soilless farming – the next generation green revolution. *Current Science* 116, 728–732.

- Rathore, I., Tarafdar, J.C., 2015. Perspectives of Biosynthesized Magnesium Nanoparticles in Foliar Application of Wheat Plant. *Journal of Bionanoscience* 9, 209–214. <https://doi.org/10.1166/jbns.2015.1296>
- Reddy, P., 2013. Impact of climate change on insect pests, pathogens and nematodes. *Pest Management in Horticultural Ecosystems*.
- Rodrigues, S.M., Demokritou, P., Dokoozlian, N., Hendren, C.O., Karn, B., Mauter, M.S., Sadik, O.A., Safarpour, M., Unrine, J.M., Viers, J., Welle, P., White, J.C., Wiesner, M.R., Lowry, G.V., 2017. Nanotechnology for sustainable food production: promising opportunities and scientific challenges. *Environ. Sci.: Nano* 4, 767–781. <https://doi.org/10.1039/C6EN00573J>
- Rosa, C., Kuo, Y.-W., Wuriyanghan, H., Falk, B.W., 2018. RNA Interference Mechanisms and Applications in Plant Pathology. *Annual Review of Phytopathology* 56, 581–610. <https://doi.org/10.1146/annurev-phyto-080417-050044>
- Rosenzweig, C., Iglesias, A., Yang, X.B., Epstein, P.R., Chivian, E., 2001. Climate Change and Extreme Weather Events; Implications for Food Production, Plant Diseases, and Pests. *Global Change & Human Health* 2, 90–104. <https://doi.org/10.1023/A:1015086831467>
- Rossi, L., Fedenia, L.N., Sharifan, H., Ma, X., Lombardini, L., 2019. Effects of foliar application of zinc sulfate and zinc nanoparticles in coffee (*Coffea arabica* L.) plants. *Plant Physiol Biochem* 135, 160–166. <https://doi.org/10.1016/j.plaphy.2018.12.005>
- Satapanajaru, T., Anurakpongsatorn, P., Pengthamkeerati, P., Boparai, H., 2008. Remediation of Atrazine-contaminated Soil and Water by Nano Zerovalent Iron. *Water Air Soil Pollut* 192, 349–359. <https://doi.org/10.1007/s11270-008-9661-8>
- Schunck, D., Magistri, F., Rosu, R.A., Cornelißen, A., Chebrolu, N., Paulus, S., Léon, J., Behnke, S., Stachniss, C., Kuhlmann, H., Klingbeil, L., 2021. Pheno4D: A spatio-temporal dataset of maize and tomato plant point clouds for phenotyping and advanced plant analysis. *PLOS ONE* 16, e0256340. <https://doi.org/10.1371/journal.pone.0256340>
- Shahrekizad, M., Gholamalizadeh Ahangar, A., Mir, N., 2015. EDTA-Coated Fe₃O₄ Nanoparticles: a Novel Biocompatible Fertilizer for Improving Agronomic Traits of Sunflower (*Helianthus Annuus*). *Journal of Nanostructures* 5, 117–127. <https://doi.org/10.7508/jns.2015.02.006>
- Shalaby, T., Bayoumi, Y., Abdalla, N., Taha, H., Alshaal, T., El-Ramady, H., Shehata, S., Amer, M., domokos-szabolcsy, E., 2016. Nanoparticles, Soils, Plants and Sustainable Agriculture. https://doi.org/10.1007/978-3-319-39303-2_10
- Shenashen, M., Derbalah, A., Hamza, A., Mohamed, A., El Safty, S., 2017. Antifungal activity of fabricated mesoporous alumina nanoparticles against root rot disease of tomato caused by *Fusarium oxysporium*. *Pest Manag Sci* 73, 1121–1126. <https://doi.org/10.1002/ps.4420>

- Shrestha, S., 2019. Effects of Climate Change in Agricultural Insect Pest. *Acta Scientific Agriculture* 3, 74–80. <https://doi.org/10.31080/ASAG.2019.03.0727>
- Singh, A., Gautam, V., Singh, S., Sarkar Das, S., Verma, S., Mishra, V., Mukherjee, S., Sarkar, A.K., 2018. Plant small RNAs: advancement in the understanding of biogenesis and role in plant development. *Planta* 248, 545–558. <https://doi.org/10.1007/s00425-018-2927-5>
- Solomon, S., Intergovernmental Panel on Climate Change, Intergovernmental Panel on Climate Change (Eds.), 2007. *Climate change 2007: the physical science basis: contribution of Working Group I to the Fourth Assessment Report of the Intergovernmental Panel on Climate Change*. Cambridge University Press, Cambridge; New York.
- Soltani, A., Rajabi, M.H., Zeinali, E., Soltani, E., 2013. Energy inputs and greenhouse gases emissions in wheat production in Gorgan, Iran. *Energy* 50, 54–61. <https://doi.org/10.1016/j.energy.2012.12.022>
- Song, X.-S., Gu, K.-X., Duan, X.-X., Xiao, X.-M., Hou, Y.-P., Duan, Y.-B., Wang, J.-X., Zhou, M.-G., 2018. A myosin5 dsRNA that reduces the fungicide resistance and pathogenicity of *Fusarium asiaticum*. *Pestic Biochem Physiol* 150, 1–9. <https://doi.org/10.1016/j.pestbp.2018.07.004>
- Stasińska-Jakubas, M., Hawrylak-Nowak, B., 2022. Protective, Biostimulating, and Eliciting Effects of Chitosan and Its Derivatives on Crop Plants. *Molecules* 27, 2801. <https://doi.org/10.3390/molecules27092801>
- Su, Y., Ashworth, V., Kim, C., Adeleye, A.S., Rolshausen, P., Roper, C., White, J., Jassby, D., 2019. Delivery, uptake, fate, and transport of engineered nanoparticles in plants: a critical review and data analysis. *Environ. Sci.: Nano* 6, 2311–2331. <https://doi.org/10.1039/C9EN00461K>
- Taliansky, M., Samarskaya, V., Zavriev, S.K., Fesenko, I., Kalinina, N.O., Love, A.J., 2021. RNA-Based Technologies for Engineering Plant Virus Resistance. *Plants* 10, 82. <https://doi.org/10.3390/plants10010082>
- Uiterkamp, A.J.M.S., Vlek, C., 2007. Practice and Outcomes of Multidisciplinary Research for Environmental Sustainability. *Journal of Social Issues* 63, 175–197. <https://doi.org/10.1111/j.1540-4560.2007.00502.x>
- Ul Haq, I., Ijaz, S., 2019. Use of Metallic Nanoparticles and Nanoformulations as Nanofungicides for Sustainable Disease Management in Plants, in: Prasad, R., Kumar, V., Kumar, M., Choudhary, D. (Eds.), *Nanobiotechnology in Bioformulations, Nanotechnology in the Life Sciences*. Springer International Publishing, Cham, pp. 289–316. https://doi.org/10.1007/978-3-030-17061-5_12
- Ustin, S.L., Jacquemoud, S., 2020. How the Optical Properties of Leaves Modify the Absorption and Scattering of Energy and Enhance Leaf Functionality, in: Cavender-Bares, J., Gamon, J.A., Townsend, P.A. (Eds.), *Remote Sensing of Plant Biodiversity*. Springer International Publishing, Cham, pp. 349–384. https://doi.org/10.1007/978-3-030-33157-3_14

- Varanasi, A., Prasad, P.V.V., Jugulam, M., 2016. Chapter Three - Impact of Climate Change Factors on Weeds and Herbicide Efficacy, in: Sparks, D.L. (Ed.), *Advances in Agronomy*, *Advances in Agronomy*. Academic Press, pp. 107–146. <https://doi.org/10.1016/bs.agron.2015.09.002>
- Venkateswarlu, B., Shanker, A., 2009. Climate change and agriculture: Adaptation and mitigation strategies. *Indian Journal of Agronomy* 54.
- Volpato, L., Pinto, F., González-Pérez, L., Thompson, I.G., Borém, A., Reynolds, M., Gérard, B., Molero, G., Rodrigues, F.A., 2021. High Throughput Field Phenotyping for Plant Height Using UAV-Based RGB Imagery in Wheat Breeding Lines: Feasibility and Validation. *Frontiers in Plant Science* 12.
- Walter, A., Liebisch, F., Hund, A., 2015. Plant phenotyping: from bean weighing to image analysis. *Plant Methods* 11, 14. <https://doi.org/10.1186/s13007-015-0056-8>
- Wang, P., Lombi, E., Zhao, F.-J., Kopittke, P.M., 2016. Nanotechnology: A New Opportunity in Plant Sciences. *Trends in Plant Science* 21, 699–712. <https://doi.org/10.1016/j.tplants.2016.04.005>
- Wang, W., Yuan, J., Jiang, C., 2021. Applications of nanobodies in plant science and biotechnology. *Plant Mol Biol* 105, 43–53. <https://doi.org/10.1007/s11103-020-01082-z>
- Wang, Z., Yue, L., Dhankher, O.P., Xing, B., 2020. Nano-enabled improvements of growth and nutritional quality in food plants driven by rhizosphere processes. *Environ Int* 142, 105831. <https://doi.org/10.1016/j.envint.2020.105831>
- Worrall, E.A., Hamid, A., Mody, K.T., Mitter, N., Pappu, H.R., 2018. Nanotechnology for Plant Disease Management. *Agronomy* 8, 285. <https://doi.org/10.3390/agronomy8120285>
- Xie, C., Yang, C., 2020. A review on plant high-throughput phenotyping traits using UAV-based sensors. *Computers and Electronics in Agriculture* 178, 105731. <https://doi.org/10.1016/j.compag.2020.105731>
- Xu, R., Li, C., 2022. A Review of High-Throughput Field Phenotyping Systems: Focusing on Ground Robots. *Plant Phenomics* 2022, 1–20. <https://doi.org/10.34133/2022/9760269>
- Xu, X., Jiao, Y., Shen, L., Li, Y., Mei, Y., Yang, W., Li, C., Cao, Y., Chen, F., Li, B., Yang, J., 2023. Nanoparticle-dsRNA Treatment of Pollen and Root Systems of Diseased Plants Effectively Reduces the Rate of Tobacco Mosaic Virus in Contemporary Seeds. *ACS Appl. Mater. Interfaces* 15, 29052–29063. <https://doi.org/10.1021/acsami.3c02798>
- Yakhin, O.I., Lubyantsev, A.A., Yakhin, I.A., Brown, P.H., 2017. Biostimulants in Plant Science: A Global Perspective. *Frontiers in Plant Science* 7.
- Yong, J., Zhang, R., Bi, S., Li, P., Sun, L., Mitter, N., Carroll, B.J., Xu, Z.P., 2021. Sheet-like clay nanoparticles deliver RNA into developing pollen to efficiently silence a

- target gene. *Plant Physiology* 187, 886–899. <https://doi.org/10.1093/plphys/kiab303>
- Yu, M., Yao, J., Liang, J., Zeng, Z., Cui, B., Zhao, X., Sun, C., Wang, Y., Liu, G., Cui, H., 2017. Development of functionalized abamectin poly(lactic acid) nanoparticles with regulatable adhesion to enhance foliar retention. *RSC Adv.* 7, 11271–11280. <https://doi.org/10.1039/C6RA27345A>
- Ze, Y., Liu, C., Wang, L., Hong, M., Hong, F., 2011. The regulation of TiO₂ nanoparticles on the expression of light-harvesting complex II and photosynthesis of chloroplasts of *Arabidopsis thaliana*. *Biol Trace Elem Res* 143, 1131–1141. <https://doi.org/10.1007/s12011-010-8901-0>
- Zhang, H., Cao, Y., Xu, D., Goh, N.S., Demirer, G.S., Cestellos-Blanco, S., Chen, Y., Landry, M.P., Yang, P., 2021a. Gold-Nanocluster-Mediated Delivery of siRNA to Intact Plant Cells for Efficient Gene Knockdown. *Nano Lett.* 21, 5859–5866. <https://doi.org/10.1021/acs.nanolett.1c01792>
- Zhang, H., Goh, N.S., Wang, J., Demirer, G.S., Butrus, S., Park, S.-J., Landry, M.P., 2021b. Nanoparticle Cellular Internalization is Not Required for RNA Delivery to Mature Plant Leaves. <https://doi.org/10.1101/2021.03.17.435888>
- Zhang, X., Zhang, J., Zhu, Y.-K., 2010. Chitosan/double-stranded RNA nanoparticle-mediated RNA interference to silence chitin synthase genes through larval feeding in the African malaria mosquito (*Anopheles gambiae*). *Insect molecular biology* 19, 683–93. <https://doi.org/10.1111/j.1365-2583.2010.01029.x>
- Zilberman, D., Liu, X., Roland-Holst, D., Sunding, D., 2004. The economics of climate change in agriculture. *Mitigation and Adaptation Strategies for Global Change* 9, 365–382. <https://doi.org/10.1023/B:MITI.0000038844.72226.13>



CHAPTER 2 - Characterization and functionalization of chitosan nanoparticles as carriers for double stranded RNA (dsRNA) molecules towards sustainable crop protection

Original Paper

First published: 10 november 2023

Bioscience Reports, BSR-2023-0817, Portland Press

DOI: 10.1042/BSR20230817

Characterization and functionalization of chitosan nanoparticles as carriers for double stranded RNA (dsRNA) molecules towards sustainable crop protection

Dora Scarpin¹, Luca Nerva², Walter Chitarra², Loredana Moffa², Francesca D'Este³, Marco Vuerich¹, Antonio Filippi³, Enrico Braidot¹, Elisa Petrusa¹

¹ Department of Agriculture, Food, Environment and Animal Sciences (DI4A), University of Udine, Via delle Scienze 206, 33100 Udine, Italy.

² Research Centre for Viticulture and Enology, Council for Agricultural Research and Economics (CREA-VE), Via XXVIII Aprile 26, 31015 Conegliano (TV), Italy.

³ Department of Medicine (DAME), University of Udine, P.le Kolbe 4, 33100 Udine, Italy.

Correspondence: enrico.braidot@uniud.it. Tel.: +39 0432558792

Keywords: Chitosan nanoparticles; dsRNAs; nanomaterial functionalization; smart delivery; RNA-interference; *Botrytis cinerea*; nanoparticle/tegument interaction.

Abbreviations

DLS: Dynamic Light Scattering

GFP dsRNA: Green Fluorescent Protein double-stranded RNA

EIA: Ethoxylated isodecyl alcohol

FITC: Fluorescein-5-isothiocyanate

NPs: Nanoparticles

NPsD: Nanoparticles from degradation treatment

NPsF: Nanoparticles from filtration treatment

RNAi: RNA interference

TEM: Transmission electron microscopy

ABSTRACT

The need to minimise the impact of phytosanitary treatments for disease control boosted researchers to implement techniques with less environmental impact. The development of technologies using molecular mechanisms based on the modulation of metabolism by short dsRNA sequences appears promising. The intrinsic fragility of polynucleotides and the high cost of these techniques can be circumvented by nanocarriers that protect the bioactive molecule enabling high efficiency delivery to the leaf surface and extending its half-life.

In this work, a specific protocol was developed aiming to assess the best methodological conditions for the synthesis of low-size chitosan nanoparticles (NPs) to be loaded with nucleotides. In particular, NPs have been functionalised with partially purified Green Fluorescent Protein dsRNAs (*GFP* dsRNA) and their size, surface charge and nucleotide retention capacity were analysed. Final NPs were also stained with FITC and sprayed on *Nicotiana benthamiana* leaves to assess, by confocal microscopy, both a distribution protocol and the fate of NPs up to 6 days after application.

Finally, to confirm the ability of NPs to increase the efficacy of dsRNA interference, specific tests were performed: by means of *GFP* dsRNA-functionalized NPs, the nucleotide permanence during time was assessed both *in vitro* on detached wild-type *N. benthamiana* leaves and *in planta*; lastly, the inhibition of *Botrytis cinerea* on single leaves was also evaluated, using a specific fungal sequence (*Bc* dsRNA) as the NPs' functionalizing agent.

The encouraging results obtained are promising in the perspective of long-lasting application of innovative treatments based on gene silencing.

INTRODUCTION

Within a very short time, the farming system is claimed to respond to several challenges in facing the predicted worldwide increase in food demand by 2050 (1). A more sustainable agriculture, such as endorsed by the EU Commission for the Farm-to-Fork program, imposes a drastic reduction in chemical pesticides and fertilizers. Indeed, it calls for development and adoption of safer alternatives, respectful for the agro-ecosystems and the environment, with low-risk for human health (2).

During recent years, research and agriculture efforts have been largely devoted to improve the use of smart technologies and tools, such as naturally derived biostimulants, able to sustain high crop productivity with a low impact on the environment, improve plant nutrient use efficiency (NUE) (3) (4) and abiotic stress tolerance (5) or boost the innate plant resistance to pathogens (6). Among these bio-based compounds, bulk chitin and chitosan, its N-deacetylated derivative, have been gaining large interest. Due to the presence of their reactive amine and hydroxyl groups, they exert multiple bioactivities in a wide range of applications in crop protection, as well as in biotechnological and biomedical fields, cosmetics, and in food quality preservation (6–8).

Differently from chitin, chitosan application is not limited by a low solubility (9), since it is easily dissolved in water under acidic solution, while it represents a safe, non-toxic, biocompatible and highly renewable bio-compound from fish production waste (10,11). Bulk chitosan has been demonstrated to display several antimicrobial and antioxidant properties against pathogenic microorganisms when applied to different crops (6,12), as well as to act as bioelicitor of natural plant immunity (13). Furthermore, the reactive functional groups present in chitosan confer elevated biodegradability, high adsorption and gel-forming capacity (11,14), high facility in chemical cross-linking and chelation, entrapment and delivery of functional compounds and negatively charged biologically active macromolecules such as nucleotides and proteins (15). As an alternative approach in integrated crop protection, innovative chitosan-based delivery systems and agro-nanochemicals have been recently developed (6,16,17). Indeed, the encapsulation of pesticides and antimicrobial or active compounds in chitosan-formulated nanostructures offers several advantages, such as enhanced precise delivery into the target plant tissues, elevated bioavailability, stability and, in turn, a limitation in run-off of toxic compounds into the environment. Several chitosan nanoformulations, carrying conventional or systemic pesticides, bioactive plant-based extracts, DNA and Cu or Ag metals, have been used in recent years, demonstrating to be very effective systems for their uptake, translocation and delivery in a wide range of crop plants (17).

The very latest alternative to conventional agrochemicals in the research of chitosan-based nanotechnology is extended to the development of nanocarriers for genetically modified (GM)-free RNA interference (RNAi) technology. This is a conserved mechanism able to recognize endogenous as well as exogenous double-stranded RNA

sequences (dsRNAs) and process them to smaller RNA molecules known as small interfering RNA (siRNAs) that lead to the degradation of homologous RNAs. Recent studies highlighted that RNAi is a natural protection strategy able to elicit plant defence responses against pathogens through post-transcriptional gene regulation (18–21). Indeed, it has been already proven that induction of RNAi can be useful for pathogens control, such as viral, fungal, insect and nematode diseases (22–25). Furthermore, the use of exogenously applied dsRNAs can be exploited to regulate plant endogenous genes to functionally characterize them or to impair fungal pathogens (26–28). However, efficiency of exogenous naked dsRNAs applications can be limited by their low persistence in the environment (*e.g.*, because of light, UV and thermal degradation) (29,30) and ability to overcome the physical barriers of the leaf surface (31). Moreover, RNAs could be sequestered (32) or degraded within the plant cell (29).

In this regard, chitosan nanoparticle (NP) formulations, in addition to other efficient nano-assisted systems such as carbon structures, gold nanoclusters and DNA nanocarriers (33), could represent very promising tools for improving dsRNA delivery and stability, and overall response in RNAi-based crop protection strategies.

The study of the combination of these two strategies has recently been carried out by Xu and co-workers (34). In this work, the effect of Chitosan quaternary ammonium salt (HACC) nanoparticles complexed with dsRNAs targeting Tobacco Mosaic Virus (TMV) inhibitory sequences has been investigated. The HACC-dsRNA complex was characterised and its fate studied by means of fluorescent probes. Four different modes of delivery were tested *in planta*, observing that all of them were able to reduce the incidence of TMV infection.

In the present work, we trace some of the analyses carried out in the aforementioned research, concentrating, however: (a) on identifying the best method for NPs synthesis; (b) in defining the best formulation for foliar application also through NPs fluorescent labelling; (c) in the use of a single delivery mode (spray distribution), the most suitable for combating the target pathogen *Botrytis cinerea*. We firstly characterize different chitosan NP preparations by size and ζ -potential and we investigate their ability to be functionalized with nucleotide sequences as naked dsRNAs (*GFP* dsRNAs). Furthermore, the permanence of *GFP* dsRNA-NPs topically applied on wild-type *Nicotiana benthamiana* leaves is evaluated both in detached leaves under UV light treatment and in plants grown in controlled environment. To confirm the effectiveness also on pathogen defence, NPs conveying specific fungal sequences (*Bc* dsRNA) are subsequently employed for the growth inhibition of *B. cinerea* mycelium.

Finally, we perform confocal imaging of FITC-labelled chitosan nanostructures to track and visualize their adhesion and distribution on foliar surface of *N. benthamiana* and to assess their absorption up to 6 days after treatment.

RESULTS

In the present work, the application of the synthesis protocol of NPs by ionic gelation (35) aimed to improve the synthesis of functionalizable chitosan nanomaterials. Such products need to be as small as possible to meet the technical requirement of easy distribution on leaf surface, an adequate capacity of adhesion and high degree of stability. Moreover, in order to exploit the properties of chitosan, already known as a bio-agent, we verified the possibility to functionalize NPs with dsRNA polymers showing a phytoiatric effect.

A slight modification of the method suggested by Zhao and Wu (36) involves an oxidation treatment that partially degrades chitosan used to produce NPs, hereafter referred to as NPsD to distinguish them from NPsF obtained by the conventional method involving a preliminary chitosan filtration. The adjustment has led to a significant increase in the efficiency of synthesis if compared to original protocol, achieving a yield of 86.06 ± 1.50 % instead of 62.58 ± 11.72 % obtainable with the filtration process ($n = 6$; t test significance $P = 0.004$)

The characterization by Dynamic Light Scattering (DLS) method showed a significant decrease in the size of NPsD in comparison to NPsF, whereas their ζ potential was substantially close to neutrality and unaffected by the synthesis treatment (Figure 1a). However, in both synthesis methods, the functionalization with dsRNAs significantly led to an increase of the NP size compared to that of the respective non-functionalized NPs, where the degradation treatment provided a significant greater value than the filtration one (Figure 1b). Again, the NPs functionalization by dsRNA did not affect the surface charge, since it remained the same as measured in the empty NPs, regardless of the applied synthesis method.

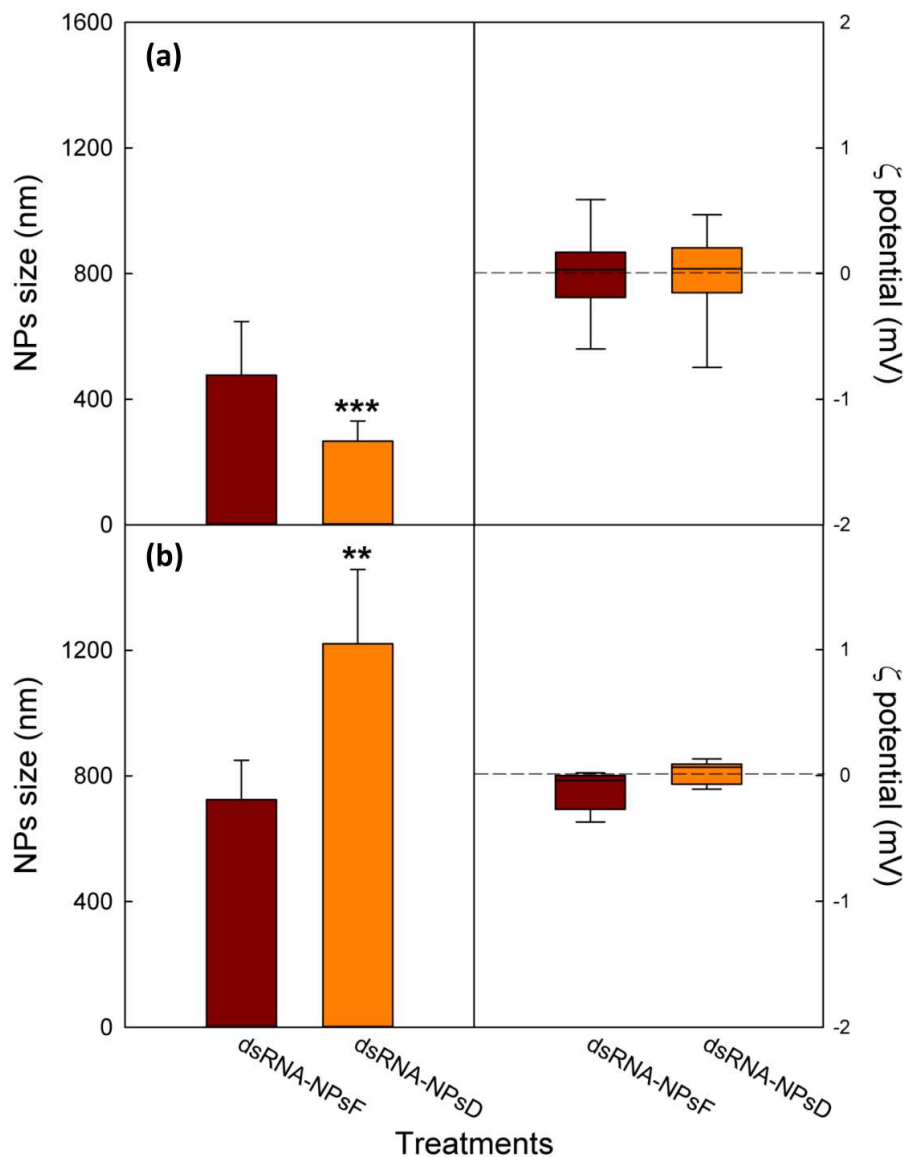


Figure 1. NPs characterization. Size and ζ potential of NPs obtained by the two preparations before (a) and after (b) their functionalization with RNA. Data ($n = 6$) are expressed: (left) as mean \pm SD; (right) as boxplot whose whiskers correspond to the data range between minimum and maximum value, excluding outliers. The significance of the applied T test is *** $P = 0.000$ (a) and ** $P = 0.017$ (b).

The dsRNA retention efficiency of NPs obtained according to the two protocols was assessed by agarose gel electrophoresis and subsequent fluorescence analysis of the nucleotide-bound signal by means of UV lamp illumination.

In Figure 2a, samples obtained by simple filtration of chitosan (NPsF) showed a much higher dsRNA retention capacity than those obtained by oxidative degradation (NPsD), if assayed either immediately after synthesis (lanes 1 and 2) or following refinement and sonication (lanes 3 and 4). This effect is confirmed by the high fluorescence signal

of NPsF functionalized by dsRNAs observed at the well level (lanes 1 and 3), whereas in the case of NPsD samples (lanes 2 and 4) nucleotides migrated along the gel with a smear pattern, similar to that detectable in the free dsRNA sample (lane 7). In the lanes of the supernatants from the two NP preparations, no smear signal was detected, as a proof of the lack of dsRNA release from the NPs after synthesis.

A further electrophoretic run has been applied to test the effect of EIA (Figure 2b), a surfactant commonly used in agronomic practices, on the retention capacity of the NPs under study. After suspension in increasing concentrations of EIA, the NPsD show a release of the nucleotide polymers (lanes 2, 4 and 6) resembling that detectable in the free dsRNA sample resuspended in 0.1% EIA (lane 7) or in the samples without EIA (lanes 2 and 4, Panel a). In the loading wells of the latter, no fluorescent signal can be found anymore, indicating an almost complete runoff following electrophoresis. The release effect is maximized by the intermediate dose (0.05%) of surfactant, as evidenced by the increased fluorescence intensity of the electrophoretic bands. In contrast, NPsF samples show no release of nucleotides in the gel and the fluorescence signal is localized only at the loading point, in the starting well (Figure 2b, lanes 1, 3 and 5).

These results have led to identify the NPsF preparation as the best choice for the following tests involving NP application on *N. benthamiana* leaves.

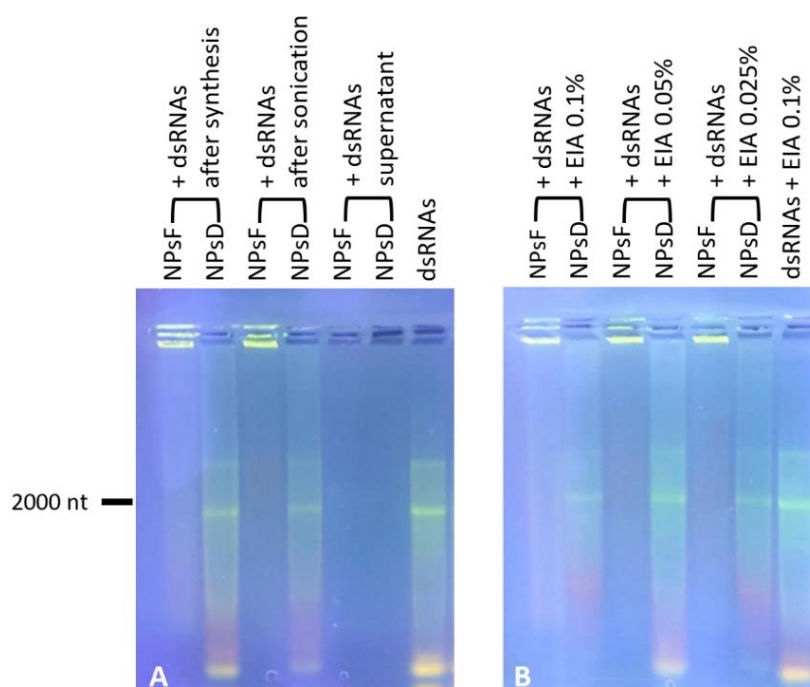


Figure 2. Gel electrophoresis on GFP dsRNA-loaded NPs. Evaluation of the dsRNA retention capacity of NPs obtained by the two different preparations (a) and after their resuspension in different concentrations of EIA (b). The amount of free dsRNA was the same as that provided to functionalized NPs.

According with the above-described results, the highest dose of EIA (0.1%) was chosen for the subsequent analyses on *N. benthamiana* leaves and plants. The further characterization of the NPsF and the observation of their distribution pattern on the leaf were obtained by functionalization with FITC probe and confocal microscopy analysis. For this purpose, FITC-doped NPsF have been characterized by DLS. As shown in Figure S4, FITC-incorporation induced a significant decrease in the hydrodynamic diameter of NP size, as well as the addition of the wetting agent to the resuspension solution. On the contrary, neither FITC nor EIA influenced the surface charge of the NPs.

Confocal microscopy analysis highlighted the ability of NPsF to cover the leaf surface with a dose-dependent distribution according to the dilution level. The most (1:20) and moderately (1:5) diluted NPs were preferentially distributed along the tangential walls of the tegumental cells, as shown in Figure 3b-f. The presence of fluorescence signal was also detected within stomatal guard cells and hairs.

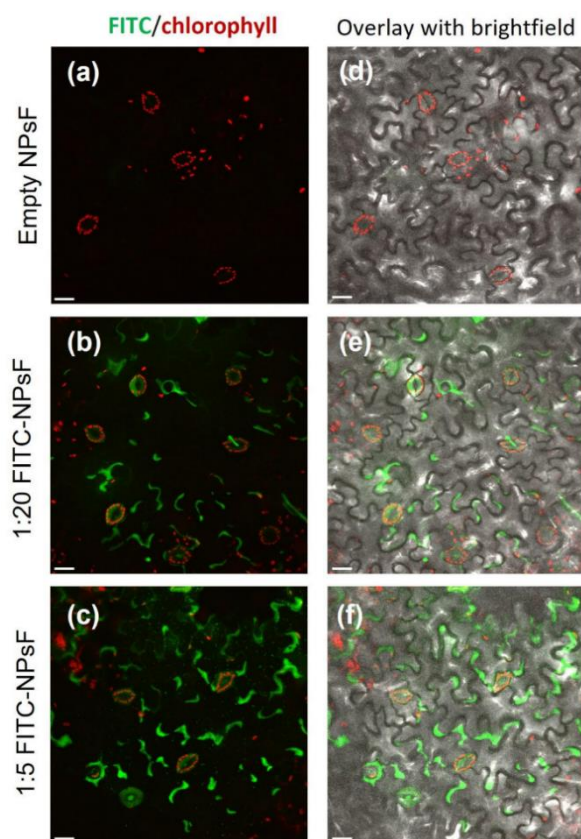


Figure 3. Confocal microscopy analysis of *N. benthamiana* abaxial side of leaf teguments sprayed with NPsF resuspended in 0.1% EIA. Panels (a) and (d): Empty NPsF; panels (b) and (e): 1:20 FITC-NPsF; panels (c) and (f): 1:5 FITC-NPsF. Left column: maximum intensity projection micrographs (green channel, FITC; red channel, chlorophyll autofluorescence); right column: overlay with corresponding brightfield images. Scalebar 20 μm .

The 3D reconstructions of the *N. benthamiana* leaves shown in Figure 4 confirmed NPsF accumulation and the correlation between the titre of the NPsF suspension used in the treatment and the amount of fluorescence detectable on leaf surface (Figure 4; see also Figure S5). Notably, the 1:1 dilution of the nanomaterial exhibited a quite complete covering effect, which probably led to an unspecific incrustation of tegument cell wall (Figure S5). In addition, the three-dimensional views highlight the predominantly external localization of NPsF due to virtually absent fluorescence signal below the epidermis. This is an expected result given the short time interval (max 4 h) between treatment and microscopy analysis, and at the same time is a demonstration of the FITC-retention capacity of the nanomaterial in comparison with free FITC (see Figure S6).

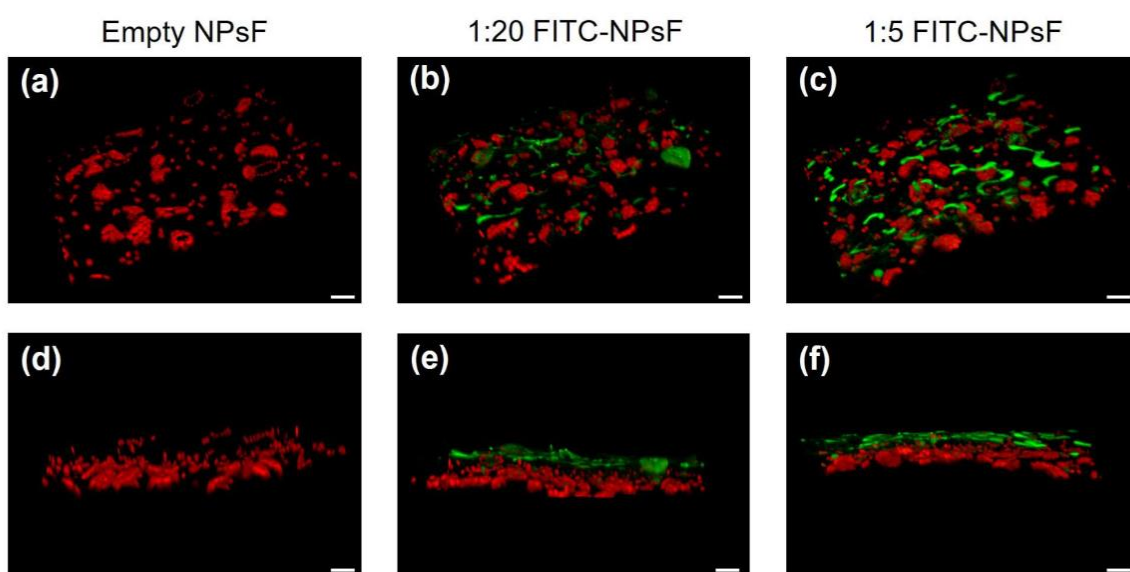


Figure 4. 3D reconstructed confocal micrographs showing the distribution of NPsF in 0.1% EIA on *N. benthamiana* leaf abaxial surface. Tilted and side views spanning from the leaf epidermis to the mesophyll are reported. Panels (a) and (d), empty NPsF; panels (b) and (e), 1:20 FITC-NPsF; panels (c) and (f), 1:5 FITC-NPsF. Green, FITC; red, chlorophyll autofluorescence. Scalebar 20 μ m.

After the choice of the most suitable concentration of FITC-NPsF (dilution 1:20), a further test was carried out to study the fate of nanoparticles that remained in contact with the leaves for up to 6 days. The results, based on the indirect evidence of the fluorescent signal of FITC probe, showed that the distribution of NPsF around the cell borders tended to spread evenly starting from 24 h after application (Figure 5c). Nanoparticles remained largely on the leaf surface until the end of the experiment, but after 72 h a faint fluorescent signal was also detected inside of the epidermal cells, reaching the chloroplast zone in the mesophyll, as observed in Figure 5e-f.

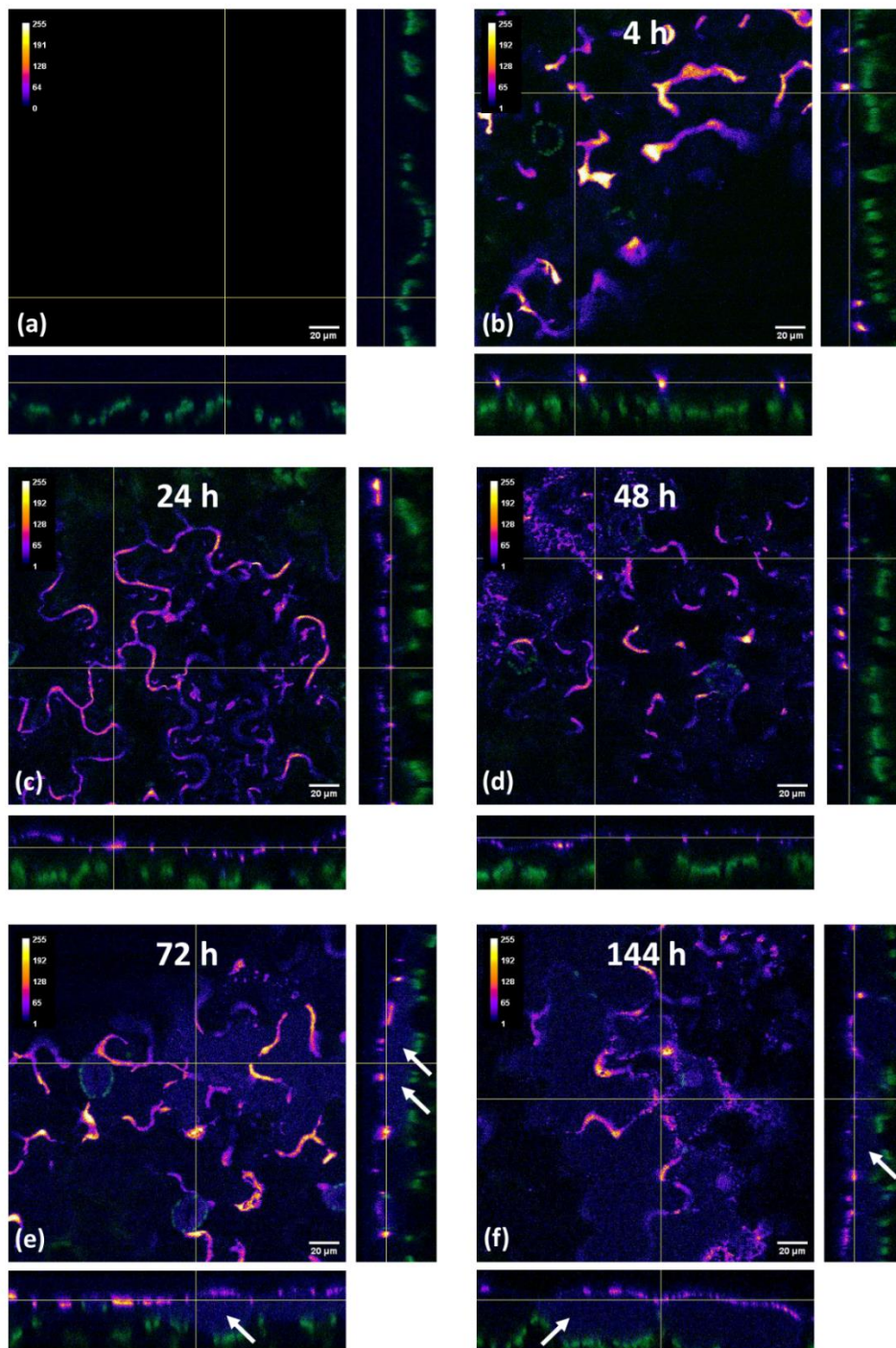


Figure 5. Analysis of the behavior of FITC-NPsF over time on *N. benthamiana* leaves. Orthogonal view of the leaf surface treated with FITC-NPs diluted 1:20 in 0.1% EIA obtained by confocal microscopy. Purple-yellow chromatic gradation: FITC signal distinguished by intensity; green: chloroplast autofluorescence. Panel (a): Control (0.1% EIA only); panels (b-f): FITC-NPsF 4 h (b); 24 h (c); 48 h (d) 72 h (e) and 144 h (f) after application. Arrows highlight signal penetration at the mesophyll level. Scalebar 20 μm .

Finally, trials were conducted to evaluate the efficacy of the dsRNAs-NPsF combination.

Firstly, NPsF were applied to detached leaves from *N. benthamiana* plants to assess capability of chitosan nanomaterial to protect dsRNAs from degradation by environmental agents and to improve their persistence on foliar surface. The first test, consisting in the exposition of NPsF-treated leaves to UV light, demonstrated that functionalisation in NPsF decreased the sensitivity of *GFP* dsRNA to denaturing radiation. In fact, as seen in Figure 6, the free genetic material sprayed on leaves was significantly degraded after 15 min of UV exposure, while that included in NPs showed no significant difference if compared to the relative control at time 0. Moreover, the analysis did not detect the presence of nucleotides on leaves exclusively treated with NPsF, thus confirming the absence of contamination during the application phase (data not shown).

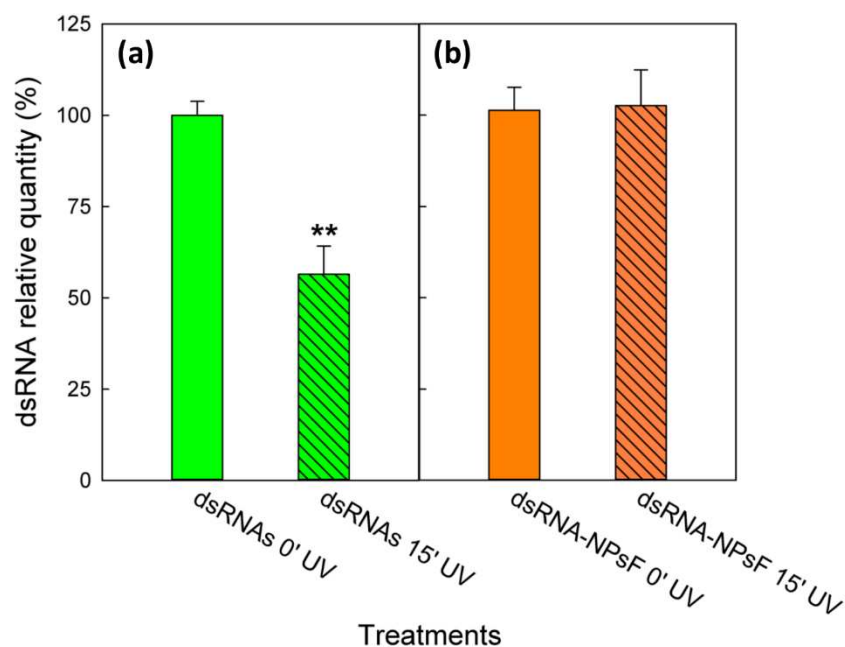


Figure 6. UV disrupting effect. Relative *GFP* dsRNA quantity on *N. benthamiana* leaves after 15 min exposition to UV light: comparison between treatment by 1:20 RNA in 0.1% EIA applied as free soluble form (a) and functionalized in NPsF (b). Data are mean \pm SD ($n = 3$). The significance of the applied T test is **P value < 0.01 .

On the contrary, the *in planta* test concerning the permanence of *GFP* dsRNA over time, did not show significant differences between the amount of free and NPsF-bound dsRNA detected after 7 and 15 days from application on *N. benthamiana* leaves, respectively (Table S1). Indeed, no significant degradation of free *GFP* dsRNA was observed even if a decreasing trend was identifiable in free-RNA-treated samples, suggesting the need for a more prolonged environmental exposure or to replicate the experiment in an open environment.

Finally, a specific nucleotide fragment expressing *B. cinerea* essential genes was employed to assess the degree of inhibition of fungal development on *N. benthamiana* leaves. As shown in Figure 7, naked *Bc* dsRNA was able to reduce mycelium growth in comparison to the control and *Botrytis* diffusion was severely restricted also when the sequence was bound to NPsF, as proven by the significance level of the treatment factor (see Table 1). In addition, the long-lasting and better protective effect exerted by dsRNA NPsF compared to naked dsRNA was confirmed by significance of statistical analysis (Table S2). In contrast, the application of empty NPsF had no effect, and necrosis developed similarly to the untreated leaves.

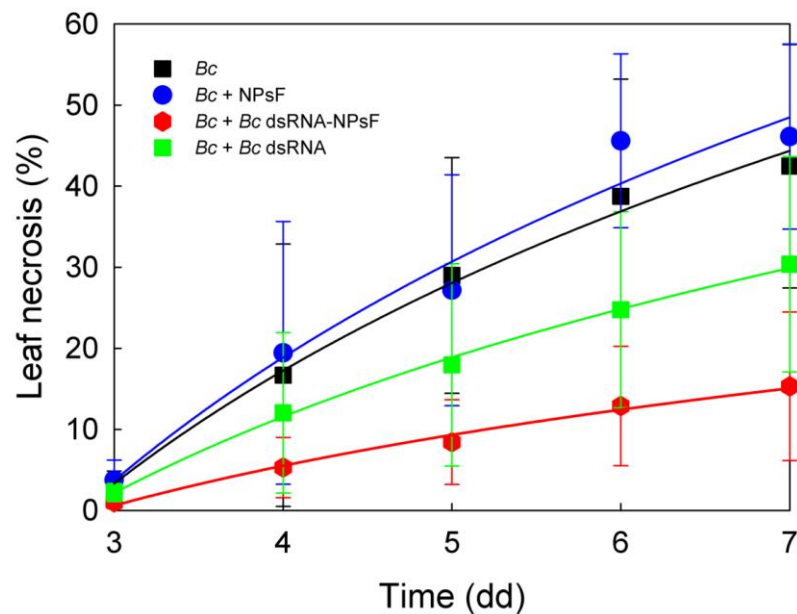


Figure 7. Development of *B. cinerea* necrosis on *N. benthamiana* leaves within 7 days. Data are expressed as the average percentage of leaf area invasion \pm SD ($n = 12$). *Bc*: *Botrytis cinerea*.

Table 1. Growth inhibition of *B. cinerea* mycelium due to the effect of dsRNA interference technique applied on *N. benthamiana* leaves. Data are expressed as mean \pm SD ($n = 12$). Significant relationships are in bold. Df = degrees of freedom; F = Fisher value; P = level of significance. "****" indicates a P significance level < 0.001 .

Response variable	Source of variability	Df	F value	P value (>F)
<i>B. cinerea</i> mycelium growth	Time	4	80.63	$<2e^{-16}$ ****
	Treatment	3	41.09	$<2e^{-16}$ ****
	Residuals	229		

DISCUSSION

Raising concerns about environmental variables have boosted the development of strategies able to increase efficacy of pest control by means of smart and low impact approaches.

According to this assumption, the application of dsRNAs as sustainable alternative to synthetic pesticides is a powerful and promising methodology, since it induces the RNAi pathway which is able to silence target genes in invading pathogens.

The rationale of present study is to investigate the characteristics of chitosan-based nanomaterials suitable for dsRNAs encapsulation, contributing to recent advances in chitosan NPs entrapping dsRNA delivery and improving RNAi-based response in plant crop protection (37).

Additionally, such an approach guarantees a protective effect on leaf-applied nucleotide sequences quite sensitive to degradation under field conditions, which limits their protection to less than seven days (38). The entrapped chitosan-dsRNA NPs could further open the opportunity for future developments involving the ability of nanomaterials to overcome leaf cuticle barrier, by-pass through cell wall and plasma membrane and avoid degrading *in vivo* nucleases (31,37). Comparably to medical treatments, low-dimension NPs may allow easy and targeted delivery of functionalizing molecules also inside plant tissue, possibly giving them free access to cell metabolism and even a long-distance distribution with systemic effects or being more efficiently uptaken by phytopathogens (39).

The most innovative and sustainable solutions require an efficient distribution and delivery of very precious and delicate material such as nucleotide sequences inside the plant, where the presence of a fully hydrophobic leaf tegument and of a cell wall creates specific conditions. Actually, there is a poor knowledge about the mechanisms underlying the different steps of nanomaterial transport in plants, namely: (i) plant surface adhesion and lifetime; (ii) internalization beyond the tegument barrier; (iii) translocation along both a short and long distance involving passive and active mechanisms and finally (iv) accumulation inside cell after crossing over cell wall and plasmalemma (40). All these steps are strictly dependent on NP size, concentration and surface charge, which are the main physico-chemical features to be considered in the design of nanomaterial able to provide the best transport efficiency.

The initial approach of the present investigation was then devoted to implement a synthesis protocol for NPs, using ionic gelation method, aiming to minimize NP dimension and to allow nucleotide retention inside NPs at the highest level possible. As reported in literature, in ionic gelation method, an optimal encapsulation of nucleic acids should be usually favored by their strong crosslinking with TPP inside the chitosan matrix, instead of depending only on electrostatic interactions, thus enhancing their potential retention ability (41,42).

Initially, to obtain small NPs that would be more functional for interaction with the leaf surface, two different synthesis protocols were defined by decreasing the polymer

molecular weight of bulk chitosan. This aim has been addressed through two modalities, namely the filtration of the stock solution or its oxidative degradation for 24h, both defined after the preliminary tests shown in Figures S1 and S2. In the first one, filtration lowered the concentration of long chains (average diameter <500 nm), therefore attenuating the effect of intermolecular interactions during synthesis with TPP, that would cause the formation of large NPs (43). Instead, the degradation process itself decreased the presence of amino groups in favor of carboxyl ones (44) and the size of the chitosan chains (36,44), favoring the synthesis of smaller NPs (<400 nm).

The size of the NPs was studied both before and after functionalization with RNA: as the NPsF were considered better in terms of lower size increase after functionalization (Figure 1) and stronger binding capacity (Figure 2), they were also subjected to a more precise dimensional analysis by TEM (Figure S3), which allowed to estimate the actual average particle size of 170 ± 61 nm.

Both NP formulations presented a neutral charge (Figure 1), which represents an optimal feature for enhancing their interaction with hydrophobic leaf epidermis thereby decreasing NP aggregation or loss due to solubilization by rainwater runoff (45).

The shift in the balance of charges in favor of anions in the chitosan polymers (44), which might have occurred during degradation treatment involved in NPsD synthesis, also negatively affects the ability to bind RNA, being itself a polyanion (43). This explains the result of gel electrophoresis analysis for complexation of dsRNA with NPs (Figure 2), where NPsD functionalized by RNA showed only a partial complexation, evidenced by a smear similar to that of free nucleotides, while the complex nucleotide-chitosan formation became optimal in the RNA-NPsF sample, where bound dsRNA did not migrate under electrophoresis. Similar results were obtained by Petrônio and collaborators (46), using coacervation synthesis protocol for obtaining small-sized chitosan-dsRNA NPs from high molecular weight bulk chitosan. The more efficient complexation of RNA sequences with NPsF compelled us to choose the filtration method for the synthesis of chitosan NPs in the following plant tests and confocal microscopy analyses.

The electrophoretic analysis provided additional information, since it was possible to demonstrate that the refinement treatments (in particular the sonication) as well as the addition of the surfactant EIA, did not affect the retention capacity of the RNA by the NPs, as confirmed by the absence of non-specific release.

The efficient functionalization with RNA was further attested by the size modification of the NPs (Figure 1), which represented an additional preferential factor toward NPsF, since they exhibited a smaller apparent hydrodynamic diameter than NPsD. Conversely, the values of the ζ potential were not affected.

In a view to future agronomic application of the NPs thus obtained, the characteristics of a formulation including a surfactant commonly used in agriculture was tested by its distribution on detached leaves of *N. benthamiana*.

With the aim to investigate the deposition and early penetration of the chitosan-based NPs suspension on the abaxial leaf surface, 3D confocal microscopy analysis was performed with small-size FITC-conjugated NPsF suspended in wetting agent and applied by foliar spray. Despite fluorescent-labelled chitosan-NPs have been largely used in medical literature, offering the advantages of tracking the extracellular and intracellular NPs delivery and allowing a stable and high fluorescence signal emission (47), analogous studies in plant systems are still scarce. Microscopic fluorescent NPs imaging showed a dose-dependent adhesion on the abaxial leaf surface and a preferential localization along the tangential walls of the tegumental cells, in agreement with the evidence of different authors (48–50). This is more marked in the NP treatments applied at 1:20 and 1:5 dilution ratio as shown in Figure 3 (panels b and e; c and f, respectively) and in Figure 4 (panels b and e; c and f, respectively). On the contrary, the thesis at 1:1 NPsF dilution showed a hedging effect likely due to an excess of large-size aggregates of particles (Figure S5), and for this reason it was not taken into consideration for further tests. In fact, the use of high concentrations of nanomaterials sprayed on plant leaf could be counterproductive, since it induces large-size aggregates formation on leaf surface probably explained by the higher probability of particle collision (51), at the expense of NPs' mono-dispersity (see Figure S5), thus ultimately affecting the effective penetration of the NPs inside the tissues and controlling their fate in plant systems.

Furthermore, this would alter the intrinsic properties related to the nanometric size of the materials, such surface charge distribution and high surface:volume ratio, while at the same time would reduce their contact surface available for interaction with the leaf epidermis.

In Figure S6 the fluorescence observed upon leaf exposure to free FITC diluted 1:1000 is compared with that obtained after application of the supernatant from low concentration (1:20) of FITC-NPsF, previously washed by centrifugation to get rid of exceeding FITC. The negligible signal in the case of the supernatant, as compared to both the corresponding suspension (see Figure 3) and the free FITC solution, supports the absence of significant dye leakage in the FITC-NP formulation.

Confocal analysis also allowed to observe a partial localization of FITC fluorescence signal within chloroplast-containing guard cells (Figure 3), suggesting that at least a portion of the NPs could pass through the stomatal rims entering the guard cells. Such fluorescence signal could be due both to intact FITC-NPsF, possibly those belonging to size classes below 20 nm (40), or to dye molecules eventually released from the functionalized NPs, once beyond the tegument barrier. Accordingly, recent evidence reported that foliar uptake of nanoparticles proceeds both via a polar pathway (*e.g.*, trichomes, stomata) and a nonpolar pathway (*e.g.*, cuticle and its pores), depending on their size, charge and form (52), but it is strongly dependent also on the plant-species dependent leaf features and wettability (53,54).

Notably, although this signal in the guard cells was observed also in the case of leaf treatment with free FITC in solution (Figures S4a and S4c), in the treatment by NPsF

supernatant (Figures S4b and S4d) only a negligible fluorescence could be retrieved at stomata level. These results suggest that the minor contribution from leaked dye present in the supernatant (marker of high retention NPs) is unlikely to explain the high signal detected in these cells upon FITC-NPsF application. In addition, the high fluorescence signal mostly associated to the guard cells implies a transport against concentration gradient. Such an activity is explainable by an energy-driven accumulation of FITC-NPsF or free FITC, since a passive accumulation-driven by a concentration gradient is hardly conceivable, given the already cited low fluorescence associated to the supernatant. Instead, it could be inferred that the permeation is limited to guard cells only, since stomata are known as the only epidermal cells able to perform an actual photosynthesis and therefore to synthesize a large amount of ATP (55). This observation is in accordance with what was recently reported by Landry and colleagues (49), working with different microscopic techniques on DNA-modified gold NPs uptake in *N. benthamiana* leaves. They suggested that, depending on size and shapes, the route for NPs delivery into plant cells is not accomplished by a simple diffusion mechanism, but could be mostly driven by an energy-dependent endocytosis process or even that the particles could accumulate in the cell walls, then releasing their cargo.

It is necessary to specify that this confocal microscopy analysis was carried out over a short period of time (no more than 4 hours from treatment). A time course experiment was subsequently performed to verify the persistence of sprayed NPs on leaf surface during longer time periods.

The images acquired by means of confocal microscope analysis showed the orthogonal view of the outer layers of the leaf cells. Although the indirect approach used, based on the fluorescence of FITC dye used as NPs doping agent, doesn't allow to discriminate between fluorescence of free released FITC or that of dye still bound to the nanoparticles, the collected images revealed a time-dependent modification of the distribution pattern. In particular, the time-course of images shows that the distribution pattern underwent a time dependent modification and from an initial localization preferably along the edge of the cell walls, in agreement with the initial short time analysis, then a more even distribution was observed within 1 or 2 days. Although the experiment was prolonged over several days with light/dark cycles, the fluorescence signal remained detectable until at least day 6, an observation that would suggest a protective effect of presumably still intact NPs against photobleaching of the doping molecule. From day 3 a weak signal was detectable inside the cells of leaf tegument, indicating that at least the free FITC had partially permeated the waterproof layer of the leaf. These results are promising as they show that NPs provide the functionalizing molecules with protection against environmental factors (light in particular), which did not result in massive fluorescence loss. The late appearance of the fluorescence inside plant tissues could be explained by a gradual and prolonged release of the doping molecule, occurring concurrently with the slow NPsF degradation. Durable adhesion on the leaf, overcoming the impermeable barrier created by the cuticle and subsequent transport into the cells are currently the weak

points for rapid diffusion of RNA interference (54). These results thus provide an additional strength point for the practical application of this smart strategy.

The promising feature of chitosan nanomaterials to enhance dsRNA stability and delivery on plants with the aim to activate RNAi response was preliminarily verified by treating *N. benthamiana* leaves with dsRNA-functionalized NPsF. Quantification of specific *GFP* dsRNA amount in leaf tissue by means of PCR technique allowed to evaluate the rate of nucleotide degradation both on detached leaves exposed under UV light, mimicking drastic environmental conditions, and on plants in a controlled environment.

In the harsher conditions, under a brief exposure to UV light, *GFP* dsRNA functionalized with NPsFs were actually protected by degradation, while leaf dsRNA content significantly decreased in leaves treated by naked RNA. Accordingly, exogenous spraying of naked dsRNAs for plant virus resistance under field conditions has been already shown to be limited by the high instability and short half-life (38,56) and this poses several controversial discussions on the successful application of exogenous dsRNA for RNAi systems (57), nonetheless several innovative nanosystems for effective RNA delivery have been proposed to overcome this challenge (58).

Unfortunately, the same approach showed no significant difference between the two treatments if applied *in planta* during a 7 to 15 days cultivation period in a growth chamber (Table S1). This result confirms on the one hand that the dsRNA molecule on leaf surface has fair stability over time and on the other hand that controlled growing conditions induce a weak environmental effect, which is very different from field conditions.

The obtained data confirmed the initial hypothesis, since dsRNAs appeared to be stable over an acceptable period of time in the perspective of future application as a molecular "smart strategy". This goal was interestingly further amplified since the distribution of functionalized NPsF, although not at a statistically significant level, suggest the presence of a more favorable behavior in the decay trend of the dsRNA and the possibility of a long-lasting coverage using RNAi technique for protection from pathogen and environmental stresses.

Such a hypothesis has been further demonstrated by the experiment described in Figure 7, where the already known antifungal effect (59) related to RNA interference approach has been further potentiated by NPs functionalization and this strengthen the feasibility of its application in the case of pests and pathogen present on the leaf surface. The observed decrease of the *Botrytis* mycelium diffusion could be almost completely ascribed to a merely protective effect of nanoparticles on nucleotide sequences, without the expected anti-mycotic effect of chitosan. This observation suggests that this smart technology based on RNAi could be even further improved in case the chitosan raw material used for NPs synthesis would exhibit antimicrobial activity by itself. Further experiments should be performed to evaluate different chitosan formulations with greater reactivity to induce an additive inhibitory action, being aware that secondary effects of phytotoxicity must be avoided.

EXPERIMENTAL PROCEDURES

Plant material

Wild-type plants of *Nicotiana benthamiana* Domin were used for all experiments. A set of 6 plants has been employed to study the NPsF by fluorescence analysis under the confocal microscope, while to study their long-term fate 10 plants were used. Evaluation of the NPsF ability to enhance the nucleotides lifetime, 18 plants were used in the case of leaf treatment and 27 for the whole plant-application. Finally, the leaves of 48 plants have been employed to study the effect of treatments by dsRNA-NPsF on *B. cinerea*.

The plants were cultivated in standard conditions at 22°C and 14 h of light per day in a growth room. For all purposes the leaves were collected at the 3rd-5th node, corresponding to the first fully expanded leaves, from plants grown for 60-90 days after germination.

Synthesis and partial purification of double-stranded RNA (dsRNA) molecules

Synthesis and partial purification of both dsRNAs molecules utilized in the present work were performed as previously detailed (59). Briefly, specific primers were designed to amplify a 376 bp amplicon from the pCBCT plasmid. Once purified the PCR product was digested with the restriction enzyme PstI and cloned into the linearized L4440 plasmid. The later was introduced into HT115-DE3 *E. coli* cells, which are defective for the RNase III gene, involved in degradation of dsRNAs, and contains T7 RNA polymerase under control of the inducible *Lac* promoter. The modified L4440 plasmid, which contains two convergent T7 promoters, was then exploited to induce the production of dsRNAs in HT115-DE3 cells by adding IPTG at the exponential growth phase. For dsRNAs targeting *B. cinerea* essential genes the plasmid previously produced was exploited (59). This plasmid contains the sequence of *BcCYP51*, *Bcchs1*, and *BcEF2* obtained by overlapping PCR. Similarly, a single fragment of the GFP coding sequence was independently cloned into the L4440 plasmid in order to obtain dsRNAs with this incorporated sequence.

Extraction of dsRNAs from bacterial cells was achieved through a classic phenol–chloroform extraction followed by isopropanol precipitation and then by DNase I treatment. dsRNA integrity was checked with a 1% agarose gel using a weighted ladder to obtain a semi-quantitative evaluation of the extracted amount.

Synthesis, functionalization and refinement of chitosan NPs

Chitosan (Acros Organics, MW: 100,000 – 300,000 g mol⁻¹) was purchased from Thermo Fisher Scientific (Fair Lawn, NJ, USA); all other reagents were from Sigma-Aldrich Chemical Co. (St. Louis, MO, USA) if not otherwise specified.

Two types of nanoparticles (NPs) were synthesized, using chitosan stock solution differently prepared. In the first case, it was obtained by dissolving chitosan powder in

an aqueous solution of acetic acid (adjusting the pH around 3.5), stirring it for more than 12 h and then filtering it with 0.2 µm syringe filters (Nalgene Syringe Filters, SFCA membrane, 25 mm diameter; Thermo Fisher Scientific). For this reason, this kind of NPs are hereinafter referred to as NPsF.

The second stock solution was instead obtained by pre-treating chitosan for 24 h (the treatment duration was determined according to previous assays, see Figure S1) with a 6% hydrogen peroxide solution, according to Zhao and Wu method (36), with the aim of degrading it and decreasing its molecular weight. Chitosan was then dried and dissolved in the same solution as above, but without carrying out the final filtration; the thus prepared NPs will be named NPsD.

Both NP types were then obtained by the ionic gelation method (35,60), using TPP (sodium triphosphate pentabasic, MW. 367.86 g mol⁻¹) as crosslinker agent and TWEEN®20 as surfactant. The amount of chitosan added for each mL of the synthetic mixture was 1.57 mg, and the ratio between low molecular weight chitosan and TPP was 5:2, in agreement with the findings of Yang and coworkers (61). The reaction was carried out at room temperature in an aqueous solution (final volume: 2.1 mL) by adding the TPP dropwise and then stirring for one hour.

The synthesis yield was evaluated through the difference between the dry weight of the chitosan used and that of the NP precipitation pellet.

The procedure followed to functionalize the NPs was the same as that for the empty ones by the simple incorporation of the doping solution during stirring, before the TPP addition. In the case of RNAi studies, the sources for the doping solutions were, as mentioned above, total RNAs obtained from a transformed *E. coli* strain able to synthesize: (a) the dsRNA of Green Fluorescent Protein (*GFP* dsRNA) or (b) a specific fragment expressing *B. cinerea* essential genes (*BcCYP51*, *Bcchs1*, and *BcEF2*. For simplicity it will be called *Bc* dsRNA) (59). For each mg of chitosan, 6 µg of *GFP* dsRNA or of *Bc* dsRNA were added. The same concentration was used for all experiments. If necessary, the pH of the synthetic solution was adjusted with acetic acid 2.4 M, buffering it to the usual values of empty NP-preparations (pH 5.0-5.5).

NPsF were also functionalized with another molecule, the fluorescein-5-isothiocyanate (FITC; Merck KGaA, Darmstadt, Germany) to allow visualization by confocal microscopy. In this case, a 1% stock solution in acetone was prepared and NPsF were loaded with 0.1% FITC taking care to avoid exposure to light as much as possible.

After synthesis, all types of NPs were subjected to a refinement process consisting in two phases of pelleting (centrifugation at 16000 *g* for 10 min) and final resuspension in 1 mL of double-distilled water. At last, aiming to improve mono-dispersity, NPs were treated with 3 sonication sessions of 15 seconds each, at the power of 50 W (Labsonic 1510; B. Braun, Bender+Hobun, Zurich, Switzerland).

EIA wetting agent addition

Aiming to formulate NP suspensions suitable for an optimal distribution on the plant canopy, the possibility of using an additive with a tackifier function was also

considered. Among the various existing commercial products, ethoxylated isodecyl alcohol wetting agent (EIA, 100 g L⁻¹; CIFO Srl, S. Giorgio di Piano, BO, Italy) was chosen since it is already widely used in agricultural practices. After refinement, a sample of NPs was therefore resuspended in three aqueous solutions with different EIA concentrations (0.025, 0.05 and 0.1%) and used for the tests of NP characterization.

Particle size and ζ potential determination

All the NPs, both empty and functionalized, were analysed to assess their properties. Their size distribution and charge were determined by Dynamic Light Scattering (DLS) using the Particle sizer/ ζ potential Analyzer PSS Nicomp 380 ZLS (Santa Barbara, California, USA). The measurement was carried out at room temperature in aqueous solution, using refined NP suspensions as samples (cuvette volume ratio: 100 μ L of sample in a total volume of 3 mL).

TEM analysis and image processing

A NPsF sample was assayed by transmission electron microscopy (TEM) to obtain additional information about their shape and size (see Figure S3).

Sample preparation was carried out as follows: the NPsF suspension was mixed with 1% uranyl acetate solution, and 5 μ L were placed on the microscope (EM 208 – Philips TEM: Philips Eindhoven, Netherland) copper grid. After a 10-minute incubation at room temperature, which was necessary to allow material settlement, the liquid excess was removed with a paper towel and the microscope analysis was performed. The instrument was equipped with a Quemesa (Olympus Soft Imaging Solutions) camera. Three different fields of the obtained images were then processed by *ImageJ* software (Java version 1.8.0 322) to measure the diameter of individual particles.

Gel retardation assay

Electrophoresis (Mini-Sub Cell®GT Agarose Gel Electrophoresis System; Bio-Rad Laboratories, Inc., CA-USA) was performed to evaluate both the *GFP* dsRNA retention capacity by the two types of NPs and whether the addition of EIA influenced it. NPs obtained from filtration treatment (NPsF) and those made from degraded chitosan (NPsD) were doped with RNA and loaded into the gel wells both before and after the refinement treatment; moreover, their final supernatant was also analysed to verify if the sonication caused the release of the RNA from NPs. Further agarose gel analysis evaluated the same samples resuspended after refinement in three different EIA concentrations mentioned above. In all cases the standard The Ambion® RNA Control 250 (Thermo Fisher Scientific, Fair Lawn, NJ, USA) was used as a reference for migrating nucleotide polymers, as indicated by the segment corresponding to a molecule of about 2000 nucleotides (see Figure 2, images are representative of at least three replicates).

The assay was carried out in agarose gel 1.5% (Agarose Type I, Sigma-Aldrich Chemical Co.) in Tris-borate-EDTA buffer (TBE - 1X), using GelGreen® (GelGreen® Nucleic Acid Stain, 10,000X; Merck KGaA, Darmstadt, Germany) to stain the nucleotides, after its dilution 1:10,000 into the molten agarose solution (precast protocol). Each well was loaded with 20 µL of the samples and 5 µL of gel loading buffer (bromophenol blue 0.01% w/v, glycerol 30% v/v). The electrophoresis was performed at 60 V for 100 min; then the gel was exposed to UV light (UV Transilluminator 2000; Bio-Rad Laboratories, Inc., CA-USA) and a photo was taken by a camera.

GFP dsRNA persistence on leaves

To explore the *GFP* dsRNA persistence (62) following both RNAs application (functionalized or naked) on *N. benthamiana* leaves, three different sprayable preparations were produced, containing NPsF, RNA-NPsF and free RNA diluted 1:20 in 0.1% EIA. The aim was to simulate a real agronomic treatment, and this explains the choice of the suspension concentration (the 1:20 dose is the only one which exhibits a potential practical application, since the amount of dsRNAs represents a limiting factor) and of the EIA dosage (whose value equals to that usually recommended by the manufacturer).

With these preparations, two different experiments were conducted. In the first one, a single-leaf treatment was performed: 500 µL of each suspension were sprayed, by means of a glass dispenser, on the adaxial side of single detached *N. benthamiana* leaves. After complete drying, half of the plant material was subjected to UV light exposure (Lamp type G30T8, power 30 W, radiation peak 253.7 nm, UV yield 13.4 W; Sankyo Denki, Japan) for 15 min, while the other half was kept as a control.

In the second experiment, the distribution was carried out on the entire plant (20 mL for each plant) aiming to evaluate the preservation over time of nucleotides due to their inclusion into the nanomaterial. In this case, samples were collected at 0, 7 and 15 days after the spray application.

In both approaches, for each condition three biological replicates were formed pooling leaves from 9 independent plants (3 leaves from 3 plants X 3 biological replicates).

In all cases, samples were freeze-dried and stored at -80 °C until use for the subsequent RT-PCR analysis.

Total RNA was isolated from leaf samples using the Spectrum™ Total RNA Kit (Sigma-Aldrich, St. Louis, MO, USA) following manufacturer's instructions and RNA concentration of the extracted samples was quantified at the NanoDrop™ (Thermo Fisher Scientific, Fair Lawn, NJ, USA). DNase treatment and cDNA synthesis was performed as previously reported using about 300 ng of total RNA (62–64). The absence of genomic DNA contamination was checked before cDNA synthesis by qPCR using specific primers of *N. benthamiana* COX (For: 5'-CGTCGCATTCCAGATTATCCA-3', Rev: 5'-CAACTACGGATATATAAGRRCRRAACTG-3') (65). RT-qPCR reactions were carried out in a final volume of 10 µL containing 5 µL of SYBR® Green Master Mix (Bio-Rad Laboratories, Inc., CA-USA), 5 µM specific primers of *GFP* (For: 5'-

GTGACCACCCTGACCTACGG-3', Rev: 5'-CTCCTGGACGTAGCCTTCGG-3') and 1:10 of diluted cDNA. Reactions were run in the CFX 96 apparatus (Bio-Rad Laboratories, Inc., CA-USA) using the following program: 10 min preincubation at 95°C, followed by 40 cycles of 15 s at 95°C, and 30 s at 60°C. Each amplification was followed by melting curve analysis (65–94°C) with a heating rate of 0.5°C every 15 s. All reactions were performed with at least two technical replicates. The relative quantification of *GFP* transcripts was quantified after normalization over the tissue quantity using *NbCOX* housekeeping gene. Gene expression data were calculated as expression ratio (Relative Quantity) to naked dsRNA application at time 0.

***B. cinerea* inhibition with *Bc* dsRNA-functionalized NPsF**

For *B. cinerea* inhibition test, preparations of naked *Bc* dsRNA, NPsF and *Bc* dsRNA-functionalized NPsF were used, all diluted at 1:20 ratio in 0.1% EIA solution. The EIA-only solution was used as a control. A volume of 500 µL of each suspension was sprayed as described above on the adaxial page of 12 leaves, which, once dried, were placed in petri dishes prepared with water agar (1 %, w/v). Each leaf was then inoculated with 10 µL of *B. cinerea* spores (1.28E+06 spores per mL) in 30% glycerol, divided into two drops. *B. cinerea* isolate was obtained and maintained on Potato Dextrose Agar as described by Vuerich et al. (2023) (66).

The plates were then placed in a humidity chamber and kept in the plant growth room for one week.

To detect the extent of fungal development, photographs were taken from day 3 to 7. A camera placed on a stand at a fixed distance was used, while the plates were backlit to highlight the necrotic spots in respect to the leaf surface. Images were processed with *ImageJ* software (Java version 1.8.0 322) *Labkit* plugin (67), in order to measure the fungal symptoms by means of a segmentation process. The results were expressed as a percentage of affected leaf area on total leaf area.

Confocal microscopy

For the initial confocal microscopy analysis, three different FITC-NPsF concentrations were tested by diluting the sample at 1:1, 1:5 and 1:20 ratio, each in the presence of 0.1% EIA. Three other preparations, diluted with the same amount of surfactant as well, were used as controls: empty NPsF (concentration 1:1), 1:1000 diluted (w/v) free FITC (mimicking the loading concentration used in 1:1 NPsF) and the supernatant from the 1:20 FITC-NPsF suspension. The latter was chosen since it was the dilution applied also for all the treatments concerning NPsF functionalized with dsRNAs. Five hundred µL of each preparation have been sprayed, by means of a glass spray dispenser, on the abaxial side of a single *N. benthamiana* leaf immediately after detachment from distinct plants. Leaves were mounted for confocal examination directly after complete drying of the treatments.

Briefly, a disk of about 1 cm² area was excised from each leaf, placed on a microscope slide and sealed, covered by a film of double-distilled water, under n. 1 thickness

coverslips using coverslip spacers and two-component silicone glue (Twinsil® Picodent, Wipperfürth, Germany).

For the time-course experiment, 5 leaves were treated as described above using the FITC-NPsF preparation diluted 1:20 in 0.1% EIA, while five others were used as controls (sprayed with 0.1% EIA only). The treated leaves were kept in the plant growth room (14-10 h light-dark cycle) in 1% water agar (1%, w/v) petri dishes for different periods of time (4, 24, 48, 72 and 144 hours) before a leaf disk was excised for slide mounting. Confocal analysis was carried out on a Leica TCS SP8 confocal microscope (Leica Microsystems, Wetzlar, Germany) equipped with a tunable white light laser source set to 495 nm for FITC excitation and to 633 nm to allow visualization of chlorophyll autofluorescence. Z-stack images, starting at the abaxial epidermal surface, were collected at 0.424 µm intervals using a Plan-Apochromat 40×/1.10 NA water immersion objective. For 3D reconstructions, the total z-scanning range was between 30 and 40 µm, largely depending on different coplanarity of each specimen, to cover an anatomical portion extending from the leaf surface to the mesophyll. Alternatively, thinner stacks recorded over approximately 10-20 µm through the epidermal layer were processed as maximum intensity projections and overlaid with corresponding single-plane brightfield images to allow visualization of cell boundaries. Micrographs were contrast-adjusted and, for brightfield images only, subjected to gamma correction to improve visibility (gamma value = 0.5).

For the time-course analysis, orthogonal views were generated from approximately 50 µm-thick z-stacks and displayed using a heatmap lookup table to better reveal low intensity FITC signals inside the leaf tissue. Image processing was performed using Leica Application Suite X (LAS X) 3.5.5 software and *ImageJ Fiji* software (Java version 1.8.0 322) (68).

Statistical analyses

Inferential statistics were performed by means of the software *Statistica*™ release 11.0 (StatSoft Hamburg, Germany) and *RStudio* (2022.02.0-443 version). ANOVA or T test was employed to analyze data and a least significant difference (LSD) test at $P < 0.05$ was utilized to evaluate mean values of different treatments.

CONCLUSIONS

The present investigation provides a synthesis method for preparing NPs using filtered chitosan as a starting raw material with specific size and surface charge characteristics, which were shown to be useful for topical foliar application, in comparison to similar NPs prepared by oxidative degradation of chitosan. The efficient leaf distribution of FITC-labelled NPs on *N. benthamiana* leaf was analysed by means of 3D fluorescence confocal microscopy, which allowed to evidence that low dilution dose (in particular 1:1 rate) induced aggregation of the nanomaterial and loss of monodispersed

distribution. When loaded with dsRNA, NPFs also ensured a stable retention of nucleotides even under an electrophoretic field. Furthermore, foliar topically applied NPFs protected the *GFP* dsRNA sequence from degradation by a brief exposure under UV radiation, although, when distributed in plants grown under climatic room conditions, RNA-functionalised nano-formulation did not significantly differ in RNA protection from naked-RNA treatment. This result could suggest that these molecules exhibited appreciable stability when exposed to mild conditions such as those of a climatic room. dsRNA-chitosan NPs tool opens interesting opportunities for the development of RNAi techniques in plant crops. In particular, this solution could be potentially applied for the pathogen control in high-value crops, in order to comply with new UE regulations, prescribing a lower use of agrochemicals and the decrease in their environmental impact. In the present work we confirmed that *Bc* dsRNA shows an inhibitory action against *B. cinerea*, a pathogen developing outside plant tissues, confirming that NPs functionalization effectively was advantageous in restricting fungal infection. In addition, we provided indirect evidence that functionalized agent bound to the NPs could permeate at least leaf epidermis, since a fluorescent signal linked to FITC dye has been detected by means of confocal microscope in an interval of 3 to 6 days after distribution to plant leaves.

AUTHOR CONTRIBUTIONS

E.B., E.P., D.S., F.D.E., W.C. and L.N. designed the research, wrote and revised the manuscript. D.S., A.F., M.V. and E.P. carried out the experiments and biochemical analysis (F.D.E. confocal microscopy analysis). D.S., L.M., L.N. and W.C. conducted the RT analysis. F.D.E., W.C. and L.N. provided analytical tools and supplied resources. E.B. and D.S. undertook data curation and statistical analysis. This manuscript was critically revised and approved by all the authors.

ACKNOWLEDGEMENTS

Part of this work was founded by Cariverona foundation in the frame of BIOPROTECT project (ID 50448, Cod. SIME 2020.0057). We thank Dr. Federica Tramer for providing us TEM images of NPs.

REFERENCES

1. Parant A. Les perspectives démographiques mondiales [World population prospects] UN DESA. *Futuribles*. 1990 Mar;(141):49–78. PMID: 12283219
2. Directorate-General for Environment (European Commission). EU biodiversity strategy for 2030: bringing nature back into our lives [Internet]. LU: Publications Office of the European Union; 2021 [cited 2021 Nov 30].
3. Regulation (EU) 2019/1009 of the European Parliament and of the Council of 5 June 2019 [Internet]. OJ L, 32019R1009 Jun 25, 2019.
4. Calvo P, Nelson L, Kloepper JW. Agricultural uses of plant biostimulants. *Plant Soil*. 2014 Oct 1;383(1):3–41. <https://doi.org/10/gg3xp4>
5. Van Oosten MJ, Pepe O, De Pascale S, Silletti S, Maggio A. The role of biostimulants and bioeffectors as alleviators of abiotic stress in crop plants. *Chemical and Biological Technologies in Agriculture*. 2017 Apr 3;4(1):5. <https://doi.org/10/ghh85p>
6. Jamiołkowska A. Natural compounds as elicitors of plant resistance against diseases and new biocontrol strategies. *Agronomy*. 2020 Feb;10(2):173. <https://doi.org/10/gnm9xj>
7. Abdel-Rahman FA, Monir GA, Hassan MSS, Ahmed Y, Refaat MH, Ismail IA, et al. Exogenously applied chitosan and chitosan nanoparticles improved apple fruit resistance to blue mold, upregulated defense-related genes expression, and maintained fruit quality. *Horticulturae*. 2021 Aug;7(8):224. <https://doi.org/10/gnm944>
8. El Hadrami A, Adam LR, El Hadrami I, Daayf F. Chitosan in plant protection. *Marine Drugs*. 2010 Apr;8(4):968–87. <https://doi.org/10/ddg7t3>
9. Shahidi F, Abuzaytoun R. Chitin, chitosan, and co-products: chemistry, production, applications, and health effects. In: *Advances in Food and Nutrition Research* [Internet]. Academic Press; 2005 [cited 2021 Nov 30]. p. 93–135. [https://doi.org/10.1016/S1043-4526\(05\)49003-8](https://doi.org/10.1016/S1043-4526(05)49003-8)
10. Raafat D, Sahl H-G. Chitosan and its antimicrobial potential – a critical literature survey. *Microbial Biotechnology*. 2009;2(2):186–201. <https://doi.org/10/bt2d8r>
11. Jiménez-Gómez CP, Cecilia JA. Chitosan: a natural biopolymer with a wide and varied range of applications. *Molecules*. 2020 Jan;25(17):3981. <https://doi.org/10/gnm973>
12. Malerba M, Cerana R. Chitosan effects on plant systems. *International Journal of Molecular Sciences*. 2016 Jul;17(7):996. <https://doi.org/10/gjfvhv>
13. Gai Q-Y, Jiao J, Wang X, Liu J, Wang Z-Y, Fu Y-J. Chitosan promoting formononetin and calycosin accumulation in *Astragalus membranaceus* hairy root cultures via mitogen-activated protein kinase signaling cascades. *Sci Rep*. 2019 Jul 17;9(1):10367. <https://doi.org/10/gh298w>
14. Chawla SP, Kanatt SR, Sharma AK. Chitosan. In: Ramawat KG, Mérillon J-M, editors. *Polysaccharides: bioactivity and biotechnology* [Internet]. Cham: Springer

- International Publishing; 2015 [cited 2021 Nov 30]. p. 219–46. https://doi.org/10.1007/978-3-319-16298-0_13
15. Rafique A, Mahmood Zia K, Zuber M, Tabasum S, Rehman S. Chitosan functionalized poly(vinyl alcohol) for prospects biomedical and industrial applications: A review. *Int J Biol Macromol*. 2016 Jun 1;87:141–54. <https://doi.org/10/f8w2mj> PMID: 26893051
 16. Kashyap PL, Xiang X, Heiden P. Chitosan nanoparticle based delivery systems for sustainable agriculture. *International Journal of Biological Macromolecules*. 2015 Jun 1;77:36–51. <https://doi.org/10/f7fzhh>
 17. Maluin FN, Hussein MZ. Chitosan-based agronanochemicals as a sustainable alternative in crop protection. *Molecules*. 2020 Jan;25(7):1611. <https://doi.org/10/gjfvmd>
 18. Dubrovina AS, Kiselev KV. Exogenous RNAs for gene regulation and plant resistance. *International Journal of Molecular Sciences*. 2019 Jan;20(9):2282. <https://doi.org/10.3390/ijms20092282>
 19. Abbas U, Khan HM, Faisal M, Ayub I, Tahir T. Role of interference RNA (RNAi) in plant disease management. *Transactions in Physical and Biochemical Sciences*. 2021;1(1):16.
 20. Borah M, Konakalla NC. RNAi technology: a novel platform in crop protection. In: Singh KP, Jahagirdar S, Sarma BK, editors. *Emerging Trends in Plant Pathology* [Internet]. Singapore: Springer; 2021 [cited 2021 Dec 9]. p. 561–75. https://doi.org/10.1007/978-981-15-6275-4_24
 21. Niu D, Hamby R, Sanchez JN, Cai Q, Yan Q, Jin H. RNAs — a new frontier in crop protection. *Current Opinion in Biotechnology*. 2021 Aug 1;70:204–12. <https://doi.org/10/gk4pc3>
 22. Giudice G, Moffa L, Varotto S, Cardone MF, Bergamini C, De Lorenzis G, et al. Novel and emerging biotechnological crop protection approaches. *Plant Biotechnol J*. 2021 Aug;19(8):1495–510. <https://doi.org/10/gjwcdk> PMID: 33945200
 23. Koch A, Wassenegger M. Host-induced gene silencing – mechanisms and applications. *New Phytologist*. 2021;231(1):54–9. <https://doi.org/10/gnnbxn>
 24. Rank AP, Koch A. Lab-to-field transition of RNA spray applications – How far are we? *Frontiers in Plant Science*. 2021;12:2243. <https://doi.org/10/gnnbx2>
 25. Zotti M, dos Santos EA, Cagliari D, Christiaens O, Taning CNT, Smagghe G. RNA interference technology in crop protection against arthropod pests, pathogens and nematodes. *Pest Management Science*. 2018;74(6):1239–50. <https://doi.org/10/gh58f6>
 26. Nityagovsky NN, Kiselev KV, Suprun AR, Dubrovina AS. Exogenous dsRNA induces RNA interference of a chalcone synthase gene in *Arabidopsis thaliana*. *Int J Mol Sci*. 2022 May 10;23(10):5325. <https://doi.org/10.3390/ijms23105325> PMID: 35628133
 27. Marcianò D, Ricciardi V, Marone Fassolo E, Passera A, Bianco PA, Failla O, et al. RNAi of a putative grapevine susceptibility gene as a possible downy mildew control strategy. *Frontiers in Plant Science* [Internet]. 2021 [cited 2023 Sep 4];12. <https://doi.org/10.3389/fpls.2021.667319>

28. Nerva L, Guaschino M, Pagliarani C, De Rosso M, Lovisolo C, Chitarra W. Spray-induced gene silencing targeting a glutathione S-transferase gene improves resilience to drought in grapevine. *Plant Cell Environ.* 2022 Feb;45(2):347–61. <https://doi.org/10.1111/pce.14228> PMID: 34799858
29. Bachman P, Fischer J, Song Z, Urbanczyk-Wochniak E, Watson G. Environmental fate and dissipation of applied dsRNA in soil, aquatic systems, and plants. *Frontiers in Plant Science.* 2020;11:21. <https://doi.org/10/gmb7sh>
30. Christiaens O, Petek M, Smaghe G, Taning CNT. The use of nanocarriers to improve the efficiency of RNAi-based pesticides in agriculture. In: Fraceto LF, S.S. de Castro VL, Grillo R, Ávila D, Caixeta Oliveira H, Lima R, editors. *Nanopesticides: from research and development to mechanisms of action and sustainable use in agriculture* [Internet]. Cham: Springer International Publishing; 2020 [cited 2021 Dec 9]. p. 49–68. https://doi.org/10.1007/978-3-030-44873-8_3
31. Bennett M, Deikman J, Hendrix B, Iandolino A. Barriers to efficient foliar uptake of dsRNA and molecular barriers to dsRNA activity in plant cells. *Front Plant Sci.* 2020 Jun 12;11:816. <https://doi.org/10/gmb7zw> PMID: 32595687
32. Uslu VV, Bassler A, Krczal G, Wassenegger M. High-pressure-sprayed double stranded RNA does not induce RNA interference of a reporter gene. *Frontiers in Plant Science.* 2020;11:1976. <https://doi.org/10/gnr952>
33. Zhang H, Cao Y, Xu D, Goh NS, Demirer GS, Cestellos-Blanco S, et al. Gold-nanocluster-mediated delivery of siRNA to intact plant cells for efficient gene knockdown. *Nano Lett.* 2021 Jul 14;21(13):5859–66. <https://doi.org/10/gmbg64>
34. Xu X, Jiao Y, Shen L, Li Y, Mei Y, Yang W, et al. Nanoparticle-dsRNA treatment of pollen and root systems of diseased plants effectively reduces the rate of tobacco mosaic virus in contemporary seeds. *ACS Appl Mater Interfaces.* 2023 Jun 21;15(24):29052–63. <https://doi.org/10.1021/acscami.3c02798>
35. Janes KA, Fresneau MP, Marazuela A, Fabra A, Alonso MJ. Chitosan nanoparticles as delivery systems for doxorubicin. *Journal of Controlled Release.* 2001 Jun 15;73(2):255–67. [https://doi.org/10.1016/S0168-3659\(01\)00294-2](https://doi.org/10.1016/S0168-3659(01)00294-2)
36. Zhao J, Wu J. Preparation and characterization of the fluorescent chitosan nanoparticle probe. *Chinese Journal of Analytical Chemistry.* 2006 Nov 1;34(11):1555–9. [https://doi.org/10.1016/S1872-2040\(07\)60015-2](https://doi.org/10.1016/S1872-2040(07)60015-2)
37. Yu J, Wang D, Geetha N, Khawar KM, Jogaiah S, Mujtaba M. Current trends and challenges in the synthesis and applications of chitosan-based nanocomposites for plants: A review. *Carbohydrate Polymers.* 2021 Jun 1;261:117904. <https://doi.org/10.1016/j.carbpol.2021.117904>
38. Landry MP, Mitter N. How nanocarriers delivering cargos in plants can change the GMO landscape. *Nat Nanotechnol.* 2019 Jun;14(6):512–4. <https://doi.org/10.1038/s41565-019-0463-5>
39. Wang Y, Yan Q, Lan C, Tang T, Wang K, Shen J, et al. Nanoparticle carriers enhance RNA stability and uptake efficiency and prolong the protection against *Rhizoctonia solani*. *Phytopathology Research.* 2023 Jan 11;5(1):2. <https://doi.org/10.1186/s42483-023-00157-1>

40. Hubbard JD, Lui A, Landry MP. Multiscale and multidisciplinary approach to understanding nanoparticle transport in plants. *Current Opinion in Chemical Engineering*. 2020 Dec 1;30:135–43. <https://doi.org/10.1016/j.coche.2020.100659>
41. Babu A, Ramesh R. Multifaceted Applications of Chitosan in Cancer Drug Delivery and Therapy. *Marine Drugs*. 2017 Apr;15(4):96. <https://doi.org/10.3390/md15040096>
42. Cao Y, Tan YF, Wong YS, Liew MWJ, Venkatraman S. Recent Advances in Chitosan-Based Carriers for Gene Delivery. *Marine Drugs*. 2019 Jun;17(6):381. <https://doi.org/10.3390/md17060381>
43. Saharan V, Pal A. Chitosan based nanomaterials in plant growth and protection [Internet]. New Delhi: Springer India; 2016 [cited 2022 Apr 14]. (SpringerBriefs in Plant Science). <https://doi.org/10.1007/978-81-322-3601-6>
44. Qin CQ, Du YM, Xiao L. Effect of hydrogen peroxide treatment on the molecular weight and structure of chitosan. *Polymer Degradation and Stability*. 2002 Jan 1;76(2):211–8. [https://doi.org/10.1016/S0141-3910\(02\)00016-2](https://doi.org/10.1016/S0141-3910(02)00016-2)
45. Su Y, Ashworth V, Kim C, Adeleye AS, Rolshausen P, Roper C, et al. Delivery, uptake, fate, and transport of engineered nanoparticles in plants: a critical review and data analysis. *Environ Sci: Nano*. 2019;6(8):2311–31. <https://doi.org/10.1039/C9EN00461K>
46. Petrônio MS, Barros-Alexandrino TT, Lima AMF, Assis OBG, Nagata AKI, Nakasu EYT, et al. Physicochemical and toxicity investigation of chitosan-based dsRNA nanocarrier formation. *Biointerface Research in Applied Chemistry*. 2022 Aug 15;12(4):14. <https://doi.org/10.33263/BRIAC124.52665279>
47. Caprifico AE, Polycarpou E, Foot PJS, Calabrese G. Biomedical and Pharmacological Uses of Fluorescein Isothiocyanate Chitosan-Based Nanocarriers. *Macromolecular Bioscience*. 2021;21(1):2000312. <https://doi.org/10.1002/mabi.202000312>
48. Hu P, An J, Faulkner MM, Wu H, Li Z, Tian X, et al. Nanoparticle charge and size control foliar delivery efficiency to plant cells and organelles. *ACS Nano*. 2020 Jul 28;14(7):7970–86. <https://doi.org/10.1021/acsnano.9b09178>
49. Zhang H, Goh NS, Wang JW, Pinals RL, González-Grandío E, Demirer GS, et al. Nanoparticle cellular internalization is not required for RNA delivery to mature plant leaves. *Nat Nanotechnol*. 2022 Feb;17(2):197–205. <https://doi.org/10.1038/s41565-021-01018-8>
50. Demirer GS, Zhang H, Goh NS, Pinals RL, Chang R, Landry MP. Carbon nanocarriers deliver siRNA to intact plant cells for efficient gene knockdown. *Science Advances*. 2020;6(26):12. <https://doi.org/10.1126/sciadv.aaz0495>
51. Maximova N, Dahl O. Environmental implications of aggregation phenomena: current understanding. *Current Opinion in Colloid & Interface Science*. 2006 Oct;11(4):246–66. <https://doi.org/10.1016/j.cocis.2006.06.001>
52. Avellan A, Yun J, Morais BP, Clement ET, Rodrigues SM, Lowry GV. Critical Review: Role of Inorganic Nanoparticle Properties on Their Foliar Uptake and in Planta Translocation. *Environ Sci Technol*. 2021 Oct 19;55(20):13417–31. <https://doi.org/10.1021/acs.est.1c00178>

53. Ballikaya P, Brunner I, Coccozza C, Grolimund D, Kaegi R, Murazzi ME, et al. First evidence of nanoparticle uptake through leaves and roots in beech (*Fagus sylvatica* L.) and pine (*Pinus sylvestris* L.). *Tree Physiology*. 2023 Feb 1;43(2):262–76. <https://doi.org/10.1093/treephys/tpac117>
54. Hoang BTL, Fletcher SJ, Brosnan CA, Ghodke AB, Manzie N, Mitter N. Rnai as a foliar spray: efficiency and challenges to field applications. *International Journal of Molecular Sciences*. 2022 Jan;23(12):6639. <https://doi.org/10.3390/ijms23126639>
55. Lawson T. Guard cell photosynthesis and stomatal function. *New Phytol*. 2009;181(1):13–34. <https://doi.org/10.1111/j.1469-8137.2008.02685.x> PMID: 19076715
56. Mitter N, Worrall EA, Robinson KE, Xu ZP, Carroll BJ. Induction of virus resistance by exogenous application of double-stranded RNA. *Current Opinion in Virology*. 2017 Oct 1;26:49–55. <https://doi.org/10.1016/j.coviro.2017.07.009>
57. Uslu VV, Wassenegger M. Critical view on RNA silencing-mediated virus resistance using exogenously applied RNA. *Current Opinion in Virology*. 2020 Jun 1;42:18–24. <https://doi.org/10.1016/j.coviro.2020.03.004>
58. Mitter N, Worrall EA, Robinson KE, Li P, Jain RG, Taochy C, et al. Clay nanosheets for topical delivery of RNAi for sustained protection against plant viruses. *Nature Plants*. 2017 Jan 9;3(2):1–10. <https://doi.org/10.1038/nplants.2016.207>
59. Nerva L, Sandrini M, Gambino G, Chitarra W. Double-stranded RNAs (dsRNAs) as a sustainable tool against gray mold (*Botrytis cinerea*) in grapevine: effectiveness of different application methods in an open-air environment. *Biomolecules*. 2020 Feb;10(2):200. <https://doi.org/10/ggkdx>
60. Grenha A. Chitosan nanoparticles: a survey of preparation methods. *Journal of Drug Targeting*. 2012 May 1;20(4):291–300. <https://doi.org/10.3109/1061186X.2011.654121> PMID: 22296336
61. Yang H-C, Wang W-H, Huang K-S, Hon M-H. Preparation and application of nanochitosan to finishing treatment with anti-microbial and anti-shrinking properties. *Carbohydrate Polymers*. 2010 Jan 5;79(1):176–9. <https://doi.org/10.1016/j.carbpol.2009.07.045>
62. Nerva L, Guaschino M, Pagliarani C, De Rosso M, Lovisolo C, Chitarra W. Spray-induced gene silencing targeting a glutathione S-transferase gene improves resilience to drought in grapevine. *Plant, Cell & Environment*. 2022;45(2):347–61. <https://doi.org/10/gpg2tg>
63. Chitarra W, Cuozzo D, Ferrandino A, Secchi F, Palmano S, Perrone I, et al. Dissecting interplays between *Vitis vinifera* L. and grapevine virus B (GVB) under field conditions. *Molecular Plant Pathology*. 2018;19(12):2651–66. <https://doi.org/10.1111/mpp.12735>
64. Nerva L, Giudice G, Quiroga G, Belfiore N, Lovat L, Perria R, et al. Mycorrhizal symbiosis balances rootstock-mediated growth-defence tradeoffs. *Biol Fertil Soils*. 2022 Jan 1;58(1):17–34. <https://doi.org/10/gpg2wf>

- 65.** Nerva L, Varese GC, Falk BW, Turina M. Mycoviruses of an endophytic fungus can replicate in plant cells: evolutionary implications. *Sci Rep.* 2017 May 15;7(1):1908. <https://doi.org/10/gc4sk7>
- 66.** Vuerich M, Petrusa E, Filippi A, Cluzet S, Fonayet JV, Sepulcri A, et al. Antifungal activity of chili pepper extract with potential for the control of some major pathogens in grapevine. *Pest Management Science.* 2023;79(7):2503–16. <https://doi.org/10.1002/ps.7435>
- 67.** Arzt M, Deschamps J, Schmied C, Pietzsch T, Schmidt D, Tomancak P, et al. LABKIT: labeling and segmentation toolkit for big image data. *Frontiers in Computer Science* [Internet]. 2022 [cited 2023 Aug 23];4. <https://doi.org/10.3389/fcomp.2022.777728>
- 68.** Schindelin J, Arganda-Carreras I, Frise E, Kaynig V, Longair M, Pietzsch T, et al. Fiji: an open-source platform for biological-image analysis. *Nat Methods.* 2012 Jul;9(7):676–82. <https://doi.org/10.1038/nmeth.2019>

SUPPORTING INFORMATION

Table S1. Relative quantity (RQ) of GFP-dsRNA on leaves detached from treated plants. Values are weighted to the quantity of GFP-dsRNA at day 0 (RQ=1). Data are expressed as mean \pm SE ($n = 3$).

Days after treatment	Treatment	GFP-dsRNA RQ
7	Empty NPsF	0.02 \pm 0.005
7	Naked RNA	0.93 \pm 0.203
7	NPsF-RNA	0.96 \pm 0.178
15	Empty NPsF	0.02 \pm 0.004
15	Naked RNA	0.79 \pm 0.140
15	NPsF-RNA	0.94 \pm 0.205

Table S2. t test between different treatments on *N. benthamiana* leaves infected by *B. cinerea*. Data are expressed as mean \pm SD ($n = 12$) and were compared by coupled double tail t test.

Treatment comparison		t test significance
<i>Bc</i>	<i>Bc</i> + NPsF	0.951
<i>Bc</i>	<i>Bc</i> + <i>Bc</i> dsRNA-NPsF	8.027E-11
<i>Bc</i>	<i>Bc</i> + <i>Bc</i> dsRNA	8.995E-06
<i>Bc</i> + NPsF	<i>Bc</i> + <i>Bc</i> dsRNA-NPsF	1.867E-10
<i>Bc</i> + NPsF	<i>Bc</i> + <i>Bc</i> dsRNA	0.001
<i>Bc</i> + <i>Bc</i> dsRNA-NPsF	<i>Bc</i> + <i>Bc</i> dsRNA	2.072E-07

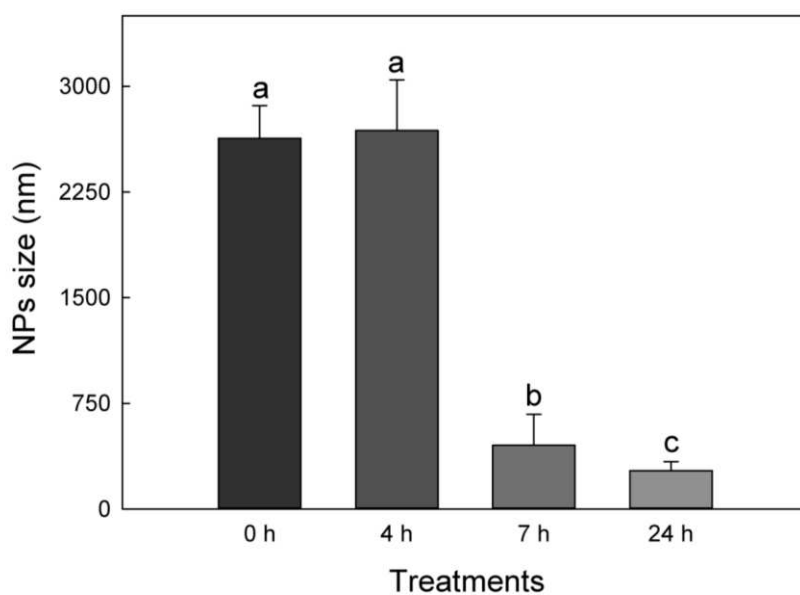


Figure S1. Effect of time duration of the chitosan degradative treatment on NP hydrodynamic diameter. Data are expressed as mean \pm SD ($n = 6$). Values with different letters are significantly different at $P > 0.05$ by post-hoc LSD test.

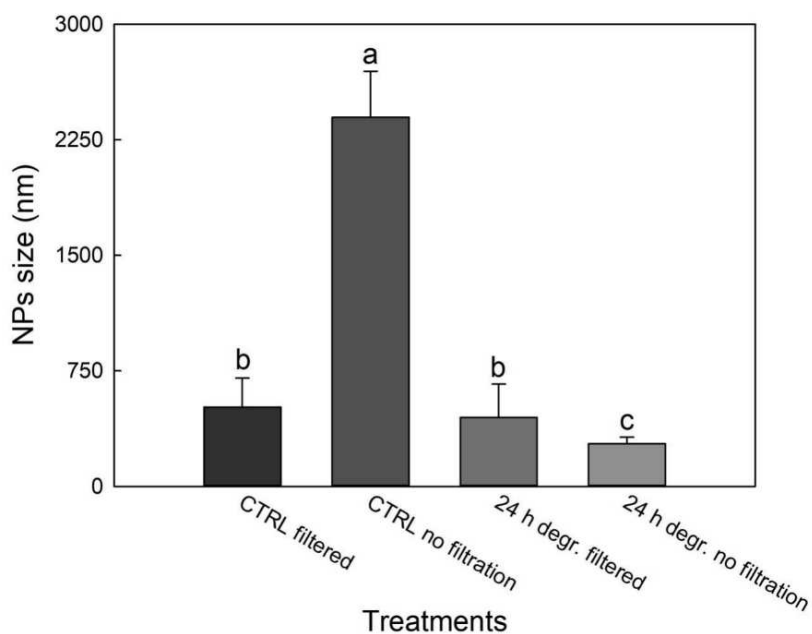


Figure S2. Effects in the size of NPs given by filtration and 24h-H₂O₂ degradation treatments on chitosan stock solution. Data are expressed as mean \pm SD ($n = 6$). Values with different letters are significantly different at $P > 0.05$ by post-hoc LSD test.

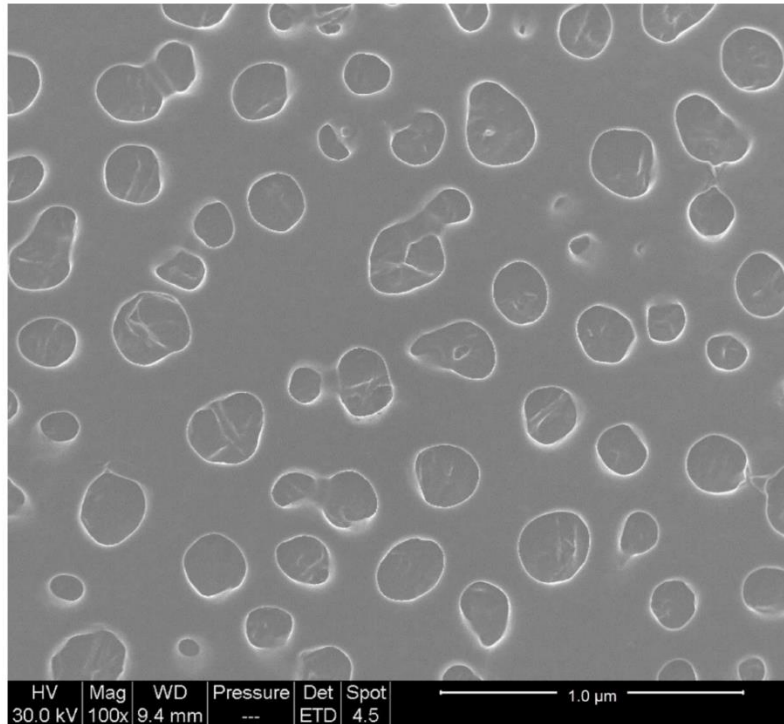


Figure S3. Image of NPsF acquired by transmission electron microscopy (TEM).

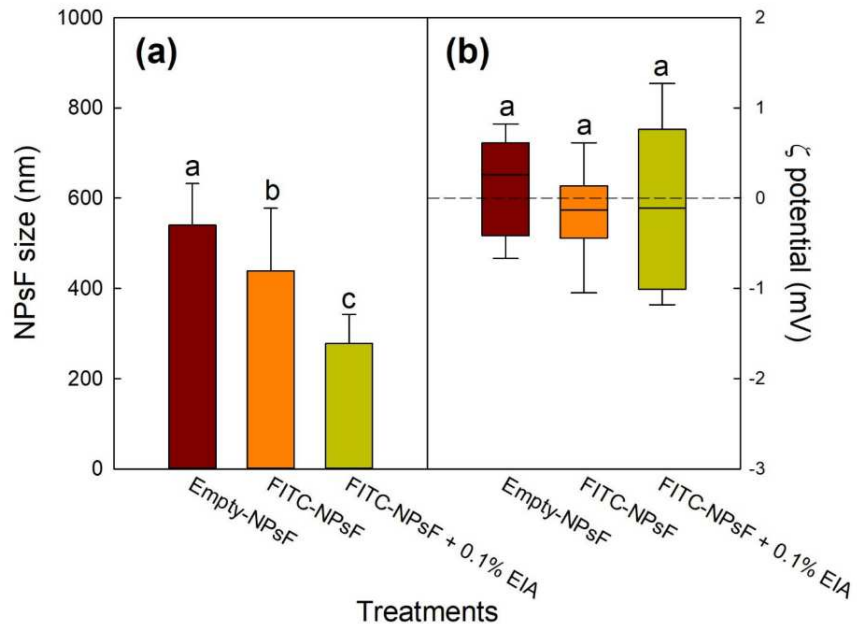


Figure S4. Determination of size (a) and ζ potential (b) of NPsF. Treatments were: NPsF as such, FITC-functionalized NPsF and FITC-functionalized NPsF suspended in 0.1% EIA solution. Data ($n = 9$) are expressed: (a) as mean \pm SD; (b) as boxplot whose whiskers correspond to the data range between minimum and maximum value, excluding outliers. Values with different letters are significantly different at $P > 0.05$ by post-hoc LSD test.

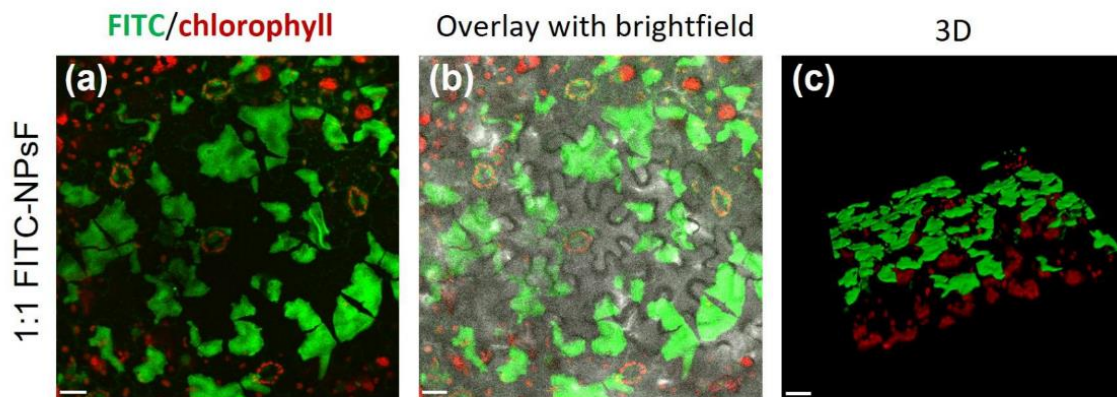


Figure S5. Confocal microscopy analysis of *N. benthamiana* leaves. Abaxial side of leaf tegument was sprayed with FITC-NPsF diluted 1:1 in 0.1% EIA. (a): Maximum intensity projection (epidermal layer); (b): projection overlay with corresponding brightfield image; (c): 3D rendering (epidermis to mesophyll; different field). Green, FITC; red, chlorophyll autofluorescence. Scalebar 20 μm .

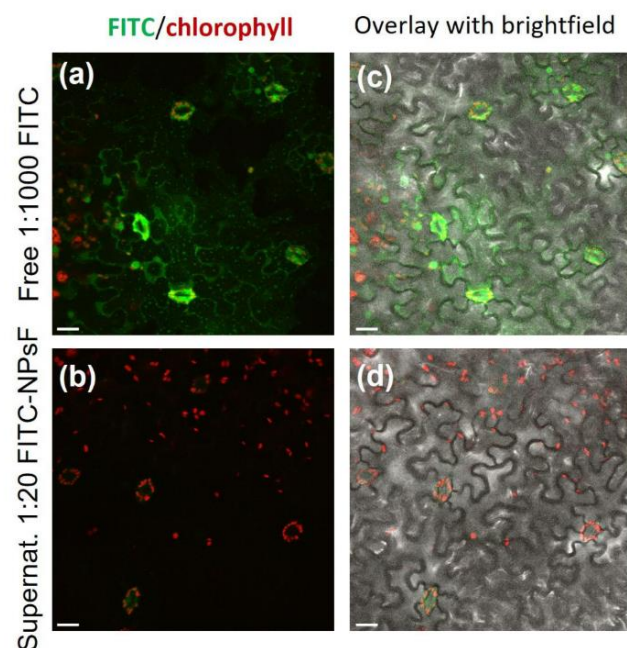



Figure S6. Maximum intensity projection confocal images of *N. benthamiana* leaves. *N. benthamiana* abaxial side of leaf teguments was sprayed with (a, c) free FITC solution (1:1000) or with (b, d) the supernatant of FITC-NPsF diluted 1:20 in 0.1% EIA (green, FITC; red, chlorophyll autofluorescence). Right column: projections are overlaid with corresponding brightfield images. Scalebar 20 μm .



CHAPTER 3 - Calcium Phosphate Particles Coated With Humic Substances: A Potential Plant Biostimulant From Circular Economy

Original Paper

First published: 10 may 2021

Molecules 2021, 26, 2810, MDPI

DOI: <https://doi.org/10.3390/molecules26092810>

Calcium Phosphate Particles Coated With Humic Substances: A Potential Plant Biostimulant From Circular Economy

Alessio Adamiano^{1,*}, Guido Fellet², Marco Vuerich², **Dora Scarpin**², Francesca Carella¹, Clara Piccirillo³, Jong-Rok Jeon⁴, Alessia Pizzutti^{2,5}, Luca Marchiol² and Michele Iafisco¹

¹Institute of Science and Technology for Ceramics (ISTEC), National Research Council (CNR), Via Granarolo 64, 48018 Faenza, Italy; francesca.carella@istec.cnr.it (F.C.); Michele.iafisco@istec.cnr.it (M.I.).

²Department of AgriFood, Animal and Environmental Sciences, University of Udine, via delle Scienze 206, 33100 Udine, Italy; guido.fellet@uniud.it (G.F.); vuerich.marco@spes.uniud.it (M.V.); scarpin.dora@spes.uniud.it (D.S.); pizzutti.alessia@spes.uniud.it (A.P.); luca.marchiol@uniud.it (L.M.).

³Institute of Nanotechnology (NANOTEC), National Research Council (CNR), Campus Ecotekne, Via Monteroni, 73100 Lecce, Italy; clara.piccirillo@nanotec.cnr.it.

⁴Department of Agricultural Chemistry, Food Science & Technology, IALS, Gyeongsang National University, Jinju 52828, Korea; jrjeon@gnu.ac.kr.

⁵Department of Life Sciences, University of Trieste, Via Licio Giorgieri 10, 34127 Trieste, Italy.

Correspondence: alessio.adamiano@istec.cnr.it. Tel.: +39-054-669-9724

Keywords: calcium phosphate; humic substances; plant biostimulants; circular economy; phosphorous; nutrients uptake.

ABSTRACT

Nowadays, the use of biostimulants to reduce agrochemical input is a major trend in agriculture. In this work, we report on calcium phosphate particles (CaP) recovered from the circular economy, combined with natural humic substances (HSs), to produce a plant biostimulant. CaPs were obtained by the thermal treatment of *Salmo salar* bones and were subsequently functionalized with HSs by soaking in a HS water solution. The obtained materials were characterized, showing that the functionalization with HS did not sort any effect on the bulk physicochemical properties of CaP, with the exception of the surface charge that was found to get more negative. Finally, the effect of the materials on nutrient uptake and translocation in the early stages of development (up to 20 days) of two model species of interest for horticulture, *Valerianella locusta* and *Diplotaxis tenuifolia*, was assessed. Both species exhibited a similar tendency to accumulate Ca and P in hypogeal tissues, but showed different reactions to the treatments in terms of translocation to the leaves. CaP and CaP-HS treatments lead to an increase of P accumulation in the leaves of *D. tenuifolia*, while the treatment with HS was found to increase only the concentration of Ca in *V. locusta* leaves. A low biostimulating effect on both plants' growth was observed, and was mainly scribed to the low concentration of HS in the tested materials. In the end, the obtained material showed promising results in virtue of its potential to elicit phosphorous uptake and foliar translocation by plants.

INTRODUCTION

Intensive farming has been extensively adopted in recent years to cope with the increasing global food demand [1]. Unfortunately, this practice often fails sustainability principles as it requires the use of massive quantities of pesticides and nutrients involving the depletion of non-renewable resources. In this context, the use of biostimulants for increasing plant nutrient use efficiency (NUE) have been proposed several times to reduce the chemical inputs of intensive farming while maintaining high productivity levels [2].

Among the various biostimulants, humic substances (HS) are among the most studied in virtue of (i) their ability to stimulate plant growth and increase nutrient uptake and hormone production; (ii) their natural occurrence in soils; and (iii) their positive interaction with soil bacterial communities [3,4]. As an example, Purwanto et al. studied the effects of different combinations of HS extracted from composted manure and P_2O_5 on different corn cultivars [5], reporting a substantial growth in the crop yields due to an increase in the crop root dimensions - that in turn boosted the P uptake - to a significant improvement of the physiological performance of plants. HSs were also found to elicit physiological processes of plants, promoting abiotic stress resistance, in particular salt tolerance and drought stress, in several plants such as *Capsicum annum*, *Oryza sativa*, and *Phaseolus vulgaris* [6–9]. Moreover, it has been proved that HSs have the ability to interact with calcium phosphates [10] and increase P bioavailability in the soil, often present in the form of insoluble complexes [6].

In a previous work, some of the authors have functionalized synthetic hydroxyapatite nanoparticles, which were already proposed for agronomic applications [11], with soil friendly HS to produce a nanocarrier that could efficiently deliver both nutrients and biostimulants toward plants [12]. The results obtained on corn plants showed that the co-release of P and HS from the nanoparticles leads to a boost of crop biomass growth and of abiotic stress resistance. In another work, we showed that calcium phosphate particles (CaP) extracted from fish bones at different temperatures (*i.e.*, in the 300–900°C range) have the ability to increase the germination rate of *Lepidium sativum* seeds, and to boost the growth of *Zea mays* coleoptiles and plants [13].

Thus, in an attempt to produce a biostimulant from circular economy with potential agronomic applications, here we report on the production of CaP obtained from the thermal treatment of salmon (*Salmo salar*) bones and on their engineering with natural HS. The rationale behind this study is that HS could be combined with CaP to obtain a biostimulant with improved performances. The obtained materials were applied on *Diplotaxis tenuifolia* and *Valerianella locusta* that were chosen as test species in virtue of their wide use in horticulture. Attention was paid to investigate the different effects on the early growth (up to 20 days), nutrient uptake, and elements translocation from the roots to the leaves, and highlight species-specific responses by the two plants.

RESULTS

1. Materials Characterization

Pictures of the materials obtained from the calcination of salmon bones and of those derived from its functionalization with HS are reported in Figure 1. The sample without HS treatment is named CaP hereafter, while that obtained by soaking CaP in a water solution of HS at 0.1 g L^{-1} is named CaP-HS. The functionalization with HS changed the color of the materials from the white of CaP to the brownish/greyish of CaP-HS.

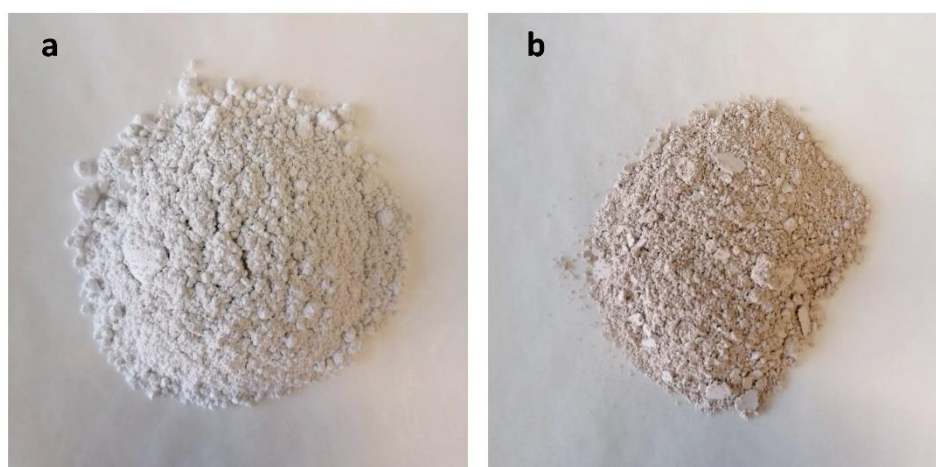


Figure 1. Pictures of the calcium phosphate before (a) and after soaking in a humic acid solution at 0.1 g mL^{-1} (b).

Samples were analyzed by XRD, and the collected spectra are reported in Figure 2. The XRD patterns indicate that both the samples consist of a bi-phasic mixture of beta-tricalcium phosphate (β -TCP, $\beta\text{-Ca}_3(\text{PO}_4)_2$) and hydroxyapatite (HA, $\text{Ca}_{10}(\text{PO}_4)_6$). In more detail, the spectra are featured by the occurrence of peaks typical of HA, located at 2θ values of 25.9° , 31.7° , 32.9° , 34.0° , 46.7° , and 49.5° corresponding to the lattice planes with Miller indexes (0 0 2), (2 1 1), (3 0 0), (2 0 2), (2 2 2), and (2 1 3), respectively, and of peaks typical of β -TCP located at 2θ values of 13.6° , 17.0° , 27.8° , 31.0° , and 34.3° , corresponding to the lattice planes (1 0 4), (1 1 0), (2 1 4), (0 2 10), (2 2 0), respectively. Finally, all of the spectra are characterized by the occurrences of sharp and resolved peaks with no difference between bare CaP and CaP-HS.

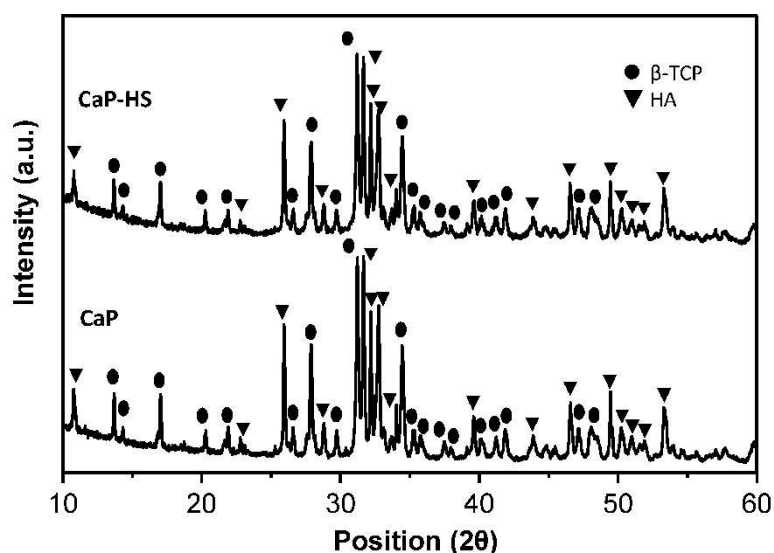


Figure 2. XRD patterns of bare CaP and CaP functionalized with HS (CaP–HS).

The crystallinity indexes (CI) calculated according to Equation (1) are displayed in Table 1, together with the phase compositions calculated by Rietveld refinement, the analysis of the main element by ICP–OES and the amount of HS determined by TGA. Both the materials are characterized by the occurrence of β -TCP and by HA with a weight ratio close to 60:40, respectively, with no difference between bare CaP and CaP–HS. The CI shows that the samples are all highly crystalline, as typically reported in the literature for calcium phosphates obtained by treating fish bones at temperatures around 800 °C, and that the HS functionalization did not have any effect on the crystallinity [13,14]. The ICP results show that samples have a similar chemical composition with no statistically significant difference among them for Ca, P, and Mg content (student-*t* test, $p < 0.05$). Finally, CaP has a slightly higher content of K and Na with respect to CaP–HS.

Table 1. Phase, chemical composition and surface charge of the samples.

Sample	CaP	CaP–HS
HA (wt.%) ^a	42.8 ± 1.7	42.6 ± 1.3
β -TCP (wt.%) ^a	57.1 ± 1.7	57.4 ± 1.2
CI (a.u.) ^a	61.4 ± 0.5	61.2 ± 0.5
Ca (wt.%) ^b	34.0 ± 0.3	33.5 ± 0.6
P (wt.%) ^b	18.7 ± 0.2	18.3 ± 0.4
K (wt.%) ^b	1.64 ± 0.02	1.11 ± 0.01
Mg (wt.%) ^b	0.69 ± 0.01	0.67 ± 0.01
Na (wt.%) ^b	1.80 ± 0.34	1.26 ± 0.03
Ca/P molar ratio ^b	1.41 ± 0.01	1.41 ± 0.01
Humic acid (wt.%) ^c	-	0.4
ζ -potential ^d	-23.0 ± 1.0	-29.5 ± 0.2

^a Determined by XRD, ^b Determined by ICP-OES, ^c Determined by TGA, ^d Determined by DLS.

The ATR spectra of the materials are reported in Figure 3 and confirmed the occurrence of β -TCP and HA in all the samples. The main IR bands of these phases, corresponding to the triply degenerated asymmetric stretching vibration mode (ν_3) of the phosphate tetrahedron, are really close, 1040 and 1042 cm^{-1} for HA and β -TCP, respectively, and are superimposed. However, the typical β -TCP bands are visible at 980 and 945 cm^{-1} , corresponding to the stretching mode (ν_1) of PO_4 , and at 590 and 550 cm^{-1} , corresponding to the triply degenerated bending mode (ν_4) of PO_4 [15]. Characteristics HA bands corresponding to the triply degenerated bending mode (ν_4) and to the asymmetric stretching mode (ν_1) of PO_4 are also visible at 962 and 562 cm^{-1} , respectively [16,17]. On the other hand, the spectrum of pure humic acid is characterized by signals ascribable to COO^- , $-\text{C}-\text{NO}_2$, and $\text{C}=\text{C}$ groups (1550 cm^{-1}), and to $-\text{CO}-\text{CH}_3$ and possibly nitrate groups (1360 cm^{-1}) [18]. These signals are absent in the spectrum of CaP, but the signal at 1550 cm^{-1} is present in that of CaP-HS, confirming the presence of HS as already detected by TGA.

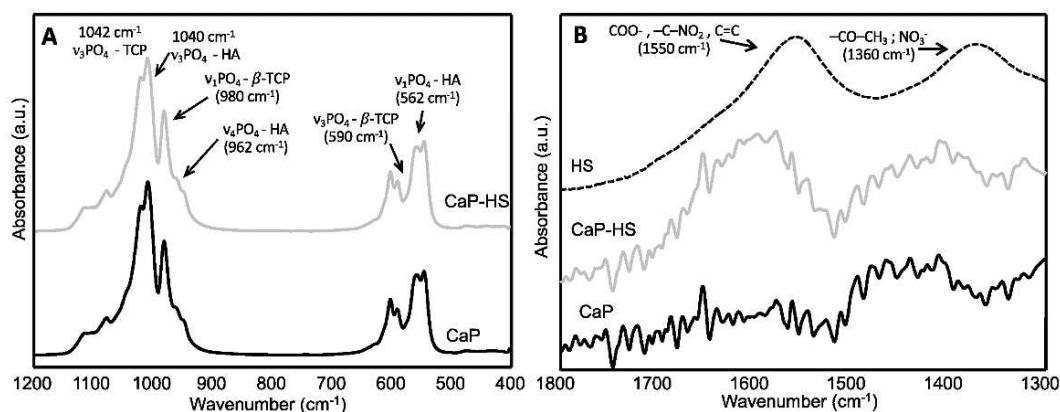


Figure 3. FT-IR spectra of CaP, CaP-HS and HS. The range of the spectra where the main IR bands of HA and β -TCP appear (1200–400 cm^{-1}) is reported on the left (A), while a magnification of the FT-IR spectra in the region where the typical IR bands of HS (1800–1300 cm^{-1}) occur is reported on the right (B).

The ζ -potential of the particles determined by DLS and reported in Table 1 was found to be more negative for the CaP coated with HS respect to the bare one. Finally, the engineering of the particles surface did not sort any effect on the specific surface area of CaP-HS (8.50 $\text{m}^2 \text{g}^{-1}$) that was very close to that of CaP (8.53 $\text{m}^2 \text{g}^{-1}$).

Micrographs of the materials at different magnifications recorded by SEM are reported in Figure 4. All the samples are featured by the occurrence of two kind of particles with a different morphology: (i) coarser and flattened particles with round shape and smooth edges, with a size in the range 1.0–2.0 μm ; and (ii) elongated rod-like particles with a minor axis in the size range 0.05–0.10 μm and a major axis with size in the range 0.1–1.0 μm . The first morphology can be ascribed to β -TCP crystals, while the second

one can be ascribed to HA [19]. No difference can be noticed between bare CaP and CaP coated with HS.

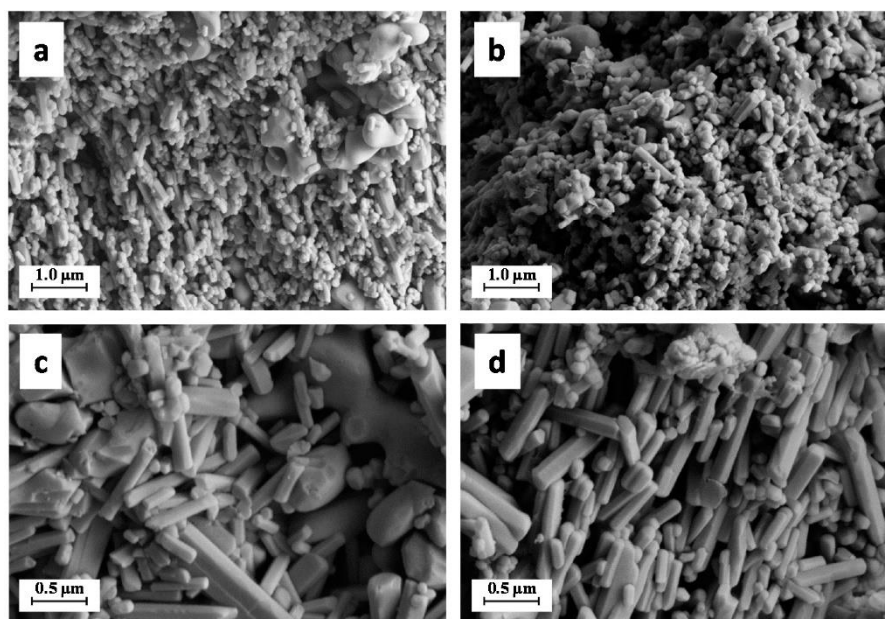


Figure 4. SEM pictures of CaP (a,c) and CaP-HS (b,d) at 50,000× magnification on the top (a,b) and 100,000× magnification on the bottom (c,d).

2. Observations on Plant Species

2.1. Germination and Seedlings Development

A two-way ANOVA was run within the species *D. Diplotaxis* and *V. tenuifolia* to highlight the effects of treatments (Tables S1–S4). Interaction effects represent the combined effects of experimental factors on the dependent parameter.

The recorded observations show that the experimental treatments did not influence seeds germination percentage. Although non-treated seeds had the lowest percentage of germination for both species, data variability has hidden statistical evidence of response to the treatments (Tables S3 and S4), which were not significant by ANOVA ($p = 0.7834$ and $p = 0.2106$, respectively for *D. tenuifolia* and *V. locusta*).

Regarding the root length, the species' response was different, this difference being statistically significant ($p < 0.01$) for *V. locusta* (Table S2) and not significant for *D. tenuifolia* respectively. In the case of *D. tenuifolia*, all treatments resulted in a reduction in the root system's development (Table 2), with seedlings treated with CaP having –12.8% in root length if compared to control plants. A similar effect was recorded for CaP-HS (–13.3%). On the contrary, in *V. locusta* seedlings the root system's development was significantly stimulated by HS and the combination of HS and CaP by 6% and 20% more compared to control, respectively (Table 3).

Table 2. Seedling root length, root, and shoot dry weight, and ATP concentration in shoots of *Diplotaxis tenuifolia*. Data are expressed as mean \pm standard deviation ($n = 4$). Different letters indicate statistically significant difference between treatments at Tukey's post-hoc test ($p \leq 0.05$).

Treatments	Root Length (mm plant ⁻¹)	Roots DW (mg plant ⁻¹)	Shoot ATP (nmol g ⁻¹ DW)	Shoot DW (mg plant ⁻¹)
Ctrl	65.0 \pm 8.83	5.08 \pm 1.75 B *	0.094 \pm 0.026	21.0 \pm 0.75 b
HS	49.3 \pm 10.4	3.88 \pm 1.72 B	0.115 \pm 0.031	24.7 \pm 2.33 ab
CaP	56.7 \pm 7.39	7.63 \pm 2.46 A	0.093 \pm 0.023	25.0 \pm 3.83 a
CaP-HS	56.4 \pm 2.33	6.28 \pm 2.56 A	0.123 \pm 0.031	21.3 \pm 2.27 ab

* Capital letters beside the figures mean that the effect of the CaP treatment is significant for the variable in question according to the Tukey's post-hoc test, while small letters mean that the interaction CaP \times HS is significant.

Table 3. Seedling root length, root and shoot dry weight, and ATP concentration in shoots of *Valerianella locusta*. Data are expressed as mean \pm standard deviation ($n = 4$). Different letters indicate statistically significant difference between treatments at Tukey's post-hoc test ($p \leq 0.05$).

Treatments	Root Length (mm plant ⁻¹)	Roots DW (mg plant ⁻¹)	Shoot ATP (nmol g ⁻¹ DW)	Shoot DW (mg plant ⁻¹)
Ctrl	45.2 \pm 4.54 b *	6.23 \pm 1.46	0.090 \pm 0.011	15.6 \pm 1.78 b *
HS	48.2 \pm 4.79 a	6.00 \pm 0.84	0.087 \pm 0.005	18.7 \pm 0.05 a
CaP	41.8 \pm 4.50 b	6.27 \pm 0.77	0.078 \pm 0.011	16.1 \pm 1.74 b
CaP-HS	54.3 \pm 5.05 a	7.73 \pm 0.33	0.083 \pm 0.006	17.7 \pm 0.33 a

* Capital letters beside figures mean that the effect of the CaP treatment is significant for the variable in question according to the Tukey's post-hoc test, while small letters mean that the interaction CaP \times HS is significant.

The accumulation of dry matter in the root tissues of *D. tenuifolia* responded significantly to treatments (Table S1). In details, the presence of CaP alone or in combination with HS stimulated a significant increase in the dry weight of the roots of +50.1% and +23.6% compared with control, respectively (Table 2). On the other hand, a negative trend for HS, although not statistically significant, was recorded for both the treatments with HS, *i.e.*, HS alone and in combination with CaP (Table 2).

In the case of *V. locusta*, treatments did not affect significantly roots dry weight; however, a different response could be observed with respect to *D. tenuifolia*, since the stimulating effect of CaP was practically nullified (Table 3). The dry matter accumulation was the highest with CaP-HS treatment (7.73 mg plant⁻¹), equal to +24% with respect to the control.

The root specific weight was calculated by combining roots' cumulative length and dry weight. In both the species, this variable was not affected by the imposed treatments (Tables S3 and S4).

Regarding the dry matter accumulation in the aerial part of plantlets, *D. tenuifolia* was affected by the interaction of CaP and HS ($p < 0.05$) (Table S1). An increase (+19%) was observed in the presence of CaP alone, whereas for CaP-HS, the shoot dry weight was similar to the control (Table 2). A more pronounced increase in DM shoot accumulation was recorded in *V. locusta* (Table 3). In this case, the treatment responses were statistically significant for HS ($p = 0.002$ *, Table S2). The effect of CaP was negligible, whereas HS stimulated the shoot biomass production (+19.8% and +13.5% compared to control, respectively) (Table 2).

The total DW per plant was calculated by adding the dry weight of plantlet fractions (Tables S3 and S4). According to the measured data, the species' treatment response was not significant for both species.

In the experimental conditions, the shoots' energetic status represented by ATP concentration was not influenced by the treatments. No statistically significant differences were observed in both species (Table 2 and Table 3).

2.2. Element Concentration in Seedling Roots and Shoot

Considering the two species separately, the effect of treatments on nutrients concentration was noticeably different, both in roots and leaves, but similarities were highlighted especially for P and Ca concentrations, whose high correlation in the global data set is certified by Figure S1.

In *D. tenuifolia*, the effect of CaP on the Ca level in the roots was significant ($p < 0.001$), with an increase in its concentration regardless of the presence of HS (Figure 5A). A similar result was found for the concentration of P in roots, with the same degree of significance (Figure 5B).

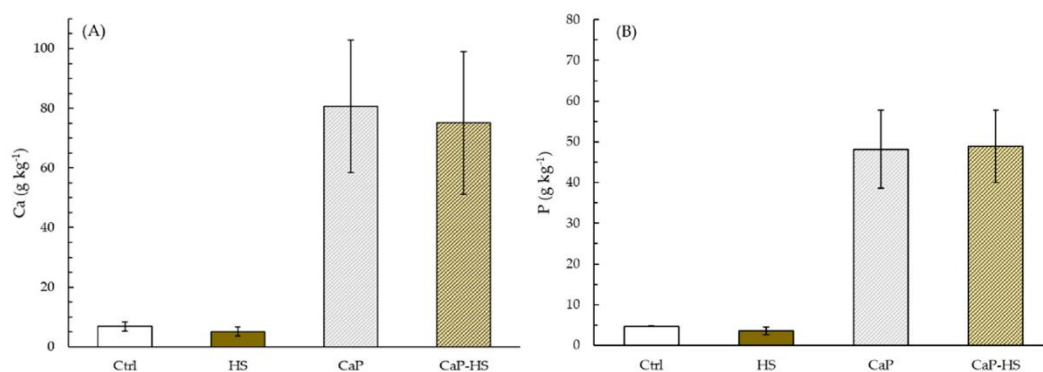


Figure 5. Concentration of Ca (A) and P (B) in root of *Diplotaxis tenuifolia*. Data are mean \pm standard deviation ($n = 4$). When the interaction between experimental factors (CaP \times HS) was significant at ANOVA, different letters were used to indicate statistically significant differences between treatments at Tukey's post-hoc test ($p \leq 0.05$).

The Mg level in root was significantly modulated by CaP and HS factors ($p < 0.001$, $p < 0.05$), showing a decreasing trend in concentration in the presence of HS if compared

to control or CaP alone, which instead slightly increased Mg content (Figure S2). The level of K in roots was affected mainly by HS treatment ($p < 0.01$), while the interaction effect between factors was low ($p = 0.027$): the presence of HS seemed to reduce K content in roots, with a strong depression particularly given by HS alone compared to the control (Figure S2).

Data obtained from leaf analysis concerning P level showed a strong statistical significance for CaP and HS treatments ($p < 0.001$), and a lower significance value for their interaction ($p < 0.05$) (Figure 6B). However, the level of P increased in plants treated with CaP and CaP–HS with an upwards trend, where the major effect was given by CaP–HS.

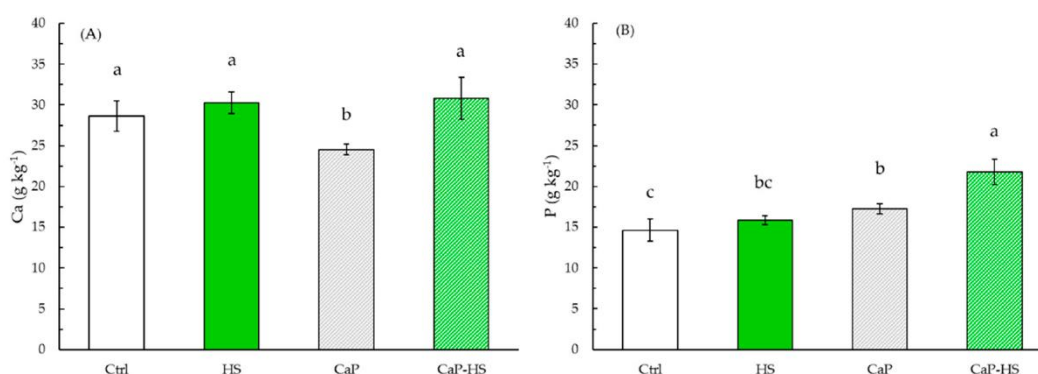


Figure 6. Concentration of Ca (A) and P (B) in leaves of *Diplotaxis tenuifolia*. Data are mean \pm standard deviation ($n = 4$). Different letters indicate statistically significant differences between means at Tukey's post-hoc test ($p \leq 0.05$).

Regarding Ca concentration, CaP and HS factors and their interaction were all significant ($p < 0.05$) (Figure 6A). Differently from P nutrient, Ca level was reduced in leaves by the application of CaP, whereas the application of both HS and CaP–HS resulted in the same Ca content of the control.

A statistical significance was also shown for HS factor ($p < 0.05$) and its interaction with CaP ($p < 0.01$) regarding K concentration in leaves: when CaP was functionalized with HS, a K-increasing effect was recorded with respect to both CaP and HS alone (Figure S3).

Considering the effect on Mg, the treatment with CaP–HS was weakly significant ($p = 0.037$). The only difference respect to the control was a slight decrease recorded for CaP treatment (Figure S3).

The response of ANOVA on data of *V. locusta* roots concerning P content showed a strong statistical significance for CaP factor ($p < 0.001$), while HS and CaP–HS factors were less significant ($p < 0.05$). While HS applied alone has given no effect on P concentration in roots compared to the control, CaP and CaP–HS showed a noticeable increase in its level, with the greatest effect being expressed by CaP (Figure 7B).

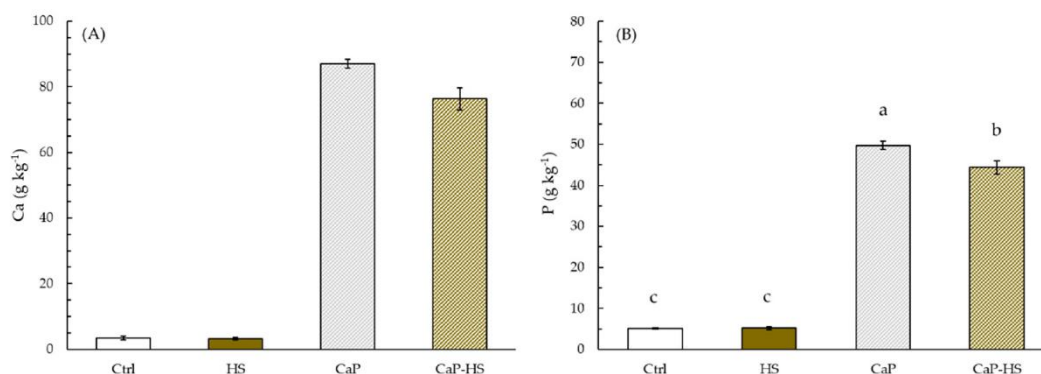


Figure 7. Concentration of Ca (A) and P (B) in roots of *Valerianella locusta*. Data are mean \pm standard deviation ($n = 4$). When the interaction between experimental factors (CaP \times HS) was significant at ANOVA, different letters were used to indicate statistically significant differences between treatments at Tukey's post-hoc test ($p \leq 0.05$).

A similar trend was also observed on Ca concentration in *V. locusta* roots (Figure 7A), but in this case only CaP factor was statistically significant ($p < 0.001$).

The tested treatments did not sort any effect on the Mg concentration in roots (data not shown), while a moderate significance ($p < 0.01$) for HS was observed from the data relating to K (Figure S4). In fact, pure HS application compared to the control showed a growing effect on K level, while when applied with CaP microparticles, the trend was the opposite.

Considering the effects on *V. locusta* leaves, also in this case we could observe a similarity between treatment's effects on P and Ca concentrations: in both of them, CaP and HS effects were statistically significant, but in the case of P, the statistical value was stronger for CaP ($p < 0.001$). Moreover, also the interaction between factors was significant for P ($p < 0.01$). In particular, when CaP was applied alone, there was a strong reduction in the concentration of P, while neither HS nor CaP-HS changed P content in leaves compared to the control (Figure 8B).

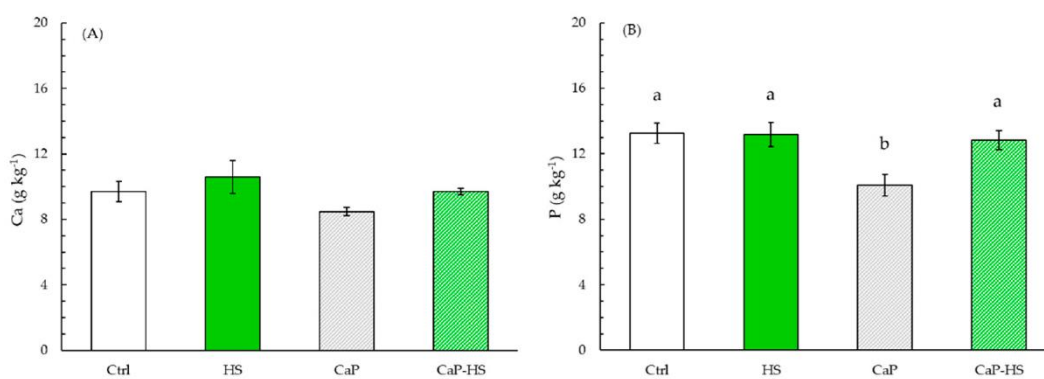


Figure 8. Concentration of Ca (A) and P (B) in leaves of *Valerianella locusta*. Data are mean \pm standard deviation ($n = 4$). When the interaction between experimental factors (CaP \times HS) was significant at ANOVA, different letters were used to indicate statistically significant differences between treatments at Tukey's post-hoc test ($p \leq 0.05$).

As for Ca level, instead, CaP and HS were equally significant ($p < 0.01$) (Figure 8A). CaP addition to nutritive substrate decreased Ca content in leaves with respect to the other treatments. On the contrary, the presence of HS, both alone and in CaP–HS, showed an increase in Ca concentration if compared with the two treatments without HS.

Finally, data regarding K and Mg concentration in leaves showed no statistical significance for none of the factors (Figure S5).

DISCUSSION

The CaP sample has been thermally extracted from salmon bones at 800 °C to be then functionalized by soaking in a water solution of HS.

As largely known in the literature, the thermal treatment of fish bones can lead to the formation of HA and β -TCP at different ratio depending on the fish species and on the temperature of treatment (usually, the higher is the temperature the larger the amount of β -TCP) [20,21]. For instance, some of the authors have previously reported that the thermal extraction of calcium phosphates from *S. aurita* bones at 900 °C leads to the formation of HA as the principal phase, and of just minor quantities of β -TCP (c.a. 5.0 wt.%) [13] differently from other fish species, such as salmon [14] and mackerel (c.a. 40.0 wt.% of β -TCP) [22]. The materials obtained from *S. aurita* are composed mainly by HA in the form of rod-like particles almost identical to the ones detected in this work for the materials extracted from *S. salar*, but do not feature flattened and larger particles ascribable to β -TCP.

The functionalization with HS did not have any effect on the main physicochemical properties of CaP. The only parameter that was found to change among the samples is, as expected, the presence of HS that was confirmed by ATR and quantified by TGA, and the ζ -potential of the particles. More in detail, the ζ -potential of bare CaP was

found to be close to that of synthetic HA [11,23], while it got more negative after the functionalization with HS. This increase in the net negative charge of the particles is due to the occurrence of HS on the surface of the CaP, and in particular to the oxygenated functional groups of natural HS getting a partial negative charge in water at neutral pH [24,25]. These data suggest that when HS is added to preformed CaP, the interaction is only superficial and HS molecules stay on the surface of the particles without penetrating the material, with no effect on its bulk structure. This is in line with what already reported in the literature for synthetic HA nanoparticles functionalized with both natural and synthetic humic substances [11,26].

HS was used in virtue of its biostimulant activity on plants and its ability to increase the water solubility of calcium phosphate particles. In more detail, HSs are complex and recalcitrant organic polymers naturally occurring in soils, having the ability to stimulate plants metabolism through genes activation, empowering their resistance to abiotic stress and increasing their germination and growth [25,27].

The aim of this work was to verify whether the coupling of HS with CaP could be useful, not only to promote the germination and development of seedlings through biostimulation, but also to facilitate the intake of nutrients in a synergistic way. In more detail, the main focus was assessing the beneficial effect on P uptake, given its limited bioavailability in mineral calcium phosphate in neutral and alkaline substrates.

What has been observed is that the response of the two chosen species was different, but, considering the effects on nutrients intake, both have shown some similarities on P and Ca concentrations, particularly in hypogeal tissues. Specifically, even if CaP has a low solubility, here it was found to be the main factor that affected P and Ca uptake in roots. On the contrary, it was observed a null effect given by HS for *D. tenuifolia*, and a possible worsening in P level in the case of *V. locusta*, when microparticles were coated with HS. This fact could be explained with a possible trade-off between the increase in CaP dissolution due to a more acidic surface and a limited contact between phosphorus and water molecules caused by HS functionalization, as already highlighted in a previous work with synthetic HA nanoparticles [11].

Considering the effect of treatments on shoots, the most interesting finding was related to P foliar content in *D. tenuifolia*: the application of CaP increased the level of P, which was further enhanced by CaP-HS. This shows the possibility of positive interaction between CaP and HS in increasing P availability, through nutrients chelation and gradual release by HS. In agreement with these results, other reports show the positive effect of humic acid applications in phosphorus fertilization [28,29] and, even more noteworthy, in calcareous soils [30,31,32].

On the contrary, in *V. locusta* Ca content in leaves was enhanced only by HS, regardless of CaP functionalization. In this case, despite an increased root absorption of this element in presence of CaP alone or CaP-HS, Ca translocation to the epigeous portion was significantly stimulated by HS, suggesting that HS could favor the xylematic transport of this macronutrient by a hormone-like activity [3,33].

At the foliar level, a similar trend was observed for Ca in the leaves of *D. tenuifolia* and Ca and P in those of *V. locusta* seedlings treated with CaP, whose concentrations were found to decrease with respect to the control. To explain these results, we hypothesized that the amount of nutrient in the medium was already sufficient to sustain plantlet metabolism and, therefore, the addition of further Ca and P through the microparticles was irrelevant or even unfavorable. In this case, the HS on the surface of CaP probably performed a restorative function through chelation, releasing the nutrients more gradually and allowing Ca and P regular translocation to the leaves; this allowed the achievement of the same saturation level already observed in the control thesis.

The fact that in some cases HS have not shown the expected biostimulating effect can be explained considering the great variability of both the experimental conditions (low concentration on the particles) and of the characteristics of the humic substances used in similar research works. For instance, Nikbakht et al. (2008) highlighted contrasting results on the effect of HS on plant nutrition, and argued that this might be partially related to different soil or growing media, origin and concentration of HS and the species treated [34]. In this light, we found a strong significance in variance of the nutrient content in foliar portion described by the species factor; in particular, it has to be underlined that *D. tenuifolia* seems to constitutively accumulate greater amount of Ca in leaf compared to *V. locusta* (approximately 30% more), confirming a feature that is inherent to other species of *Brassicaceae* [35], although no difference was observed among species at the root level.

On the contrary, in *V. locusta* this feature was not observed, despite both Ca transport to shoot and growth stimulation (described as shoot dry weight and root length increase) were dependent on HS application alone or in combination with CaP. Such evidence suggests that this species probably adopts different absorption and translocation mechanisms.

MATERIALS AND METHODS

CaP-HS Production and Characterization

CaP Extraction from Fish Bones

Salmon (*Salmo salar*) fish bones resulting from the filleting were collected from a local shop (Italy). Before any treatment, fish bones were separated from offal and heads, scraped and soaked in hot water (80 °C) up to 2 h to remove organic tissues, placed on paper towel, and then dried in an oven at 50 °C overnight. The bones were then placed in an open furnace and heated in air by a 100 °C h⁻¹ thermal ramp followed by a one-hour isotherm at the temperature of 800 °C. After that, the resulting material was cooled at room temperature and then placed in a mortar to be grinded. The resulting powder was finally passed through a 270 mesh sieve before being characterized and used.

CaP Coating with HS

The coating of CaP extracted from salmon bones with HS (humic acids, MycSA, AG, Brownsville, TX, USA) was performed as already reported by Yoon et al. [11] with slight modification. Briefly, HS was dissolved in autoclaved distilled water at 0.10 g mL^{-1} . The solution was centrifuged at 13,000 rpm for 10 min to remove water-insoluble HS; after, 1 g of CaP was added to 10 mL of the resulting solution to be vigorously vortexed and then placed under gentle agitation in an incubator for 24 h at room temperature. To collect HS-coated CaP, the solution was centrifuged at 13,000 rpm for 10 min and the resulting pellet was rinsed with distilled water. Finally, the materials were recovered by centrifugation and dried overnight at $50 \text{ }^{\circ}\text{C}$.

Samples Characterization

The morphology of the samples was analyzed by scanning electron microscopy with a field-emission microscope (FEG-SEM, SIGMA, ZEISS NTS GmbH, Oberkochen, Germany). The samples were powdered and deposited on carbon tape mounted on an aluminum SEM stub and sputter-coated (Polaron E5100, Polaron Equipment, Watford, Hertfordshire, UK) with 10 nm of gold for electrical conductance. Accelerating voltages in the 3 to 10 keV range were used to observe the samples in the secondary electron imaging mode.

Fourier transform infrared spectroscopy analyses in the attenuated total reflection mode (FTIR-ATR) were carried out using a Nicolet iS5 spectrometer (Thermo Fisher Scientific Inc., Waltham, MA, USA) with a resolution of 1 cm^{-1} by accumulation of 16 scans covering the 4000 to 400 cm^{-1} range, using a diamond ATR accessory model iD7. Thermal Gravimetric Analysis (TGA) were performed using STA 449 Jupiter (Netzsch GmbH, Selb, Germany) apparatus. About 10 mg of powdered samples were heated from room temperature to $1100 \text{ }^{\circ}\text{C}$ under air flow with a heating rate of $10 \text{ }^{\circ}\text{C min}^{-1}$ in an alumina crucible. The amount of HS on CaP-HS was determined as the weight loss occurring between $550 \text{ }^{\circ}\text{C}$ and $950 \text{ }^{\circ}\text{C}$.

Dynamic Light Scattering (DLS) analyses were performed by using a Zetasizer Nano instrument ZSP (Malvern Instruments, Worcestershire, UK). For the analysis, samples were dispersed in water at a concentration of 0.5 mg mL^{-1} at pH 7.0. ζ -potentials were quantified by laser Doppler velocimetry as the electrophoretic mobility at $25 \text{ }^{\circ}\text{C}$ using a disposable electrophoretic cell (DTS1061, Malvern Ltd., Worcestershire, UK) of three separate measurements (maximum 100 runs each). Hydroxyapatite refractive index (1.63), water refractive index (1.33), and viscosity (1 cps) were used as working parameters for the samples and the solvent, respectively.

The chemical composition of the samples was determined using inductively coupled plasma optical emission spectrometry (ICP-OES) on a Liberty 200 spectrometer (Agilent Technologies 5100 ICP-OES, Varian, Palo Alto, Santa Clara, CA USA). 20 mg of CaP and CaP-HS were added to 15 mL of a HNO_3 solutions and placed in an ultrasonic bath sonicator at $37 \text{ }^{\circ}\text{C}$ until samples complete dissolution. Solutions were then cooled

at room temperature and added with water up to 100 mL before the ICP analysis. Ca, P, and Mg concentration were then measured by their atomic emission at the following wavelengths: 422.673 nm for Ca, 213.618 nm for P and 279.553 nm for Mg.

Specific surface areas of samples were measured through N₂ gas adsorption by the Brunauer–Emmett–Teller (BET) method using a Surfer instrument (Thermo Fisher Scientific Inc., Waltham, MA, USA). Samples were degassed at 100 °C for 3 h under vacuum before the analysis.

Samples X-Ray Diffraction (XRD) patterns were collected by a DS Advance Diffractometer (Bruker), equipped with a Lynx-eye position sensitive detector, with a CuK α radiation ($\lambda = 1.54178 \text{ \AA}$), at 40 kV and 40 mA. The spectra were recorded in the 10–60° 2 θ range with a step size of 0.02° and a scanning speed of 0.5 s. Rietveld refinement for phase quantification was performed with the software TOPAS5, and the percentage of each phase in terms of wt.% was refined considering a multiphase system, using tabulated atomic coordinates of hydroxyapatite (ASTM Card file No. 09-0432), and β -TCP (ASTM Card file No. 09-0169).

Equation (1) was used to calculate the crystallinity degree of each sample:

$$\text{Crystallinity [\%]} = 100 \cdot C / (A + C) \quad (1)$$

where C was the sum of peaks area and A was the area between the peaks and the background in the diffraction pattern [36].

Scherrer's formula was used to calculate the size of hydroxyapatite crystallites along the c-axis and along the a/b-axis [37] taking into accounts the diffraction peaks located at 2 θ values of 25.8° and 39.7° corresponding to the (002) and (310) reflections, respectively.

Plant Experiment Setup

Seeds of *Diplotaxis tenuifolia* L. and *Valerianella locusta* L. cv Trophy were purchased from TuttoGIARDINO (Udine, Italy). The experiment was carried out under controlled conditions (temperature: within 20 °C–23 °C, PAR: 500 $\mu\text{mol m}^{-2} \text{ s}^{-1}$, 12 h day⁻¹). Respectively, 25 and 20 seeds were soaked in deionized water for 15 min and placed into each 90 mm Petri dishes containing 40 mL of half-strength 0.5%-agar-solidified the Hoagland solution (adjusted to pH = 7.0), which represented the control treatment (i) as well as the substrate for preparing the following treatments: (ii) humic substance (HS, 16 mg L⁻¹), (iii) CaP (4000 mg L⁻¹), (iv) CaP coated with HS (CaP-HS, 4000 mg kg⁻¹). The CaP microparticles were sonicated for 20 min in 20 mL of deionized water before adding to the Hoagland solution for treatments (iii) and (iv); the addition was done when the solution temperature fell between 60 °C and solidification temperature, while stirring.

The duration of the experiment from sowing to harvest was 20 days (Figure S6). Four replicates for each treatment and for each species were prepared for a total of 32 Petri dishes that were kept closed for the whole duration of the experiment. At harvest, germination was calculated as the ratio of germinated seeds out of the total seeds in

each Petri dish. Seedlings were carefully removed, washed with deionized water and photographed; photos were processed with the public domain Java image processing software Image J [38] to measure the root lengths that were calculated for each petri dish as the average of the longest root of the plants. For each treatment, half of the plants of each dish were used for the ATP activity while the other half were used for the element content and the biometric parameters (root length, wet and dry weight).

Cellular ATP Activity Determination

For the determination of cellular ATP, shoot portions were weighted (100 ± 20 mg DW) and frozen by liquid nitrogen. A fine powder was obtained by grinding, and it was used for cellular ATP measurement, according to Mattiello et al. [39]. An aliquot (20 ± 2 μ L) of shoot soluble fraction was added to the incubation mixture. The ATP calibration curve was performed for each experiment and the sample concentrations were then calculated by interpolation.

Macroelements in Plant Seedlings

To quantify the total content of Ca, K, Mg, and P in roots and shoots of the plant species, seedlings were rinsed with deionized water and were oven-dried at 60 °C for three days. The total biomass of each fraction was digested on a microwave oven (ETHOS EASY digestion system, Milestone, Italy), using 9 mL of HNO₃ and 1 mL of H₂O₂ in Teflon cylinders at 180 °C, following the USEPA test method 3052 (1996). Plant extracts were filtered with PTFE 0.45 μ m membrane syringe filters and diluted prior the ICP–OES (5800, Agilent Technologies Inc., Palo Alto, Santa Clara, CA USA) analysis; scandium was used as internal standard.

Data Analysis

All statistical analyses were performed in R (v. 4.0.3) [40]. Effects of HS presence, CaP presence and their interaction on parameters considered were assessed by two-way ANOVA. When necessary, variables were subjected to logarithmic transformation prior to analysis in order to achieve ANOVA assumptions. A posteriori comparison of individual means was performed using Tukey's test ($p < 0.05$).

CONCLUSIONS

In this work, calcium phosphate particles (CaPs) were extracted from *Salmo salar* bones following a circular economy approach. The obtained materials were then functionalized with humic substances (HS) by a straightforward process. The presence of HS did not alter the bulk physicochemical properties of CaP, with the exception of the net surface charge that became more negative. CaP–HS together with the respective controls were tested against *Diplotaxis tenuifolia* and *Valerianella locusta* seedlings up to 20 days. The results showed that, even though they exhibited

a similar tendency to accumulate Ca and P in hypogeal tissues, the two species have different reactions to the treatments in terms of nutrient uptake and translocation. At the foliar level, CaP and CaP–HS were found to significantly increase the accumulation of P in the leaves of *D. tenuifolia*, while the treatment with HS was found to increase only that of Ca in *V. locusta* leaves. Notably, CaP was found to decrease the translocation of Ca in the leaves of *D. tenuifolia* and of both Ca and P in the leaves of *V. locusta*. Finally, the combination of HS with CaP showed promising results in terms of P uptake and translocation only for *D. tenuifolia*, but its biostimulating effect in the early stage growth of plants was low. We hypothesize that this was due to (i) HS low concentration on CaP; (ii) experimental conditions used for seedling growth; and (iii) low response of the tested species to the selected HS. These aspects will be taken into account and investigated more in depth in future works.

AUTHOR CONTRIBUTIONS

Conceptualization, A.A. and M.I.; methodology, F.C., G.F. and A.P.; software, M.V. and D.S.; validation, L.M. and J.-R.J.; formal analysis, M.V., L.M. and G.F.; investigation, A.A., L.M. and J.-R.J.; data curation, L.M., F.C., D.S., G.F., A.P. and M.V.; writing-original draft preparation, A.A., M.I. and L.M.; writing-review and editing, J.-R.J. and C.P.; visualization, F.C. and M.V.; supervision, A.A., M.I. and L.M. All authors have read and agreed to the published version of the manuscript.

ACKNOWLEDGMENTS

The authors acknowledge the Elsevier Green and Sustainable Chemistry Foundation for providing support to the project “phos-FATE: Empowering fishing communities for climate change”. The authors also acknowledge the United Nations for Industrial Development Organization and the Italian Embassy of Seoul -in particular F. Canganella- for supporting this research. C.P. thanks Fondazione con il Sud for funding the project HApECOrk (grant number 2015-0243).

REFERENCES

1. RHorrihan, L.; Lawrence, R.S.; Walker, P. How sustainable agriculture can address the environmental and human health harms of industrial agriculture. *Environ. Health Perspect.* 2002, *110*, 445–456.
2. Calvo, P.; Nelson, L.; Kloepper, J.W. Agricultural uses of plant biostimulants. *Plant Soil* 2014, *383*, 3–41.
3. Jindo, K.; Canellas, L.P.; Albacete, A.; dos Santos, L.F.; Frinhani Rocha, R.L.; Carvalho Baia, D.; Oliveira Aguiar Canellas, N.; Goron, T.L.; Olivares, F.L. Interaction between humic substances and plant hormones for phosphorous acquisition. *Agronomy* 2020, *10*, 640.
4. Olivares, F.L.; Busato, J.G.; de Paula, A.M.; da Silva Lima, L.; Aguiar, N.O.; Canellas, L.P. Plant growth promoting bacteria and humic substances: Crop promotion and mechanisms of action. *Chem. Biol. Technol. Agric.* 2017, *4*.
5. Purwanto, B.H.; Wulandari, P.; Sulistyaningsih, E.; Utami, S.N.H.; Handayani, S.; Lisetskii, F. Improved Corn Yields When Humic Acid Extracted from Composted Manure Is Applied to Acid Soils with Phosphorus Fertilizer. *Appl. Environ. Soil Sci.* 2021, *2021*, 1–12.
6. Gerke, J. Review Article: The effect of humic substances on phosphate and iron acquisition by higher plants: Qualitative and quantitative aspects. *J. Plant Nutr. Soil Sci.* 2021.
7. Çimrin, K.M.; Türkmen, Ö.; Turan, M.; Tuncer, B. Phosphorus and humic acid application alleviate salinity stress of pepper seedling. *Afr. J. Biotechnol.* 2010, *9*, 5845–5851.
8. García, A.C.; Santos, L.A.; Izquierdo, F.G.; Sperandio, M.V.L.; Castro, R.N.; Berbara, R.L.L. Vermicompost humic acids as an ecological pathway to protect rice plant against oxidative stress. *Ecol. Eng.* 2012, *47*, 203–208.
9. Aydin, A.; Kant, C.; Turan, M. Humic acid application alleviate salinity stress of bean (*Phaseolus vulgaris* L.) plants decreasing membrane leakage. *Afr. J. Agric. Res.* 2012, *7*, 1073–1086.
10. Alewell, C.; Ringeval, B.; Ballabio, C.; Robinson, D.A.; Panagos, P.; Borrelli, P. Global phosphorus shortage will be aggravated by soil erosion. *Nat. Commun.* 2020, *11*, 1–12.
11. Yoon, H.Y.; Lee, J.G.; Esposti, L.D.; Iafisco, M.; Kim, P.J.; Shin, S.G.; Jeon, J.-R.; Adamiano, A. Synergistic release of crop nutrients and stimulants from hydroxyapatite nanoparticles functionalized with humic substances: Toward a multifunctional nanofertilizer. *ACS Omega* 2020, *5*, 6598–6610.
12. Alvarez, R.; Evans, L.A.; Milham, P.J.; Wilson, M.A. Effects of humic material on the precipitation of calcium phosphate. *Geoderma* 2004, *118*, 245–260.
13. Carella, F.; Seck, M.; Degli Esposti, L.; Diadiou, H.; Maienza, A.; Baronti, S.; Vignaroli, P.; Vaccari, F.P.; Iafisco, M.; Adamiano, A. Thermal conversion of fish bones into

fertilizers and biostimulants for plant growth—A low tech valorization process for the development of circular economy in least developed countries. *J. Environ. Chem. Eng.* 2021, 9, 104815.

14. Piccirillo, C.; Adamiano, A.; Tobaldi, D.M.; Montalti, M.; Manzi, J.; Castro, P.M.L.; Panseri, S.; Montesi, M.; Sprio, S.; Tampieri, A. Luminescent calcium phosphate bioceramics doped with europium derived from fish industry byproducts. *J. Am. Ceram. Soc.* 2017, 100, 3402–3414.
15. Ben-Nissan, B. *Advances in Calcium Phosphate Biomaterials*; Springer: Berlin/Heidelberg, Germany; Hong-Kong, China, 2014.
16. Fowler, B.; Moreno, E.; Brown, W. Infra-red spectra of hydroxyapatite, octacalcium phosphate and pyrolysed octacalcium phosphate. *Arch. Oral. Biol.* 1966, 11, 477–492.
17. Adamiano, A.; Sangiorgi, N.; Sprio, S.; Ruffini, A.; Sandri, M.; Sanson, A.; Gras, P.; Grossin, D.; Francès, C.; Chatzipanagis, K. Biomineralization of a titanium-modified hydroxyapatite semiconductor on conductive wool fibers. *J. Mat. Chem. B* 2017, 5, 7608–7621.
18. Tatzber, M.; Stemmer, M.; Spiegel, H.; Katzlberger, C.; Haberhauer, G.; Mentler, A.; Gerzabek, M.H. FTIR-spectroscopic characterization of humic acids and humin fractions obtained by advanced NaOH, Na₄P₂O₇, and Na₂CO₃ extraction procedures. *J. Plant. Nutr. Soil Sci.* 2007, 170, 522–529.
19. Iafisco, M.; Marchetti, M.; Gómez Morales, J.; Hernández-Hernández, M.A.; Garcia Ruiz, J.M.; Roveri, N. Silica gel template for calcium phosphates crystallization. *Cryst. Growth Des.* 2009, 9, 4912–4921.
20. Terzioglu, P.; Ogut, H.; Kalemteş, A. Natural calcium phosphates from fish bones and their potential biomedical applications. *Mater. Sci. Eng. C Mater. Biol. Appl.* 2018, 91, 899–911.
21. Ozawa, M.; Suzuki, S. Microstructural development of natural hydroxyapatite originated from fish-bone waste through heat treatment. *J. Am. Ceram. Soc.* 2002, 85, 1315–1317.
22. Hamada, M.; Nagai, T.; Kai, N.; Tanoue, Y.; Mae, H.; Hashimoto, M.; Miyoshi, K.; Kumagai, H.; Saeki, K. Inorganic constituents of bone of fish. *Fish Sci.* 1995, 61, 517–520.
23. Marchiol, L.; Iafisco, M.; Fellet, G.; Adamiano, A. Nanotechnology support the next agricultural revolution: Perspectives to enhancement of nutrient use efficiency. *Adv. Agron.* 2020, 161, 27–116.
24. García, A.C.; De Souza, L.G.A.; Pereira, M.G.; Castro, R.N.; García-Mina, J.M.; Zonta, E.; Lisboa, F.J.G.; Berbara, R.L.L. Structure-property-function relationship in humic substances to explain the biological activity in plants. *Sci. Rep.* 2016, 6, 1–10.
25. Vekariya, R.L.; Sonigara, K.K.; Fadadu, K.B.; Vaghasiya, J.V.; Soni, S.S. Humic acid as a sensitizer in highly stable dye solar cells: Energy from an abundant natural polymer soil component. *ACS Omega* 2016, 1, 14–18.

26. Jeong, H.J.; Cha, J.-Y.; Choi, J.H.; Jang, K.-S.; Lim, J.; Kim, W.-Y.; Seo, D.-C.; Jeon, J.-R. One-pot transformation of technical lignins into humic-like plant stimulants through fenton-based advanced oxidation: Accelerating natural fungus-driven humification. *ACS Omega* 2018, 3, 7441–7453.
27. Savy, D.; Mazzei, P.; Drosos, M.; Cozzolino, V.; Lama, L.; Piccolo, A. Molecular characterization of extracts from biorefinery wastes and evaluation of their plant biostimulation. *ACS Sustain. Chem. Eng.* 2017, 5, 9023–9031.
28. David, P.; Nelson, P.; Sanders, D. A humic acid improves growth of tomato seedling in solution culture. *J. Plant Nutr.* 1994, 17, 173–184.
29. Wang, X.J.; Wang, Z.Q.; Li, S. The effect of humic acids on the availability of phosphorus fertilizers in alkaline soils. *Soil Use Manage.* 1995, 11, 99–102.
30. Delgado, A.; Madrid, A.; Kassem, S.; Andreu, L.; Del Campillo, M.D.C. Phosphorus fertilizer recovery from calcareous soils amended with humic and fulvic acids. *Plant Soil* 2002, 245, 277–286.
31. Benedetti, A.; Figliolia, A.; Izza, C.; Canali, S.; Rossi, G. Some thoughts on the physiological effects of humic acids: Interactions with mineral fertilisers. *Agrochimica* 1996, 40, 229–240.
32. Bermudez, D.; Juarez, M.; Sanchez-Andreu, J.; Jorda, J. Role of eddha and humic acids on the solubility of soil phosphorus. *Commun. Soil Sci. Plant Anal.* 1993, 24, 673–683.
33. Zhang, X.; Ervin, E.; Schmidt, R. Physiological effects of liquid applications of a seaweed extract and a humic acid on creeping bentgrass. *J. Am. Soc. Hortic. Sci.* 2003, 128, 492–496.
34. Nikbakht, A.; Kafi, M.; Babalar, M.; Xia, Y.P.; Luo, A.; Etemadi, N.-A. Effect of humic acid on plant growth, nutrient uptake, and postharvest life of gerbera. *J. Plant Nutr.* 2008, 31, 2155–2167.
35. Broadley, M.R.; White, P.J. Eats roots and leaves. Can edible horticultural crops address dietary calcium, magnesium and potassium deficiencies? *Proc. Nutr. Soc.* 2010, 69, 601–612.
36. Adamiano, A.; Fabbri, D.; Falini, G.; Belcastro, M.G. A complementary approach using analytical pyrolysis to evaluate collagen degradation and mineral fossilisation in archaeological bones: The case study of Vicenne-Campochiaro necropolis (Italy). *J. Anal. Appl. Pyrolysis* 2013, 100, 173–180.
37. Klug, H.P.; Alexander, L.E. *X-Ray Diffraction Procedures: For Polycrystalline and Amorphous Materials*; Wiley: Hoboken, NJ, USA, 1974.
38. Rueden, C.T.; Schindelin, J.; Hiner, M.C.; DeZonia, B.E.; Walter, A.E.; Arena, E.T.; Eliceiri, K.W. ImageJ2: ImageJ for the next generation of scientific image data. *BMC Bioinf.* 2017, 18, 1–26.
39. Mattiello, A.; Filippi, A.; Pošćić, F.; Musetti, R.; Salvatici, M.C.; Giordano, C.; Vischi, M.; Bertolini, A.; Marchiol, L. Evidence of phytotoxicity and genotoxicity in *Hordeum vulgare* L. exposed to CeO₂ and TiO₂ nanoparticles. *Front. Plant. Sci.* 2015, 6, 1043.

40. Team RDC. *R: A Language and Environment for Statistical Computing*; R Foundation for Statistical Computing: Vienna, Austria, 2010; Available online: <http://www.R-project.org> (accessed on 4 February 2021).

SUPPORTING INFORMATION

Table S1. Two-way ANOVA applied on morphological and biochemical variables measured on *Diplotaxis tenuifolia*. Data are mean \pm standard deviation ($n = 4$). Different symbols indicate statistical significance of the analyzed factors (***, $p \leq 0.001$; **, $p \leq 0.01$; *, $p \leq 0.05$).

Parameter	Treatment	Df	F-value	p-value
Roots DW	CaP	1,14	5.5	0.034 *
Shoot DW	HS	1,12	0.00	0.985
	CaP	1,12	0.05	0.832
	CaP x HS	1,12	8.49	0.013 *
log(Ca root)	CaP	1, 14	274	$2 \cdot 10^{-10}$ ***
log(P root)	CaP	1,14	210	$8 \cdot 10^{-10}$ ***
K root	HS	1,12	11.08	0.006 ***
	CaP	1,12	1.16	0.302
	CaP x HS	1,12	6.29	0.027 *
Mg root	HS	1,13	6.44	0.025 *
	CaP	1,13	19.29	$7 \cdot 10^{-4}$ ***
Ca leaf	CaP	1,12	4.96	0.046 *
	HS	1,12	7.11	0.021 *
	CaP x HS	1,12	7.20	0.020 *
P leaf	HS	1,11	28.1	$3 \cdot 10^{-4}$ ***
	CaP	1,11	54.3	$1 \cdot 10^{-5}$ ***
	CaP x HS	1,11	8.5	0.014 *
K leaf	HS	1,12	7.75	0.017 *
	CaP	1,12	0.22	0.646
	CaP x HS	1,12	14.47	0.002 **
Mg leaf	HS	1,12	0.17	0.689
	CaP	1,12	1.60	0.230
	CaP x HS	1,12	5.51	0.037 *

Table S2. Two-way ANOVA applied on morphological and biochemical variables measured on *Valerianella locusta*. Data are mean \pm standard deviation ($n = 4$). Different symbols indicate statistical significance of the analyzed factors (***, $p \leq 0.001$; **, $p \leq 0.01$; *, $p \leq 0.05$).

Parameter	Treatment	Df	F-value	p-value
Root length	HS	1,14	9.37	0.009 **
Shoot DW	HS	1,14	14.2	0.002 **
log(Ca root)	CaP	1, 13	3487	$2 \cdot 10^{-16}$ ***
log(P root)	HS	1,11	5.29	0.042 *
	CaP	1,11	9299.74	$2 \cdot 10^{-16}$ ***
	CaP x HS	1,11	8.29	0.015 *
K root	HS	1,12	2.57	0.135
	CaP	1,12	0.24	0.631
	CaP x HS	1,12	10.96	0.006 **
Mg root	HS	1, 13	9.96	0.008 **
Ca leaf	HS	1,13	12.5	0.004 **
	CaP	1,13	12.8	0.003 **
P leaf	CaP	1,12	28.8	$2 \cdot 10^{-4}$ ***
	HS	1,12	16.6	0.002 **
	CaP x HS	1,12	18.6	0.001 **
K leaf	CaP	1,13	7.64	0.016 *

Table S3. Germination percentage, root specific weight, and total seedling dry weight of *Diplotaxis tenuifolia*. Data are mean \pm standard deviation ($n = 4$). Different letters indicate statistically significant difference between treatments at Tukey's post-hoc test ($p \leq 0.05$).

Treatments	Germination (%)	Root specific weight (mg mm ⁻¹)	Total DW (mg plant ⁻¹)
Ctrl	54 \pm 8.33 a	0.077 \pm 0.02 a	26.1 \pm 2.12 a
HS	58 \pm 2.31 a	0.079 \pm 0.03 a	28.6 \pm 3.99 a
CaP	59 \pm 5.03 a	0.135 \pm 0.04 a	32.6 \pm 5.28 a
CaP-HS	56 \pm 10.3 a	0.113 \pm 0.05 a	27.5 \pm 4.33 a

Table S4. Germination percentage, root specific weight, and total seedling dry weight of *Valerianella locusta*. Data are mean \pm standard deviation ($n = 4$). Different letters indicate statistically significant difference between treatments at Tukey's post-hoc test ($p \leq 0.05$).

Treatments	Germination (%)	Root specific weight (mg mm ⁻¹)	Total DW (mg plant ⁻¹)
Ctrl	44 \pm 4.79 a	0.140 \pm 0.04 a	21.8 \pm 2.94 a
HS	53 \pm 2.89 a	0.125 \pm 0.02 a	24.7 \pm 0.84 a
CaP	51 \pm 4.78 a	0.152 \pm 0.03 a	22.4 \pm 2.41 a
CaP-HS	50 \pm 7.07 a	0.143 \pm 0.02 a	25.4 \pm 0.51 a

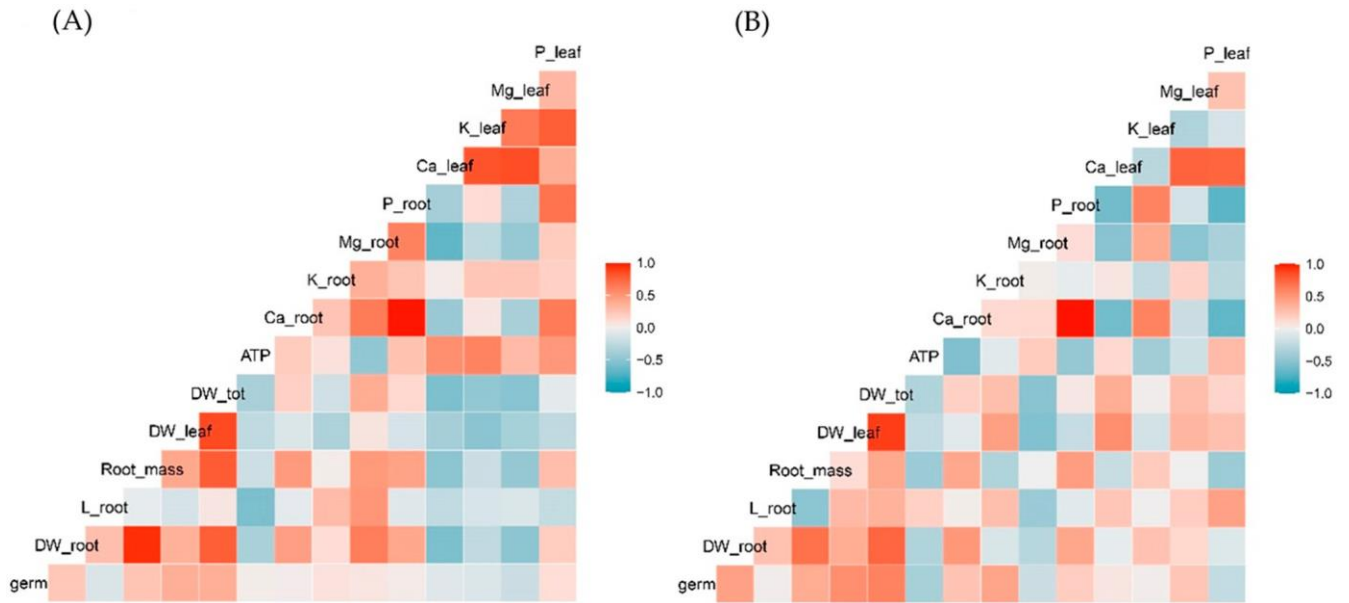


Figure S1. Correlation plot performed on global data set comparing all the considered variables measured for for *Diplotaxis tenuifolia* (A) and *Valerianella locusta* (B). Chromatic palet on the left indicates the correlation degree.

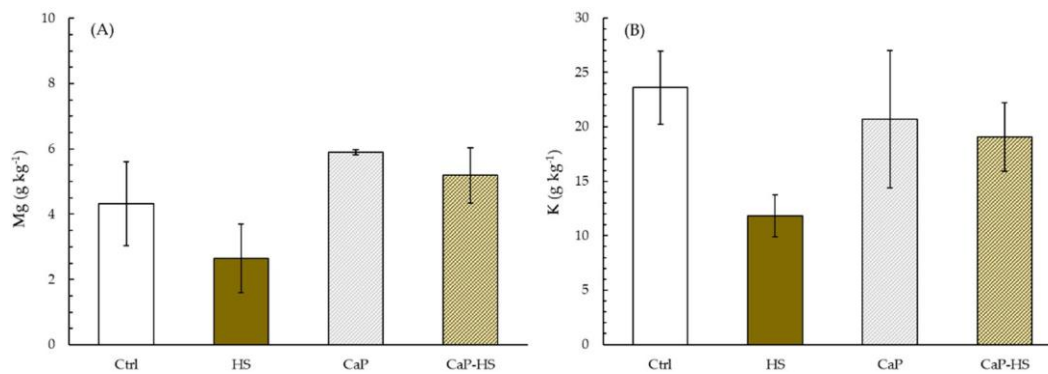


Figure S2. Concentration of Mg (A) and K (B) in roots of *Diplotaxis tenuifolia*. Data are mean \pm standard deviation ($n = 4$). When the interaction between experimental factors (CaP \times HS) was significant at ANOVA, different letters were used to indicate statistically significant differences between treatments at Tukey's post-hoc test ($p \leq 0.05$).

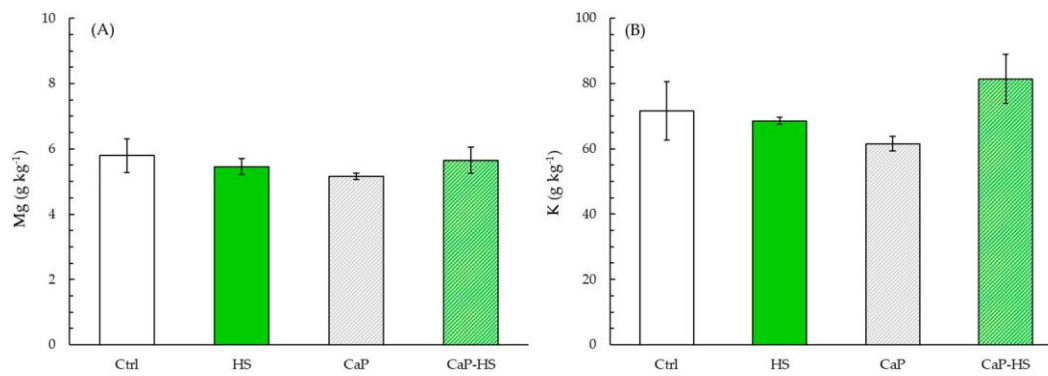


Figure S3. Concentration of Mg (A) and K (B) in leaves of *Diplotaxis tenuifolia*. Data are mean \pm standard deviation ($n = 4$). When the interaction between experimental factors (CaP \times HS) was significant at ANOVA, different letters were used to indicate statistically significant differences between treatments at Tukey's post-hoc test ($p \leq 0.05$).

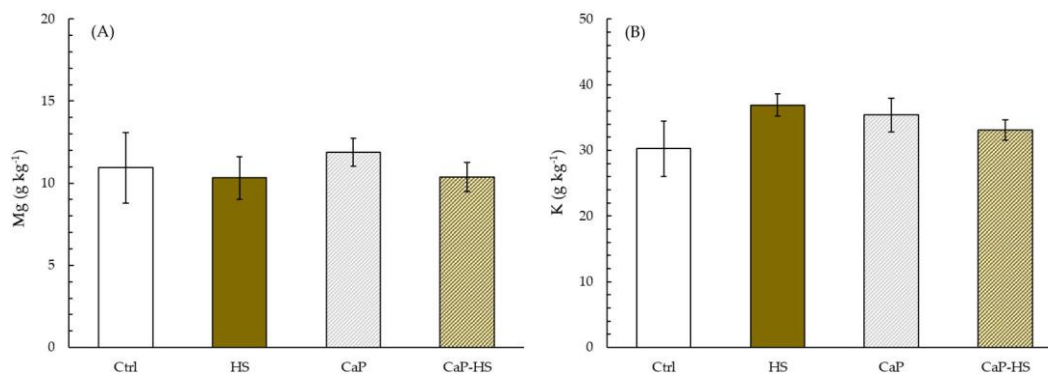


Figure S4. Concentration of Mg (A) and K (B) in roots of *Valerianella locusta*. Data are mean \pm standard deviation ($n = 4$). When the interaction between experimental factors (CaP \times HS) was significant at ANOVA, different letters were used to indicate statistically significant differences between treatments at Tukey's post-hoc test ($p \leq 0.05$).

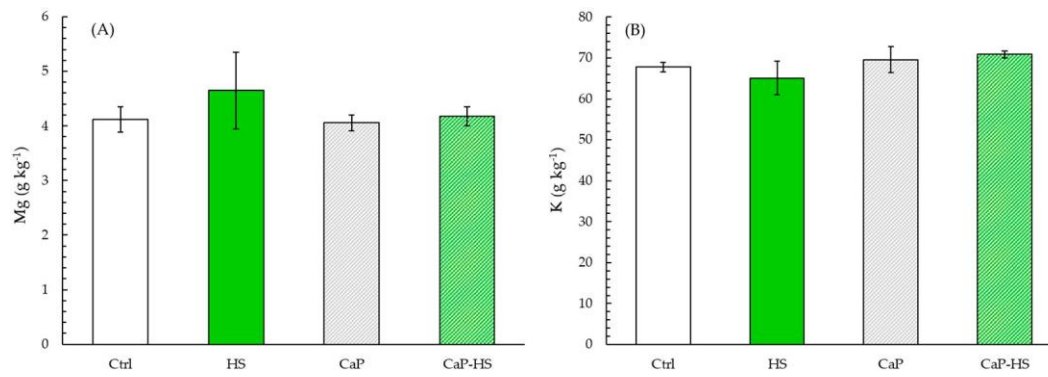


Figure S5. Concentration of Mg (A) and K (B) in leaves of *Valerianella locusta*. Data are mean \pm standard deviation ($n=4$). When the interaction between experimental factors (CaP \times HS) was significant at ANOVA, different letters were used to indicate statistically significant differences between treatments at Tukey's post-hoc test ($p \leq 0.05$).

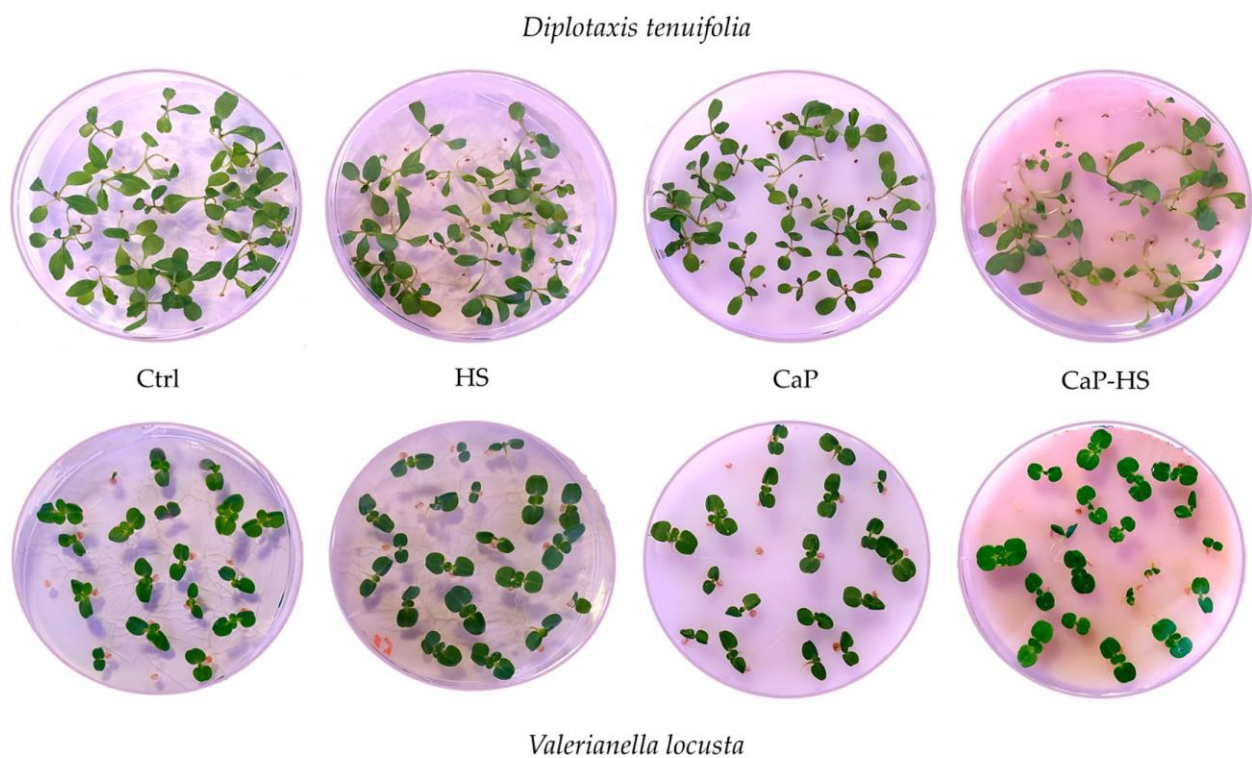


Figure S6. Plantlets of *Diplotaxis tenuifolia* and *Valerianella locusta* in Petri dishes 20 days after sowing.

CHAPTER 4 - Innovative multi-scale approach to study leaf phenotypic plasticity in weedy *Amaranthus* spp. young seedlings

Original Paper

Submitted to: *Plant Biology*, Wiley

Innovative multi-scale approach to study leaf phenotypic plasticity in weedy *Amaranthus* spp. young seedlings

Dora Scarpin¹, Giacomo Este¹, Francesca D'Este², Francesco Boscutti¹, Andrea Milani³, Silvia Panozzo³, Serena Varotto⁴, Marco Vuerich¹, Elisa Petrusa¹, Enrico Braidot¹

¹Department of Agriculture, Food, Environment and Animal Sciences (DI4A), University of Udine, Via delle Scienze 206, 33100 Udine, Italy

²Department of Medicine (DAME), University of Udine, P.le Kolbe 4, 33100 Udine, Italy

³Institute for Sustainable Plant Protection (IPSP) - National Research Council (CNR), Viale dell'Università 16, 35020 Legnaro (PD), Italy

⁴Department of Agronomy Animal Food Natural Resources and Environment (DAFNAE), University of Padova, Viale dell'Università 16, 35020 Legnaro (PD), Italy

Correspondence: elisa.petrussa@uniud.it Phone: +39 0432 558779

Keywords: Plant phenotyping; imaging; *Amaranthus*; confocal reflection microscopy; juvenile leaf; leaf traits.

ABSTRACT

- Plant phenotyping on plant morpho-anatomical traits can be achieved by imaging analysis, ranging from microscope images up to high-scale acquisitions through remote sensing. This technique represents a low-invasive tool providing insight into physiological and structural trait diversity, as well as the plant-environment interaction. The high phenotypic plasticity in the *Amaranthus* genus has already attracted much interest, due to the inclusion in annual weed species with high invasiveness and great impact on important summer crops, as well as nutritive grain or vegetable crops of great economic value. Identification of morpho-anatomic characters in leaf at very young stage across some weedy amaranths could be thereby useful for a better comprehension of the structural traits related to their performance in the agroecosystem.
- In this work, we focused on an innovative multi-scale approach phenotyping analysis of about 20 single-leaf morphometric traits of 4 *Amaranthus* species through the processing of photographic and confocal microscopy acquisitions.
- The results evidenced that determination of leaf traits at different investigation levels can highlight species-specific traits even at a juvenile stage, crucial for plant development and competition establishment. More specifically, leaf shape and hairiness Aspect Ratio variables were those explaining better discrimination among *A. tuberculatus* and the other species.
- The methodology proved to be a promising, reliable and low-impact approach for the functional characterization of phylogenetically related species and statistical quantification of traits involved in taxonomy and biodiversity studies.

INTRODUCTION

Plants fitness is determined by the relationship between the genotype and the environmental factors, which are leading to phenotype expression, evaluable as representation of different functional types [1]. Gene sequencing technologies have greatly enhanced our knowledge of plant biology [2] but predicting the performance of an individual in a given environment cannot be complete if only its gene pool is considered [1]. The integrated study of the phenotype therefore becomes fundamental, moreover considering the enormous plasticity that affects the adaptation of plants to different growth conditions [1,3] and generates further challenges for modern quantitative analyses [4].

In this context, the development of phenotyping science and techniques is increasingly emerging as a strategy linking genomics with plant ecophysiology [5]. Thanks to the rapid development of imaging technology, computer-assisted analysis has greatly facilitated scientific research and is now an important tool for plant phenotyping as a complement or alternative to the more limiting and time-consuming manual measurements [6].

High throughput plant phenotyping, in particular, deals with the analysis of image sequences acquired in different controlled environment conditions [6], and allows the acquisition of a large amount of information useful for both holistic (the whole plant) and component (single organs) analyses [7].

One branch of phenotyping methodologies is the so-called "Anatomics", the study and quantification of anatomical plant traits through imaging techniques [8]. In accordance, these techniques allow to assess variation in leaf vein architecture, hairiness and stomata density, as well as surface traits, which are strictly related to environment adaptation of photosynthetic efficiency and water transport function of the plant [9]. Methods for high-throughput anatomical phenotyping would be useful in many areas of plant science, from basic research to crop breeding, as plant anatomy is a regulator of several fundamental biological processes, as well as interaction with other organisms [10]. However, the measurement and analysis of anatomical phenotypes in detail has been limited in research, resulting in a lack of understanding of the extent of phenotypic variation between species and its correlation to fitness [8]. Nowadays, new technologies can facilitate both the measurement and quantification of anatomical characters, acquiring more in-depth information and allowing studies even with field-grown plants [8].

Phenotyping could represent a further application for more integrated investigation on interaction between crop and weed plants, as this analysis would be informative for development of future target-directed and less invasive treatments against weeds. Among the latter, amaranths represent good candidates as plant model for this analysis.

The *Amaranthus* genus include 70 species, mostly annual herbaceous plants, spread all over the world, covering a range of different habitats [11]. More than twenty species

have been reported in the Italian flora, comprising just only three native species, while the others are considered alien, mostly neophytes native to the Americas [12]. *Amaranthus* is among the few dicotyledon plants with a C4 metabolism, which allows these species to survive in arid, dry and high-salinity environments [13] and to show high competitiveness against crops such as soybean, maize, tomato, etc. due to higher photosynthetic efficiency. The high capacity to hybridise, the production of allelopathic substances and the high seed production are further aspects that make many amaranth species extremely invasive [14]: the high yield losses they cause is the main reason why some of these are considered among the most noxious weeds [11,15,16]. The lack of weed control has become a widespread phenomenon that is difficult to manage due to the repeated use of these pesticides [11] and resistant populations have been reported worldwide [17]. In particular, dioecious species are likely to evolve resistant biotypes rapidly, because they are subject to cross fertilisation unlike monoecious species, so they show greater genetic recombination and thus high genetic and phenotypic variability [18]. Examples of species that have already developed resistance are the monoecious *A. hybridus* L. and *A. retroflexus* L., and the dioecious *A. palmeri* S. Wats. and *A. tuberculatus* (Moq.) J. D. Sauer [17]. Resistant biotypes of these four species have also been reported in Italy, sometimes infesting the same field [11,19].

In this work, we conducted a phenotyping study on leaf morpho-anatomical traits of the above mentioned *Amaranthus* species, analysing in depth the characteristics of the adaxial blade of young leaves. The choice was determined by the fact that amaranth plants begin to be competitive during the crop emergence phase, when they are both in the early stages of development [20,21]. Secondly, amaranths are perfectly controlled by post-emergence herbicides at early stage-development, whereas the treatment of larger plants favours the selection of metabolic resistance mechanisms. Besides, plant phenotyping conducted at high resolution scale of cellular and tissue organization is far less common compared to what carried out at whole-plant organism/ecosystem level [22,23] and combined analyses with a top-down approach have recently been increasingly called to address this shortcoming [24]. Therefore, we expected that specific leaf anatomical traits could significantly discriminate the leaf plasticity across the amaranths investigated, allowing to add taxonomic information on vegetative traits. In particular, we hypothesized these traits being more evident at juvenile stages than those related to morphological leaf shape and size at higher scale of investigation.

MATERIALS AND METHODS

Plant material

Four *Amaranthus* species were used: *A. hybridus* L., *A. palmeri* S. Wats., *A. retroflexus* L. and *A. tuberculatus* (Moq.) J. D. Sauer.

The species were obtained from local populations in Veneto region, Italy. The four populations were well-characterized and susceptible checks routinely used for herbicide screenings were carried out by IPSP-CNR [19]. The preliminary cultivation phases were performed at the IPSP - CNR site in Legnaro (PD). Seeds were sown in agar 0.6% plastic boxes and placed in a germination chamber at 18/28 °C night/day and 12 h photoperiod using neon tubes with a photon flux density suitable for photosynthesis ($15\text{-}30 \mu\text{mol m}^{-2} \text{s}^{-1}$). The pre-germinated seeds were transplanted into plastic pots (11 cm x 10.1 cm) filled with a standard substrate (60% loamy soil, 15% sand, 15% perlite and 10% peat) and were grown in a greenhouse (30/20 °C day/night) with a photoperiod of 16 h light/day [25]. At least eighteen plants of each species have been examined at the growth stage 13-16 according to the weed-extended BBCH scale [26]: the third or fourth leaf from the apex, including the petiole, was collected, and all measurements have been performed on the same leaf.

Image acquisition

The image acquisition phase was conducted at the University of Udine immediately after transferring the plants.

Leaf traits were measured and analysed according to a scale criterion, which allowed to define three different groups of morpho-anatomical traits, divided as follows:

1. Macroscopic traits (full scale leaf analysis)
2. Surface-related microscopic traits (leaf surface microscopic analysis)
3. Evapotranspiration (ET)-related traits (full scale and microscopic leaf analysis).

Leaves were placed on a white light LED panel (RaLeno Photographic Equipment, Shenzhen, China) for full scale image acquisition, with the adaxial page facing upwards. A glass sheet was used to keep them flattened (Fig. S1). Photos were taken using a Panasonic DC-GH5 camera (Panasonic Corporation, Osaka, Japan) at a 60 mm focal length (settings: f/22, 1/800 sec, ISO 800), placed with tripod at a known constant distance from the leaf.

Leaf surface imprints [27,28] were prepared to examine the morphological parameters of the epidermal cells, the number of stomata and the roughness-related traits at the epidermal tissue level: the median portion of the adaxial leaf page was coated with a double layer of transparent nail polish, allowing the first coat to dry before applying the second one. After complete hardening, the resulting imprint was removed using adhesive tape and tweezers and was mounted in distilled water on a microscope slide, under a # 1 coverslip sealed with the same polish.

Samples were imaged in reflection mode on a Leica TCS SP8 confocal microscope (Leica Microsystems, Wetzlar, Germany) using a 40x/1.10 NA water immersion objective and a 488 nm laser line. Z-stacks covering reflection from the whole surface of the field were collected at 1 AU pinhole aperture and 0.422 μm step-size. Maximum intensity projection images (Fig. S2) were generated using Leica Application Suite X

(LAS X) 3.5.5 software. Alternatively, the z-series were processed for roughness-related traits analysis as specified below.

Image analysis

The images were analysed using *Fiji* software (*win-64* version) [29] to measure the different morpho-anatomical parameters.

All the morpho-anatomical traits examined are reported in detail in Table 1.

1. Macroscopic traits

Both the software's default tools and the *LeafJ* plugin [30] were used to analyse morpho-anatomical macroscopic leaf traits. The following parameters were measured: leaf area, circularity, length, aspect ratio (AR), solidity and petiole length (see Table 1).

After image acquisition was completed, leaves were placed in an oven at 70°C overnight and then weighed to determine their Dry Weight (DW). This parameter, together with the previously measured leaf area, was used to calculate the Specific Leaf Area (SLA) [31,32].

2. Surface-related microscopic traits

The confocal maximum intensity projections were used to analyse the morpho-anatomical parameters of tegument cells; in this case, the analysis was conducted by combining the use of *Fiji* software with that of *LeafNet* website [33]. Specifically, *LeafNet* was used to segment tegument cells, while cell counting and the measurement of cell area, circularity and Aspect Ratio (AR) (see Table 1) was performed with *Fiji* thresholding tools. Finally, a series of parameters concerning the roughness-related traits were measured from the confocal reflection z-stacks of the nail polish imprint, according to McNaughton protocol [34]. Firstly, data was processed with the *Extended Depth of Field* [35] *Fiji* plugin, followed by analysis of the resulting height map with *SurfCharJ_1q* [36] plugin to calculate Rsk, Rv, Rp, FPO, FAD, MRV values (see Table 1) [36].

3. ET-related traits

Vessel Analysis plugin [37] was used to measure Density of Leaf Veins (DLV) [38] percentage, while *Fiji* thresholding tools were applied to measure hairiness area, perimeter, circularity, Aspect Ratio (AR) and solidity (see Table 1). Moreover, a manual counting was performed for stomatal density using maximum intensity projections of the confocal reflection z-stacks; the obtained value was then transformed into the number of stomata per leaf area.

Statistical analysis

A Multivariate Analysis of Variance (MANOVA) was carried out using the *R Studio* software (2022.02.0-443 version) to test the trait differences between the study species. Where significant ($P < 0.05$), the MANOVA models were used to perform a Canonical Discriminant Analysis (CDA). For each CDA analysis, a Likelihood Ratio test was performed to verify the model accuracy (results not shown). MANOVA and CDA were performed on each trait group, separately (leaf macroscopic, surface- and ET-related traits).

Following the outcomes obtained from the CDAs, the variables that showed a high score and therefore had a relevant effect in the statistical model were chosen for further univariate analyses. For all variables (see Table 3) a Shapiro-Wilk normality test was performed to determine the normal distribution of the data. In the case of variables without a normal distribution, their transformation was performed by means of conversion with appropriate functions (Table 3). An ANOVA was then performed to test the differences between the study species for each selected trait ($P < 0.05$). Where significant, a *post hoc* analysis using the LSD Fisher test was used to check the pairwise comparisons between species.

RESULTS

According to the rationale of the scientific project, several traits of amaranth leaf were measured at different scale level, starting from a macroscopic (full-scale) level down to a microscopic level. This approach aimed to build a phenotyping model to describe more accurately as possible the variability of morpho-anatomical traits in the four amaranth species under study.

MANOVA analysis

The analysed variables (Table 1) were grouped into three different sets according to their morpho-anatomical role and subjected to multivariate variance analysis (MANOVA) in order to highlight not only the percentage of variance explained by the model, but also the correlations existing between the factor species and the different traits measured experimentally.

Table 1. Definitions of the non-correlated variables analysed by means of MANOVA. Abbreviation list: ET = Evapotranspiration.

Leaf analysis level	Non-correlated traits	Meaning
Macroscopic traits	Leaf area	Area of the leaf (mm ²)
	Leaf circularity	Circularity = 4π Leaf area / (Leaf perimeter) ² (non-dimensional)
	Leaf solidity	Area of the convex hull bounds the leaf shape as a polygon (mm ²)
	Leaf length	Leaf major axis (mm)
	Leaf AR	Aspect Ratio = leaf major axis / leaf minor axis (non-dimensional)
	Petiole length	Length of petiole (mm)
	DW	Dry Weight (mg)
	SLA	Specific Leaf Area = leaf area / leaf dry mass (mm ² /mg)
Surface-related microscopic traits	Cell area	Area of the cell (μm ²)
	Cell circularity	Cell circularity = 4π [cell area / (cell perimeter) ²] (non-dimensional)
	Cell AR	Aspect Ratio = cell major axis / cell minor axis (non-dimensional)
	Rsk	Skewness of the assessed epidermis profile
	Rv	Lowest valley
	Rp	Highest peak height
	FPO	Average polar facet orientation (between 0 and 90 sexagesimal degrees)
	FAD	Average direction of azimuthal facets (between 0 and 360 sexagesimal degrees)
MRV	Vector resulting from the average of the inclinations of all cellular facets	
ET-related traits	Hairiness area	Tomentosity area (mm ²)
	Hairiness perimeter	Tomentosity perimeter (mm)
	Hairiness AR	Aspect Ratio of the hairs = hair major axis / hair minor axis (non-dimensional)
	Hairiness circularity	Hair cell circularity = 4π [hair area / (hair perimeter) ²]
	Hairiness solidity	Area of the convex hull bounds the hair shape as a polygon (mm ²)
	DLV	Density of Leaf Veins = total vein length / area (mm/mm ² or %) (Price <i>et al.</i> 2011)
	Stomata Density	(Stomata / mm ²)

Table 2 shows that the multivariate analysis model has a high significance in all three areas considered. These conclusions were confirmed by the subsequent execution of the Canonical Discriminant Analysis (CDA), the results of which are summarised in Figs. 1-3.

Table 2. MANOVA of morpho-anatomical leaf traits at different scale levels. Abbreviation list: Df= degree of freedom; Pillai = Pillai value; F= Fisher; Num-Den Df = numerator - denominator of Df; P = P value; ET = Evapotranspiration. Significance level: "****" = $P < 0.001$.

Leaf analysis level	MANOVA	Df	Pillai	approx. F	Num-Den Df	P	Significance
Macroscopic traits	(Intercept)	1	0.999	69697.0	8-61	<0.001	***
	Species	3	1.125	5.0	24-189	<0.001	***
	Residuals	68					
Surface-related microscopic traits	(Intercept)	1	0.998	5361.3	9-60	<0.001	***
	Species	3	0.855	2.7	27-186	<0.001	***
	Residuals	68					
ET-related traits	(Intercept)	1	0.996	2512.4	7-62	<0.001	***
	Species	3	0.963	4.3	21-192	<0.001	***
	Residuals	68					

Aiming to simplify the analysis of the different traits under study, a criterion of subdivision according to the scale level of the analysis or the regulatory function of leaf exchange was adopted. Fig. 1 describes the CDA performed on the leaf traits measured on a macroscopic level. Canonical variable 1 (Can1) explains a significant percentage of the variance, which exceeds 98% if Can2 is also considered. The CDA showed that the data for *A. tuberculatus* are in the negative portion of the biplot and are clearly distinguishable from the other three ellipsoids related to the species *A. hybridus*, *A. retroflexus* and *A. palmeri*. Furthermore, the distribution of the vectors associated with the different traits makes it clear that these species share a strong positive correlation with the trait leaf circularity and to some extent DW and leaf area, while a negative correlation with the leaf length parameter can be found, as evidenced by the DIM plot associated with the CDA (Fig. S3). The graph confirms that *A. tuberculatus* shows exactly the opposite trend.

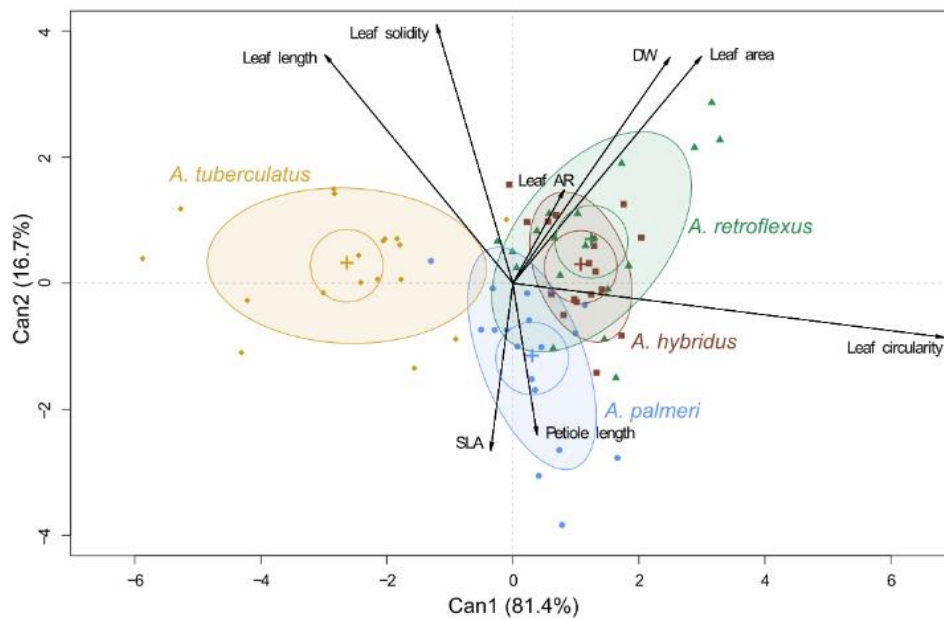


Figure 1. Canonical Discriminant Analysis biplot concerning morpho-anatomical leaf traits analysed at macroscopic scale level. Abbreviation list: Can1 and Can2 = the two first canonical variables; DW = Dry Weight; SLA = Specific Leaf Area.

The CDA analysis applied to the second group of variables comprising traits related to leaf surface measurable on a microscopic scale shows a more homogeneous distribution between the two canonical variables of the explained variance, which altogether reaches a value close to 83%.

Again, *A. tuberculatus* is clearly distinct from the other 3 species, whose ellipsoids are in the positive portion of the biplot and showed a high positive correlation with the traits in this range, especially with some roughness-related variables such as Rsk, Rv and FPO, while the level is milder for cellular parameters such as area, circularity and AR (Fig. 2). The only Rp character is positively correlated with *A. tuberculatus*, which again shows mirrored layout compared to the other three species under study. The negative score attributed to it in the DIM plot (Fig. S4) is therefore attributable to the correlation with the traits negatively correlated with Can1 (Rp and FAD) and further to the inverse correlation it shows with Rsk Rv and FPO, variables that positively influence the score. In any case, the absolute values of the scores vary little, confirming the fact that the analysis in this second area returned a Can1 parameter capable of explaining only 50% of the variability.

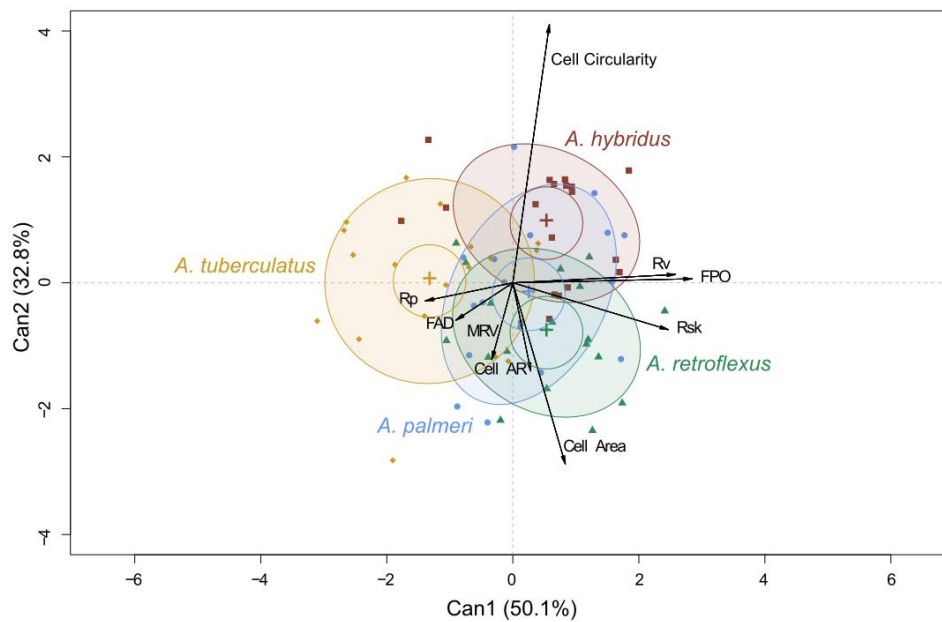


Figure 2. Canonical Discriminant Analysis biplot concerning morpho-anatomical traits of the leaf surface analysed at microscopic scale level. Abbreviation list: Can1 and Can2 = the two first canonical variables; Rp = highest peak height of surface; FAD = average direction of azimuthal facets; MRV = vector resulting from the average of the inclinations of all cellular facets; Cell AR = cell Aspect Ratio; Rv = lowest valley of surface; FPO = average polar facet orientation; Rsk = skewness of the assessed epidermis profile.

The CDA analysis of the characters involved in leaf evapotranspiration is shown in Figs. 3 and S5. The variability explained by the two main canonical variables is collectively 98% and the percentage difference between Can1 and Can2 is small. Fig. 3 again shows that *A. tuberculatus* differs from the other species when considering traits involved in leaf conductivity. In fact, the ellipsoid relative to *A. tuberculatus* is in the right portion of the biplot, unlike the other ellipsoids, which are positioned in the left-hand side. Apart from *A. retroflexus*, the other species are graphically separated on the y-axis constructed on Can1, which therefore proves capable of distinguishing *A. tuberculatus*, *A. palmeri* and *A. hybridus* from each other.

The trait "hairiness AR" is described by a vector with a positive direction almost parallel to the x-axis of Can1, while the vector "hairiness perimeter", also parallel to the abscissa, has a negative direction.

The DIM plot (Fig. S5) with the box-plot analysis confirms that *A. retroflexus* has a positive score due to the high positive correlation with the hairiness AR and the partial correlation with the hairiness circularity, and *A. palmeri*, the other dioecious species, also shows a value slightly higher than 0. On the contrary, the two monoecious species, *A. hybridus* and *A. tuberculatus*, are characterised by negative scores that can be

explained by the high correlation with the negative vectors of the traits "hairiness perimeter", "hairiness area" and "stomata density".

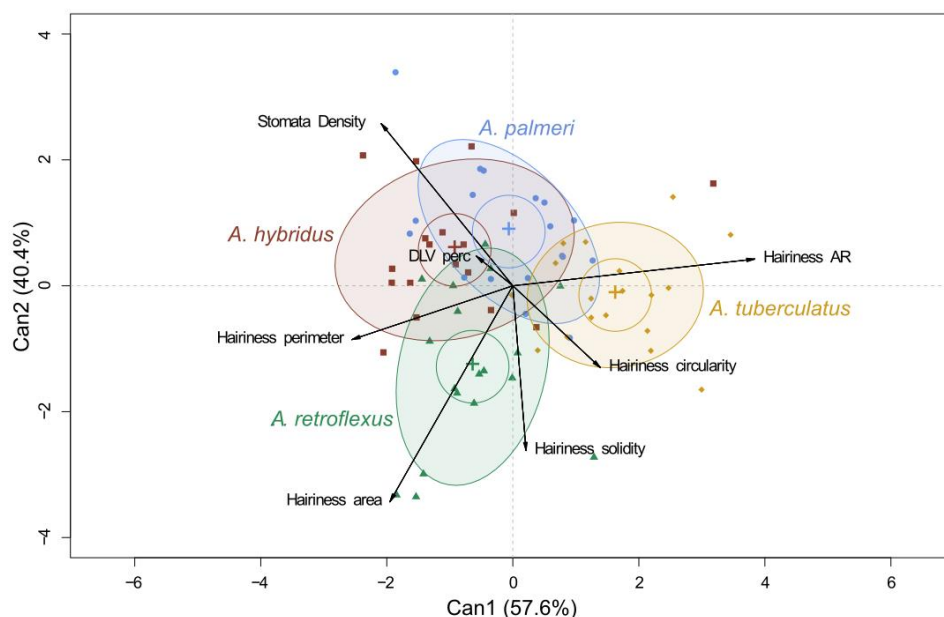


Figure 3. Canonical Discriminant Analysis biplot concerning morpho-anatomical leaf traits related to evapotranspiration (ET) analysed at microscopic scale level. Abbreviation list: Can1 and Can2 = the two first canonical variables; Hairiness AR = hairiness Aspect Ratio; DLV perc = Density of Leaf Veins percentage.

The results obtained from the CDA allowed to highlight which trait was a significant factor in discriminating the different amaranth species from each other and which also had a high correlation with the multivariate model and was therefore able to adequately explain the variability observed.

ANOVA evidencing most effective traits

As confirmation of the evidence provided by the CDA, these traits were individually subjected to ANOVA one-way tests, as described in Table 3.

Table 3. ANOVA of morpho-anatomical leaf traits at different scale levels. Abbreviation list: Df = degree of freedom; Sum Sq = Sum of Squares; F = Fisher, P = P value; ET = Evapotranspiration. Significance level: "***" = $P < 0.01$; "****" = $P < 0.001$.

Leaf analysis level	Trait		Df	Sum Sq	F value	P	Significance	
Macroscopic traits	<i>Leaf area</i>	Transformation: ln (<i>Leaf area</i>)						
		Species	3	1.22	4.988	0.003	**	
		Residuals	68	5.54				
	<i>Leaf circularity</i>	Transformation: (<i>Leaf circularity</i>) ³						
		Species	3	0.47	35.644	<0.001	***	
		Residuals	68	0.30				
	<i>Leaf length</i>	Transformation: none						
		Species	3	298.61	4.882	0.004	**	
		Residuals	68	1386.43				
Surface-related microscopic traits	<i>FPO</i>	Transformation: (<i>FPO</i>) ⁵						
		Species	3	3.64 e ⁺¹⁸	4.852	0.004	**	
		Residuals	68	1.70 e ⁺¹⁹				
	<i>Cell Area</i>	Transformation: sqrt (<i>Cell area</i>)						
		Species	3	392.55	4.456	0.006	**	
		Residuals	68	1996.81				
	<i>Cell circularity</i>	Transformation: none						
		Species	3	0.11	6.813	<0.001	***	
		Residuals	68	0.37				
ET-related traits	<i>Hairiness AR</i>	Transformation: 1/ <i>Hairiness AR</i>						
		Species	3	0.26	11.929	<0.001	***	
		Residuals	68	0.49				
	<i>Stomata density</i>	Transformation: sqrt (<i>Stomata density</i>)						
		Species	3	114254.00	5.686	0.002	**	
	Residuals	68	455456.00					

All the considered variables showed a high degree of significance in the ANOVA test (at least $P < 0.01$) and in some cases also revealed significant differences if the LSD post hoc test was applied. Among the macroscopic traits, leaf area had a high significance

(Table 3) due to the higher averages measured in the two monoecious species. The post hoc analysis revealed that only *A. retroflexus* and *A. tuberculatus* were significantly different for this trait (Fig. S6). The leaf circularity variable significantly differed among species and again the mean of *A. tuberculatus* was significantly lower on the LSD test when compared to the other species (Fig. S7). The leaf length similarly showed that the mean value of this trait measured in *A. tuberculatus* was significantly higher than in *A. palmeri* (Fig. S8).

Regarding the microscopic characters related to roughness, the ANOVA showed a more differentiated pattern. On the one hand, the variable FPO again showed a significantly different mean value between *A. palmeri* and *A. retroflexus* at the LSD test (Fig. S9), which is known to cause different leaf surface behaviour when studying the Bi-directional Scattering Distribution Function [39]. On the other hand, the tegument cell area in the two monoecious varieties was significantly different in the LSD test, because the epidermal cell area of *A. retroflexus* was about one third greater than that of *A. hybridus* (Fig. S10).

Cell circularity showed a further significant pattern of response in the *Amaranthus* species under study. The shape of the cells of *A. hybridus* most closely approximated a circumference and differentiates them significantly from those of *A. palmeri* and *A. retroflexus* for this specific trait (Fig. S11).

The last group of variables considered includes the traits capable of modulating the exchanges between the leaf and its environment and, in accordance with the CDA, the significance of the species as independent variable was demonstrated by means of the ANOVA test. In particular, the hairiness AR of the hairs distributed along the leaf perimeter showed a high ratio between the major and minor axis in *A. tuberculatus* (Fig. S12), which the LSD test demonstrated to be significantly different from that of the other species investigated. Similarly, it was possible to show that the stomata density of *A. tuberculatus* (Fig. S13) was the lowest of the four species examined and was significantly different from that of *A. hybridus*. Although without any significance, considering the averages of the other two species concerning this trait, a different behaviour of the two monoecious species compared to the dioecious species is conceivable.

DISCUSSION

In recent years, non-invasive imaging techniques have been developed for quantitative studies of plant traits related to plant growth and adaptation to biotic and abiotic stress, extending from single microscope acquisitions to high-scale imaging through remote sensing [5,40]. Here we conducted an integrated multi-scale (whole leaf, tissue and cells) approach analysis on single leaf phenotypic variation among four phylogenetically related *Amaranthus* summer weeds (*A. hybridus*, *A. retroflexus*, *A. palmeri*, and *A. tuberculatus*). These species are commonly invading soybean fields of northern Italy, becoming more and more noxious for the ability of several populations

to evolve cross-resistance to the herbicide Mode of Action most used for their control, the acetolactate synthase (ALS) inhibitors [11,19,41].

We combined conventional digital leaf morphometrics with further analysis by scaling down at a higher spatial resolution, through the processing of reflection confocal microscopy acquisitions on adaxial surface imprints. The latter technique avoids time-consuming histochemical sample preparations and allows the visualization of leaf surface and cell structure of epidermis, as well as hairiness, thus providing quantitative anatomical traits deeply related to functional processes of the leaf/plant, such as photosynthesis, hydraulic conductance or plastic acclimation and adaptation responses to environmental changes [8,24]. In this respect, many authors advocate the necessity of filling the lack of integration between high-throughput, whole plant phenotyping analysis and quantification of in-depth anatomical or molecular traits of leaves at different scale of organization [24,42,43]. This could represent one of the major challenges in plant phenotyping approach, as valid technology useful for implementation and transition to precision and digital agriculture [23] and development of more resilient agroecosystems [44].

In addition to a synchronization in the analysis of different species at a very similar early growth stage, another challenging issue we faced in the present investigation was to assess the multi-scale phenotyping analysis on younger, still maturing foliar blade of the weed plants, when for example leaf hairs are not completely differentiated [45]. This approach was chosen with two levels of rationale: (i) effective weed control management of these species requires foliar application at very juvenile stage (6-9 true leaf stage, corresponding to BBCH 12-14 [26]) and (ii) so far identification of leaf phenotypic plasticity has been mainly performed at adult stage only across crop *Amaranthus* spp. and cultivars aiming to link green colour to nutritional state [46] or climate conditions [47], for selection of varieties with desirable traits. On the other hand, few reports analysing leaf morphometrics of weed amaranth species are available to the best of our knowledge [48,49]. Indeed, taxonomic identification studies [12] and simplified botanical keys [11] recently arranged in Italy on *Amaranthus* spp. mostly rely on reproductive traits. The presented results revealed that multi-scale phenotyping analysis on young leaf was accurate, reproducible and reliable, capable of discriminating across the four amaranth species. In addition to quantitative (continuous) parameters, the present analysis also includes automated assessment of qualitative (categorical) variables, usually relied on visual inspection in traditional manual phenotyping and not included in statistical analysis of variance in most studies, because of difficulty of quantification. More specifically, we highlighted through CDA analysis that the variables comprising leaf blade shape and size (leaf circularity, and to a lesser extent, leaf area and leaf length) and hairiness traits (hairiness Aspect Ratio) were the most important in explaining the highest percentage of variance, by markedly distinguishing *A. tuberculatus* from the other three species. Some of these results were expected, given the elongated, lance-shaped leaves observed in the first species, visually noticeable also at the first stages of development (Fig. S1). Also, our results confirmed that the relationships between leaf shape and size traits are strongly

correlated [50] and attest that the taxonomic basis is one of the main drivers of leaf shape variation also at juvenile stage. We found that *A. tuberculatus* is the species that possesses more distinctive macroscopic morpho-anatomical characters and therefore may have undergone to a separate evolutionary path more than others. Supporting this statement, recent studies on phylogenetic relationships and size of the genome in the genus *Amaranthus* confirm that the monoecious *A. retroflexus* and *A. hybridus* belong to the same subgenus *Amaranthus*, while the two dioecious species *A. palmeri* and *A. tuberculatus*, although included in the same subgenus *Acnida*, have been described as phylogenetically divergent [51,52].

Leaf phenotyping variation associated to leaf shape and Aspect Ratio is extremely tuned up for optimizing leaf photosynthetic capacity and plant growth, by influencing light absorption and gas exchanges [53,54]. In particular, *A. tuberculatus* had smaller leaf circularity values, an indirect shape descriptor representing the ratio between leaf area and true perimeter, which is linked to serrations and lobes and linked to elongated shapes [55]. This morphometric parameter, as well as Aspect Ratio and solidity, have previously been used to measure the genetic basis of shape variation in several crop species, being strongly related to important yield traits [53,56–58].

Among morphometrical traits explaining leaf variation in respect to evapotranspiration, hairiness AR of marginal trichomes was an additional parameter, useful in distinguishing *A. tuberculatus* from the other species. In fact, this species showed to possess significantly high values of hairiness Aspect Ratio (inversely correlated to hairiness roundness) compared to the other amaranth species. The structure of leaf surface is influenced at three different levels by trichome shape and density and protruding veins, by cell size shape and undulation and by shape and size of the epicuticular wax system [59,60]. All these traits concur to affect plant health and adaptation to multiple environmental stresses [61,62], and pesticide wetting [63] by influencing herbicide distribution and absorption. However, it must be stressed that the other variables of leaf tegument structure at this plant stage did not discriminate across specific leaf phenotypes and inconclusive relationships could be extrapolated within the studied amaranths, apart from stomata density for which *A. tuberculatus* can be significantly distinguished only from *A. hybridus*. These results could be rationalized because in juvenile leaves epidermal cells generally do not produce epidermal hairs, except along the leaf margins or tip [64], so that trichome differentiation on the adaxial page of leaf non-margin area was not still completed at the time of image acquisition. For this reason, we cannot rule out that at older stage the hairiness trait module could better explain the effects of genotype or environment on leaf phenotypic plasticity of these amaranths. Even though trichomes and stomata may possess species-specific form with taxonomic value, also in part characterized in *Amaranthus* genus [48,49], we did not find further distinct traits for these components across the studied species.

Similarly, the variables inherent to the microscopic features and describing the surface roughness-related traits and the shape of epidermal cells were analysed. The investigation has highlighted a pattern in which the species under consideration overlapped greatly and did not show specific significant differences among them.

These traits were ones of the main internal factors in addition to hairiness and stomatal density influencing leaf wettability, as well as representing the first response barrier against several types of natural environment stresses and plant diseases [60]. If these traits have shown strong similarities among the young leaves of the four amaranths, we may suppose that the individual species would respond in a similar way or have common patterns of response to stresses and to different agronomic management practices.

Partially contrary to our expectations, the results of the low-impact multi-scale phenotyping proposed in the present work proved that leaf plasticity at juvenile stage across weed amaranths is mainly driven by the morphometric traits associated to leaf size and shape module, often traditionally used as diagnostic of species [65], and, at in-depth anatomical level, only to stomata density and hairiness AR among the water-related leaf traits analysed.

In contrast, image-based phenotyping of leaf surface structure at microscopic scale highlighted that these traits at younger stages contributed to a lesser extent in unravelling taxonomic leaf variation across these species. Similar conclusions were also highlighted for juvenile-to-adult phase change in grasses, in which leaf shape resulted to be a more reliable proxy than leaf anatomical traits [66]. Also, the question if the pattern of correlations among multiple leaf characters, defined as phenotyping integration [67], can change or not during ontogeny is still a unresolved debate [67,68]. However, phenotyping of the leaf surface-traits, being the latter strongly related to photosynthetic capacity, water conservation strategy of the plant and even water/surface interaction, could instead result more consistent to quantitative investigation of traits related to adaptive responses in an ecological context [69,70], as an innovative opportunity in supporting the definition of next generation strategies for the sustainable management of the agro-ecosystem.

More in general, multi-scale leaf phenotyping analysis could integrate further advanced detection techniques, such as remote sensing [44,71], and easily extended and adapted for ecophysiological studies concerning amaranth-crop interaction, also in the perspective of climate change adaptations.

AUTHOR CONTRIBUTIONS

All the authors conceived the project. A. Milani, S. Panozzo and S. Varotto provided the plant material. F. D'Este performed the confocal analyses. G. Este, E. Petrusa and D. Scarpin performed the other measurements. G. Este processed the images to collect the data. F. Boscutti, M. Vuerich, D. Scarpin and E. Braidot performed the statistical analyses. D. Scarpin, E. Braidot, E. Petrusa, F. Boscutti wrote the manuscript. A. Milani, S. Panozzo and S. Varotto and F. D'Este revised the manuscript, with the assistance of all co-authors.

REFERENCES

1. R. Pieruschka, U. Schurr, Plant Phenotyping: Past, Present, and Future, *Plant Phenomics*. 2019 (2019) 1–6. <https://doi.org/10.34133/2019/7507131>.
2. W.-B. Jiao, K. Schneeberger, The impact of third generation genomic technologies on plant genome assembly, *Current Opinion in Plant Biology*. 36 (2017) 64–70. <https://doi.org/10.1016/j.pbi.2017.02.002>.
3. S.E. Sultan, Phenotypic plasticity for plant development, function and life history, *Trends in Plant Science*. 5 (2000) 537–542. [https://doi.org/10.1016/S1360-1385\(00\)01797-0](https://doi.org/10.1016/S1360-1385(00)01797-0).
4. D. Houle, D. Govindaraju, S. Omholt, Phenomics: The next challenge, *Nature Reviews. Genetics*. 11 (2010) 855–66. <https://doi.org/10.1038/nrg2897>.
5. Z. Li, R. Guo, M. Li, Y. Chen, G. Li, A review of computer vision technologies for plant phenotyping, *Computers and Electronics in Agriculture*. 176 (2020) 105672. <https://doi.org/10.1016/j.compag.2020.105672>.
6. S.D. Choudhury, S. Goswami, S. Bashyam, T. Awada, A. Samal, Automated Stem Angle Determination for Temporal Plant Phenotyping Analysis, in: 2017 IEEE International Conference on Computer Vision Workshops (ICCVW), 2017: pp. 2022–2029. <https://doi.org/10.1109/ICCVW.2017.237>.
7. S. Das Choudhury, S. Bashyam, Y. Qiu, A. Samal, T. Awada, Holistic and component plant phenotyping using temporal image sequence, *Plant Methods*. 14 (2018). <https://doi.org/10.1186/s13007-018-0303-x>.
8. C.F. Strock, H.M. Schneider, J.P. Lynch, Anatomics: High-throughput phenotyping of plant anatomy, *Trends in Plant Science*. 27 (2022) 520–523. <https://doi.org/10.1016/j.tplants.2022.02.009>.
9. J. Kattge, G. Bönisch, S. Díaz, S. Lavorel, I.C. Prentice, P. Leadley, S. Tautenhahn, G.D.A. Werner, T. Aakala, M. Abedi, A.T.R. Acosta, G.C. Adamidis, K. Adamson, M. Aiba, C.H. Albert, J.M. Alcántara, C. Alcázar C, I. Aleixo, H. Ali, B. Amiaud, C. Ammer, M.M. Amoroso, M. Anand, C. Anderson, N. Anten, J. Antos, D.M.G. Apgaua, T.-L. Ashman, D.H. Asmara, G.P. Asner, M. Aspinwall, O. Atkin, I. Aubin, L. Bastrup-Spohr, K. Bahalkeh, M. Bahn, T. Baker, W.J. Baker, J.P. Bakker, D. Baldocchi, J. Baltzer, A. Banerjee, A. Baranger, J. Barlow, D.R. Barneche, Z. Baruch, D. Bastianelli, J. Battles, W. Bauerle, M. Bauters, E. Bazzato, M. Beckmann, H. Beeckman, C. Beierkuhnlein, R. Bekker, G. Belfry, M. Belluau, M. Beloiu, R. Benavides, L. Benomar, M.L. Berdugo-Lattke, E. Berenguer, R. Bergamin, J. Bergmann, M. Bergmann Carlucci, L. Berner, M. Bernhardt-Römermann, C. Bigler, A.D. Bjorkman, C. Blackman, C. Blanco, B. Blonder, D. Blumenthal, K.T. Bocanegra-González, P. Boeckx, S. Bohlman, K. Böhning-Gaese, L. Boisvert-Marsh, W. Bond, B. Bond-Lamberty, A. Boom, C.C.F. Boonman, K. Bordin, E.H. Boughton, V. Boukili, D.M.J.S. Bowman, S. Bravo, M.R. Brendel, M.R. Broadley, K.A. Brown, H. Bruelheide, F. Brumnich, H.H. Bruun, D. Bruy, S.W. Buchanan, S.F. Bucher, N. Buchmann, R. Buitenwerf, D.E. Bunker, J. Bürger, S. Burrascano, D.F.R.P. Burslem, B.J. Butterfield, C. Byun, M. Marques, M.C. Scalon, M. Caccianiga, M. Cadotte, M. Cailleret, J. Camac, J.J. Camarero, C. Company, G. Campetella, J.A.

Campos, L. Cano-Arboleda, R. Canullo, M. Carbognani, F. Carvalho, F. Casanoves, B. Castagneyrol, J.A. Catford, J. Cavender-Bares, B.E.L. Cerabolini, M. Cervellini, E. Chacón-Madrigal, K. Chapin, F.S. Chapin, S. Chelli, S.-C. Chen, A. Chen, P. Cherubini, F. Chianucci, B. Choat, K.-S. Chung, M. Chytrý, D. Ciccarelli, L. Coll, C.G. Collins, L. Conti, D. Coomes, J.H.C. Cornelissen, W.K. Cornwell, P. Corona, M. Coyea, J. Craine, D. Craven, J.P.G.M. Crowsigt, A. Csecserits, K. Cufar, M. Cuntz, A.C. da Silva, K.M. Dahlin, M. Dainese, I. Dalke, M. Dalle Fratte, A.T. Dang-Le, J. Danihelka, M. Dannoura, S. Dawson, A.J. de Beer, A. De Frutos, J.R. De Long, B. Dechant, S. Delagrange, N. Delpierre, G. Derroire, A.S. Dias, M.H. Diaz-Toribio, P.G. Dimitrakopoulos, M. Dobrowolski, D. Doktor, P. Dřevojan, N. Dong, J. Dransfield, S. Dressler, L. Duarte, E. Ducouret, S. Dullinger, W. Durka, R. Duursma, O. Dymova, A. E-Vojtkó, R.L. Eckstein, H. Ejtehadi, J. Elser, T. Emilio, K. Engemann, M.B. Erfanian, A. Erfmeier, A. Esquivel-Muelbert, G. Esser, M. Estiarte, T.F. Domingues, W.F. Fagan, J. Fagúndez, D.S. Falster, Y. Fan, J. Fang, E. Farris, F. Fazlioglu, Y. Feng, F. Fernandez-Mendez, C. Ferrara, J. Ferreira, A. Fidelis, B. Finegan, J. Firn, T.J. Flowers, D.F.B. Flynn, V. Fontana, E. Forey, C. Forgiarini, L. François, M. Frangipani, D. Frank, C. Frenette-Dussault, G.T. Freschet, E.L. Fry, N.M. Fyllas, G.G. Mazzochini, S. Gachet, R. Gallagher, G. Ganade, F. Ganga, P. García-Palacios, V. Gargaglione, E. Garnier, J.L. Garrido, A.L. de Gasper, G. Gea-Izquierdo, D. Gibson, A.N. Gillison, A. Giroldo, M.-C. Glasenhardt, S. Gleason, M. Gliesch, E. Goldberg, B. Gödel, E. Gonzalez-Akre, J.L. Gonzalez-Andujar, A. González-Melo, A. González-Robles, B.J. Graae, E. Granda, S. Graves, W.A. Green, T. Gregor, N. Gross, G.R. Guerin, A. Günther, A.G. Gutiérrez, L. Haddock, A. Haines, J. Hall, A. Hambuckers, W. Han, S.P. Harrison, W. Hattingh, J.E. Hawes, T. He, P. He, J.M. Heberling, A. Helm, S. Hempel, J. Hentschel, B. Hérault, A.-M. Hereş, K. Herz, M. Heuertz, T. Hickler, P. Hietz, P. Higuchi, A.L. Hipp, A. Hirons, M. Hock, J.A. Hogan, K. Holl, O. Honnay, D. Hornstein, E. Hou, N. Hough-Snee, K.A. Hovstad, T. Ichie, B. Igić, E. Illa, M. Isaac, M. Ishihara, L. Ivanov, L. Ivanova, C.M. Iversen, J. Izquierdo, R.B. Jackson, B. Jackson, H. Jactel, A.M. Jagodzinski, U. Jandt, S. Jansen, T. Jenkins, A. Jentsch, J.R.P. Jespersen, G.-F. Jiang, J.L. Johansen, D. Johnson, E.J. Jokela, C.A. Joly, G.J. Jordan, G.S. Joseph, D. Junaedi, R.R. Junker, E. Justes, R. Kabzems, J. Kane, Z. Kaplan, T. Kattenborn, L. Kavelenova, E. Kearsley, A. Kempel, T. Kenzo, A. Kerkhoff, M.I. Khalil, N.L. Kinlock, W.D. Kissling, K. Kitajima, T. Kitzberger, R. Kjølner, T. Klein, M. Kleyer, J. Klimešová, J. Klipel, B. Kloeppel, S. Klotz, J.M.H. Knops, T. Kohyama, F. Koike, J. Kollmann, B. Komac, K. Komatsu, C. König, N.J.B. Kraft, K. Kramer, H. Kreft, I. Kühn, D. Kumarathunge, J. Kuppler, H. Kurokawa, Y. Kurosawa, S. Kuyah, J.-P. Laclau, B. Lafleur, E. Lallai, E. Lamb, A. Lamprecht, D.J. Larkin, D. Laughlin, Y. Le Bagousse-Pinguet, G. le Maire, P.C. le Roux, E. le Roux, T. Lee, F. Lens, S.L. Lewis, B. Lhotsky, Y. Li, X. Li, J.W. Lichstein, M. Liebergesell, J.Y. Lim, Y.-S. Lin, J.C. Linares, C. Liu, D. Liu, U. Liu, S. Livingstone, J. Llusià, M. Lohbeck, Á. López-García, G. Lopez-Gonzalez, Z. Lososová, F. Louault, B.A. Lukács, P. Lukeš, Y. Luo, M. Lussu, S. Ma, C. Maciel Rabelo Pereira, M. Mack, V. Maire, A. Mäkelä, H. Mäkinen, A.C.M. Malhado, A. Mallik, P. Manning, S. Manzoni, Z. Marchetti, L. Marchino, V. Marcilio-Silva, E. Marcon, M. Marignani, L. Markesteijn, A. Martin, C. Martínez-Garza, J.

Martínez-Vilalta, T. Mašková, K. Mason, N. Mason, T.J. Massad, J. Mase, I. Mayrose, J. McCarthy, M.L. McCormack, K. McCulloh, I.R. McFadden, B.J. McGill, M.Y. McPartland, J.S. Medeiros, B. Medlyn, P. Meerts, Z. Mehrabi, P. Meir, F.P.L. Melo, M. Mencuccini, C. Meredieu, J. Messier, I. Mészáros, J. Metsaranta, S.T. Michaletz, C. Michelaki, S. Migalina, R. Milla, J.E.D. Miller, V. Minden, R. Ming, K. Mokany, A.T. Moles, A. Molnár V, J. Molofsky, M. Molz, R.A. Montgomery, A. Monty, L. Moravcová, A. Moreno-Martínez, M. Moretti, A.S. Mori, S. Mori, D. Morris, J. Morrison, L. Mucina, S. Mueller, C.D. Muir, S.C. Müller, F. Munoz, I.H. Myers-Smith, R.W. Myster, M. Nagano, S. Naidu, A. Narayanan, B. Natesan, L. Negoita, A.S. Nelson, E.L. Neuschulz, J. Ni, G. Niedrist, J. Nieto, Ü. Niinemets, R. Nolan, H. Nottebrock, Y. Nouvellon, A. Novakovskiy, T.N. Network, K.O. Nystuen, A. O'Grady, K. O'Hara, A. O'Reilly-Nugent, S. Oakley, W. Oberhuber, T. Ohtsuka, R. Oliveira, K. Öllerer, M.E. Olson, V. Onipchenko, Y. Onoda, R.E. Onstein, J.C. Ordonez, N. Osada, I. Ostonen, G. Ottaviani, S. Otto, G.E. Overbeck, W.A. Ozinga, A.T. Pahl, C.E.T. Paine, R.J. Pakeman, A.C. Papageorgiou, E. Parfionova, M. Pärtel, M. Patacca, S. Paula, J. Paule, H. Pauli, J.G. Pausas, B. Peco, J. Penuelas, A. Perea, P.L. Peri, A.C. Petisco-Souza, A. Petraglia, A.M. Petritan, O.L. Phillips, S. Pierce, V.D. Pillar, J. Pisek, A. Pomogaybin, H. Poorter, A. Portsmouth, P. Poschlod, C. Potvin, D. Pounds, A.S. Powell, S.A. Power, A. Prinzing, G. Puglielli, P. Pyšek, V. Raavel, A. Rammig, J. Ransijn, C.A. Ray, P.B. Reich, M. Reichstein, D.E.B. Reid, M. Réjou-Méchain, V.R. de Dios, S. Ribeiro, S. Richardson, K. Riibak, M.C. Rillig, F. Riviera, E.M.R. Robert, S. Roberts, B. Robroek, A. Roddy, A.V. Rodrigues, A. Rogers, E. Rollinson, V. Rolo, C. Römermann, D. Ronzhina, C. Roscher, J.A. Rosell, M.F. Rosenfield, C. Rossi, D.B. Roy, S. Royer-Tardif, N. Rüger, R. Ruiz-Peinado, S.B. Rumpf, G.M. Rusch, M. Ryo, L. Sack, A. Saldaña, B. Salgado-Negret, R. Salguero-Gomez, I. Santa-Regina, A.C. Santacruz-García, J. Santos, J. Sardans, B. Schamp, M. Scherer-Lorenzen, M. Schleuning, B. Schmid, M. Schmidt, S. Schmitt, J.V. Schneider, S.D. Schowanek, J. Schrader, F. Schrod, B. Schuldt, F. Schurr, G. Selaya Garvizu, M. Semchenko, C. Seymour, J.C. Sfair, J.M. Sharpe, C.S. Sheppard, S. Sheremetiev, S. Shiodera, B. Shipley, T.A. Shovon, A. Siebenkäs, C. Sierra, V. Silva, M. Silva, T. Sitzia, H. Sjöman, M. Slot, N.G. Smith, D. Sodhi, P. Soltis, D. Soltis, B. Somers, G. Sonnier, M.V. Sørensen, E.E. Sosinski Jr, N.A. Soudzilovskaia, A.F. Souza, M. Spasojevic, M.G. Sperandii, A.B. Stan, J. Stegen, K. Steinbauer, J.G. Stephan, F. Sterck, D.B. Stojanovic, T. Strydom, M.L. Suarez, J.-C. Svenning, I. Svitková, M. Svitok, M. Svoboda, E. Swaine, N. Swenson, M. Tabarelli, K. Takagi, U. Tappeiner, R. Tarifa, S. Tauugourdeau, C. Tavsanoğlu, M. te Beest, L. Tedersoo, N. Thiffault, D. Thom, E. Thomas, K. Thompson, P.E. Thornton, W. Thuiller, L. Tichý, D. Tissue, M.G. Tjoelker, D.Y.P. Tng, J. Tobias, P. Török, T. Tarin, J.M. Torres-Ruiz, B. Tóthmérész, M. Treurnicht, V. Trivellone, F. Trolliet, V. Trotsiuk, J.L. Tsakalos, I. Tsiripidis, N. Tysklind, T. Umehara, V. Usoltsev, M. Vadeboncoeur, J. Vaezi, F. Valladares, J. Vamosi, P.M. van Bodegom, M. van Breugel, E. Van Cleemput, M. van de Weg, S. van der Merwe, F. van der Plas, M.T. van der Sande, M. van Kleunen, K. Van Meerbeek, M. Vanderwel, K.A. Vanselow, A. Vårhammar, L. Varone, M.Y. Vasquez Valderrama, K. Vassilev, M. Vellend, E.J. Veneklaas, H. Verbeek, K. Verheyen, A. Vibrans, I. Vieira, J. Villacís, C. Violle, P. Vivek,

- K. Wagner, M. Waldram, A. Waldron, A.P. Walker, M. Waller, G. Walther, H. Wang, F. Wang, W. Wang, H. Watkins, J. Watkins, U. Weber, J.T. Weedon, L. Wei, P. Weigelt, E. Weiher, A.W. Wells, C. Wellstein, E. Wenk, M. Westoby, A. Westwood, P.J. White, M. Whitten, M. Williams, D.E. Winkler, K. Winter, C. Womack, I.J. Wright, S.J. Wright, J. Wright, B.X. Pinho, F. Ximenes, T. Yamada, K. Yamaji, R. Yanai, N. Yankov, B. Yguel, K.J. Zanini, A.E. Zanne, D. Zelený, Y.-P. Zhao, J. Zheng, J. Zheng, K. Ziemińska, C.R. Zirbel, G. Zizka, I.C. Zo-Bi, G. Zotz, C. Wirth, TRY plant trait database – enhanced coverage and open access, *Global Change Biology*. 26 (2020) 119–188. <https://doi.org/10.1111/gcb.14904>.
10. J.P. Lynch, C.F. Strock, H.M. Schneider, J.S. Sidhu, I. Ajmera, T. Galindo-Castañeda, S.P. Klein, M.T. Hanlon, Root anatomy and soil resource capture, *Plant Soil*. 466 (2021) 21–63. <https://doi.org/10.1007/s11104-021-05010-y>.
 11. A. Milani, L. Scarabel, M. Sattin, A family affair: resistance mechanism and alternative control of three *Amaranthus* species resistant to acetolactate synthase inhibitors in Italy, *Pest Management Science*. 76 (2020) 1205–1213. <https://doi.org/10.1002/ps.5667>.
 12. D. Iamónico, Taxonomic revision of the genus *Amaranthus* (Amaranthaceae) in Italy, *Phytotaxa*. 199 (2015) 1. <https://doi.org/10.11646/phytotaxa.199.1.1>.
 13. O.N. Ruth, K. Unathi, N. Nomali, M. Chinsamy, Underutilization Versus Nutritional-Nutraceutical Potential of the *Amaranthus* Food Plant: A Mini-Review, *Applied Sciences*. 11 (2021) 6879. <https://doi.org/10.3390/app11156879>.
 14. S.M. Ward, T.M. Webster, L.E. Steckel, Palmer Amaranth (*Amaranthus palmeri*): A Review, *Weed Technology*. 27 (2013) 12–27. <https://doi.org/10.1614/WT-D-12-00113.1>.
 15. X. Ma, H. Wu, W. Jiang, Y. Ma, Y. Ma, Interference between Redroot Pigweed (*Amaranthus retroflexus* L.) and Cotton (*Gossypium hirsutum* L.): Growth Analysis, *PLoS ONE*. 10 (2015) e0130475. <https://doi.org/10.1371/journal.pone.0130475>.
 16. L.M. Schwartz, J.K. Norsworthy, B.G. Young, K.W. Bradley, G.R. Kruger, V.M. Davis, L.E. Steckel, M.J. Walsh, Tall Waterhemp (*Amaranthus tuberculatus*) and Palmer amaranth (*Amaranthus palmeri*) Seed Production and Retention at Soybean Maturity, *Weed Technology*. 30 (2016) 284–290. <https://doi.org/10.1614/WT-D-15-00130.1>.
 17. I. Heap, The International Herbicide-Resistant Weed Database, [www.Weedscience.Org](http://www.weedscience.org). (2023). <https://www.weedscience.org/Home.aspx> (accessed October 24, 2023).
 18. J.M. Kreiner, J.R. Stinchcombe, S.I. Wright, Population Genomics of Herbicide Resistance: Adaptation via Evolutionary Rescue, *Annu Rev Plant Biol*. 69 (2018) 611–635. <https://doi.org/10.1146/annurev-arplant-042817-040038>.
 19. A. Milani, S. Panozzo, S. Farinati, D. Iamónico, M. Sattin, D. Loddo, L. Scarabel, Recent Discovery of *Amaranthus palmeri* S. Watson in Italy: Characterization of ALS-Resistant Populations and Sensitivity to Alternative Herbicides, *Sustainability*. 13 (2021) 7003. <https://doi.org/10.3390/su13137003>.

20. R.A. Massinga, R.S. Currie, M.J. Horak, J. Boyer, Interference of Palmer amaranth in corn, *Weed Science*. 49 (2001) 202–208. [https://doi.org/10.1614/0043-1745\(2001\)049\[0202:IOPAIC\]2.0.CO;2](https://doi.org/10.1614/0043-1745(2001)049[0202:IOPAIC]2.0.CO;2).
21. C.N. Bensch, M.J. Horak, D. Peterson, Interference of redroot pigweed (*Amaranthus retroflexus*), Palmer amaranth (*A. palmeri*), and common waterhemp (*A. rudis*) in soybean, *Weed Science*. 51 (2003) 37–43. [https://doi.org/10.1614/0043-1745\(2003\)051\[0037:IORPAR\]2.0.CO;2](https://doi.org/10.1614/0043-1745(2003)051[0037:IORPAR]2.0.CO;2).
22. J. Schiefelbein, Molecular phenotyping of plant single cell-types enhances forward genetic analyses, *Front Plant Sci*. 6 (2015) 509. <https://doi.org/10.3389/fpls.2015.00509>.
23. J.M. Costa, J. Marques da Silva, C. Pinheiro, M. Barón, P. Mylona, M. Centritto, M. Haworth, F. Loreto, B. Uzilday, I. Turkan, M.M. Oliveira, Opportunities and Limitations of Crop Phenotyping in Southern European Countries, *Frontiers in Plant Science*. 10 (2019). <https://doi.org/10.3389/fpls.2019.01125>.
24. C. Amitrano, A. Junker, N. D’Agostino, S. De Pascale, V. De Micco, Integration of high-throughput phenotyping with anatomical traits of leaves to help understanding lettuce acclimation to a changing environment, *Planta*. 256 (2022) 68. <https://doi.org/10.1007/s00425-022-03984-2>.
25. L. Scarabel, S. Varotto, M. Sattin, A European biotype of *Amaranthus retroflexus* cross-resistant to ALS inhibitors and response to alternative herbicides, *Weed Research*. 47 (2007) 527–533. <https://doi.org/10.1111/j.1365-3180.2007.00600.x>.
26. M. Hess, G. Barralis, H. Bleiholder, L. Buhr, Th. Eggers, H. Hack, R. Stauss, Use of the extended BBCH scale—general for the descriptions of the growth stages of mono; and dicotyledonous weed species, *Weed Research*. 37 (1997) 433–441. <https://doi.org/10.1046/j.1365-3180.1997.d01-70.x>.
27. T. Sun, V. Lazouskaya, Y. Jin, Polydimethylsiloxane replicas efficacy for simulating fresh produce surfaces and application in mechanistic study of colloid retention, *Journal of Food Science*. 84 (2019) 524–531. <https://doi.org/10.1111/1750-3841.14479>.
28. I. Zajicova, E. Tihlarikova, P. Cifrova, P. Kyjakova, V. Nedela, J. Sechet, L. Havelkova, J. Kloutvorova, K. Schwarzerova, Analysis of apple epidermis in respect to ontogenic resistance against *Venturia inaequalis*, *Biologia Plant*. 63 (2019) 662–670. <https://doi.org/10.32615/bp.2019.134>.
29. J. Schindelin, I. Arganda-Carreras, E. Frise, V. Kaynig, M. Longair, T. Pietzsch, S. Preibisch, C. Rueden, S. Saalfeld, B. Schmid, J.-Y. Tinevez, D.J. White, V. Hartenstein, K. Eliceiri, P. Tomancak, A. Cardona, Fiji: an open-source platform for biological-image analysis, *Nat Methods*. 9 (2012) 676–682. <https://doi.org/10.1038/nmeth.2019>.
30. J.N. Maloof, K. Nozue, M.R. Mumbach, C.M. Palmer, LeafJ: An ImageJ Plugin for Semi-automated Leaf Shape Measurement, *JoVE*. (2013) 50028. <https://doi.org/10.3791/50028>.
31. E.G. de la Riva, M. Olmo, H. Poorter, J.L. Ubera, R. Villar, Leaf Mass per Area (LMA) and Its Relationship with Leaf Structure and Anatomy in 34 Mediterranean Woody

- Species along a Water Availability Gradient, *PLOS ONE*. 11 (2016) e0148788. <https://doi.org/10.1371/journal.pone.0148788>.
32. G. Kutbay, A. çakmak, H. Yilmaz, B. Sürmen, Comparison of Leaf Traits (SLA And LMA) on Different Populations of *Alcea apterocarpa*, *Hacettepe Journal of Biology and Chemistry*. 2 (2016) 125–125. <https://doi.org/10.15671/HJBC.20164417630>.
 33. S. Li, L. Li, W. Fan, S. Ma, C. Zhang, J.C. Kim, K. Wang, E. Russinova, Y. Zhu, Y. Zhou, LeafNet: a tool for segmenting and quantifying stomata and pavement cells, *The Plant Cell*. 34 (2022) 1171–1188. <https://doi.org/10.1093/plcell/koac021>.
 34. A. McNaughton, Measuring Surface Roughness Using Confocal Microscopy and ImageJ (or Fiji variant), (2012). https://www.otago.ac.nz/_data/assets/pdf_file/0020/273440/surface-roughness-684709.pdf (accessed October 24, 2023).
 35. B. Forster, D. Van De Ville, J. Berent, D. Sage, M. Unser, Complex wavelets for extended depth-of-field: a new method for the fusion of multichannel microscopy images, *Microsc Res Tech*. 65 (2004) 33–42. <https://doi.org/10.1002/jemt.20092>.
 36. G. Chinga Carrasco, P. Johnsen, R. Dougherty, E. Berli, J. Walter, Quantification of the 3-D micro-structure of SC surfaces, *Journal of Microscopy*. 227 (2007) 254–65. <https://doi.org/10.1111/j.1365-2818.2007.01809.x>.
 37. Vessel Analysis, ImageJ Wiki. (2023). <https://imagej.github.io/plugins/vessel-analysis> (accessed September 14, 2023).
 38. C.A. Price, O. Symonova, Y. Mileyko, T. Hilley, J.S. Weitz, Leaf Extraction and Analysis Framework Graphical User Interface: Segmenting and Analyzing the Structure of Leaf Veins and Areoles, *Plant Physiology*. 155 (2011) 236–245. <https://doi.org/10.1104/pp.110.162834>.
 39. A. Comar, F. Baret, F. Viénot, L. Yan, B. de Solan, Wheat leaf bidirectional reflectance measurements: Description and quantification of the volume, specular and hot-spot scattering features, *Remote Sensing of Environment*. 121 (2012) 26–35. <https://doi.org/10.1016/j.rse.2011.01.028>.
 40. L. Li, Q. Zhang, D. Huang, A Review of Imaging Techniques for Plant Phenotyping, *Sensors*. 14 (2014) 20078–20111. <https://doi.org/10.3390/s141120078>.
 41. Gruppo Italiano Resistenza Erbicidi (GIRE), (n.d.). <http://gire.ipsp.cnr.it/> (accessed October 23, 2023).
 42. C. Granier, F. Tardieu, Multi-scale phenotyping of leaf expansion in response to environmental changes: the whole is more than the sum of parts, *Plant, Cell & Environment*. 32 (2009) 1175–1184. <https://doi.org/10.1111/j.1365-3040.2009.01955.x>.
 43. F. Eeuwijk, D. Bustos-Korts, E. Millet, M. Boer, W. Kruijer, A. Thompson, M. Malosetti, H. Iwata, Q. Roberto, C. Kuppe, O. Muller, K. Blazakis, K. Yu, F. Tardieu, S. Chapman, Modelling strategies for assessing and increasing the effectiveness of new phenotyping techniques in plant breeding, *Plant Science*. (2018). <https://doi.org/10.1016/j.plantsci.2018.06.018>.
 44. M. Janni, R. Pieruschka, Plant phenotyping for a sustainable future, *Journal of Experimental Botany*. 73 (2022) 5085–5088. <https://doi.org/10.1093/jxb/erac286>.

45. A. Telfer, K.M. Bollman, R.S. Poethig, Phase change and the regulation of trichome distribution in *Arabidopsis thaliana*, *Development*. 124 (1997) 645–654. <https://doi.org/10.1242/dev.124.3.645>.
46. W.A. Nyonje, R. Schafleitner, M. Abukutsa-Onyango, R.-Y. Yang, A. Makokha, W. Owino, Precision phenotyping and association between morphological traits and nutritional content in Vegetable Amaranth (*Amaranthus* spp.), *Journal of Agriculture and Food Research*. 5 (2021) 100165. <https://doi.org/10.1016/j.jafr.2021.100165>.
47. U.K.S. Khanam, S. Oba, Phenotypic Plasticity of Vegetable Amaranth, *Amaranthus tricolor* L. under a Natural Climate, *Plant Production Science*. 17 (2014) 166–172. <https://doi.org/10.1626/pps.17.166>.
48. A.A. El-Ghamery, A.M. Sadek, O.H. Abdelbar, Comparative anatomical studies on some species of the genus *Amaranthus* (Family: *Amaranthaceae*) for the development of an identification guide, *Annals of Agricultural Sciences*. 62 (2017) 1–9. <https://doi.org/10.1016/j.aos.2016.11.001>.
49. S. Terzieva, N. Grozeva, K. Velichkova, Morphological studies on three *Amaranthus* species, *Bulgarian Journal of Agricultural Science*. 25 (2019) 136–140.
50. J. Wäldchen, P. Mäder, Plant Species Identification Using Computer Vision Techniques: A Systematic Literature Review, *Arch Comput Methods Eng*. 25 (2018) 507–543. <https://doi.org/10.1007/s11831-016-9206-z>.
51. J.J. Wassom, P.J. Tranel, Amplified Fragment Length Polymorphism-Based Genetic Relationships Among Weedy *Amaranthus* Species, *Journal of Heredity*. 96 (2005) 410–416. <https://doi.org/10.1093/jhered/esi065>.
52. M.G. Stetter, K.J. Schmid, Analysis of phylogenetic relationships and genome size evolution of the *Amaranthus* genus using GBS indicates the ancestors of an ancient crop, *Mol Phylogenet Evol*. 109 (2017) 80–92. <https://doi.org/10.1016/j.ympev.2016.12.029>.
53. D.H. Chitwood, A. Ranjan, C.C. Martinez, L.R. Headland, T. Thiem, R. Kumar, M.F. Covington, T. Hatcher, D.T. Naylor, S. Zimmerman, N. Downs, N. Raymundo, E.S. Buckler, J.N. Maloof, M. Aradhya, B. Prins, L. Li, S. Myles, N.R. Sinha, A Modern Ampelography: A Genetic Basis for Leaf Shape and Venation Patterning in Grape1[C][W][OPEN], *Plant Physiol*. 164 (2014) 259–272. <https://doi.org/10.1104/pp.113.229708>.
54. M. Zhang, B. Liu, Y. Fei, X. Yang, L. Zhao, C. Shi, Y. Zhang, N. Lu, C. Wu, W. Ma, J. Wang, Genetic architecture of leaf morphology revealed by integrated trait module in *Catalpa bungei*, *Horticulture Research*. 10 (2023) uhad032. <https://doi.org/10.1093/hr/uhad032>.
55. M. Li, H. An, R. Angelovici, C. Bagaza, A. Batushansky, L. Clark, V. Coneva, M. Donoghue, E. Edwards, D. Fajardo, H. Fang, M. Frank, T. Gallaher, S. Gebken, T. Hill, S. Jansky, B. Kaur, P. Klahs, L. Klein, D. Chitwood, Topological Data Analysis as a Morphometric Method: Using Persistent Homology to Demarcate a Leaf Morphospace, *Frontiers in Plant Science*. 9 (2018). <https://doi.org/10.3389/fpls.2018.00553>.

56. D.H. Chitwood, R. Kumar, A. Ranjan, J.M. Pelletier, B.T. Townsley, Y. Ichihashi, C.C. Martinez, K. Zumstein, J.J. Harada, J.N. Maloof, N.R. Sinha, Light-Induced Indeterminacy Alters Shade-Avoiding Tomato Leaf Morphology, *Plant Physiol.* 169 (2015) 2030–2047. <https://doi.org/10.1104/pp.15.01229>.
57. S. Gupta, D.M. Rosenthal, J.R. Stinchcombe, R.S. Baucom, The remarkable morphological diversity of leaf shape in sweet potato (*Ipomoea batatas*): the influence of genetics, environment, and G×E, *New Phytologist*. 225 (2020) 2183–2195. <https://doi.org/10.1111/nph.16286>.
58. S.D. Rowland, K. Zumstein, H. Nakayama, Z. Cheng, A.M. Flores, D.H. Chitwood, J.N. Maloof, N.R. Sinha, Leaf shape is a predictor of fruit quality and cultivar performance in tomato, *New Phytologist*. 226 (2020) 851–865. <https://doi.org/10.1111/nph.16403>.
59. L. Boize, C. Gudin, G. Purdue, The influence of leaf surface roughness on the spreading of oil spray drops, *Annals of Applied Biology*. 84 (1976) 205–211. <https://doi.org/10.1111/j.1744-7348.1976.tb01749.x>.
60. H. Wang, H. Shi, Y. Wang, The Wetting of Leaf Surfaces and Its Ecological Significances. *Wetting and Wettability*, IntechOpen, 2015. <https://www.intechopen.com/chapters/49090> (accessed September 13, 2023).
61. A. Garcia, L. Talavera-Mateo, M.E. Santamaria, An automatic method to quantify trichomes in *Arabidopsis thaliana*, *Plant Science*. 323 (2022) 111391. <https://doi.org/10.1016/j.plantsci.2022.111391>.
62. R.D. Peters, S.D. Noble, Characterization of leaf surface phenotypes based on light interaction, *Plant Methods*. 19 (2023) 26. <https://doi.org/10.1186/s13007-023-01004-2>.
63. N.M. Johnson, R.S. Baucom, The double life of trichomes: understanding their dual role in herbivory and herbicide resistance, (2023) 2023.04.28.538721. <https://doi.org/10.1101/2023.04.28.538721>.
64. D.K. Bongard-Pierce, M.M.S. Evans, R.S. Poethig, Heteroblastic Features of Leaf Anatomy in Maize and Their Genetic Regulation, *International Journal of Plant Sciences*. 157 (1996) 331–340. <https://doi.org/10.1086/297353>.
65. J.S. Cope, D. Corney, J.Y. Clark, P. Remagnino, P. Wilkin, Plant species identification using digital morphometrics: A review, *Expert Systems with Applications*. 39 (2012) 7562–7573. <https://doi.org/10.1016/j.eswa.2012.01.073>.
66. A.W. Sylvester, V. Parker-Clark, G.A. Murray, Leaf shape and anatomy as indicators of phase change in the grasses: comparison of maize, rice, and bluegrass, *Am J Bot.* 88 (2001) 2157–2167.
67. X. Damián, J. Fornoni, C.A. Domínguez, K. Boege, Ontogenetic changes in the phenotypic integration and modularity of leaf functional traits, *Functional Ecology*. 32 (2018) 234–246. <https://doi.org/10.1111/1365-2435.12971>.
68. C.M. Mason, L.A. Donovan, Does investment in leaf defenses drive changes in leaf economic strategy? A focus on whole-plant ontogeny, *Oecologia*. 177 (2015) 1053–1066. <https://doi.org/10.1007/s00442-014-3177-2>.

- 69.** N. Pérez-Harguindeguy, S. Díaz, E. Garnier, S. Lavorel, H. Poorter, P. Jaureguiberry, M.S. Bret-Harte, W.K. Cornwell, J.M. Craine, D.E. Gurvich, C. Urcelay, E.J. Veneklaas, P.B. Reich, L. Poorter, I.J. Wright, P. Ray, L. Enrico, J.G. Pausas, A.C. De Vos, N. Buchmann, G. Funes, F. Quétier, J.G. Hodgson, K. Thompson, H.D. Morgan, H. Ter Steege, L. Sack, B. Blonder, P. Poschlod, M.V. Vaieretti, G. Conti, A.C. Staver, S. Aquino, J.H.C. Cornelissen, New handbook for standardised measurement of plant functional traits worldwide, *Aust. J. Bot.* 61 (2013) 167. <https://doi.org/10.1071/BT12225>.
- 70.** W. Liu, L. Zheng, D. Qi, Variation in leaf traits at different altitudes reflects the adaptive strategy of plants to environmental changes, *Ecol Evol.* 10 (2020) 8166–8175. <https://doi.org/10.1002/ece3.6519>.
- 71.** M. Machwitz, R. Pieruschka, K. Berger, M. Schlerf, H. Aasen, S. Fahrner, J. Jiménez-Berni, F. Baret, U. Rascher, Bridging the Gap Between Remote Sensing and Plant Phenotyping—Challenges and Opportunities for the Next Generation of Sustainable Agriculture, *Frontiers in Plant Science.* 12 (2021). <https://doi.org/10.3389/fpls.2021.749374>.

SUPPORTING INFORMATION



Figure S1. Sample image of leaf appearance of the four *Amaranthus* species.

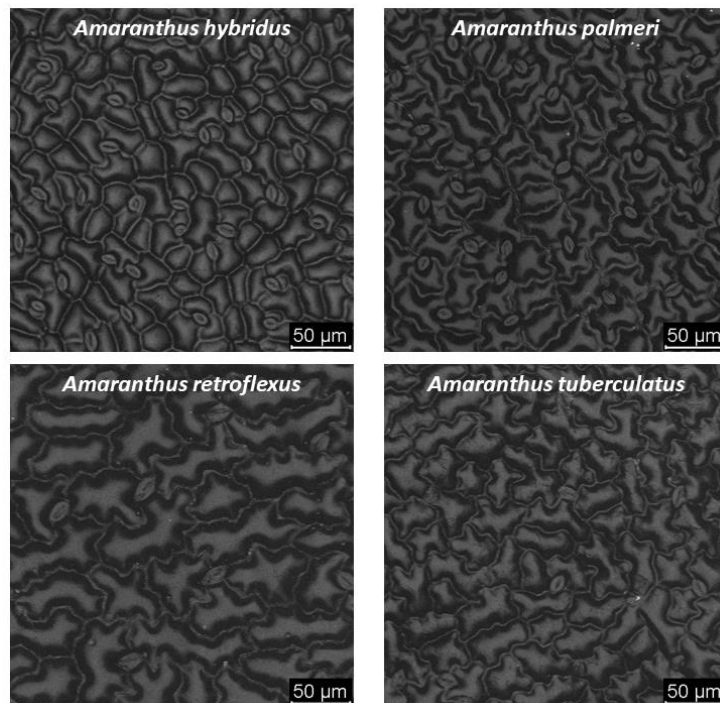


Figure S2. Maximum intensity projections of confocal z-stacks acquired in reflection mode. Samples consist of nail polish imprints of the four *Amaranthus* species, obtained from the adaxial leaf surface.

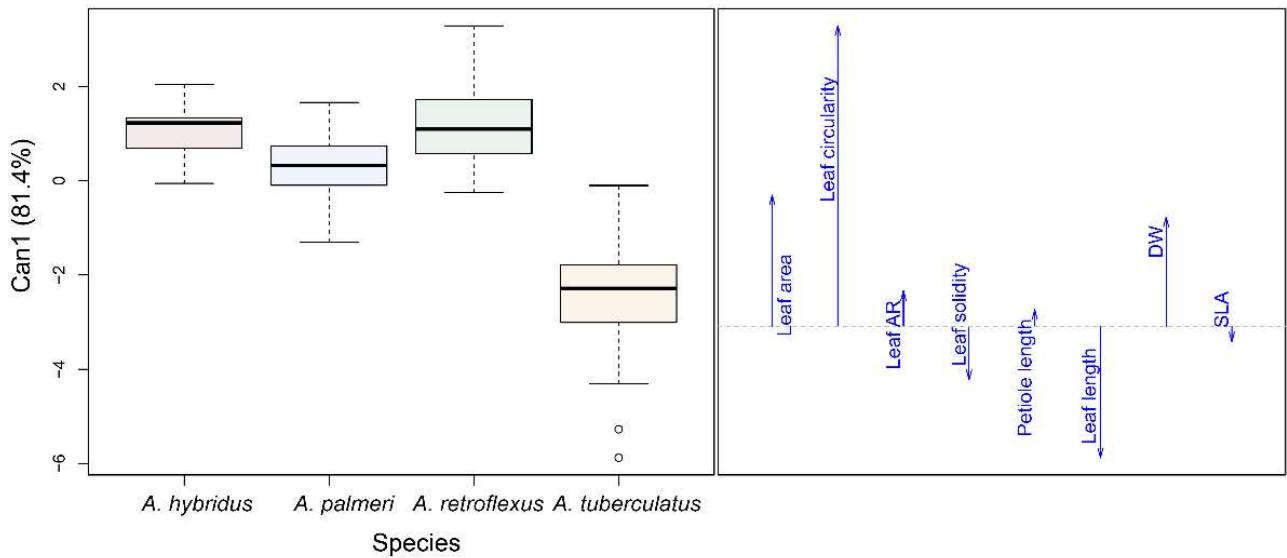


Figure S3. DIM plot concerning morpho-anatomical leaf traits analysed at macroscopic scale level. Left panel shows the canonical scores of the different species calculated considering Can1 only. Right panel describes the positive or negative correlation with Can1 of morpho-anatomical traits, calculated on the basis of the canonical scores.

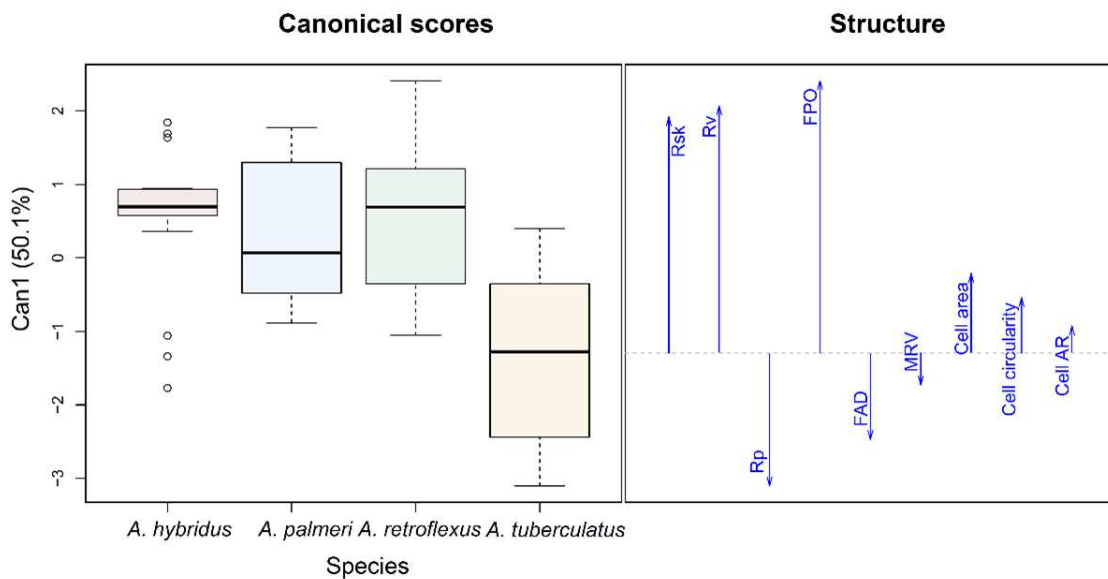


Figure S4. DIM plot concerning morpho-anatomical traits of the leaf surface analysed at microscopic scale level. Left panel shows the canonical scores of the different species calculated considering Can1 only. Right panel describes the positive or negative correlation with Can1 of morpho-anatomical traits, calculated on the basis of the canonical scores.

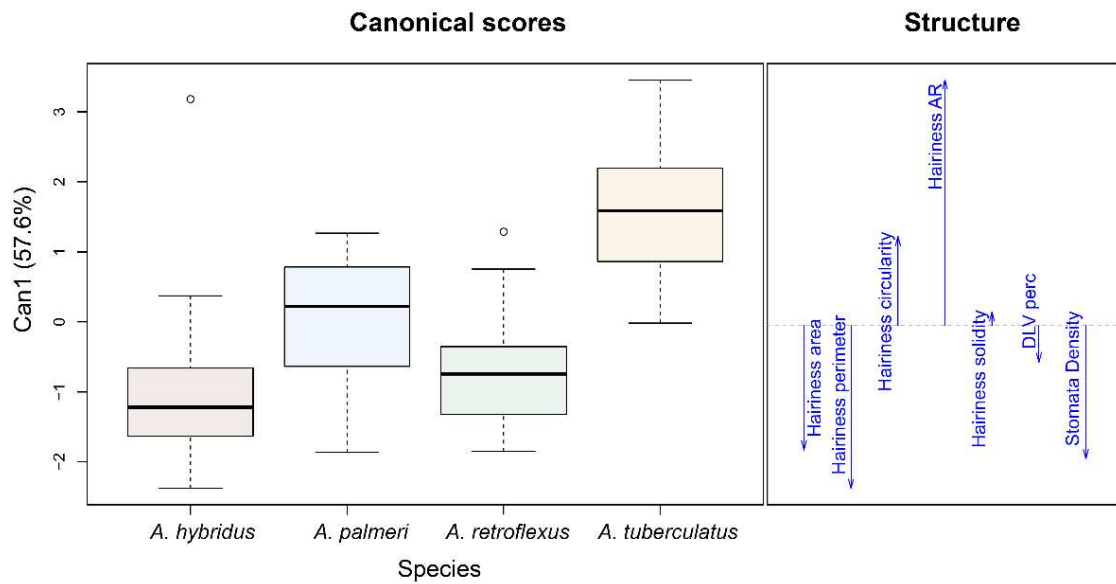


Figure S5. DIM plot concerning morpho-anatomical leaf traits related to evapotranspiration. Left panel shows the canonical scores of the different species calculated considering Can1 only. Right panel describes the positive or negative correlation with Can1 of morpho-anatomical traits, calculated on the basis of the canonical scores.

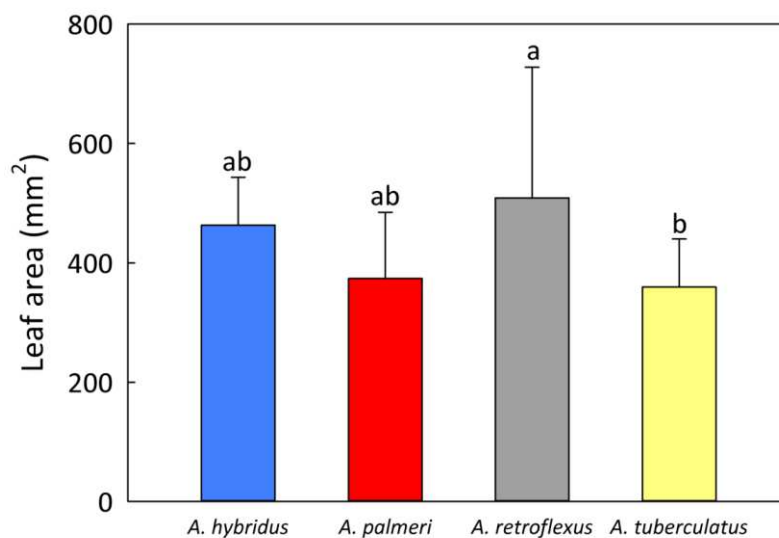


Figure S6. Mean values and LSD test response for the leaf area trait of the four *Amaranthus* species. Bars with different letters indicate significant differences ($P < 0.05$) when LSD test is applied.

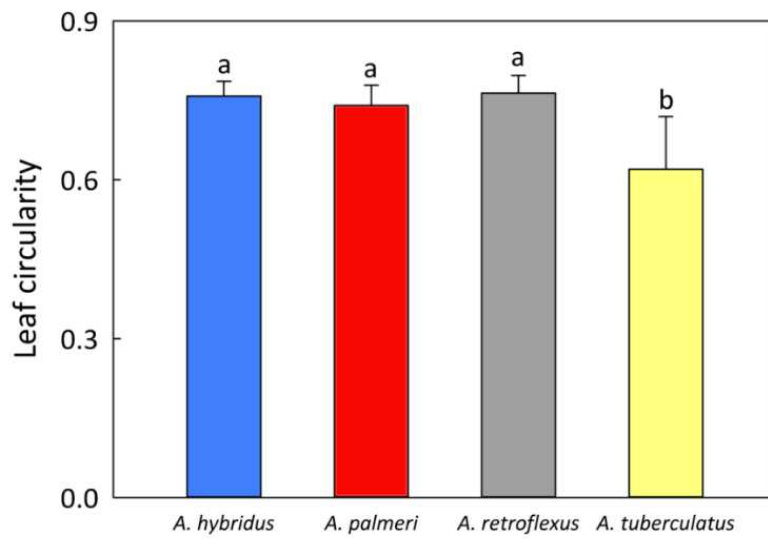


Figure S7. Mean values and LSD test response for the leaf circularity trait of the four *Amaranthus* species. Bars with different letters indicate significant differences ($P < 0.05$) when LSD test is applied.

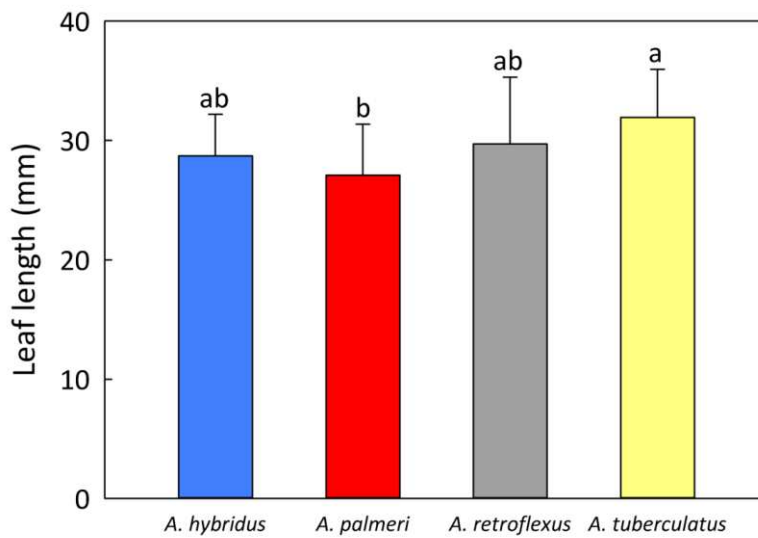


Figure S8. Mean values and LSD test response for the leaf length trait of the four *Amaranthus* species. Bars with different letters indicate significant differences ($P < 0.05$) when LSD test is applied.

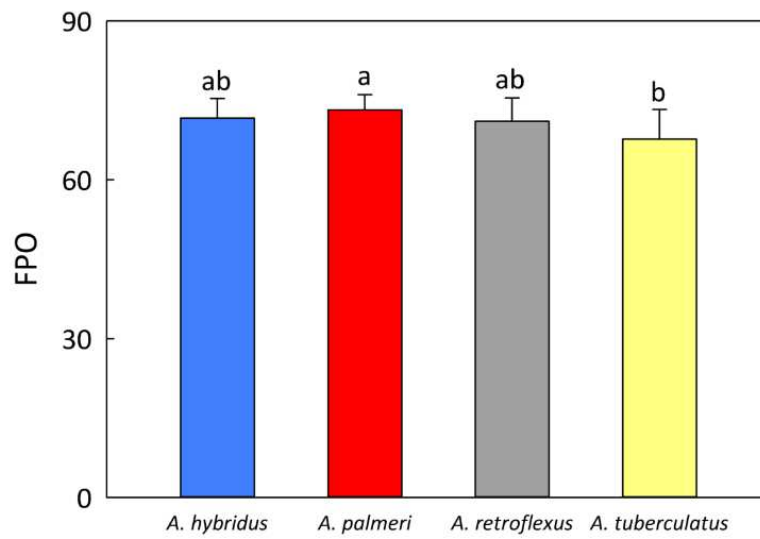


Figure S9. Mean values and LSD test response for the FPO trait of the four Amaranthus species. Bars with different letters indicate significant differences ($P < 0.05$) when LSD test is applied.

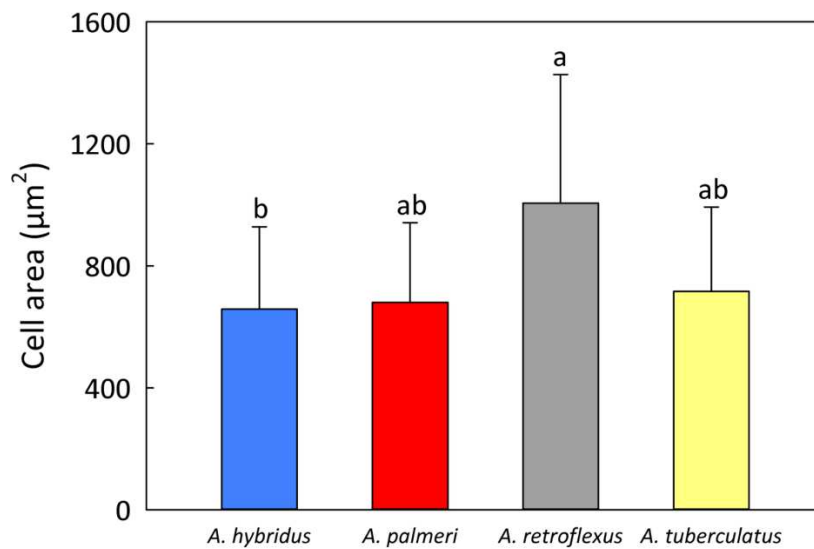


Figure S10. Mean values and LSD test response for the cell area trait of the four Amaranthus species. Bars with different letters indicate significant differences ($P < 0.05$) when LSD test is applied.

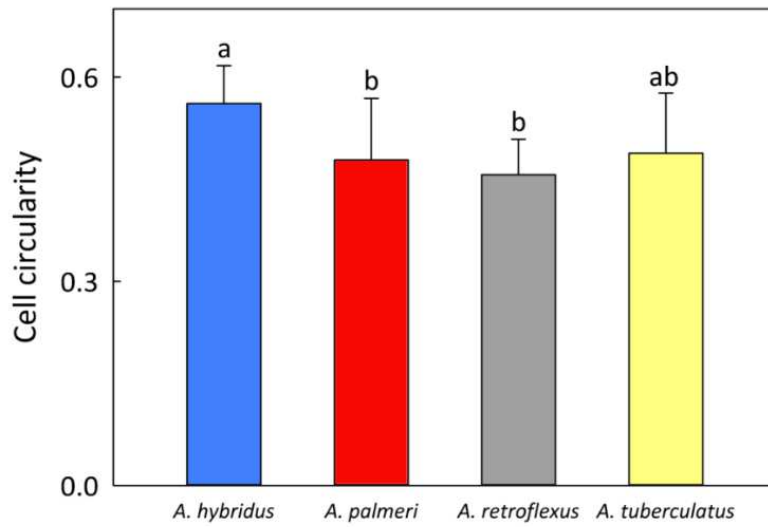


Figure S11. Mean values and LSD test response for the cell circularity trait of the four *Amaranthus* species. Bars with different letters indicate significant differences ($P < 0.05$) when LSD test is applied.

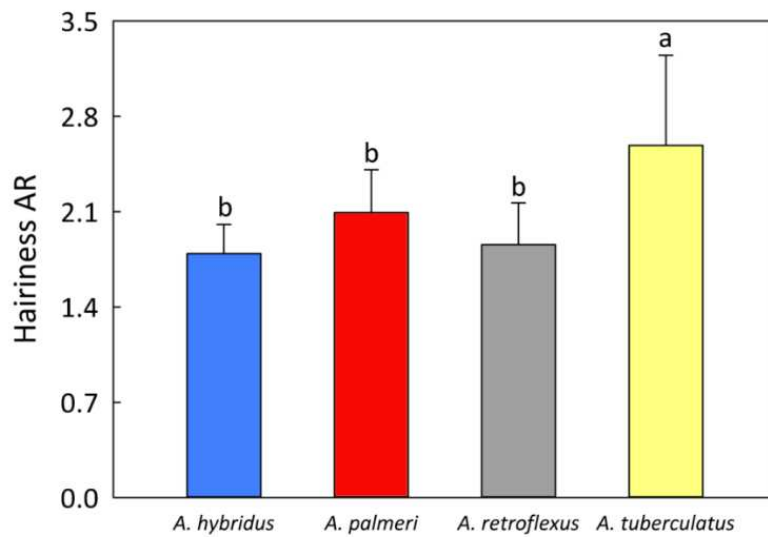


Figure S12. Mean values and LSD test response for the hairiness AR trait of the four *Amaranthus* species. Bars with different letters indicate significant differences ($P < 0.05$) when LSD test is applied.

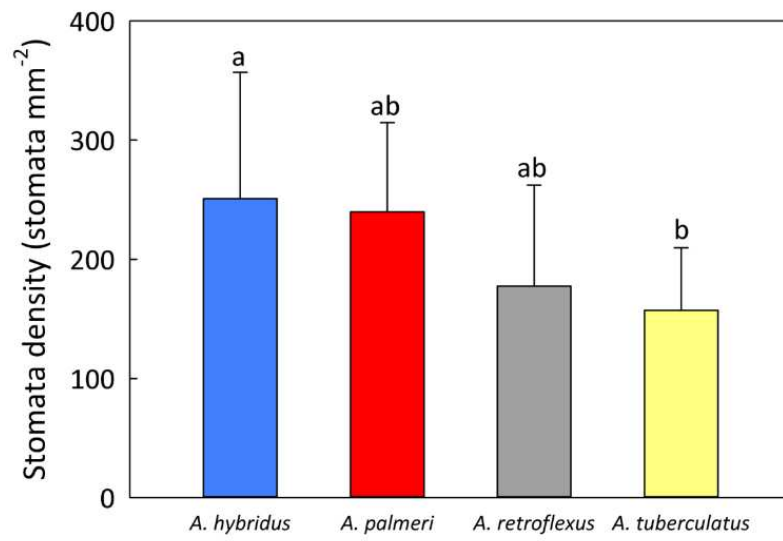


Figure S13. Mean values and LSD test response for the stomata density trait of the four *Amaranthus* species. Bars with different letters indicate significant differences ($P < 0.05$) when LSD test is applied.

CHAPTER 5 - From plant traits to ecosystem: new perspective for the upscaling of salt marsh response to flooding stress with remote sensing tools

Original Paper

Submitted to: *Scientific Reports*, Springer Nature

From plant traits to ecosystem: new perspective for the upscaling of salt marsh response to flooding stress with remote sensing tools

Marco Vuerich¹, Paolo Cingano¹, Giacomo Trotta^{1,2}, Elisa Petrusa¹, Enrico Braidot¹, **Dora Scarpin**¹, Annelore Bezzi³, Michele Mestroni⁴, Elisa Pellegrini¹ and Francesco Boscutti¹

¹DI4A Department of Agricultural, Food, Environmental and Animal Sciences, University of Udine, Udine 33100, Italy

²Department of Environmental and Life Sciences (DSV), University of Trieste, 34127, Trieste, Italy

³Department of Mathematics and Geosciences, University of Trieste, Trieste 34128, Italy

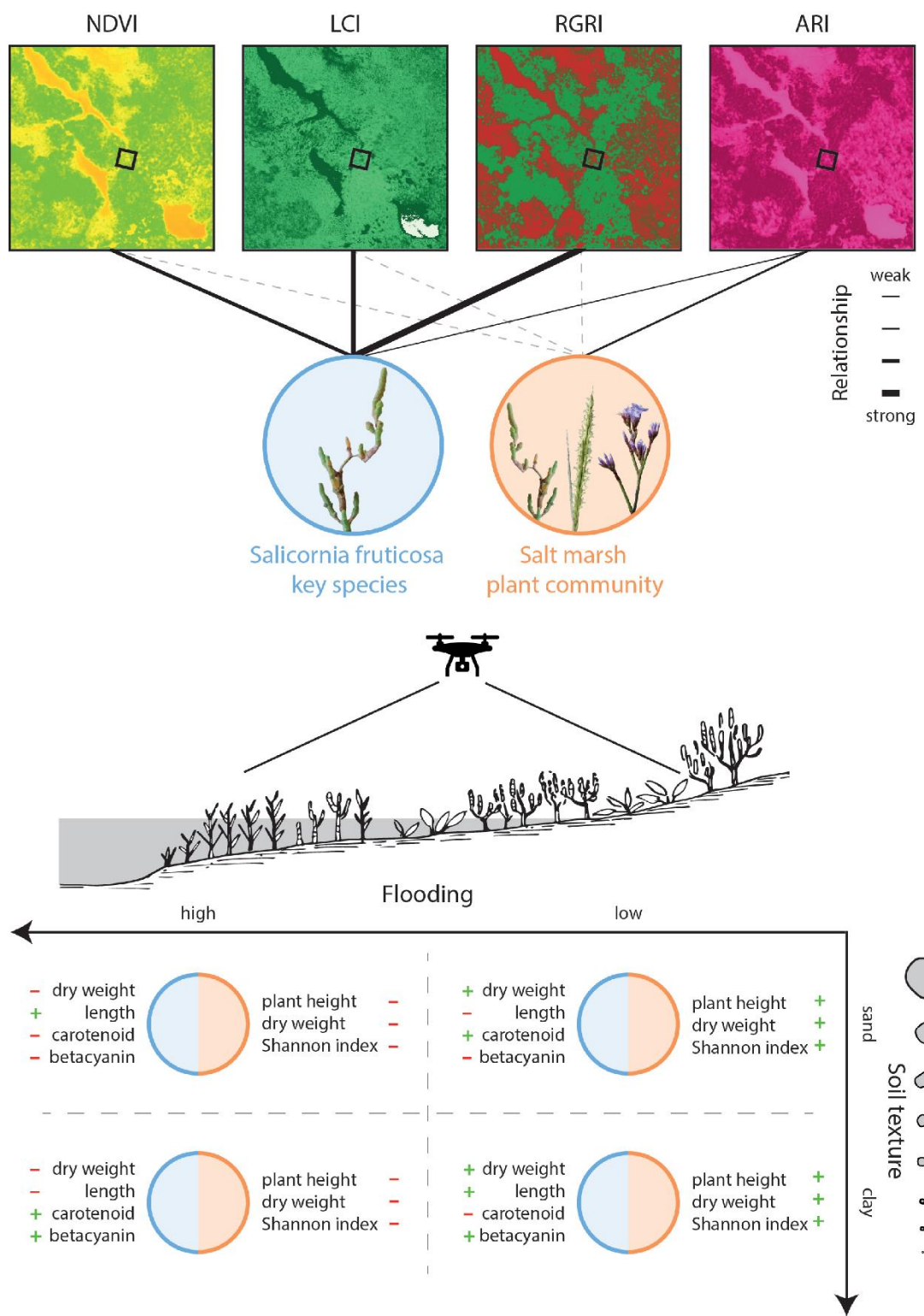
⁴Agricoltura innovativa Mestroni, Mereto di Tomba (UD), 33036, Italy

Correspondence: marco.vuerich@uniud.it. Tel: +39 0432 558727

Keywords: Ecosystem upscaling; flooding; global change biology; phenotypic plasticity; plant-soil interaction; remote sensing; salt marsh; sea level rise.

ABSTRACT

Understanding the response of salt marshes to flooding is crucial to foresee the fate of these fragile ecosystems, requiring an upscaling approach. In this study we related plant species and community response to multispectral indices aiming at parsing the power of remote sensing to detect the environmental stress due to flooding in lagoon salt marshes. We studied the response of *Salicornia fruticosa* (L.) L. and associated plant community along a flooding and soil texture gradient in nine lagoon salt marshes in northern Italy. We considered community (*i.e.*, species richness, dry biomass, plant height, dry matter content) and individual traits (*i.e.*, annual growth, pigments, and secondary metabolites) to analyze the effect of flooding depth and its interplay with soil properties. We also carried out a drone multispectral survey, to obtain remote sensing-derived vegetation indices for the upscaling of plant responses to flooding. Plant diversity, biomass and growth all declined as inundation depth increased. The increase of soil clay content exacerbated flooding stress shaping *S. fruticosa* growth and physiological responses. Multispectral indices were negatively related with flooding depth. We found key species traits rather than other community traits to better explain the variance of multispectral indices. In particular stem length and pigment content (*i.e.*, betacyanin, carotenoids) were more effective than other community traits to predict the spectral indices in an upscaling perspective of salt marsh response to flooding. We proved multispectral indices to potentially capture plant growth and plant eco-physiological responses to flooding at the large scale. These results represent a first fundamental step to establish long term spatial monitoring of marsh acclimation to sea level rise with remote sensing. We further stressed the importance to focus on key species traits as mediators of the entire ecosystem changes, in an ecological upscaling perspective.



Graphical abstract Our findings shed new light on the potential use of the remote sensing tool for the understanding of the response of vegetation to the future increase of the sea level. We stressed the power of the remote sensing tools for monitoring plant eco-physiological responses to flooding at the large scale, underlying the importance to parse the eco-physiological response of key species (e.g., pigments and secondary metabolites accumulation) as fundamental traits for future remote sensing monitoring and ecological upscaling.

INTRODUCTION

Coastal areas are considered among the most valuable but endangered ecosystems globally due to their susceptibility to global change and other anthropogenic factors [1–3]. Among coastal environments, salt marshes represent the most important sea-land transitional ecosystem of estuarine and lagoon systems [4–7], undergoing rapid alterations due to climate change aftermaths [8,9]. Climate-induced sea level rise (SLR) and storm surges threaten the integrity and functionality of salt marshes by increasing the frequency and intensity of flooding stress [3,10,11]. For SLR in particular, the salt marsh survival depends on their accretion ability in relation to the sediment inputs and flooding stress increase [12,13]. In fact, any reduction in plant growth may affect the capacity of the marsh to attenuate waves (especially in storms) and trap sediment [14], influencing salt marsh accretion [15]. Moreover, decreased root or rhizome production may weaken marsh bank stability leading to increased susceptibility to erosion [16,17]. The ultimate consequence is the salt marsh area shrinkage and, eventually, its migration or disappearance [18]. For these reasons understanding how salt marsh plants acclimate to flooding and monitoring such processes is of the utmost importance in depicting future scenarios and possible mitigation actions.

Tidal flooding is a pivotal factor driving plant species growth, distribution, and zonation in salt marshes [19–22]. In an equilibrium state, tidal flooding is mainly determined by land morphology [23] and soil texture (*i.e.*, soil permeability) [24]. As a consequence, flooding influences crucial soil features, such as the availability of oxygen [25,26], triggering intense plant-soil feedback [27]. An increase of flooding stress might cause the reduction of plant performance in a soil-mediated process that can have repercussions on the overall biodiversity and productivity [27].

Plant-soil feedback is often modulated by plant functional traits of key species of the community [27,28], that in salt marsh plants are represented by both morphological and physiological traits determining the phenotypic response of a plant to flooding [29,30,31]. A functional traits approach is hence crucial to predict the response of key species of the ecosystems, which changes could also affect the entire ecosystem processes and properties (*e.g.*, nutrient cycles, biodiversity) [32,33], opening important upscaling perspectives.

Among the most promising tools for scale-up of ecological processes, remote sensing has been used across different ecological scales and systems [34–38]. In salt marsh, application of remote sensing tools (*e.g.*, satellite and unmanned aerial vehicle (UAV) images) has been limited to plant community discrimination [39,40], plant phenology detection [41,42], plant-plant interactions [43] and to survey overall ecosystem properties [44]. In these ecosystems, while remote sensing has been applied for the monitoring of some gross ecosystem properties (*e.g.*, net primary production), linking the mechanistic response of individual plants (*e.g.*, growth traits, physiological response) to the ecosystem level remains unexplored and promising.

We studied the response of salt marsh plant communities by upscaling the functional response of the key species *Salicornia fruticosa* (L.) L. across a flooding gradient in a lagoon system. We further linked the functional response of *S. fruticosa* (*i.e.*, secondary metabolites, plant growth traits) to multispectral indices with the aim to extend the potential effect of plant response to a broader spatial and ecological scale.

We expected that high flooding stress has a direct effect on *S. fruticosa* response and the properties of the whole salt marsh ecosystem. We did expect flooding to shape the phenotypic plasticity of *S. fruticosa* by reducing individual growth traits (*i.e.*, stem elongation), photosynthetic pigment contents, and increasing secondary metabolites production (flavonoids, betacyanins). We expected a decrease of community productivity (biomass) and biodiversity with an increase of the stress (flooding). We also explored the potential of high-resolution multispectral image acquisition to depict the link between traits and community response to the environmental stress. We finally expected multispectral indices to be affected by both community and key species functional traits, in relation to an alteration of vegetation spectral firm induced by individual mean functional changes.

RESULTS

Salt marsh plant community response to flooding and soil texture gradient

All the community traits mean and range values are shown in table 1. Community plant height and dry weight were significantly affected by flooding depth, but not by soil clay content (Tab. 2), explaining 28.1 % and 26.3% of the total variance. At higher levels of flooding, plant communities were short (*i.e.*, mean plant height) (Fig. 1a) and with a low overall aboveground biomass (*i.e.*, total dry weight) (Fig. 1b). In contrast, plant community dry matter content was not affected neither by flooding depth nor by soil clay content (Tab. 2). Finally, plant diversity (*i.e.*, Shannon index) decreased along the flooding gradient (Fig. 1c) but did not show any relationship with soil clay content (Tab. 2).

***S. fruticosa* response to flooding and soil texture gradient**

All the *S. fruticosa* traits mean and range values are shown in table 1. The functional response of *S. fruticosa* was mainly modulated by flooding depth and its interaction with soil texture (*i.e.*, clay content). (Tab. 3). *S. fruticosa* shoot dry weight showed a significant decrease along the flooding depth gradient (Fig. 2a), whereas betacyanin shoot content was also significantly affected by soil clay content, showing a significant positive relationship (Tab. 3, Fig. 2b and 2c). *S. fruticosa* shoot length and carotenoid content were shaped by the interaction between flooding depth and soil clay content (Tab. 3). In particular, in soil with high content of clay the shoot length sharply decreased along the increase of flooding depth, while in soils poor in clay (*i.e.*, sandy soils) the increase of flooding depth slightly increased the annual plant stem

elongation (shoot length) (Fig. 2d). A high stem carotenoid content was caused by high flooding depth levels and high percentage of clay in the soil, whereas a low carotenoid content was observed in more sandy soil more subjected to flooding (Fig. 2e). As for total dry matter content of plant community, also shoot dry matter content was affected neither by flooding nor by clay soil content.

Upscaling of plant community and *S. fruticosa* functional responses by means of remote sensing signals

Flooding depth reduced all the vegetation indices considered. (Tab. S2).

For NDVI about 27% of the total variance was explained by plant traits (CI = [0.17 - 0.60]) while community trait (*i.e.*, total dry weight and height) did not contribute (Fig. 3, Tab. S3). Most of the variance was assigned to shoot length (part $R^2 = 0.10$, CI = [0.00 - 0.23]) and betacyanin shoot content (part $R^2 = 0.08$, CI = [0.00 - 0.22]).

Plant traits explained 23% of the LCI total variance (CI = [0.13 - 0.44]) (Fig. 3, Tab. S3). Shoot length was the main trait contributing the variance (part $R^2 = 0.12$, CI = [0.00 - 0.23]) along with carotenoids (part $R^2 = 0.06$, CI = [0.04 - 0.28]) and betacyanin shoot content (part $R^2 = 0.05$, CI = [0.03 - 0.28]).

The 37% of the variance of RGRI mainly explained by shoot length, carotenoid and betacyanin content (namely part $R^2 = 0.12$, CI = [0.05- 0.34]; part $R^2 = 0.10$, CI = [0.04 - 0.32]; part $R^2 = 0.10$, CI = [0.04 - 0.33]), (Fig. 3, Tab. S3).

For ARI about 23% of the total variance was explained only by community and *S. fruticosa* traits (CI = [0.16 - 0.39]). Community dry weight and carotenoid shoot content were the variables mostly contributing to this proportion (both part $R^2 = 0.06$, CI = [0.04 - 0.19]). Community plant height explained only 3% of the variance (CI = [0.01 - 0.15]), whereas annual shoot length and betacyanin content did not affect this index (Fig. 3, Tab. S3).

Table 1. Descriptive statistics of environmental, plant community and *Salicornia fruticosa* variables.

Variable	Mean	Std. Dev	Max	Min
<i>Flooding depth (cm)</i>	1.59	1.03	4.14	0.01
<i>Clay content (%)</i>	19.55	6.26	30.91	5.84
<i>Species richness</i>	4.15	1.38	8	2
<i>Shannon index</i>	0.69	0.35	1.47	0.06
<i>Salicornia fruticosa cover value (%)</i>	74.45	16.75	99.01	28.37
<i>Plant height (cm)</i>	25.87	6.89	42.00	14.80
<i>Total dry weight (g)</i>	131.07	54.83	264.00	64.2
<i>Total dry matter content</i>	320.48	58.35	429.52	214.61
<i>Shoot dry weight (g)</i>	0.03	0.01	0.05	0.02
<i>Shoot dry matter content</i>	139.68	16.67	174.93	110.11
<i>Shoot length (cm)</i>	4.10	0.89	6.76	2.64
<i>Chlorophyll concentration ($\mu\text{g g}^{-1}$)</i>	481.66	139.27	877.63	286.39
<i>Pheophytin content</i>	32.19	14.42	68.18	16.28
<i>Carotenoid concentration ($\mu\text{g g}^{-1}$)</i>	90.58	12.03	113.60	64.02
<i>Flavonoid concentration ($\mu\text{g g}^{-1}$)</i>	23.86	8.40	40.83	7.96
<i>Betacyanin concentration ($\mu\text{g g}^{-1}$)</i>	24.30	15.18	60.57	2.91

Table 2. Results of the LMMs relating the salt marsh community traits (i.e., plant height, total dry weight, total dry matter content, Shannon index) with flooding depth and soil clay content. Significant relationships are in bold ($p < 0.05$). Degrees of freedom (Df), estimate, standard error (SE), t-values and p-values are shown.

Dependent variable	Independent variable	Df	Estimate	SE	t-Value	p-Value
<i>Plant height</i>	Flooding	1,16	-5.93	1.20	-4.92	< 0.001
	Clay content	1,16	0.07	0.17	0.40	0.698
<i>Total dry weight</i>	Flooding	1,16	-23.33	9.21	-2.53	0.022
	Clay content	1,16	2.09	1.53	1.36	0.191
<i>Total dry matter content</i>	Flooding	1,16	-1.97	11.19	-0.18	0.863
	Clay content	1,16	1.97	1.86	1.06	0.306
<i>Shannon index</i>	Flooding	1,15	-0.14	0.06	-2.48	0.026
	Clay content	1,15	-0.01	0.01	-1.09	0.295

Table 3. Results of the LMMs relating the *S. fruticosa* traits (i.e., shoot dry weight, shoot dry matter content, shoot length, chlorophyll, carotenoids, flavonoids, betacyanin content) with flooding depth, soil clay content and their interaction. Significant relationships are in bold ($p < 0.05$). Degrees of freedom (Df), estimate, standard error (SE), t-values and p-values are shown.

Dependent variable	Independent variable	Df	Estimate	SE	t-Value	p-Value
<i>log(Shoot dry weight)</i>	Flooding	1,16	-0.11	0.06	-2.05	0.050
	Clay content	1,16	0.01	0.01	1.16	0.265
<i>Shoot dry matter content</i>	Flooding	1,16	-1.05	3.41	-0.31	0.762
	Clay content	1,16	0.11	0.51	0.20	0.841
<i>Shoot length</i>	Flooding	1,14	1.18	0.54	2.20	0.046
	Clay content	1,14	0.15	0.03	4.69	< 0.001
	Flooding*Clay content	1,14	-0.08	0.03	-2.77	0.015
<i>Chlorophyll</i>	Flooding	1,16	-6.39	25.60	-0.25	0.806
	Clay content	1,16	-4.09	3.74	-1.09	0.290
<i>Carotenoids</i>	Flooding	1,12	-31.19	8.93	-3.49	0.004
	Clay content	1,12	-0.85	0.44	-1.94	0.076
	Flooding*Clay content	1,12	1.56	0.48	3.29	0.007
<i>Flavonoids</i>	Flooding	1,16	-0.29	1.60	-0.18	0.858
	Clay content	1,16	-0.34	0.27	-1.26	0.226
<i>log(Betacyanin)</i>	Flooding	1,15	0.27	0.13	2.27	0.038
	Clay content	1,15	0.05	0.02	2.97	0.010

Table 4. List, formula and brief interpretation description of the multispectral vegetation indices selected for the study.

Vegetation index and formula	Interpretation
$NDVI = \frac{NIR - RED}{NIR + RED}$	estimation of geometrical features and green biomass production [95]
$LCI = \frac{NIR - RED\ EDGE}{NIR + RED}$	estimation of chlorophyll content and distribution in leaves [96]
$RGRI = \frac{RED}{GREEN}$	estimation of the course of leaf development in canopies and indicator of leaf production and stress [97,98]
$ARI = \frac{1}{GREEN} - \frac{1}{RED\ EDGE}$	estimation of anthocyanin content in plant biomass [75]

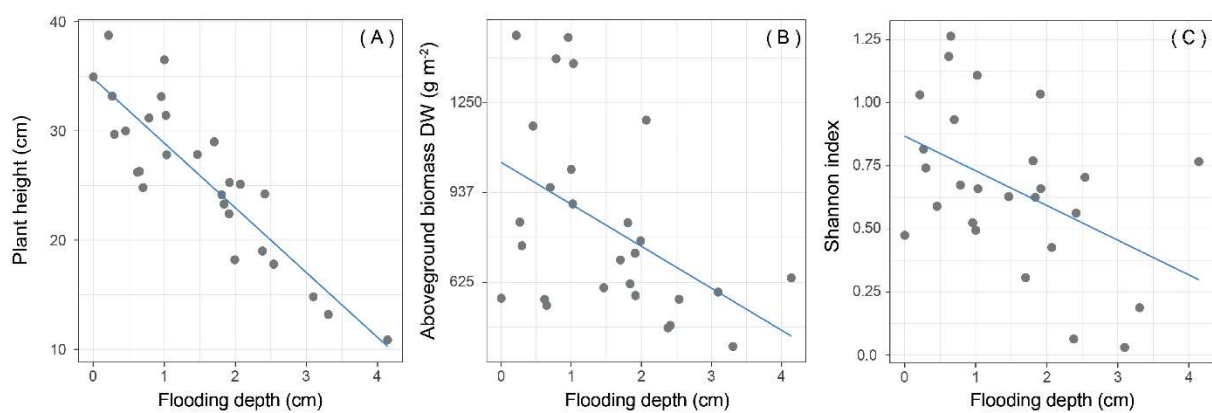


Figure 1. Effect plots of flooding depth on salt marsh plant community traits, namely plant height (A), aboveground biomass dry weight (DW), (B) and Shannon index (C).

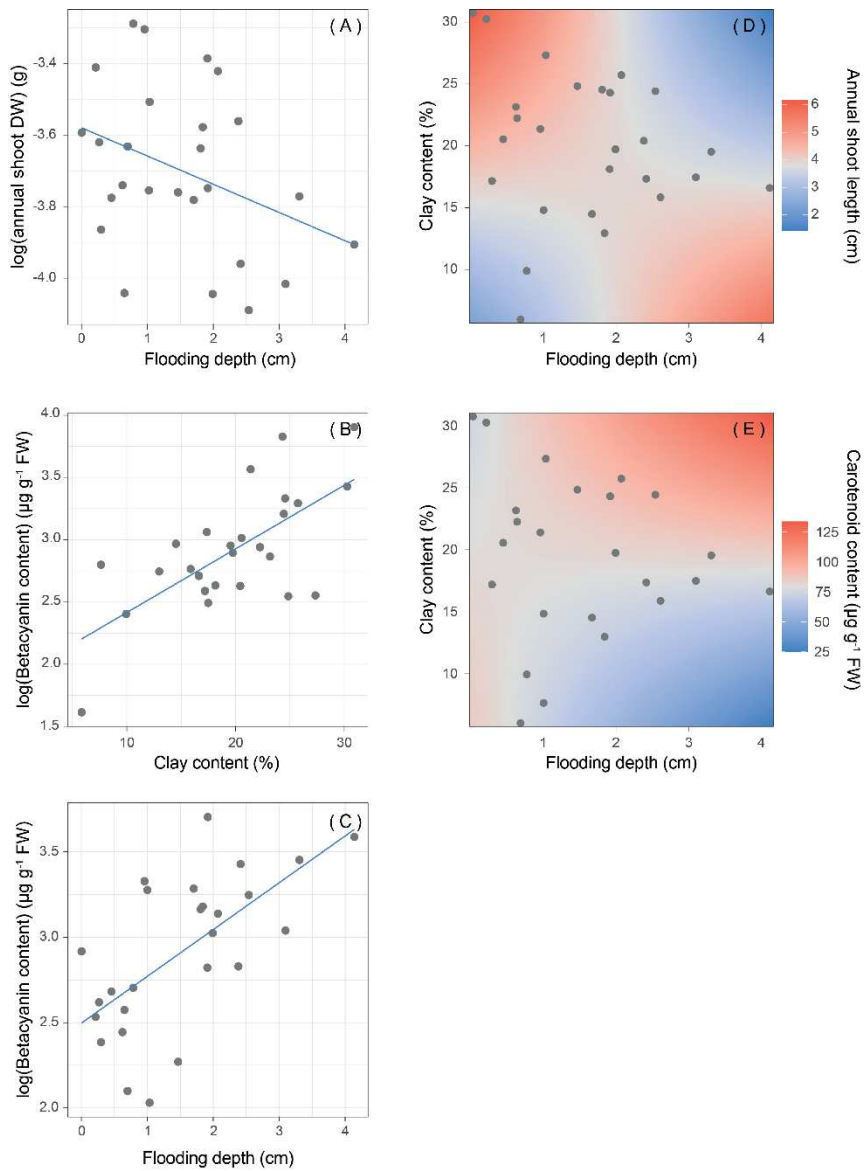


Figure 2. Effect plots of flooding depth, clay content and their interaction on *S. fruticosa* traits. Changes of annual shoot dry weight (DW)(A) betacyanin content (B,C) annual shoot length (D) and carotenoid content (E) along the flooding gradient, the clay content, and their interaction.

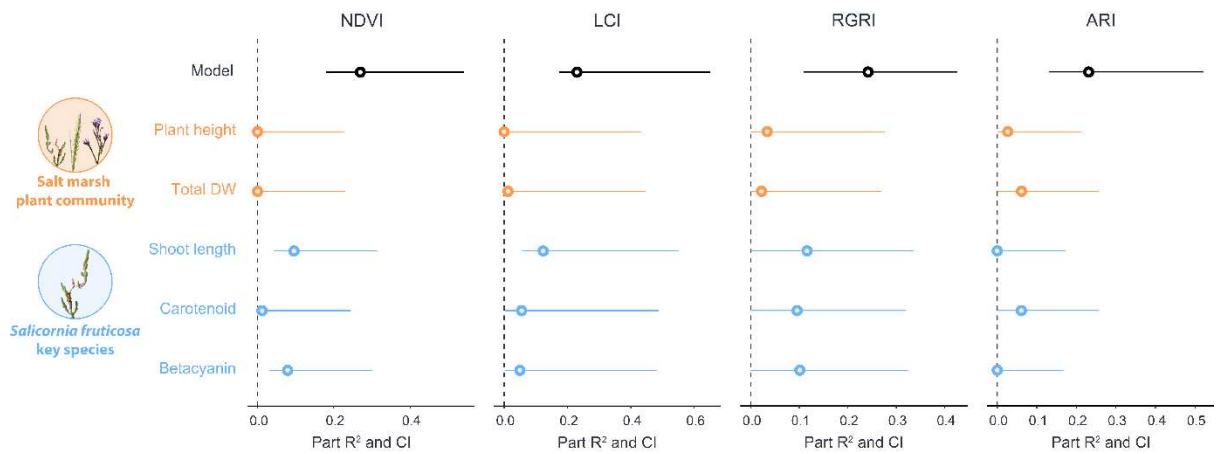


Figure 3. Contribution of salt marsh plant community traits and *S. fruticosa* traits to vegetation indices. Proportions of vegetation indices (i.e., NDVI, LCI, RGRI, ARI) variance explained by plant community traits (i.e., plant height and total dry weight) and *S. fruticosa* traits (i.e., shoot length, carotenoid and betacyanin content).

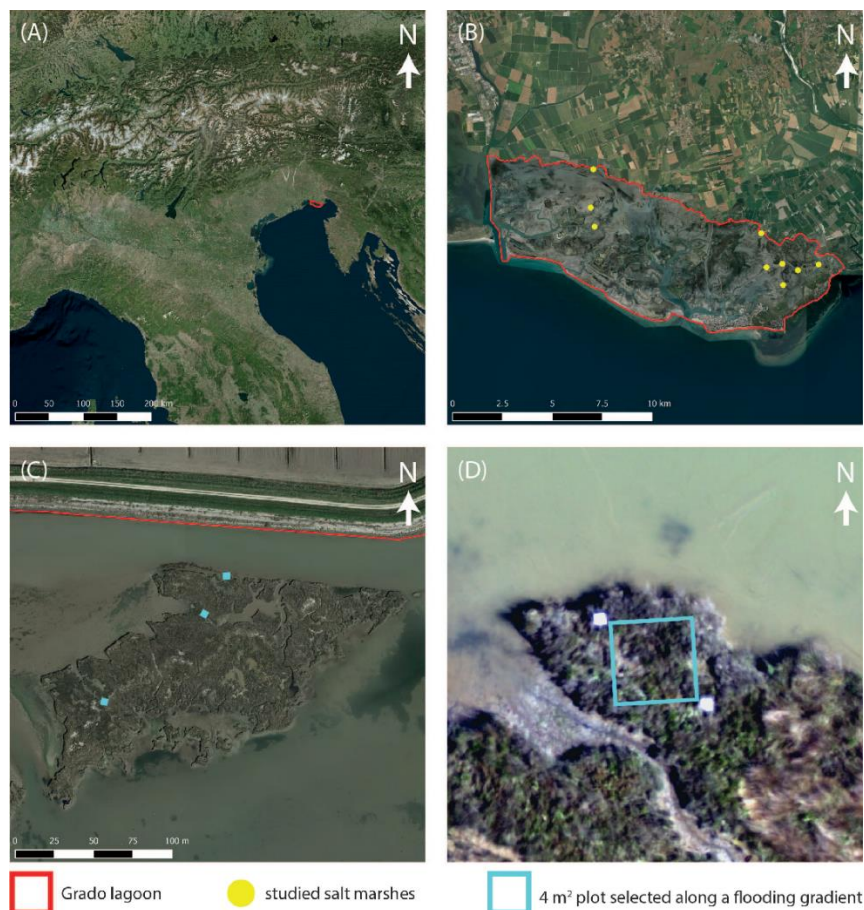


Figure 4. The study area of the Grado lagoon in the northern Adriatic Sea (A), the 9 studied salt marshes (B), the 3 sampling plots chosen along a flooding gradient in one of the studied salt marshes (C) and the 4 m² plot delimited by ground control point (D).

DISCUSSION

Our findings confirmed flooding depth to be the main driver shaping plant communities in tidal salt marshes. Interestingly, flooding depth was the only driver directly affecting plant community features (*i.e.*, biomass, plant height, and diversity), while its interaction with soil clay content shaped the functional response of *Salicornia fruticosa* (*i.e.*, shoot length, shoot carotenoid content), probably via increasing soil anoxia soil [24].

By exploring the relationships between plant community and *S. fruticosa* functional traits and high-resolution remote sensing derived indices we found key species traits, in particular stem length and pigment content (*i.e.*, betacyanin, carotenoids), to be more effective than others for an upscaling perspective in tidal salt marshes. This suggests that the response of the key species, already demonstrated to be important drivers for the modulation of the whole ecosystem responses to environmental changes [27,32], should not be neglected in the upscaling process of the vegetation response to flooding, from the plot to ecosystem level.

Salt marsh response to flooding and soil texture gradient

Community response

An increase of flooding depth produced a significant decrease in plant diversity, biomass and plant height. Due to the harsh environmental conditions, salt marshes are generally recognized as low-diversity plant communities, where well adapted species are dominant, and few other species can occur [45–47].

Further, flooding depth has been already linked to the reduction of salt marsh productivity, by modulating plant growth [48,49].

Clay content did not affect plant community traits, while it contributes for the shaping of *S. fruticosa* response, that, in turn, can facilitate other species along the abiotic stress gradient caused by flooding depth and soil clay, causing plausible feedback at the community level [24,50].

Salicornia fruticosa response

As hypothesized flooding depth significantly affected *S. fruticosa* growth and physiological response, but its effect was often modulated by soil texture (*i.e.*, clay content).

Deeply flooded plants of *S. fruticosa* showed a low increment in annual biomass (*i.e.*, annual shoot dry weight), while their elongation (shoot length) was finely modulated by the interaction of clay content and flooding depth, showing the lowest values in sites deeper flooded and with high soil clay content. These findings suggest that elongation of plants, often used to avoid complete submergence, is used by plants only in sites where soil conditions are less harsh (*i.e.*, sandy soils where complete anoxia is rarely reached), while plants could be severely limited in growth in compact clayey

soils, including their shoot elongation [51]. This is induced by the variation of parameters such as (i) the limited diffusion of O₂ and CO₂ [52], (ii) the increase of toxic volatile substances [53], (iii) the limitation of nutrients [54], and (iv) the increase in osmotic stress. In this light, the elongation of *S. fruticosa* annual shoot could represent a common escape strategy to cope with submergence, shared with other wetland plants [27,55].

As expected, deep flooding stimulated the production of secondary pigments such carotenoids but did not affect chlorophyll content of photosynthetic stems. Other contributions showed carotenoids and chlorophyll content to be particularly sensitive to flooding depth [56,57]. Here we found that carotenoids reached their maximum values when deep flooding was combined with high clay content in the soil, consistently with what found in other species [58], as probable response to hypoxia [59,60]. Instead on highly permeable soils the flooding induced a decrease of carotenoids, this was consistent to what evidenced in other studies where the mere application of flooding decreased all pigments production, carotenoids included [56,57]. It is thus probable that only a strong soil hypoxia due to the interplay of deep flooding and soil clay content can activate the protective role of a high carotenoid concentration. Flooding did not affect flavonoids, while a greater content of betacyanins was found in *S. fruticosa* plants growing on clayey soils and with deep flooding. Flavonoids seem to play in response to water-related stress [61,62], while were demonstrated to be primarily related to soil hypoxia [63]. Albeit not significant, we found an increase of flavonoids in soils with more clay content, and hence, more subjected to lack of oxygen.

Such as for anthocyanins, betacyanins accumulation in vegetative organs has been generally related to their protection from environmental stress [64,65]. Consistently, we observed an increase of betacyanins under flooding stress in soil with high clay content that might be related to their capacity to attenuate effects of soil hypoxia on plants as effective scavengers of reactive oxygen species and osmotic photo-protectants [66–68].

Potential upscaling of plant response by remote sensing

Multispectral images have been already used to indirectly quantify the submersion in salt marsh vegetation [69]. Here, we evidenced the selected multispectral indices to be consistently good indicators of the analyzed stress gradient, also able to depict the interplay of flooding and soil clay content. In this light, our fine-tuning monitoring of the flooding effect on the key species response might be useful to monitor the acclimation mechanisms by remote sensing tools. In particular, the rate of sea level rise (1.5 mm year⁻¹) in the norther Adriatic Sea is consistent with our narrow tidal frame, also in relation to the salt marsh accretion, deemed to attenuate the effects of sea rise [70]. Despite the narrow flooding gradient species and community responses were remarkable, therefore offering a wide array of plant and community responses. We found *S. fruticosa* growth (*i.e.*, stem length) and physiological traits (*i.e.*, betacyanin,

carotenoids) to be the plant traits that mostly explained multispectral derived indices. Many authors already evidenced the direct relationship between indices and the whole community response to flooding, proposing for instance NDVI for the quantification of biomass and other ecosystem properties [71–73]. Instead, we found the individual response of the key species *S. fruticosa* to be more important than the whole plant community in determining the multispectral signal of vegetation. The community response to flooding (*i.e.*, biomass, plant diversity) results from a reduction in the biomass of the key species *S. fruticosa*, suggesting a possible upscaling link between the studied species and the response of the entire ecosystem, regardless of the environmental stress intensity considered. This is indicating that remote sensing monitoring over time might reveal the acclimation of salt marshes to sea level rise by intercepting the response of the key species *S. fruticosa*, opening new perspective in the multispectral image interpretation. Salt marsh key species has been already linked to the community response by plant trait-soil interactions [24,27]. Our findings suggest that this feedback might also drive the remote sensing-vegetation relationships for the monitoring of the ecosystem properties. NDVI is one of the most used indices for numerous upscaling purposes [9,74]. The application of NDVI in our sites was informative about the *S. fruticosa* growth response and betacyanin stem content. We further suggest that other indices, namely LCI, RGRI and ARI might improve the upscaling of salt marsh response to flooding. The LCI was mainly explained by plant growth and at a lesser extent by carotenoids and betacyanins. This index was originally proposed as very sensitive for estimation of chlorophyll content and distribution in leaves. In our study area it seems to better represent the overall status of the *S. fruticosa*, similarly to RGRI that showed similar, but higher partial regression values for the physiological and growth traits. ARI captured most of the carotenoid signal, being lower at high concentrations of carotenoids. ARI is mainly used for detection of anthocyanin content [75], but in our study it appears to better evidence changes in carotenoids and community biomass. This might be related either to a negative relationship between anthocyanins (not measured) and carotenoids or to a species-specific shift in plant reflectance due to its succulent growth form [76]. These results also suggest to further investigate the relationship between stress and modification of the spectral signature of plant species. In salt marsh halophytes, a decisive role could be played by the accumulation of pigments and other metabolites that can also shift a sensible visible change in plant chromaticism [30,79]. We only partially parsed such a complex physiological response, which study in the future could increase the upscaling perspectives of plant eco-physiological acclimation to abiotic stresses.

Conclusions

We suggest remote sensing as a promising tool able to merge different ecological scales, proving far reach achievements for the understanding of spatial distribution and to forecast the vegetation changes due to abiotic stress gradient. In this light, our fine-tuning monitoring of the flooding effect on the key species response might be useful to monitor the acclimation mechanisms by remote sensing tools, being

consistent with local sea level rise rates. Our findings might represent a novel approach to assess and monitoring the impacts of the ongoing rising sea level rise in wetland areas. We evidenced that the ongoing sea level rise can lead to a progressive reduction of plant cover and biomass, as well as the height of the populations, by increasing the areas subjected to high levels of submersion stress. Nonetheless, further improvements are needed. We also highlighted that some physiological processes such as the accumulation of pigments and secondary metabolites in relation to increasing levels of stress could play a fundamental role for future remote sensing monitoring and upscaling. These finding suggest that the acclimation of salt marshes to sea level rise could be revealed through remote sensing monitoring over time by intercepting the response of the key species *S. fruticosa*. These upscaling perspectives applied to 'sentinel ecosystems', such as salt marshes, might provide an early warning on global and regional changes, with fundamental understanding of future scenarios of the entire coastal system.

MATERIALS AND METHODS

Study area and sampling design

The study was conducted in the Grado lagoon (from 45°42'10.5"N 13°9'17.8" E to 45°40'49.8"N 13°21'31.2" E) in the Northern Adriatic Sea (Friuli Venezia Giulia, Italy) (Fig. 4a). The site is designated as both a Special Area of Conservation (SAC) and a Special Protection Area (SPA) in the Natura 2000 network (site code IT3320037). The mean annual rainfall is 974 mm, with an average temperature ranging from 3.1°C in January to 29.0°C in July. The lagoon is morphologically classified as a leaky lagoon [80]. It is strongly influenced by tides which are semi-diurnal, with a mean range of 0.65 m and spring and neap ranges of 1.05 m and 0.22 m, respectively [81].

The sampling was performed during May 2021 in 9 salt marshes (Fig. 4b). In each salt marsh, 3 sampling areas (plots) of 4 m² (2 m x 2 m) (Fig. 4c and 4d) were chosen along a flooding gradient according to ground micro-morphology of salt marshes, for a total of 27 plots.

Flooding and soil texture

The flooding depth and flooding duration were measured at each sampling site (27 plots) by using a water level data logger (HOBO U-20L-01, Onset, resolution: 0.02 kPa, 0.21 cm; water level accuracy $\pm 0.1\%$). The sensors were positioned at the ground level, with a recording interval of 5 min along a complete tidal cycle (2 weeks, including a shift from spring tide to neap tide). For an accurate flooding measurement, in each monitored salt marsh a reference datalogger was positioned in high elevation point never subjected to water submersion. Pressure data, recorded with the loggers, were automatically compared with reference air pressure measurements, and hence, converted to the height of the water column submerging the soil, using the

HOBOWare® Pro software (version 3.7.14, Onset). Flooding depth was expressed as the mean height (cm) of the water column of a complete tidal cycle, while the flooding duration as the percentage of time the logger was flooded during a complete tidal cycle. We used mean depth to better represent the average conditions of water column. However, we verified the occurrence of a high correlation between mean height and maximum height of water depth ($r=0.89$; $p<0.001$), considering them interchangeable. The studied tidal range (Tab. 1) represent a significant shift in ecological conditions and was already demonstrated to trigger remarkable changes in salt marshes plant communities [27]. Moreover, the range is also representing a good proxy of the sea level rise that in the norther Adriatic Sea have an increasing rate of 1.5 mm year^{-1} over the last decades.

A soil sample was collected at the center of each plot using a cylindrical tube (height: 12 cm, width: 3.5 cm, volume: 115.5 cm^3), transported to the laboratory for soil texture analyses. All soil samples ($n=27$) were processed by removing any visible vegetal remain and shell, wet-sieved through a 2 mm sieve and treated by hydrogen peroxide (H_2O_2) 3% and distilled water 1:4 for 48 hours. Grain size analysis ($2000\text{-}0.2 \text{ }\mu\text{m}$) was performed through a Laser Diffraction Particle Size Analyzer (Malvern Mastersizer 2000) coupled with an autosampler. For further analyses we used only the clay percentage of the sample (particle size $< 4 \text{ }\mu\text{m}$).

***Salicornia fruticosa* morphological and physiological traits**

In each sampling plot, fourteen annual shoots of *S. fruticosa* were randomly collected from different individuals, sealed in plastic bags, stored in portable fridge, and transported to the laboratory. Five annual shoots were used to measure mean shoot length and fresh weight and later oven-dried at 70°C for 72 h, weighed again (dry weight) and used for calculating the dry matter content of selected plant shoots.

The remaining nine annual shoots were used for quantifying chlorophyll, carotenoid, flavonoid and betacyanin content. The samples were pooled in three subsets (3 annual shoot x subset) and ground into fine powder under liquid nitrogen. Chlorophyll (*i.e.*, chlorophyll *a* and *b*) and carotenoid concentration analysis was measured following Marchiol et al. [82] protocol and expressed per gram fresh weight ($\mu\text{g g}^{-1}$) (for the calculation methods see Wellburn [83]). Pheophytin content was estimated indirectly as a percentage compared to the amount of chlorophyll [84]. The flavonoid content was quantified according to the method described by Filippi et al., [85] with minor changes and expressed as quercetin-eq content per gram fresh weight ($\mu\text{g quercetin-eq g}^{-1}$).

The betacyanin concentration was determined by extraction from liquid nitrogen-pulverized samples using a 50 mM ascorbic acid in 80% methanol solution. The material was treated with a cold ultrasonic bath for 2 minutes, incubated for 30 minutes at -20°C and finally centrifuged at 15000 g for 10 minutes at room temperature. A supernatant volume of 0.5 ml was diluted 1:1 with distilled water and its absorbance

was measured at 538 nm. The determination of the betacyanin content was performed following Priatni & Pradita method [86].

Plant community traits

The occurrence and the estimated cover value (% of plant cover compared to plot area) of all vascular plants were recorded in each plot. Species nomenclature followed Bartolucci *et al.* [87]. The identification of the plant material was performed by Francesco Boscutti, Paolo Cingano and Marco Vuerich in the field or in laboratory, using the national flora references [88]. All samplings were performed in accordance with national and international legislation [89,90]. None of the species employed in the study belong to any national and international protective species list nor to the the IUCN Red List of endangered species. In particular, the amount of *S. fruticosa* samples collected was below the threshold limit set by regional legislation [90]. No voucher specimen of the plant material has been deposited in a publicly available herbarium. The height of 10 plants randomly selected of different species within each plot was measured in the field and subsequently the total aboveground plant biomass (all individuals of different species occurring) was harvested from a sub-plot (0.4 x 0.4 m), sealed in plastic bags, and transported in a portable fridge to the laboratory where it was fresh weighed, oven-dried at 70°C for 72 h and weighed again (dry weight). Dry weight was then expressed as grams per square meters. Dry matter content was later calculated as the ratio of fresh weight to dry weight.

UAV and Remote sensing indices

The hexacopter Zephyr Exos UAV (Zephyr SRL, Forlì, Italy) equipped with a Parrot Sequoia multispectral camera (Parrot Drones SAS, Paris, France) was used to acquire multispectral images of each salt marshes. The hexacopter UAV was controlled via a hand-held remote controller, which sends waypoint navigation information to the aircraft allowing the hexacopter UAV to follow a flight path, at an altitude and speed defined by the user. The flight altitude above ground level was set at 40 m and the speed was 2 m s⁻¹ for all nine flights. Each flight lasted for ~15 min and was performed close to solar noon with wind speed of <1 m s⁻¹, during the low-tide cycle concurrently to vegetation surveys and collection of plant and soil samples. Each flight path over the trial area was designed with an 85% forward and side overlap. The Parrot Sequoia multispectral camera has four sensors for four spectral bands: green (wavelength = 550 nm, bandwidth = 40 nm), red (wavelength = 660 nm, bandwidth = 40 nm), red-edge (wavelength = 735 nm, bandwidth = 10 nm), and near infrared (NIR) (wavelength = 790 nm, bandwidth = 40 nm). Before and after each flight was taken a picture of the calibrated reflectance panel (CRP), which is a Lambertian surface with a reflectance calibration curve associated that allows to convert raw pixels values into absolute reflectance. Moreover, to minimize the error during image capture due to change of the light, a downwelling light sensor (DLS) has been coupled to the multispectral camera to automatically adjust the readings to ambient light. For identifying each

sampling site, two ground control points were located diagonally to the sampling site. Post-processing of the raw images was carried out using the Pix4Dmapper Pro software (version 4.0, PIX4D, Lausanne, Switzerland). Firstly, a geometric correction for each single-band raw image was performed using the camera calibration parameters included for each sensor. The post-processed images were then used to generate orthomosaic images including aligning photos, optimizing alignment, building a dense cloud, building digital surface models (DSMs) and building orthomosaics with a spatial resolution of 4 cm pixel⁻¹. The orthomosaic images were radiometrically transformed to reflectance using the known reflectance of the CRP and with the DLS. Multispectral vegetation indices were calculated with the R package “terra” [91]. The calculated vegetation indices were: (i) Normalized Difference Vegetation Index (NDVI), (ii) Leaf Chlorophyll Index (LCI), (iii) Red Green Ratio Index (RGRI) and (iv) Anthocyanin Reflectance Index (ARI) (Tab. 4). The mean value of each vegetation index was calculated for each vegetation plot (2x2 m), as the average value of the pixel included in the plot.

Statistical analysis

Prior to analysis, all pseudo replicates of the considered traits were averaged per each plot (n=27). Plant community diversity was assessed by calculating the Shannon diversity index, based on the estimated cover value of the vascular plants recorded in each plot. The collinearity of the independent variables (*i.e.*, flooding depth, flooding duration, clay content) was tested by the Pearson correlation test. As flooding depth and flooding duration showed a significant positive correlation ($r = 0.44$, $p = 0.02$), we cautiously decided to test only for flooding depth effects. Clay content did not show any significant correlation with flooding (flooding depth vs soil clay: $r = -0.12$, $p = 0.54$; flooding duration vs soil clay: $r = -0.25$, $p = 0.20$). Linear mixed effects models (LMMs) were applied to examine the effect of flooding depth, clay content and their interaction (*i.e.*, dependent variable ~ flooding depth*clay content) on community traits (*i.e.*, plant height, dry weight, dry matter content, Shannon index), on *S. fruticosa* traits (*i.e.*, shoot dry weight, shoot dry matter content, shoot length, chlorophyll, carotenoids, flavonoids and betacyanin content) and on vegetation indices (*i.e.*, NDVI, LCI, RGRI, ARI). The salt marsh was considered as random factor. LMMs were applied using the “nlme” R package [92]. Model assumptions were verified using diagnostic plots and Shapiro-Wilk normality test ($p > 0.05$) on model residuals. Where model residuals violated any linear model assumption (*i.e.*, shoot dry weight and betacyanin content), variables were log-transformed or evident outliers were discarded. The model interactions were manually removed when not significant ($p > 0.05$). Full model outcomes are reported in Table S1.

In order to assess the potential of remote sensing to upscale the community and species response, we assessed the contribution of each trait significantly varying along the studied gradients to the vegetation indices total variance. In particular, variance partitioning tools were used to quantify the vegetation indices (*i.e.*, NDVI, LCI, RGRI,

ARI) variance explained by community (*i.e.*, plant height, dry weight) and *S. fruticosa* traits (*i.e.*, shoot length, carotenoid and betacyanin content). At this stage we did not include any abiotic variable to better encompass the contribution of plant response to remote sensing indices, in the upscaling perspective. Semi-partial coefficients of determination (part R^2) to partition the variance explained by individual traits were calculated with R package "partR2" (version 0.9.1) [93].

All graphs and statistical analyses were performed in R statistical software [94].

AUTHOR CONTRIBUTIONS

FB, PC, MV conceived the ideas and designed methodology; PC, MV, MM collected data; FB, MV, GT, DS, AB analyzed the data; FB and MV led the writing of the manuscript. All authors contributed critically to the drafts and gave final approval for publication.

ACKNOWLEDGEMENTS

We thank Stefano Sponza, Marco Bertè, Lorenzo Orzan for the help during field work.

REFERENCES

1. Blankespoor, B.; Dasgupta, S.; Laplante, B. Sea-Level Rise and Coastal Wetlands. *Ambio* 2014, 43, 996–1005, doi:10.1007/s13280-014-0500-4.
2. Crosby, S.C.; Sax, D.F.; Palmer, M.E.; Booth, H.S.; Deegan, L.A.; Bertness, M.D.; Leslie, H.M. Salt Marsh Persistence Is Threatened by Predicted Sea-Level Rise. *Estuar. Coast. Shelf Sci.* 2016, 181, 93–99, doi:10.1016/j.ecss.2016.08.018.
3. Hanley, M.E.; Bouma, T.J.; Mossman, H.L. The Gathering Storm: Optimizing Management of Coastal Ecosystems in the Face of a Climate-Driven Threat. *Ann. Bot.* 2020, 125, 197–212, doi:10.1093/aob/mcz204.
4. Noto, A.E.; Shurin, J.B. Early Stages of Sea-Level Rise Lead To Decreased Salt Marsh Plant Diversity through Stronger Competition in Mediterranean-Climate Marshes. *PLOS ONE* 2017, 12, e0169056, doi:10.1371/journal.pone.0169056.
5. Kelleway, J.J.; Saintilan, N.; Macreadie, P.I.; Baldock, J.A.; Ralph, P.J. Sediment and Carbon Deposition Vary among Vegetation Assemblages in a Coastal Salt Marsh. *Biogeosciences* 2017, 14, 3763–3779, doi:10.5194/bg-14-3763-2017.
6. Pedersen, O.; Perata, P.; Voesenek, L.A.C.J. Flooding and Low Oxygen Responses in Plants. *Funct. Plant Biol. FPB* 2017, 44, iii–vi, doi:10.1071/FPv44n9_FO.
7. Lin, H.; Sun, T.; Adams, M.P.; Zhou, Y.; Zhang, X.; Xu, S.; Gu, R. Seasonal Dynamics of Trace Elements in Sediment and Seagrass Tissues in the Largest *Zostera Japonica* Habitat, the Yellow River Estuary, Northern China. *Mar. Pollut. Bull.* 2018, 134, 5–13, doi:10.1016/j.marpolbul.2018.02.043.
8. Adam, P. Saltmarshes in a Time of Change. *Environ. Conserv.* 2002, null, 39–61, doi:10.1017/S0376892902000048.
9. Simas, T.; Nunes, J.P.; Ferreira, J.G. Effects of Global Climate Change on Coastal Salt Marshes. *Ecol. Model.* 2001, 139, 1–15, doi:10.1016/S0304-3800(01)00226-5.
10. Van Wijnen, H.J.; Bakker, J.P. Long-Term Surface Elevation Change in Salt Marshes: A Prediction of Marsh Response to Future Sea-Level Rise. *Estuar. Coast. Shelf Sci.* 2001, 52, 381–390, doi:10.1006/ecss.2000.0744.
11. Nicholls, R.J.; Cazenave, A. Sea-Level Rise and Its Impact on Coastal Zones. *Science* 2010, 328, 1517–1520, doi:10.1126/science.1185782.
12. Bouma, T.J.; van Belzen, J.; Balke, T.; van Dalen, J.; Klaassen, P.; Hartog, A.M.; Callaghan, D.P.; Hu, Z.; Stive, M.J.F.; Temmerman, S.; et al. Short-Term Mudflat Dynamics Drive Long-Term Cyclic Salt Marsh Dynamics. *Limnol. Oceanogr.* 2016, 61, 2261–2275, doi:10.1002/lno.10374.
13. Ganju, N.K.; Defne, Z.; Kirwan, M.L.; Fagherazzi, S.; D’Alpaos, A.; Carniello, L. Spatially Integrative Metrics Reveal Hidden Vulnerability of Microtidal Salt Marshes. *Nat. Commun.* 2017, 8, 14156, doi:10.1038/ncomms14156.
14. Voss, C.M.; Christian, R.R.; Morris, J.T. Marsh Macrophyte Responses to Inundation Anticipate Impacts of Sea-Level Rise and Indicate Ongoing Drowning of North Carolina Marshes. *Mar. Biol.* 2013, 160, 181–194, doi:10.1007/s00227-012-2076-5.

- 15.** Nyman, J.A.; Walters, R.J.; Delaune, R.D.; Patrick, W.H. Marsh Vertical Accretion via Vegetative Growth. *Estuar. Coast. Shelf Sci.* 2006, 69, 370–380, doi:10.1016/j.ecss.2006.05.041.
- 16.** Deegan, L.A.; Johnson, D.S.; Warren, R.S.; Peterson, B.J.; Fleeger, J.W.; Fagherazzi, S.; Wollheim, W.M. Coastal Eutrophication as a Driver of Salt Marsh Loss. *Nature* 2012, 490, 388–392, doi:10.1038/nature11533.
- 17.** De Battisti, D.; Griffin, J.N. Below-Ground Biomass of Plants, with a Key Contribution of Buried Shoots, Increases Fore-dune Resistance to Wave Swash. *Ann. Bot.* 2020, 125, 325–334, doi:10.1093/aob/mcz125.
- 18.** Stralberg, D.; Brennan, M.; Callaway, J.C.; Wood, J.K.; Schile, L.M.; Jongsomjit, D.; Kelly, M.; Parker, V.T.; Crooks, S. Evaluating Tidal Marsh Sustainability in the Face of Sea-Level Rise: A Hybrid Modeling Approach Applied to San Francisco Bay. *PLOS ONE* 2011, 6, e27388, doi:10.1371/journal.pone.0027388.
- 19.** Marani, M.; Lanzoni, S.; Silvestri, S.; Rinaldo, A. Tidal Landforms, Patterns of Halophytic Vegetation and the Fate of the Lagoon of Venice. *J. Mar. Syst.* 2004, 51, 191–210, doi:10.1016/j.jmarsys.2004.05.012.
- 20.** Lang, F.; von der Lippe, M.; Schimpel, S.; Scozzafava-Jaeger, T.; Straub, W. Topsoil Morphology Indicates Bio-Effective Redox Conditions in Venice Salt Marshes. *Estuar. Coast. Shelf Sci.* 2010, 87, 11–20, doi:10.1016/j.ecss.2009.12.002.
- 21.** Vittori Antisari, L.; Ferronato, C.; Pellegrini, E.; Boscutti, F.; Casolo, V.; de Nobili, M.; Vianello, G. Soil Properties and Plant Community Relationship in a Saltmarsh of the Grado and Marano Lagoon (Northern Italy). *J. Soils Sediments* 2017, 17, 1862–1873, doi:10.1007/s11368-016-1510-6.
- 22.** Lan, Z.; Huang, H.; Chen, Y.; Liu, J.; Chen, J.; Li, L.; Li, L.; Jin, B.; Chen, J. Testing Mechanisms Underlying Responses of Plant Functional Traits to Flooding Duration Gradient in a Lakeshore Meadow. *J. Freshw. Ecol.* 2019, 34, 481–495, doi:10.1080/02705060.2018.1550022.
- 23.** Wang, A.; Gao, S.; Jia, J. Impact of the Cord-Grass *Spartina Alterniflora* on Sedimentary and Morphological Evolution of Tidal Salt Marshes on the Jiangsu Coast, China. *Acta Oceanol. Sin.* 2006, 25, 32–42.
- 24.** Pellegrini, E.; Incerti, G.; Pedersen, O.; Moro, N.; Foscarelli, A.; Casolo, V.; Contin, M.; Boscutti, F. Flooding and Soil Properties Control Plant Intra- and Interspecific Interactions in Salt Marshes. *Plants* 2022, 11, 1940, doi:10.3390/plants11151940.
- 25.** Davy, A.J.; Brown, M.J.H.; Mossman, H.L.; Grant, A. Colonization of a Newly Developing Salt Marsh: Disentangling Independent Effects of Elevation and Redox Potential on Halophytes. *J. Ecol.* 2011, 99, 1350–1357, doi:10.1111/j.1365-2745.2011.01870.x.
- 26.** Fagherazzi, S.; Mariotti, G.; Wiberg, P.L.; McGLATHERY, K.J. Marsh Collapse Does Not Require Sea Level Rise. *Oceanography* 2013, 26, 70–77.
- 27.** Pellegrini, E.; Boscutti, F.; De Nobili, M.; Casolo, V. Plant Traits Shape the Effects of Tidal Flooding on Soil and Plant Communities in Saltmarshes. *Plant Ecol.* 2018, 219, 823–835, doi:10.1007/s11258-018-0837-z.

- 28.** Pellegrini, E.; Boscutti, F.; Alberti, G.; Casolo, V.; Contin, M.; De Nobili, M. Stand Age, Degree of Encroachment and Soil Characteristics Modulate Changes of C and N Cycles in Dry Grassland Soils Invaded by the N₂-Fixing Shrub *Amorpha fruticosa*. *Sci. Total Environ.* 2021, 792, 148295, doi:10.1016/j.scitotenv.2021.148295.
- 29.** Casolo, V.; Tomasella, M.; De Col, V.; Braidot, E.; Savi, T.; Nardini, A. Water Relations of an Invasive Halophyte (*Spartina patens*): Osmoregulation and Ionic Effects on Xylem Hydraulics. *Funct. Plant Biol.* 2015, 42, 264–273, doi:10.1071/FP14172.
- 30.** Pellegrini, E.; Forlani, G.; Boscutti, F.; Casolo, V. Evidence of Non-Structural Carbohydrates-Mediated Response to Flooding and Salinity in *Limonium narbonne* and *Salicornia fruticosa*. *Aquat. Bot.* 2020, 166, 103265, doi:10.1016/j.aquabot.2020.103265.
- 31.** An, Y.; Gao, Y.; Tong, S.; Liu, B. Morphological and Physiological Traits Related to the Response and Adaptation of *Bolboschoenus planiculmis* Seedlings Grown Under Salt-Alkaline Stress Conditions. *Front. Plant Sci.* 2021, 12.
- 32.** Boscutti, F.; Casolo, V.; Beraldo, P.; Braidot, E.; Zancani, M.; Rixen, C. Shrub Growth and Plant Diversity along an Elevation Gradient: Evidence of Indirect Effects of Climate on Alpine Ecosystems. *PLOS ONE* 2018, 13, e0196653, doi:10.1371/journal.pone.0196653.
- 33.** Cardinale, B.J.; Duffy, J.E.; Gonzalez, A.; Hooper, D.U.; Perrings, C.; Venail, P.; Narwani, A.; Mace, G.M.; Tilman, D.; Wardle, D.A.; et al. Biodiversity Loss and Its Impact on Humanity. *Nature* 2012, 486, 59–67, doi:10.1038/nature11148.
- 34.** Anderson, M.C.; Neale, C.M.U.; Li, F.; Norman, J.M.; Kustas, W.P.; Jayanthi, H.; Chavez, J. Upscaling Ground Observations of Vegetation Water Content, Canopy Height, and Leaf Area Index during SMEX02 Using Aircraft and Landsat Imagery. *Remote Sens. Environ.* 2004, 92, 447–464, doi:10.1016/j.rse.2004.03.019.
- 35.** Ustin, S.L.; Gamon, J.A. Remote Sensing of Plant Functional Types. *New Phytol.* 2010, 186, 795–816, doi:10.1111/j.1469-8137.2010.03284.x.
- 36.** Asner, G.P.; Martin, R.E.; Anderson, C.B.; Kryston, K.; Vaughn, N.; Knapp, D.E.; Bentley, L.P.; Shenkin, A.; Salinas, N.; Sinca, F.; et al. Scale Dependence of Canopy Trait Distributions along a Tropical Forest Elevation Gradient. *New Phytol.* 2017, 214, 973–988, doi:10.1111/nph.14068.
- 37.** Steenweg, R.; Hebblewhite, M.; Kays, R.; Ahumada, J.; Fisher, J.T.; Burton, C.; Townsend, S.E.; Carbone, C.; Rowcliffe, J.M.; Whittington, J.; et al. Scaling-up Camera Traps: Monitoring the Planet's Biodiversity with Networks of Remote Sensors. *Front. Ecol. Environ.* 2017, 15, 26–34, doi:10.1002/fee.1448.
- 38.** Konings, A.G.; Rao, K.; Steele-Dunne, S.C. Macro to Micro: Microwave Remote Sensing of Plant Water Content for Physiology and Ecology. *New Phytol.* 2019, 223, 1166–1172, doi:10.1111/nph.15808.
- 39.** Belluco, E.; Camuffo, M.; Ferrari, S.; Modenese, L.; Silvestri, S.; Marani, A.; Marani, M. Mapping Salt-Marsh Vegetation by Multispectral and Hyperspectral Remote Sensing. *Remote Sens. Environ.* 2006, 105, 54–67, doi:10.1016/j.rse.2006.06.006.

40. Schmidt, K.S.; Skidmore, A.K. Spectral Discrimination of Vegetation Types in a Coastal Wetland. *Remote Sens. Environ.* 2003, 85, 92–108, doi:10.1016/S0034-4257(02)00196-7.
41. Gao, Z.G.; Zhang, L.Q. Multi-Seasonal Spectral Characteristics Analysis of Coastal Salt Marsh Vegetation in Shanghai, China. *Estuar. Coast. Shelf Sci.* 2006, 69, 217–224, doi:10.1016/j.ecss.2006.04.016.
42. Vrieling, A.; Meroni, M.; Darvishzadeh, R.; Skidmore, A.K.; Wang, T.; Zurita-Milla, R.; Oosterbeek, K.; O'Connor, B.; Paganini, M. Vegetation Phenology from Sentinel-2 and Field Cameras for a Dutch Barrier Island. *Remote Sens. Environ.* 2018, 215, 517–529, doi:10.1016/j.rse.2018.03.014.
43. Chen, B.J.W.; Teng, S.N.; Zheng, G.; Cui, L.; Li, S.; Staal, A.; Eitel, J.U.H.; Crowther, T.W.; Berdugo, M.; Mo, L.; et al. Inferring Plant–Plant Interactions Using Remote Sensing. *J. Ecol.* 2022, 110, 2268–2287, doi:10.1111/1365-2745.13980.
44. Doughty, C.L.; Cavanaugh, K.C. Mapping Coastal Wetland Biomass from High Resolution Unmanned Aerial Vehicle (UAV) Imagery. *Remote Sens.* 2019, 11, 540, doi:10.3390/rs11050540.
45. Casanova, M.T.; Brock, M.A. How Do Depth, Duration and Frequency of Flooding Influence the Establishment of Wetland Plant Communities? *Plant Ecol.* 2000, 147, 237–250, doi:10.1023/A:1009875226637.
46. Kunza, A.E.; Pennings, S.C. Patterns of Plant Diversity in Georgia and Texas Salt Marshes. *Estuaries Coasts* 2008, 31, 673–681, doi:10.1007/s12237-008-9058-3.
47. Vitti, S.; Pellegrini, E.; Casolo, V.; Trotta, G.; Boscutti, F. Contrasting Responses of Native and Alien Plant Species to Soil Properties Shed New Light on the Invasion of Dune Systems. *J. Plant Ecol.* 2020, 13, 667–675, doi:10.1093/jpe/rtaa052.
48. Janousek, C.N.; Mayo, C. Plant Responses to Increased Inundation and Salt Exposure: Interactive Effects on Tidal Marsh Productivity. *Plant Ecol.* 2013, 214, 917–928, doi:10.1007/s11258-013-0218-6.
49. Buffington, K.J.; Janousek, C.N.; Dugger, B.D.; Callaway, J.C.; Schile-Beers, L.M.; Borgnis Sloane, E.; Thorne, K.M. Incorporation of Uncertainty to Improve Projections of Tidal Wetland Elevation and Carbon Accumulation with Sea-Level Rise. *PLoS ONE* 2021, 16, e0256707, doi:10.1371/journal.pone.0256707.
50. Edge, R.S.; Sullivan, M.J.P.; Pedley, S.M.; Mossman, H.L. Species Interactions Modulate the Response of Saltmarsh Plants to Flooding. *Ann. Bot.* 2020, 125, 315–324, doi:10.1093/aob/mcz120.
51. Bradley, P.M.; Morris, J.T. Physical Characteristics of Salt Marsh Sediments: Ecological Implications. *Mar. Ecol. Prog. Ser.* 1990, 61, 245–252.
52. Geigenberger, P. Response of Plant Metabolism to Too Little Oxygen. *Curr. Opin. Plant Biol.* 2003, 6, 247–256, doi:10.1016/S1369-5266(03)00038-4.
53. Colmer, T.D.; Voeselek, L.A.C.J. Flooding Tolerance: Suites of Plant Traits in Variable Environments. *Funct. Plant Biol.* 2009, 36, 665, doi:10.1071/FP09144.
54. Koch, M.S.; Mendelssohn, I.A.; McKee, K.L. Mechanism for the Hydrogen Sulfide-Induced Growth Limitation in Wetland Macrophytes. *Limnol. Oceanogr.* 1990, 35, 399–408, doi:10.4319/lo.1990.35.2.0399.

55. Lou, Y.; Pan, Y.; Gao, C.; Jiang, M.; Lu, X.; Xu, Y.J. Response of Plant Height, Species Richness and Aboveground Biomass to Flooding Gradient along Vegetation Zones in Floodplain Wetlands, Northeast China. *PLOS ONE* 2016, 11, e0153972, doi:10.1371/journal.pone.0153972.
56. Guan, B.; Yu, J.; Wang, X.; Fu, Y.; Kan, X.; Lin, Q.; Han, G.; Lu, Z. Physiological Responses of Halophyte *Suaeda salsa* to Water Table and Salt Stresses in Coastal Wetland of Yellow River Delta. *CLEAN – Soil Air Water* 2011, 39, 1029–1035, doi:10.1002/clen.201000557.
57. Yang, F.; Wang, Y.; Wang, J.; Deng, W.; Liao, L.; Li, M. Different Eco-Physiological Responses between Male and Female *Populus deltoides* Clones to Waterlogging Stress. *For. Ecol. Manag.* 2011, 262, 1963–1971, doi:10.1016/j.foreco.2011.08.039.
58. Barickman, T.C.; Simpson, C.R.; Sams, C.E. Waterlogging Causes Early Modification in the Physiological Performance, Carotenoids, Chlorophylls, Proline, and Soluble Sugars of Cucumber Plants. *Plants* 2019, 8, 160, doi:10.3390/plants8060160.
59. Logan, D.C.; Knight, M.R. Mitochondrial and Cytosolic Calcium Dynamics Are Differentially Regulated in Plants. *Plant Physiol.* 2003, 133, 21–24, doi:DOI 10.1104/pp.103.026047.
60. Tracewell, C.A.; Vrettos, J.S.; Bautista, J.A.; Frank, H.A.; Brudvig, G.W. Carotenoid Photooxidation in Photosystem II. *Arch. Biochem. Biophys.* 2001, 385, 61–69, doi:10.1006/abbi.2000.2150.
61. Copolovici, L.; Lupitu, A.; Moisa, C.; Taschina, M.; Copolovici, D.M. The Effect of Antagonist Abiotic Stress on Bioactive Compounds from Basil (*Ocimum Basilicum*). *Appl. Sci.* 2021, 11, 9282, doi:10.3390/app11199282.
62. Yang, L.; Wen, K.-S.; Ruan, X.; Zhao, Y.-X.; Wei, F.; Wang, Q. Response of Plant Secondary Metabolites to Environmental Factors. *Molecules* 2018, 23, 762, doi:10.3390/molecules23040762.
63. Blokhina, O.; Virolainen, E.; Fagerstedt, K.V. Antioxidants, Oxidative Damage and Oxygen Deprivation Stress: A Review. *Ann. Bot.* 2003, 91, 179–194, doi:10.1093/aob/mcf118.
64. Duarte, B.; Santos, D.; Marques, J.C.; Caçador, I. Ecophysiological Adaptations of Two Halophytes to Salt Stress: Photosynthesis, PS II Photochemistry and Anti-Oxidant Feedback – Implications for Resilience in Climate Change. *Plant Physiol. Biochem.* 2013, 67, 178–188, doi:10.1016/j.plaphy.2013.03.004.
65. Hayakawa, K.; Agarie, S. Physiological Roles of Betacyanin in a Halophyte, *Suaeda japonica* Makino. *Plant Prod. Sci.* 2010, 13, 351–359, doi:10.1626/pp.13.351.
66. Ibraheem, F.; Al-Zahrani, A.; Mosa, A. Physiological Adaptation of Three Wild Halophytic *Suaeda* Species: Salt Tolerance Strategies and Metal Accumulation Capacity. *Plants* 2022, 11, 537, doi:10.3390/plants11040537.
67. Jain, G.; Gould, K.S. Are Betalain Pigments the Functional Homologues of Anthocyanins in Plants? *Environ. Exp. Bot.* 2015, 119, 48–53, doi:10.1016/j.envexpbot.2015.06.002.

- 68.** Li, Y.; Cui, L.; Yao, X.; Ding, X.; Pan, X.; Zhang, M.; Li, W.; Kang, X. Trade-off between Leaf Chlorophyll and Betacyanins in *Suaeda salsa* in the Liaohe Estuary Wetland in Northeast China. *J. Plant Ecol.* 2018, 11, 569–575, doi:10.1093/jpe/rtx025.
- 69.** Yeo, S.; Lafon, V.; Alard, D.; Curti, C.; Dehouck, A.; Benot, M.-L. Classification and Mapping of Saltmarsh Vegetation Combining Multispectral Images with Field Data. *Estuar. Coast. Shelf Sci.* 2020, 236, 106643, doi:10.1016/j.ecss.2020.106643.
- 70.** Warren, R.S.; Niering, W.A. Vegetation Change on a Northeast Tidal Marsh: Interaction of Sea-Level Rise and Marsh Accretion. *Ecology* 1993, 74, 96–103, doi:10.2307/1939504.
- 71.** Rocchini, D.; Salvatori, N.; Beierkuhnlein, C.; Chiarucci, A.; de Boissieu, F.; Förster, M.; Garzon-Lopez, C.X.; Gillespie, T.W.; Hauffe, H.C.; He, K.S.; et al. From Local Spectral Species to Global Spectral Communities: A Benchmark for Ecosystem Diversity Estimate by Remote Sensing. *Ecol. Inform.* 2021, 61, 101195, doi:10.1016/j.ecoinf.2020.101195.
- 72.** Sun, C.; Fagherazzi, S.; Liu, Y. Classification Mapping of Salt Marsh Vegetation by Flexible Monthly NDVI Time-Series Using Landsat Imagery. *Estuar. Coast. Shelf Sci.* 2018, 213, 61–80, doi:10.1016/j.ecss.2018.08.007.
- 73.** Villoslada Peciña, M.; Bergamo, T.F.; Ward, R.D.; Joyce, C.B.; Sepp, K. A Novel UAV-Based Approach for Biomass Prediction and Grassland Structure Assessment in Coastal Meadows. *Ecol. Indic.* 2021, 122, 107227, doi:10.1016/j.ecolind.2020.107227.
- 74.** Bai, Y.; Zhang, S.; Zhang, J.; Wang, J.; Yang, S.; Magliulo, V.; Vitale, L.; Zhao, Y. Using Remote Sensing Information to Enhance the Understanding of the Coupling of Terrestrial Ecosystem Evapotranspiration and Photosynthesis on a Global Scale. *Int. J. Appl. Earth Obs. Geoinformation* 2021, 100, 102329, doi:10.1016/j.jag.2021.102329.
- 75.** Gitelson, A.A.; Merzlyak, M.N.; Chivkunova, O.B. Optical Properties and Nondestructive Estimation of Anthocyanin Content in Plant Leaves. *Photochem. Photobiol.* 2001, 74, 38–45, doi:10.1562/0031-8655(2001)074<0038:OPANEO>2.0.CO;2.
- 76.** Sims, D.A.; Gamon, J.A. Relationships between Leaf Pigment Content and Spectral Reflectance across a Wide Range of Species, Leaf Structures and Developmental Stages. *Remote Sens. Environ.* 2002, 81, 337–354, doi:10.1016/S0034-4257(02)00010-X.
- 77.** de Jong, S.M.; Addink, E.A.; Hoogenboom, P.; Nijland, W. The Spectral Response of *Buxus sempervirens* to Different Types of Environmental Stress – A Laboratory Experiment. *ISPRS J. Photogramm. Remote Sens.* 2012, 74, 56–65, doi:10.1016/j.isprsjprs.2012.08.005.
- 78.** Sanches, I.D.; Souza Filho, C.R.; Kokaly, R.F. Spectroscopic Remote Sensing of Plant Stress at Leaf and Canopy Levels Using the Chlorophyll 680nm Absorption Feature with Continuum Removal. *ISPRS J. Photogramm. Remote Sens.* 2014, 97, 111–122, doi:10.1016/j.isprsjprs.2014.08.015.

- 79.** Marchesini, V.A.; Guerschman, J.P.; Schweiggert, R.M.; Colmer, T.D.; Veneklaas, E.J. Spectral Detection of Stress-Related Pigments in Salt-Lake Succulent Halophytic Shrubs. *Int. J. Appl. Earth Obs. Geoinformation* 2016, 52, 457–463, doi:10.1016/j.jag.2016.07.002.
- 80.** Boscutti, F.; Vitti, S.; Casolo, V.; Roppa, F.; Tamburlin, D.; Sponza, S. Seagrass Meadow Cover and Species Composition Drive the Abundance of Eurasian Wigeon (*Mareca Penelope* L.) in a Lagoon Ecosystem of the Northern Adriatic Sea. *Ecol. Res.* 2019, 34, 320–327, doi:10.1111/1440-1703.1070.
- 81.** Fontolan, G.; Pillon, S.; Bezzi, A.; Villalta, R.; Lipizer, M.; Triches, A.; D’Aietti, A. Human Impact and the Historical Transformation of Saltmarshes in the Marano and Grado Lagoon, Northern Adriatic Sea. *Estuar. Coast. Shelf Sci.* 2012, 113, 41–56, doi:10.1016/j.ecss.2012.02.007.
- 82.** Marchiol, L.; Filippi, A.; Adamiano, A.; Degli Esposti, L.; Iafisco, M.; Mattiello, A.; Petrusa, E.; Braidot, E. Influence of Hydroxyapatite Nanoparticles on Germination and Plant Metabolism of Tomato (*Solanum Lycopersicum* L.): Preliminary Evidence. *Agronomy* 2019, 9, 161, doi:10.3390/agronomy9040161.
- 83.** Wellburn, A.R. The Spectral Determination of Chlorophylls a and b, as Well as Total Carotenoids, Using Various Solvents with Spectrophotometers of Different Resolution. *J. Plant Physiol.* 1994, 144, 307–313, doi:10.1016/S0176-1617(11)81192-2.
- 84.** Mobin, M.; Khan, N.A. Photosynthetic Activity, Pigment Composition and Antioxidative Response of Two Mustard (*Brassica Juncea*) Cultivars Differing in Photosynthetic Capacity Subjected to Cadmium Stress. *J. Plant Physiol.* 2007, 164, 601–610, doi:10.1016/j.jplph.2006.03.003.
- 85.** Filippi, A.; Braidot, E.; Petrusa, E.; Fabro, M.; Vuerich, M.; Boscutti, F. Plant Growth Shapes the Effects of Elevation on the Content and Variability of Flavonoids in Subalpine Bilberry Stands. *Plant Biol.* 2021, 23, 241–249, doi:https://doi.org/10.1111/plb.13194.
- 86.** Priatni, S.; Pradita, A. Stability Study of Betacyanin Extract from Red Dragon Fruit (*Hylocereus Polyrhizus*) Peels. *Procedia Chem.* 2015, 16, 438–444, doi:10.1016/j.proche.2015.12.076.
- 87.** Bartolucci, F.; Peruzzi, L.; Galasso, G.; Albano, A.; Alessandrini, A.; Ardenghi, N.M.G.; Astuti, G.; Bacchetta, G.; Ballelli, S.; Banfi, E.; et al. An Updated Checklist of the Vascular Flora Native to Italy. *Plant Biosyst. - Int. J. Deal. Asp. Plant Biol.* 2018, 152, 179–303, doi:10.1080/11263504.2017.1419996.
- 88.** Pignatti, S. *Flora d’Italia*. Edagricole: Milano, 2017; ISBN 978-88-506-5243-3.
- 89.** Council Directive 92/43/EEC of 21 May 1992 on the Conservation of Natural Habitats and of Wild Fauna and Flora; 2013;
- 90.** Friuli Venezia Giulia Regional Law 23 Aprile 2007, n. 9.
- 91.** Hijmans, R.J.; Bivand, R.; Pebesma, E.; Sumner, M.D. *Terra: Spatial Data Analysis* 2023.
- 92.** Pinheiro, J.; Bates, D.; DebRoy, S.; Sarkar, D.; R Core Team. *nlme: Linear and Nonlinear Mixed Effects Models*. R package Version 3.1-152 2021.

93. Stoffel, M.A.; Nakagawa, S.; Schielzeth, H. partR2: Partitioning R2 in Generalized Linear Mixed Models. *PeerJ* 2021, 9, e11414, doi:10.7717/peerj.11414.
94. R Core Team R: A Language and Environment for Statistical Computing. R Foundation for Statistical Computing; Vienna, Austria, 2022;
95. Rouse, J.W.; Haas, R.H.; Schell, J.A.; Deering, D.W. Monitoring Vegetation Systems in the Great Plains with ERTS.; January 1 1974.
96. Pu, R.; Gong, P.; Yu, Q. Comparative Analysis of EO-1 ALI and Hyperion, and Landsat ETM+ Data for Mapping Forest Crown Closure and Leaf Area Index. *Sensors* 2008, 8, 3744–3766, doi:10.3390/s8063744.
97. Gamon, J.A.; Surfus, J.S. Assessing Leaf Pigment Content and Activity with a Reflectometer. *New Phytol.* 1999, 143, 105–117, doi:10.1046/j.1469-8137.1999.00424.x.
98. Verrelst, J.; Schaepman, M.E.; Koetz, B.; Kneubühler, M. Angular Sensitivity Analysis of Vegetation Indices Derived from CHRIS/PROBA Data. *Remote Sens. Environ.* 2008, 112, 2341–2353, doi:10.1016/j.rse.2007.11.001.

SUPPORTING INFORMATION

Table S1. Results of the LMMs relating the salt marsh community traits (i.e., plant height, total DW, total DMC, Shannon index), the *S. fruticosa* traits (i.e., shoot DW, shoot DMC, shoot length, chlorophyll, carotenoids, flavonoids, betacyanin content) the vegetation indices (i.e., NDVI, LCI, RGRI, ARI) with flooding depth, soil clay content and their interaction. Significant relationships are in bold. Degrees of freedom (Df), estimate, standard error (SE), t-values and p-values are shown.

Dependent variable	Independent variable	Df	Estimate	SE	t-Value	p-Value
<i>Plant height</i>	Flooding depth	1,15	0.46	5.2	0.08	0.931
	Clay content	1,15	0.38	0.3	1.32	0.205
	Flooding depth*Clay content	1,15	-0.24	0.3	-0.85	0.405
<i>Total DW</i>	Flooding depth	1,15	-39.78	42.3	-0.94	0.361
	Clay content	1,15	1.12	2.5	0.44	0.664
	Flooding depth*Clay content	1,15	0.81	2.1	0.39	0.705
<i>Total DMC</i>	Flooding depth	1,15	-13.98	51.54	-0.27	0.790
	Clay content	1,15	1.23	3.09	0.39	0.696
	Flooding depth*Clay content	1,15	0.87	2.59	0.34	0.741
<i>Shannon index</i>	Flooding depth	1,15	-0.11	0.29	-0.38	0.706
	Clay content	1,15	-0.01	0.01	-0.58	0.567
	Flooding depth*Clay content	1,15	-0.00	0.01	-0.00	0.998
<i>log(Shoot DW)</i>	Flooding depth	1,15	-0.04	0.25	-0.16	0.875
	Clay content	1,15	0.01	0.01	0.90	0.383
	Flooding depth*Clay content	1,15	-0.00	0.01	-0.30	0.769
<i>Shoot DMC</i>	Flooding depth	1,15	-5.02	13.98	-0.36	0.724
	Clay content	1,15	-0.07	0.78	-0.09	0.929
	Flooding depth*Clay content	1,15	0.21	0.74	0.28	0.780
<i>Shoot length</i>	Flooding depth	1,14	1.18	0.54	2.20	0.046
	Clay content	1,14	0.15	0.03	4.69	< 0.001
	Flooding depth*Clay content	1,14	-0.08	0.03	-2.77	0.015

<i>Chlorophyll</i>	Flooding depth	1,15	128.12	97.21	1.32	0.207
	Clay content	1,15	1.69	5.31	0.32	0.755
	Flooding depth*Clay content	1,15	-7.24	5.24	-1.38	0.187
<i>Carotenoids</i>	Flooding depth	1,12	-31.19	8.93	-3.49	0.004
	Clay content	1,12	-0.85	0.44	-1.94	0.076
	Flooding depth*Clay content	1,12	1.56	0.48	3.29	0.007
<i>Flavonoids</i>	Flooding depth	1,15	-5.21	7.27	-0.71	0.484
	Clay content	1,15	-0.57	0.43	-1.33	0.203
	Flooding depth*Clay content	1,15	0.20	0.37	0.552	0.589
<i>log(Betacyanin)</i>	Flooding depth	1,15	0.47	0.72	0.81	0.430
	Clay content	1,15	0.05	0.03	1.46	0.164
	Flooding depth*Clay content	1,15	-0.01	0.03	-0.41	0.684
<i>NDVI</i>	Flooding depth	1,15	0.05	0.05	1.05	0.310
	Clay content	1,15	0.00	0.00	1.53	0.147
	Flooding depth*Clay content	1,15	-0.00	0.00	-1.89	0.077
<i>LCI</i>	Flooding depth	1,15	0.04	0.03	1.48	0.159
	Clay content	1,15	0.00	0.00	1.75	0.100
	Flooding depth*Clay content	1,15	-0.00	0.00	-2.23	0.041
<i>RGRI</i>	Flooding depth	1,15	0.01	0.05	0.16	0.879
	Clay content	1,15	0.00	0.00	0.19	0.852
	Flooding depth*Clay content	1,15	0.00	0.00	0.69	0.495
<i>ARI</i>	Flooding depth	1,15	1.73	0.89	1.94	0.071
	Clay content	1,15	0.04	0.05	0.87	0.396
	Flooding depth*Clay content	1,15	-0.11	0.05	-2.37	0.031

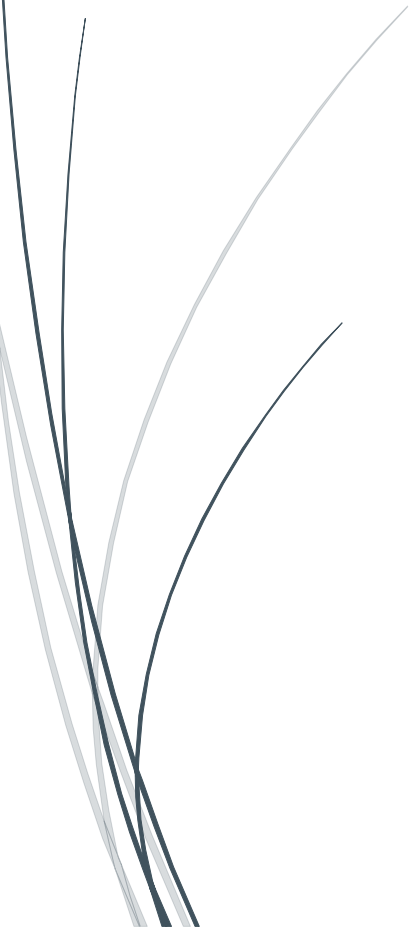
Table S2. Results of the LMMs relating the vegetation indices (i.e., NDVI, LCI, RGRI, ARI) with flooding depth, soil clay content and their interaction. Significant relationships are in bold. Degrees of freedom (Df), estimate, standard error (SE), t-values and p-values are shown.

Dependent variable	Independent variable	Df	Estimate	SE	t-Value	p-Value
<i>NDVI</i>	Flooding	1,16	-0.04	0.01	-3.14	0.006
	Clay content	1,16	0.00	0.00	0.17	0.865
<i>LCI</i>	Flooding depth	1,15	0.04	0.03	1.48	0.159
	Clay content	1,15	0.00	0.00	1.75	0.100
	Flooding depth*Clay content	1,15	-0.00	0.00	-2.23	0.041
<i>RGRI</i>	Flooding	1,16	0.04	0.01	3.49	0.003
	Clay content	1,16	0.00	0.00	1.06	0.303
<i>ARI</i>	Flooding depth	1,15	1.73	0.89	1.94	0.071
	Clay content	1,15	0.04	0.05	0.87	0.396
	Flooding depth*Clay content	1,15	-0.11	0.05	-2.37	0.031

Table S3. Contribution of salt marsh plant community traits and *S. fruticosa* traits to vegetation indices. Proportions of vegetation indices (i.e., NDVI, LCI, RGRI, ARI) variance explained by plant community traits (i.e., plant height and total DW) and *S. fruticosa* traits (i.e., shoot length, carotenoid and betacyanin content).

Dependent variable	Independent variables	Df	t Value	p-Value	Part-R²
NDVI	Plant height	1,11	0.78	0.448	0.00
	Total DW	1,11	-0.76	0.456	0.00
	Shoot length	1,11	2.83	0.014	0.10
	Carotenoid	1,11	1.30	0.212	0.01
	Betacyanin	1,11	-2.33	0.036	0.08
LCI	Plant height	1,12	0.22	0.828	0.00
	Total DW	1,12	-1.86	0.085	0.01
	Shoot length	1,12	2.94	0.011	0.12
	Carotenoid	1,12	2.04	0.062	0.06
	Betacyanin	1,12	-1.81	0.093	0.05
RGRI	Plant height	1,11	0.54	0.592	0.03
	Total DW	1,11	-0.47	0.644	0.02
	Shoot length	1,11	-1.99	0.068	0.12
	Carotenoid	1,11	-1.91	0.079	0.10
	Betacyanin	1,11	1.57	0.140	0.10
ARI	Plant height	1,11	0.82	0.424	0.03
	Total DW	1,11	-2.34	0.036	0.06
	Shoot length	1,11	2.24	0.043	0.00
	Carotenoid	1,11	-1.61	0.162	0.06
	Betacyanin	1,11	-0.75	0.467	0.00

CHAPTER 6 - Final Dissertation



IMPACT OF THIS WORK AND FUTURE PROSPECTS

The present PhD thesis has provided a contribution to the investigation and development of new technologies for the ecological transition in agriculture and to expand expertise in the field of environmental monitoring.

Nanotechnology

With regard to the development of nano-enabled agriculture, the results showed that this technology may indeed have a great potential. Functionalised nanoparticles, although of different composition, proved to be excellent tools for the targeted transport of bioactive molecules or nutrients: they were able to release them in a controlled and sustained manner and to protect them from degradation or loss due to environmental factors. Conversely, the expected biostimulating effect was not always confirmed, since in the case of CaP-HS it was moderate and in that of chitosan NPs it was not observed at all. This demonstrates that refinement studies are still needed, which could concern either the type (*e.g.*, chitosan of different origin or molecular weight) or quantity (HS) of the material to be used.

Beyond these specific cases, the development of next-generation agrochemicals using nanotechnology still requires in-depth study before they can enter the market (Saritha et al., 2022). Firstly, there is a great need to test formulations in the open field, to deeply understand inner mechanisms of action in target organisms and to verify the absence of adverse or side-effects on complex environmental matrices and in terrestrial and aquatic ecosystems through a science-based risk assessment (Saritha et al., 2022). Apart from these unavoidable verifications, one of the main limitations is the great variety of these nanomaterials. In fact, the topic has been at the forefront in recent years and there is a great deal of research on the subject, but it is very variable. Adding further complexity, the molecules to be used as functionalisers and the target organisms are also numerous (Jiang et al., 2021; Saritha et al., 2022; Worrall et al., 2018). As a result, it becomes complicated to standardise possible products and achieve a high level of scientific maturity.

The same issues arise with the application of molecular methods for crop protection, where the social acceptability of such tools needs to be considered (Giudice et al., 2021; Mezzetti et al., 2020). Although the main criticism concerns cisgenesis and genome editing, which tend to be compared with GMOs (Giudice et al., 2021), the use of SIGS may also raise some doubts, mainly due to public incompetence. In this case, the best approach for the introduction of these techniques is to widely test the safety of the method and to adopt a transparent dissemination strategy of the obtained results.

In addition to the necessary investigations already mentioned for NPs, the use of *RNA-interference* in agriculture requires further verifications due to the specificity of the sequences to be used. Indeed, the application of dsRNAs as bio-based pesticides needs specific knowledge of the target organisms and of the mechanisms underlying

the recognition and triggering of the interference machinery (Giudice et al., 2021). Discrepancies in the susceptibility to dsRNAs among organisms and even genera are known (Giudice et al., 2021), as well as in the length of the dsRNAs used, where a size from 150 to 500 bp seems the most efficient in inducing the activation of the RNAi pathway (Das and Sherif, 2020; Höfle et al., 2020). Another of the most limiting factors for field implementation of these technique is the cost-effectiveness of the approach, *i.e.*, the amount of supplied dsRNAs, which would affect not only the success of the treatment (Das and Sherif, 2020), but also its cost. Therefore, integrating molecular techniques with nanotechnologies becomes advantageous, in order to obtain efficient, long-lasting and economically accessible products by reducing the quantity of dsRNAs employed (Dalakouras et al., 2020; Giudice et al., 2021).

Ultimately, the objective of the next years will be to overcome the mentioned challenges and develop inexpensive nano-formulations with suitable properties, such as prolonged shelf life, ease of transport and handling, and a high degree of efficiency, safety and eco-compatibility. This would both overcome the existing legislative limitations (Saritha et al., 2022) and induce farmers to favourably introduce these products in their business (Singh et al., 2021).

Phenotyping

The two works concerning multi-scale plant phenotyping proved to be useful not only for the results obtained regarding the examined species and ecosystem, but also for their expandability to other research topics. In fact, these methods enable to identify morphometric and functional traits capable of describing the adaptive responses of plants, forming the basis of many investigation fields. In the agronomic sector, this information could be supportive for genotype studies and to develop sustainable methods for crop management, *e.g.*, indicating which trait is crucial for resistance of susceptibility responses. In the environmental sphere, instead, they become fundamental for territorial planning and for predicting changes in ecosystems in response to climate change.

In detail, the first work led to the identification of morpho-anatomical traits that allowed to find distinguishing elements in four weedy *Amaranthus* species. This technique proved extremely useful for the possibility of defining, with a statistical validation, taxonomic differences among species at a juvenile stage, that is usually difficult to analyse. The study could also be further extended to higher levels of investigation, using upscaling techniques such as remote sensing, similar to those employed in the last work of the present thesis. In this case, the multi-scale assessment provided far-reaching results for understanding the behaviour of vegetation in response to stresses. In addition, the comparison with conventional destructive laboratory analyses allowed further validation of the method and of the reliability of the obtained indices. Moreover, both methods showed to be advantageous demonstrating to be practical, repeatable and non-destructive towards the whole plant, factors that are of primary importance in new phenotyping techniques (Langstroff et al., 2022).

The implications of all these results are remarkable, as it would be possible to apply imaging techniques on any plant species for a great variety of purposes. Indeed, the obtainable information could be integrative for either ecophysiological studies (Noda et al., 2021) and smart crop management (Ullo and Sinha, 2021; Volpato et al., 2021; Xu and Li, 2022).

For example, combining wide to low scale survey levels with additional analysis methods, information could be obtained to predict:

- the development of different species in a specific (agro-) ecosystem and their interactions with others (also weed-crop competition) (Aharon et al., 2020);
- the acclimatisation of plants in response to environmental factors, anticipating modifications due to climate change (Arnold et al., 2019; Langstroff et al., 2022);
- the responses to both biotic and abiotic stresses, helping, in the agronomic sector, to plan more sustainable disease and nutrition management (Fiorani and Schurr, 2013; Gill et al., 2022; Zhang and Zhang, 2018).

Finally, such a level of detail in the knowledge of plant morpho-anatomical and physiological traits could also be the turning point in the development of next-generation eco-compatible agronomic products. In fact, as seen in the case of nano-agrochemicals and *RNA-interference*, the comprehension of their interaction with plant leaf surface and subsequent internalization is crucial to obtain cost-effective formulations (Giudice et al., 2021; Jiang et al., 2021). This investigation could be assessed and implemented through low-scale phenotyping. On the contrary, remote sensing techniques would facilitate verification of the functionality and effectiveness of these products by extending testing from the laboratory to the open field.

Conclusions

As seen, topics at the forefront nowadays, such as bio-based nanotechnology and imaging techniques, have indeed proven to be valuable and multi-purpose tools. In the perspective of sustainable development, they can provide a significant contribution to making agronomic or environmental management practices more efficient, especially by integrating them together and with other complementary expertises.

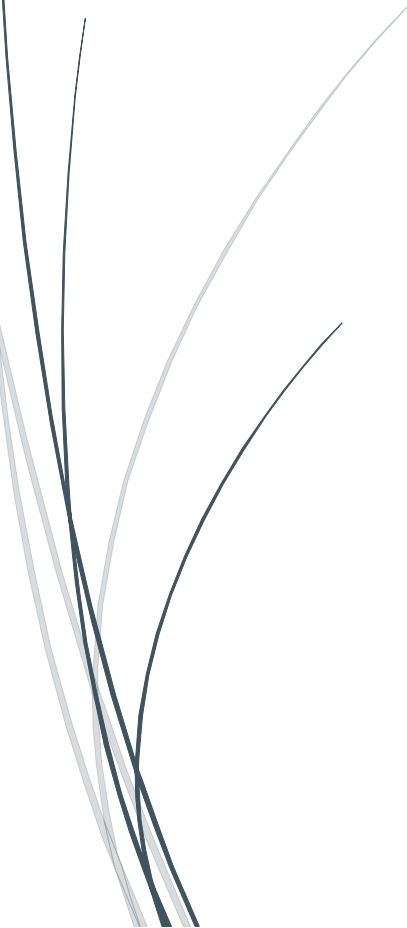
This multi-disciplinary approach, with the introduction of new tools to cope with and simultaneously mitigate the effects of climate change, is the key to reorganising human activities, maintaining the balance between our development needs and environmental sustainability.

REFERENCES

- Aharon, S., Peleg, Z., Argaman, E., Ben-David, R., Lati, R.N., 2020. Image-Based High-Throughput Phenotyping of Cereals Early Vigor and Weed-Competitiveness Traits. *Remote Sensing* 12, 3877. <https://doi.org/10.3390/rs12233877>
- Arnold, P.A., Kruuk, L.E.B., Nicotra, A.B., 2019. How to analyse plant phenotypic plasticity in response to a changing climate. *New Phytologist* 222, 1235–1241. <https://doi.org/10.1111/nph.15656>
- Dalakouras, A., Wassenegger, M., Dadami, E., Ganopoulos, I., Pappas, M.L., Papadopoulou, K., 2020. Genetically Modified Organism-Free RNA Interference: Exogenous Application of RNA Molecules in Plants. *Plant Physiol.* 182, 38–50. <https://doi.org/10.1104/pp.19.00570>
- Das, P.R., Sherif, S.M., 2020. Application of Exogenous dsRNAs-induced RNAi in Agriculture: Challenges and Triumphs. *Front. Plant Sci.* 11, 946. <https://doi.org/10.3389/fpls.2020.00946>
- Fiorani, F., Schurr, U., 2013. Future Scenarios for Plant Phenotyping. *Annual Review of Plant Biology* 64, 267–291. <https://doi.org/10.1146/annurev-arplant-050312-120137>
- Gill, T., Gill, S.K., Saini, D.K., Chopra, Y., de Koff, J.P., Sandhu, K.S., 2022. A Comprehensive Review of High Throughput Phenotyping and Machine Learning for Plant Stress Phenotyping. *Phenomix* 2, 156–183. <https://doi.org/10.1007/s43657-022-00048-z>
- Giudice, G., Moffa, L., Varotto, S., Cardone, M.F., Bergamini, C., Lorenzis, G.D., Velasco, R., Nerva, L., Chitarra, W., 2021. Novel and emerging biotechnological crop protection approaches. *Plant Biotechnology Journal* n/a. <https://doi.org/10.1111/pbi.13605>
- Höfle, L., Biedenkopf, D., Werner, B.T., Shrestha, A., Jelonek, L., Koch, A., 2020. Study on the efficiency of dsRNAs with increasing length in RNA-based silencing of the *Fusarium CYP51* genes. *RNA Biol* 17, 463–473. <https://doi.org/10.1080/15476286.2019.1700033>
- Jiang, M., Song, Y., Kanwar, M.K., Ahammed, G.J., Shao, S., Zhou, J., 2021. Phytonanotechnology applications in modern agriculture. *Journal of Nanobiotechnology* 19, 430. <https://doi.org/10.1186/s12951-021-01176-w>
- Langstroff, A., Heuermann, M.C., Stahl, A., Junker, A., 2022. Opportunities and limits of controlled-environment plant phenotyping for climate response traits. *Theor Appl Genet* 135, 1–16. <https://doi.org/10.1007/s00122-021-03892-1>
- Mezzetti, B., Smagghe, G., Arpaia, S., Christiaens, O., Dietz-Pfeilstetter, A., Jones, H., Kostov, K., Sabbadini, S., Opsahl-Sorteberg, H.-G., Ventura, V., Taning, C.N.T., Sweet, J., 2020. RNAi: What is its position in agriculture? *J Pest Sci* 93, 1125–1130. <https://doi.org/10.1007/s10340-020-01238-2>

- Noda, H.M., Muraoka, H., Nasahara, K.N., 2021. Plant ecophysiological processes in spectral profiles: perspective from a deciduous broadleaf forest. *J Plant Res* 134, 737–751. <https://doi.org/10.1007/s10265-021-01302-7>
- Saritha, G.N.G., Anju, T., Kumar, A., 2022. Nanotechnology - Big impact: How nanotechnology is changing the future of agriculture? *Journal of Agriculture and Food Research* 10, 100457. <https://doi.org/10.1016/j.jafr.2022.100457>
- Singh, H., Sharma, A., K. Bhardwaj, S., Kumar Arya, S., Bhardwaj, N., Khatri, M., 2021. Recent advances in the applications of nano-agrochemicals for sustainable agricultural development. *Environmental Science: Processes & Impacts* 23, 213–239. <https://doi.org/10.1039/D0EM00404A>
- Ullo, S.L., Sinha, G.R., 2021. Advances in IoT and Smart Sensors for Remote Sensing and Agriculture Applications. *Remote Sensing* 13, 2585. <https://doi.org/10.3390/rs13132585>
- Volpato, L., Pinto, F., González-Pérez, L., Thompson, I.G., Borém, A., Reynolds, M., Gérard, B., Molero, G., Rodrigues, F.A., 2021. High Throughput Field Phenotyping for Plant Height Using UAV-Based RGB Imagery in Wheat Breeding Lines: Feasibility and Validation. *Frontiers in Plant Science* 12.
- Worrall, E.A., Hamid, A., Mody, K.T., Mitter, N., Pappu, H.R., 2018. Nanotechnology for Plant Disease Management. *Agronomy* 8, 285. <https://doi.org/10.3390/agronomy8120285>
- Xu, R., Li, C., 2022. A Review of High-Throughput Field Phenotyping Systems: Focusing on Ground Robots. *Plant Phenomics* 2022, 1–20. <https://doi.org/10.34133/2022/9760269>
- Zhang, Y., Zhang, N., 2018. Imaging technologies for plant high-throughput phenotyping: a review. *Front. Agr. Sci. Eng.* 5, 406–419. <https://doi.org/10.15302/J-FASE-2018242>

APPENDIX - Conferences, Other Contributions, Training Activities



CONFERENCES AND WORKSHOPS – ABSTRACTS

Oral communications

Higher Education for Sustainable Food Production: 3rd Joint Meeting of Agriculture-oriented PhD Programs at Unict, Unifg and Uniud – Giovinazzo (BA, Italy), 11-15 October 2021. [Link](#)

Chitosan nanoparticles doped with dsRNA as a tool for sustainable viticulture: preliminary results

Dora Scarpin¹, Enrico Braidot¹, Elisa Petrusa¹

¹Department of Agriculture, Food, Environmental and Animal Sciences (DI4A), University of Udine, Via delle Scienze 91, 33100 Udine, Italy.

Agriculture is recently undergoing a period of transition towards sustainability, with the aim of providing sufficient food for the growing population by reducing the environmental impact. In this context, nanotechnologies are arousing interest in research thanks to the versatility and peculiar properties of some nanomaterials, which appear promising to make some agronomic practices, such as nutrition and crop protection, more eco-sustainable. Chitosan (CH) is an interesting organic polymer to be used to obtain nanoparticles (NPs), thanks to its biocompatibility and to the possibility of sourcing it through the circular economy. CH is known for its ability to induce several biological responses in plants concerning their growth and their defense against diseases, and it shows also good performances as a shuttle for a variety of molecules. This opens the possibility both to profit from the CH carrier function and its protective action against external agents, and to obtain a synergistic effect between it and the transported molecule. In our case, the goal is the functionalization of CH-NPs with specific dsRNA sequences of grapevine pathogens to exploit the *RNA-interference* (RNAi) mechanism, which has been suggested as an innovative strategy to limit pathogen infections.

Preliminary results will be here presented, concerning the development of a protocol for the synthesis of CH-NPs, their characterization and the first information regarding their interaction with dsRNA sequences. Two variants of NPs have been produced (from chitosan as it is, or treated with hydrogen peroxide), which were doped with dsRNA sequences of Esca disease pathogens. The difference in synthesis procedures determined opposite interactions with nucleotides, resulting in a lower dimensional size and greater retention of the doping agent by the NPs obtained with untreated chitosan.

55th SISV Congress: "Vegetation Science and Global Changes: Scenarios, Challenges and Innovation" – L'Aquila (Italy), 16-17 June 2022. Oral communication by Dr. Giacomo Trotta. [Link](#)

Remote sensing tools to parse the acclimation response of saltmarshes to flooding stress: upscaling perspectives in lagoon systems

Giacomo Trotta^{1,2}, Marco Vuerich¹, Paolo Cingano¹, [Dora Scarpin](#)¹, Elisa Petrusa¹, Enrico Braidot¹, Francesco Boscutti¹

¹Department of Agriculture, Food, Environmental and Animal Sciences, University of Udine (DI4A), Via delle Scienze 91, 33100 Udine, Italy.

²Department of Environmental and Life Sciences (DSV), University of Trieste, Via Licio Giorgieri 5, 34127, Trieste, Italy.

Sea level rise is considered a prominent aftermath of the ongoing global warming, which is expected to seriously treat the worldwide coasts. Among coastal environments, saltmarshes harbor plant communities particularly sensitive to the increase of flooding. Although saltmarshes might contrast sea level rise by accretion and niche shifting, sea rise rates and the coastal squeeze phenomenon undermine the acclimation capacity of such plant communities. For these reasons, parsing the underlying mechanisms of the response of saltmarshes to flooding is of outmost importance to foresee the future scenarios for these important ecosystems. In this light, linking different ecological scales using an upscaling approach might provide new insight into the ecological processes involved. We analyzed main traits of plant community and the growth of the key species *Salicornia fruticosa* (L.) L. in 9 saltmarshes along the flooding gradient (Marano and Grado lagoon, northern Adriatic Sea). In particular, we considered community (*i.e.* species richness, dry biomass, dry matter content) and individual growth (*i.e.* shoot annual growth, dry biomass, dry matter content, plant height) and physiological traits (*i.e.* pigments and secondary metabolite content) in response to flooding gradient. Concurrently we carried out a UAV (Unmanned Aerial Vehicle) multispectral survey, in order to obtain remote sensing-derived vegetation indices (*i.e.* NDVI - Normalized Difference Vegetation Index, LCI - Leaf Chlorophyll Index, ARI - Anthocyanin Reflectance Index) for the upscaling of plant responses. We found that the flooding gradient produced a significant decrease of plant biomass and growth, affecting both plant traits and plant community features. We also found remote sensing-derived indices to be related to the analyzed plant traits, showing promising perspectives for the upscaling plant flooding stress response. In particular, NDVI was mainly linked to individual annual plant shoot elongation while the other indices were also related to stem pigments and secondary metabolites content. Our findings shed new light on the potential use of the remote sensing tool for the understanding of the response of saltmarshes vegetation to the future increase of the sea level, proving to be a promising method for long-term monitoring of these plant communities.

Higher Education for Sustainable Food Production: 4th Joint Meeting of Agriculture-oriented PhD Programs at Unict, Unifg and Uniud – Paluzza (UD, Italy), 3-7 October 2022. [Link](#)

Chitosan nanoparticles for sustainable agriculture: interactions with leaf surface and protective effect on dsRNA as functionalising agent

Dora Scarpin¹, Enrico Braidot¹, Elisa Petrusa¹

¹Department of Agriculture, Food, Environmental and Animal Sciences, University of Udine (DI4A), Via delle Scienze 91, 33100 Udine, Italy.

Collaboration: Research Centre for Viticulture and Enology, Council for Agricultural Research and Economics (CREA-VE), Via XXVIII Aprile 26, 31015 Conegliano (TV), Italy.

Climate change and population growth are causing significant issues in the agricultural world, among which the worsening of environmental stresses suffered by crops and the inefficient use of resources must be highlighted. That's why it's necessary to find eco-sustainable solutions that can guarantee adequate production efficiency without affecting environmental health. Among the most advanced technologies, the development of nanomaterials partially replacing the conventional treatments with synthetic pesticides and fertilizers, stands out, given their more efficient transport of bioactive substances to plants and protection from damaging factors. Considering organic materials, nano-chitosan is even eco-compatible and obtainable through circular economy.

Another innovation concerning the defense of crops is the exploitation of the so-called *RNA-interference* mechanism. Specific dsRNAs targeting an essential gene of a pathogen or weed can be applied exogenously, triggering a pathway that leads to gene silencing into the organism. A major issue, however, consists in the easy degradability of these sequences if applied naked, which makes the technology still unlikely for agricultural up-scaling.

In this regard, the aim of our research was to verify the feasibility of dsRNA application on plants by means of functionalized chitosan nanoparticles (NPs), thus allowing its efficient delivery and protection. After defining the best synthesis protocol of NPs, these were used for different tests. To verify their ability to adhere to the leaf surface, they were observed by confocal microscope on two plant species thanks to a fluorescent probe. Subsequently, after their functionalization with nucleotides, their protective capacity was studied. These tests proved to be fundamental for the prosecution of the work concerning the evaluation of the formulation efficacy on plant pathogens.

2nd Summer School "Nanotechnology in Agriculture", University of Udine and NanoInnovation 2023 – Udine (Italy), 29-30 June 2023. [Link](#)

Recycling of waste compounds: chitosan of biological origin as a raw material for ENMs production

Dora Scarpin¹

¹Department of Agriculture, Food, Environmental and Animal Sciences, University of Udine (DI4A), Via delle Scienze 91, 33100 Udine, Italy.

Chitosan is one of the most abundant biopolymers on earth, together with cellulose, and is easily obtainable from chitin-based waste (crustaceans, fungi, insects) using circular economy processes. Therefore, considerable interest is conferred to its application in developing new technologies for eco-sustainability in agriculture, especially in synthesizing nanomaterials. Furthermore, it is known that its beneficial properties, such as the induction of biological responses concerning plant defense against stresses, are enhanced when the polymer is in a nanometric form. Furthermore, chitosan nanostructures show better interaction with plant teguments and an appreciated durability and stability; hence, they are also suitable as carriers for bioactive molecules to be used as new-generation agronomic formulations for crop nutrition or protection.

Given their potential in the future, this lesson will take an in-depth look at the properties and synthesis of chitosan nanoparticles, including some examples of plant pathology applications.

Higher Education for Sustainable Food Production: 5th Joint Meeting of Agriculture-oriented PhD Programs at Unict, Unifg and Uniud – Catania (Italy), 25-28 September 2023. [Link](#)

New technologies for the Ecological Transition in agriculture: nanomaterials, SIGS and plant phenotyping

Dora Scarpin¹, Enrico Braidot¹, Elisa Petrusa¹

¹Department of Agriculture, Food, Environmental and Animal Sciences, University of Udine (DI4A), Via delle Scienze 91, 33100 Udine, Italy.

Affiliations: Research Centre for Viticulture and Enology, Council for Agricultural Research and Economics (CREA-VE), Via XXVIII Aprile 26, 31015 Conegliano (TV), Italy; Department of Agronomy Animal Food Natural Resources and Environment (DAFNAE), University of Padova, Viale dell'Università 16, 35020 Legnaro (PD), Italy; Institute for Sustainable Plant Protection (IPSP) - National Research Council (CNR), Viale dell'Università 16, 35020 Legnaro (PD), Italy.

Increased anthropogenic activity and consequent climate change are causing significant damages in the agro-ecosystem, including worsening environmental stresses on crops and inefficient use of resources. Hence, it becomes essential to develop sustainable solutions to ensure adequate production efficiency and limited impact. Recent innovations include alternatives to be used as partial replacement of agrochemicals for crop protection or nutrition, as well as smart technologies to detect vegetation responses to environment in order to improve agronomic management planning.

In this context, the present research firstly aimed to develop efficient ways for sustainable crop protection using natural nanomaterials obtained through circular economy (mainly chitosan-based). These nanoparticles (NPs) have also been employed as carriers for specific double stranded-RNA sequences, aimed at making the so-called *Spray-Induced Gene Silencing* technology more efficient. This strategy, through topical application of RNAs targeting pathogen genes to plant material, may enable disease control. For this purpose, after preliminary analyses on NPs' properties (alone and functionalized) and on their behavior when sprayed on tobacco leaves, inhibition tests on *Botrytis cinerea* were carried out. To do it, NPs conveying dsRNAs with interfering function on fungal metabolism have been employed.

Secondly, another experiment was conducted with the aim of developing an investigation method for plant phenotyping. Different traits of the leaf surface of four invasive *Amaranthus* species were studied, using imaging techniques and multivariate statistical analysis. This method has made it possible to identify traits able to describe plant adaptive responses, useful as supporting information for genotype studies.

Both lines of research, as innovative and complementary, are worthy of being developed for the eco-sustainable management of the agro-ecosystem.

Poster communications

Plant Biology Europe 2021 – Turin (Italy), 28 June - 01 July 2021. [Link](#)

Calcium phosphate nanoparticles doped with copper ions as efficient tools for downy mildew prevention

Dora Scarpin¹, Marco Vuerich¹, Enrico Braidot¹, Elisa Petrusa¹, Guido Fellet¹, Giorgio Honsell¹, Paolo Sivilotti¹, Luca Marchiol¹, Lorenzo Degli Esposti², Alessio Adamiano², Michele Iafisco²

¹Department of Agriculture, Food, Environmental and Animal Sciences, University of Udine (DI4A), Via delle Scienze 91, 33100 Udine, Italy.

²Institute of Science and Technology for Ceramics (ISTEC), National Research Council (CNR), Via Granarolo 64, 48018 Faenza, Italy.

Nowadays the management of crops requires the use of a large quantity of pesticides, herbicides and fertilizers, especially in high-income crops such as vines, which undergo several treatments per year. Their use, however, is highly inefficient, with considerable losses that have harmful effects on the environment and human health. For this reason, the interest towards methods able to make agronomic practice more sustainable is growing noticeably. Particular attention is paid to nanotechnology applied in agriculture, as this could lead to the development of nano-agrochemicals more effective than conventional ones, concerning leaching and treatment persistence on plant. In fact, nanomaterials allow to bind the molecules of interest and to transport them directly to the target site in the plant, thus reducing the overall doses used and their dispersion into the environment.

According to this perspective, in this work two types of calcium - phosphate nanoparticles were applied on Chardonnay grapevine cultivar: the aim was to evaluate their potential as vectors for low amounts of ionic elements, which may have a nourishing or biocidal function. In particular, two different methodologies have been used for functionalization with copper (Cu II), aiming to investigate its inhibitory action on *Plasmopara viticola* infection and to verify its entry into the leaves.

III convegno AISSA#UNDER40: La ricerca scientifica nel processo di transizione ecologica in agricoltura – Bolzano (Italy), 14-15 July 2022. [Link](#)

Chitosan nanocarriers-mediated delivery of double-stranded RNA *in planta*

Dora Scarpin¹, Walter Chitarra², Luca Nerva², Loredana Moffa², Francesca D'Este³, Marco Vuerich¹, Antonio Filippi³, Enrico Braidot¹, Elisa Petrusa¹

¹Department of Agriculture, Food, Environmental and Animal Sciences, University of Udine (DI4A), Via delle Scienze 91, 33100 Udine, Italy.

²Research Centre for Viticulture and Enology, Council for Agricultural Research and Economics (CREA-VE), Via XXVIII Aprile 26, 31015 Conegliano (TV), Italy.

³Department of Medicine (DAME), University of Udine, P.le Kolbe 4, 33100 Udine, Italy.

Agriculture is currently facing numerous challenges: the rapid rise of the world population, the consequent growth in food demand, the global decrease in crop yield. Particularly regarding the last issue, climate change is worsening the environmental stresses that commonly affect crops, and the use of resources – such as fertilizers and pesticides – is highly inefficient and pollutant. In this context, research is looking for new approaches to improve crop productivity by more efficient and environmentally friendly practices. It has been shown that nanomaterials are suitable for the development of cutting-edge technologies with the aim of improving the delivery of bioactive substances on plants and to promote their resistance to biotic and abiotic stresses. Among organic polymers, chitosan, if used in the nanoscale form, shows both properties; it can induce biological responses concerning plant defense against diseases and pathogen attack, and it is particularly suitable as a carrier for several molecules. Another innovative method for the defense of crops is the exploitation of the spray-induced gene silencing (SIGS) based on the activation of the so-called *RNA-interference* (RNAi). It involves exogenous double stranded RNAs (dsRNAs) targeting an essential pathogen gene, which trigger the RNAi pathway leading to the translational repression by degradation of target homologous mRNAs. In our case, the research aimed to verify the feasibility of dsRNA distribution on plant surface by means of functionalized chitosan nanoparticles (CH-NPs), thus allowing the protection of the doping agent and its efficient delivery. Here we show the preliminary results regarding the characterization of CH-NPs, their loading with dsRNAs and their interaction with the leaf surface of *Nicotiana benthamiana* plants. The effects of the dose-dependent distribution were analyzed by confocal microscopy upon incorporation of a fluorescent probe.

LXV SIGA Annual Congress "From genes to fork - On Mendel's footsteps" – Piacenza (Italy), 6-9 September 2022. Poster communication by Dr. Serena Bordignon. [Link](#)

Development of a non-chemical RNAi-based strategy for *Amaranthus hybridus* L. weed management

Bordignon S.¹, Panozzo S.¹, Farinati S.², Milani A.¹, Scarabel L.¹, Scarpin D.³, Braidot E.³, Petrusa E.³, D'Este F.⁴, and Varotto S.²

¹Institute for Sustainable Plant Protection (IPSP) - National Research Council (CNR), Viale dell'Università 16, 35020 Legnaro (PD), Italy.

²Department of Agronomy Animal Food Natural Resources and Environment (DAFNAE), University of Padova, Viale dell'Università 16, 35020 Legnaro (PD), Italy.

³Department of Agriculture, Food, Environmental and Animal Sciences, University of Udine (DI4A), Via delle Scienze 91, 33100 Udine, Italy.

⁴Department of Medicine (DAME), University of Udine, P.le Kolbe 4, 33100 Udine, Italy.

Weeds are one of the major issues in cropping systems, responsible for significant yield losses. Herbicide applications are the most effective strategy to control weeds, but stricter legislation has resulted in a significant reduction in the number of herbicides available on the market. Furthermore, the recent European legislation on the sustainable use of pesticides will require farmers to drastically reduce chemical use over the next ten years while promoting integrated weed management strategies that improve environmental sustainability and lower the risks to animal and human health. In addition, the over-reliance on chemical control has resulted in the evolution of resistant biotypes. As a result, new technologies to effectively manage weeds and weed resistance should be developed. In this regard, the development of a non-chemical weed control strategy based on RNA interference (RNAi) technology could: i) represent a potential non-chemical weed control strategy, ii) provide an emerging GMO-free strategy for managing invasive and resistant weeds, and iii) provide a valid opportunity to go inside the molecular mechanisms of weed biology.

In this study, the acetolactate synthase (*ALS*) gene of *Amaranthus hybridus* L. has been used as the target to assess the effectiveness and applicability of *in-vitro* synthesized double-stranded RNAs (dsRNAs) direct application for endogenous gene silencing and weed control. *A. hybridus* is a monoecious and self-pollinated weed that has evolved multiple resistance to herbicides with different sites of action, including ALS inhibitors, which are the most used herbicides in soybean. *ALS* represents an ideal target for the development and future application of dsRNA-mediated gene silencing because it is an intronless, nucleotide-stable, and single-copy gene. We have produced dsRNAs of various lengths (ranging from 218 to 460bp) targeting three distinct *ALS* regions: the 5'- and 3'-ends, and a central region. dsRNAs molecules were transcribed *in-vitro* by T7 RNA polymerase and externally applied to the abaxial leaf surface of *A. hybridus* plants at 4-6 true leaves developmental stage by: i) mechanical inoculation, or ii) high-

pressure spraying. Despite the expression of *ALS* gene transcripts was found to be lightly downregulated when synthetic *ALS*-dsRNAs were applied, no phenotypic effects were observed. Our current research focuses on the determination of the effectiveness of *ALS*-dsRNAs silencing using agroinfiltration techniques, and on dsRNAs delivery techniques through the use of nanomaterials to maximize the effectiveness of gene silencing by exogenous dsRNAs application. This second approach was preliminary studied by RNA electrophoretic mobility of functionalized nanomaterial and by means of confocal microscopy on *A. hybridus* leaves. In parallel, we are examining the expression patterns of genes thought to be involved in the RNAi pathway in *A. hybridus* to verify if their expression is triggered by dsRNA applications.

Plant Biology Europe 2023 – Marseille (France), 03-06 July 2023. [Link](#)

Comparison of leaf morpho-anatomical characters in *Amaranthus* spp.: phenotyping as an investigative tool for environmental and agricultural sciences

Dora Scarpin¹, Giacomo Este¹, Francesca D'Este², Andrea Milani³, Silvia Panozzo³, Serena Varotto⁴, Marco Vuerich¹, Francesco Boscutti¹, Elisa Petrusa¹, Enrico Braidot¹

¹Department of Agriculture, Food, Environment and Animal Sciences (DI4A), University of Udine, Via delle Scienze 206, 33100 Udine, Italy.

²Department of Medicine (DAME), University of Udine, P.le Kolbe 4, 33100 Udine, Italy.

³Institute for Sustainable Plant Protection (IPSP) - National Research Council (CNR), Viale dell'Università 16, 35020 Legnaro (PD), Italy.

⁴Department of Agronomy Animal Food Natural Resources and Environment (DAFNAE), University of Padova, Viale dell'Università 16, 35020 Legnaro (PD), Italy.

Plant phenotyping is an important tool that can provide insight into the interaction between plants and the environment, often as supporting information for genotype studies. The resulting knowledge can be useful in eco-physiological research, to understand how species adapt to their growing conditions and to biotic competition. In recent years, phenotyping techniques for the study of plant morpho-anatomical traits have developed in the field of the imaging analysis, starting from microscope images up to high scale acquisitions through remote sensing. In this work, we focused on the detailed study of single-leaf morphometric traits through the processing of photographic and confocal microscope acquisitions. Four species of *Amaranthus* were used, being plants of interest due to their high invasiveness into fields. Their morphological traits could become a useful tool to describe their adaptative responses and to define strategies for the sustainable management of the agro-ecosystem.

Novel approach to link the physiological response of maize to drought and the occurrence of mycotoxins

Marco Vuerich¹, Giacomo Boscarol¹, Giacomo Trotta^{1,2}, Elisa Petrusa¹, [Dora Scarpin](#)¹, Enrico Braidot¹, Valentino Volpe³, Stefano Barbieri³, Michele Fabro³, Francesco Boscutti¹

¹Department of Agricultural Food, Animal and Environmental Sciences, University of Udine Via delle Scienze 99, 33100 Udine, Italy.

²Department of Life Sciences, University of Trieste, Via Licio Giorgieri, 5, 34127 Trieste, Italy.

³Servizio fitosanitario e chimico, ricerca, sperimentazione e assistenza tecnica, ERSA, Pozzuolo del Friuli, Italy.

Increased frequency of heatwaves and droughts are some of the aspects by which climate change threatens maize cultivation (*Zea mays* L.), thus playing a crucial role in global food security. The impact of drought on maize production is multifaceted. Firstly, drought stress during the critical stages of germination, flowering and pollination can lead to decreased plant growth, pollen production, nutrient uptake and ultimately to lower grain yields (1). In addition, prolonged periods of drought increase the spread of pests and diseases, which further exacerbate the vulnerability of maize crop and may compromise yield quality (2). However, the introduction of irrigation could only partially limit the damaging effects of severe water stress on maize performance. Therefore, improving the knowledge of the physiological response to water scarcity of this crop may be crucial for agronomic choices in the field.

In this context, we monitored 20 maize fields, characterized by the simultaneous presence of irrigated and non-irrigated areas, along a soil grain size gradient in the Friuli Venezia Giulia region throughout the growing season, at four phenological stages (*i.e.*, beginning of stem elongation, flowering, milk maturation, dent maturation). In particular, we considered the plant individual functional response (*i.e.*, plant height, SLA, leaf DMC, leaf chlorophyll, carotenoid and flavonoid content, kernel DW, kernel C:N, kernel $\delta^{13}C$), and the aflatoxin and fumonisin content of the kernel in relation to irrigation conditions and climate data (*i.e.*, total precipitation, mean temperature).

We found that the soil structure effect is overruled by the effect of climate and/or irrigation. As we expected the absence of irrigation and low total precipitation led to a reduction of plant biomass and kernel production whereas interaction between irrigation and phenological stage had significant effect on leaf pigments (*i.e.*, chlorophyll) and secondary metabolites (*i.e.*, flavonoid). Moreover, irrigation enhanced the kernel C:N ratio and $\delta^{13}C$, whereas reduced the amount of aflatoxins.

Our further investigations aim at evaluating the interplay between the climatic variables, the soil structure and the individual traits on the ultimate content of mycotoxins in the kernel, with two distinct irrigation regimes and at the given different phenological stages adopting a structural equation modelling approach.

- 1) A. Challinor, J. Watson, D. Lobell, S.M. Howden, D.R. Smith, N. Chhetri (2014) *Nature Clim Change* 4, 287–291.
- 2) S. Savary, L. Willocquet, S.J. Pethybridge, P. Esker, N. McRoberts , A. Nelson (2019) *Nat Ecol Evol* 3, 430–439.

Alien plant invasion during early succession stages of dune systems is driven by soil properties

Giacomo Trotta^{1,2}, Marco Vuerich², Elisa Pellegrini², Elisa Petrusa², [Dora Scarpin](#)², Enrico Braidot², Francesco Boscutti²

¹Dipartimento di Scienze della Vita, Università di Trieste, Via L. Giorgieri, 10, 34127 Trieste, Italy.

²Department of Agriculture, Food, Environmental and Animal Sciences, University of Udine, via delle Scienze 208, 33100 Udine, Italy.

Biological invasion is nowadays recognised as one of the major threats to biodiversity (1). This is particularly true for coastal habitats, where dunes are considered one of the most invaded habitats worldwide. Many studies linked the success of alien plant invasion in dune ecosystems to human disturbances, but less is known about the role of soil properties in plant invasion. Soil properties can directly affect plant dune colonization and the final community composition (2,3). This is expected to be linked to the interplay of soil and the plant functional response, generating important plant-soil feedbacks able to reverberate on the community structure and composition. Plant-soil interactions are thus expected to be crucial in explaining the invasion processes, but their role in dune alien colonization is mostly unknown.

We performed a manipulative experiment in a barrier island of the Marano and Grado's lagoon, Northern Adriatic Sea. The whole plant community of backdune was erased by a soil miller in the selected plots to trigger a new ecological succession and test the mechanism of alien plant invasion during the early stages of plant colonization. In 8 experimental blocks, we altered soil properties by adding salt, nitrogen and organic matter (*i.e.* peat) and combining those treatments in 1 m² plots with a factorial design (*i.e.* 8 replicates × 8 treatments = 64 plots). We recorded the emergence of seedlings with a camera system every 15 days. At the end of experiments, we recorded the plant community composition and measured the following traits: plant height, species cover, number of individuals, leaf pigments, SLA. Moreover, those traits were calculated for the overall community and for the key species (*Cakile maritima* Scop.) We also estimated the decomposition rate of the soil using the Tea Bag Index. In addition, the same parameters were collected in 8 reference plots (*i.e.* surrounding unaltered plant community).

The results showed that most of the treatments decreased the species richness of alien plants, in particular where soil salt content was enhanced. Moreover, some treatments had positive effects on the native plant cover and decreased the overall number of alien individuals, potentially reducing the initial propagule pressure due to the soil seed bank and, hence, changing the further plant community trajectories. This study provides new information on conservation and management efforts in this ecologically

sensitive area, giving new insight into the dynamics of biological invasion and the impacts on native ecosystems.

1) F. Lami, S. Vitti, L. Marini, E. Pellegrini, V. Casolo, G. Trotta, M. Sigura, F. Boscutti (2021) *Ecological Indicators*, 133, 108450.

2) M. Vilà, C. Basnou, P. Pyšek, M. Josefsson, P. Genovesi, S. Gollasch, W. Nentwig, S. Olenin, A. Roques, D. Roy (2010) *Frontiers in Ecology and the Environment*, 8, 135–144.

3) S. Vitti, E. Pellegrini, V. Casolo, G. Trotta, F. Boscutti (2020) *Journal of Plant Ecology*, 13, 667–675.

IX International Plant Science Conference (IPSC) – Pisa (Italy), 13 - 16 September 2023.
Poster communication by Dr. Giacomo Boscarol. [Link](#)

Interactions between plant response to environment and fungal microbiome in developing maize silks in relation to mycotoxin risk

Giacomo Boscarol¹, Francesco Boscutti¹, Alessandra Di Francesco¹, Giuseppe Firrao¹, Marco Vuerich¹, [Dora Scarpin](#)¹, Giacomo Trotta^{1,2}, Enrico Braidot¹, Valentino Volpe³, Thomas Lazzarin³, Maurizio Martinuzzi³, Michele Fabro³, Elisa Petrusa¹

¹Department of Agriculture, Food, Environmental and Animal Sciences, University of Udine, via delle Scienze 208, 33100 Udine, Italy.

²Dipartimento di Scienze della Vita, Università di Trieste, Via L. Giorgieri, 10, 34127 Trieste, Italy.

³Servizio fitosanitario e chimico, ricerca, sperimentazione e assistenza tecnica, ERSA, Pozzuolo del Friuli, Italy.

Maize (*Zea mays* L.) is one of the most important crops worldwide both in terms of yield and land surface used, which are constantly increasing. One of the most critical stages for maize reproduction and seed establishment is the emergence of silk from cob: silks are particularly susceptible to environmental stresses and represent a preferential entry route for mycotoxin-producing fungi such as *Fusarium verticillioides* and *Aspergillus flavus* (1). Moreover, from elongation to senescence, silks become a sink organ enriched in nutrients (e.g., Non-Structural Carbohydrates (NSC)), and a crossway for various primary and secondary metabolites. In maize silks, these metabolites are expected to be significantly affected by environmental stress conditions (2) and by the maturation stage of silk tissues themselves, possibly affecting the fungal colonization of the ear tissues. In temperate regions of cultivated maize, also pathogen growth and mycotoxin production are thought to be affected by environmental factors, such as alterations in temperature, rainfall and humidity (3), which are strictly related to climate change.

The aim of this study is to investigate the impact of the environmental conditions on the fungal microbiome in maize developing silks at two different phenological stages. To do so, some eco-physiological parameters have been measured in 5 plots under contrasting climate conditions, and the complete fungal microbiome has been sequenced for each plot, both at the beginning of emergence and at the senescence of silks.

In this study we expect to get new insights into the interplay of the environmental conditions, i.e. precipitation and temperature, and phenological stage of silks in determining the fungal microbiome of maize silks. We do believe that climate-induced plant response might be pivotal in shaping the microbiome communities by favouring some fungal groups and disfavouring others during early silk colonization.

- 1) Thompson, M. E. H. & Raizada M. N. Fungal pathogens of maize gaining free passage along the silk road. *Pathogens*, 7(4), 81 (2018).
- 2) Slewinski, T. L. Non-structural carbohydrate partitioning in grass stems: a target to increase yield stability, stress tolerance, and biofuel production. *Journal Of Experimental Botany*, Vol. 63, No. 13, pp. 4647-4670 (2012).
- 3) Magan, N. & Medina, A. Integrating gene expression, ecology and mycotoxin production by *Fusarium* and *Aspergillus* species in relation to interacting environmental factors. *World Mycotoxin J.* 9, 673–684 (2016).

Educational activities

Scarpin D. Nanomateriali a base di chitosano per un'agricoltura sostenibile – *PTCO DI4A La qualità in agricoltura*, University of Udine, 2021

Albuta A., Braidot E., Petrusa E., Scarpin D. Caratterizzazione e applicazioni di nanoparticelle di chitosano quali vettori di biomolecole – *Bachelor's thesis in Agricultural Sciences (L-25)*, University of Udine, 2022. [Link](#)

Bertè M., Boscutti F., Scarpin D., Vuerich M. Effetti della sommersione sul contenuto di pigmenti in *Salicornia fruticosa* L.: upscaling della risposta eco-fisiologica delle specie di barena ai cambiamenti globali – *Bachelor's thesis in Environmental Sciences (L-32)*, University of Udine, 2022. [Link](#)

Morossi G., Zancani M., Scarpin D. Isolamento e caratterizzazione di esosomi ottenuti da colture cellulari di caffè – *Master's thesis in Agricultural Sciences and Technologies (LM-69)*, University of Udine, 2023. [Link](#)

Este G., Braidot E., Petrusa E., Scarpin D. Caratteri morfo-anatomici in *Amaranthus* spp. L. Fenotipizzazione mediante analisi a diversi livelli di scala – *Master's thesis in Environmental Analysis and Management (LM-75)*, University of Udine and University of Trieste, 2023. [Link](#)

Training activities

Agricultural Science and Biotechnology PhD Winter School 2021: *Systems Biology* – University of Udine, 16 March-20 April 2021, Udine, Italy.

R basics course: *Corso R base: Introduzione a R per l'analisi dei dati e la statistica applicata* – Turtles of the Adriatic Organization APS, 19-26 February 2022 (online course).

Agricultural Science and Biotechnology PhD Winter School 2022: *Lab Techniques* – University of Udine, 27-28 April and 16-17 May 2022, Udine, Italy.

Summer School: *Nanotechnology in Agriculture*, 1st Edition – University of Tuscia, 30 June-01 July 2022, Viterbo, Italy.

Agricultural Science and Biotechnology PhD Winter School 2023: *Statistics with R* – University of Udine, 07 March-21 April 2023, Udine, Italy.

Summer School: *Nanotechnology in Agriculture*, 2nd Edition – University of Udine, 29-30 June 2023, Udine, Italy.

ACKNOWLEDGEMENTS

First of all, I thank my supervisors Enrico and Elisa, who accompanied me on this journey with great support and enthusiasm.

I thank the whole Plant Biology group, for their cooperation, friendship, helpfulness and for always making me feel welcome, inside and outside the University.

I thank people from other research groups without whom we could not have achieved these results: Francesca from DAME, Walter, Luca and their group at CREA, the other colleagues from Udine and Padua who collaborated with us.

Finally, I thank all those people who are not colleagues, but who have been extremely important in my path: my family, friends and Daniel, who have always heeded my endless complaints, my doubts, my concerns for the future. They always supported me, especially in the last year, which has been perhaps one of the most difficult in my life so far.

The teaching I learned from this whole experience is this: every event, choice, or action has a purpose, which is to make you learn something. If you feel like you have made a wrong decision, actually this step was necessary at that precise moment in your life. Solutions or revelations come, you just have to wait patiently.

Thank you all!